Tasting light through hydrogen peroxide: Molecular mechanisms and neural circuits

by

Nikhil Bhatla

B.S., Product Design, Stanford University, 2002

Submitted to the Department of Brain and Cognitive Sciences
in Partial Fulfillment of the Requirements for the Degree of

Doctor of Philosophy in Neuroscience

at the

Massachusetts Institute of Technology

June 2014

Signature of Author _____
Department of Brain and Cognitive Sciences
April 4, 2014

Certified by _____
H. Robert Horvitz
Professor of Biology
Thesis Advisor

Accepted by _____
Matthew A. Wilson
Sherman Fairchild Professor of Neuroscience and Picower Scholar
Director of Graduate Education for Brain and Cognitive Sciences

Tasting light through hydrogen peroxide: Molecular mechanisms and neural circuits

by

Nikhil Bhatla

Submitted to the Department of Brain and Cognitive Sciences on April 4, 2014
in Partial Fulfillment of the Requirements for the Degree of Doctor of Philosophy

Abstract

The most fascinating function of the nervous system is its ability to generate consciousness, the subjective experience or qualia that distinguishes awake life from dreamless sleep. How consciousness is generated is an ancient philosophical question which has proven resistant to scientific analysis. While the human brain is known to generate consciousness, its complexity prevents acquisition of a mechanistic understanding of consciousness. Therefore, I chose to study the much simpler nervous system of the nematode *Caenorhabditis elegans*. I tested worms for a specific kind of learning, called trace conditioning, which correlates with conscious awareness in humans, under the assumption that if worms were able to trace condition, they might also be capable of conscious awareness. However, I was not able to show trace conditioning in worms, so the question of whether worms exhibit consciousness remains unresolved.

In the process of using light in learning experiments, I noticed that worms stop feeding immediately after being exposed to short wavelength (UV) light. Curious about whether worms might actually have a subjective experience in response to light akin to primitive vision, I investigated the molecular and neural mechanisms that control this behavioral response. I identified the I2 pharyngeal neuron as a cellular light sensor required for the speed of feeding inhibition. Hydrogen peroxide elicited behavioral and cellular responses strikingly similar to those caused by light. The sensing of both light and hydrogen peroxide were mediated by the LITE-1 and GUR-3 proteins, both putative gustatory receptors, as well as by the conserved antioxidant enzyme peroxiredoxin PRDX-2. My results suggest that the LITE-1/GUR-3 family of receptors likely detects light through its generation of hydrogen peroxide or of another redox product. This is a novel mechanism by which light can be sensed.

Additionally, by studying the worm's feeding response to light, I identified a pattern of neural function in which neurons appear to act independently to control sequential phases of a behavior. In the first phase, light rapidly inhibited feeding, with the I2 neuron sensing light and releasing glutamate likely onto pharyngeal muscle, where it was received by the AVR-15 glutamate-gated chloride channel. In the second phase, the inhibition of feeding was maintained via a circuit that included the extrapharyngeal neuron RIP and pharyngeal neurons I1 and MC. Finally, in the third phase, light stimulated pharyngeal contractions via the M1 neuron. These three circuits appear to be independent. I conclude that what initially appeared to be a simple reflex is instead a sequence of behavioral responses coordinated by independent neural circuits, suggesting a motif I term "parallel temporal tiling."

Although I am still uncertain about whether worms have a subjective experience of light, this research will serve as a foundation for future work aimed at this very question.

Thesis advisor: H. Robert Horvitz, Professor of Biology

Biographical Note

I was born in 1981 and grew up in Santa Monica, California, where I went to Pilgrim Lutheran Elementary School, followed by Windward High School. For college I went to Stanford University, where I majored in Product Design, an interdisciplinary major consisting of Mechanical Engineering and Art, and minored in Computer Science. During and after Stanford I pursued various entrepreneurial interests. I went to work at Google as a product manager, where I helped lead the development of Google Desktop, Google Video and the main Google.com user experience. Following my work at Google I went to graduate school in neuroscience at MIT.

After graduating from MIT, I intend to develop scientific software for organizing knowledge as well as continue my pursuit of the biological mechanisms that underly consciousness.

Acknowledgements

I thank Bob Horvitz, my advisor, for taking a chance on me as someone with no previous biology experience. Bob has been continuously generous with his resources and advice over the past 7 years. Niels Ringstad was my on-the-ground mentor and taught me everything a first-year biology student should have already known (how to run PCR, how to cut plasmids, how to use a microscope) and then a whole lot more. If I wanted to have an interesting conversation on nearly any topic, I could always talk to Niels. Shunji Nakano was my benchmate, and I have fond memories of our conversations about consciousness and trace conditioning. He taught me how to know if an experiment was worth doing: if either outcome from an experiment did not lead to a definitive result or another experiment, the experiment was probably not worth doing. Nick Paquin and Kostas Boulias *really* taught me molecular biology when I was struggling, and Nick has scientific expertise, and a memory unlike anyone else I know. Kostas, my roommate, has been an excellent friend over the past few years, always interested in hearing me yammer on about my project and usually offering very sage advice. He is my Greek brother. Christoph Engert, a fellow grad student, is a very good friend; he is one of the few people who sees things as I see them and he is always interested in listening to my latest results and offering fresh, creative ideas. Dan Pagano, another fellow grad student, also became a very good friend and I thank him for his camaraderie, mealmanship and friendship. I am grateful for the friendship of Andrew Bolton, a classmate, for our great conversations about consciousness, science and everything else that matters while eating at Beantown Taqueria.

My dad, Ajay Bhatla, and my mom, Poonam Bhatla, have been excellent parents and supported my life's efforts. My brother, Nitin Bhatla, has taught me things that only our differences could have. Finally, I am most appreciative of the continuing companionship of my lovefriend, Becca Loya. While I signed up to learn about neuroscience by coming to grad school, she did not. Nonetheless, she is an exceptional listener and now knows more about *C. elegans* biology than anyone who has never intended to know anything at all.

I appreciate the time, guidance and advice that Chip Quinn, Troy Littleton and Michale Fee have given me as members of my thesis committee.

Table of Contents

Table of Figures

Chapter 1:

Introduction

A. General introduction

Of all the types of cells, neurons are unique in their capacity to rapidly and spatially target signals. Neurons evolved as a specialized cell type for precisely this function, and the neural circuits that they constitute have also evolved in support of animal survival. Neural circuits control operations on very fast timescales, such as the roughly 100 milliseconds that it takes for light to be perceived (Tovee 1994), as well as on slow timescales, such as the hours between sleep/wake and hunger cycles (Saper..Lu 2005, Sternson..Cao 2013). Neural circuits control behavior, such as reaching for an apple, and regulate physiology, such as by secreting hormones to control cortisol levels. The human brain is made up of an innumerable number of neural circuits, and it remains an outstanding mystery as to how the brain accomplishes all of its functions. The expectation is that, piece by piece, the neural circuits that underly all functions of the brain will be identified. In this context, it is important to consider which piece of this puzzle one should participate in assembling.

B. Motivation and a point-of-view

Within the field of neuroscience, what should one study? In general, neuroscientists and biologists study a specific phenomenon because they want to understand how that phenomenon is caused. This can be a purely intellectual pursuit in its own right, without any further application. One might simply derive personal satisfaction from solving the problem, akin to completing the day's crossword puzzle. But should the focus of one's work be as arbitrary as the questions on a crossword puzzle? I believe that a scientist should choose their phenomenon of interest carefully, and that certain types of phenomena should receive greater attention than others.

a. Medically-relevant phenomena

There are 3 categories of phenomena that warrant high priority. The first category is phenomena which are medically relevant. Instead of working on any biological process, one could limit their focus to processes that are known or suspected to function in human disease. This is in fact part of the National Institutes of Health mission: "To seek fundamental knowledge about the nature and behavior of living systems and the application of that knowledge to enhance health, lengthen life, and reduce illness and disability" (NIH website). By studying a neurological disease at all levels, from the molecular to the behavioral, one hopes that their research will lead to development of drugs and therapies.

b. Artificial intelligence

The second category of priority is phenomena related to artificial intelligence. The brain is the only artifact known to possess a wide variety of "intelligent" functions, such as visual object recognition and the ability to coordinate complex locomotion (e.g. leaps of a squirrel atop fence posts). These tasks have so far resisted emulation by computational and robotic systems. The ability to create artificial systems that employ similar intelligence capabilities as the brain would certainly lead to substantial advances in technology and the associated enhancements in ease of living. Studying how the brain implements these intelligent functions might facilitate the generation of artificial intelligence.

c. Consciousness

The final category of priority is the phenomenon of consciousness, which I will discuss in detail in Chapter 2.

d. Which topic to study?

For both disease treatment and artificial intelligence, I question whether biological research is either necessary or an efficient approach to achieving these goals. Many drugs provide relief without a validated understanding of the underlying mechanism. Fluoxetine (Prozac) functions as a successful antidepressant with limited knowledge of how it alters the brain circuits that account for depression (Nestler..Monteggia 2002). Some advances in artificial intelligence have relied at least partially on basic insights from neuroscience, such as the hierarchical neural network models used in deep learning, which form the algorithmic basis for modern voice recognition (Hinton..Teh 2006). However, whether additional insight will be provided by more detailed understanding of neural circuits remains to be seen.

Of the three high priority areas of neuroscience research, I chose to focus my work on the study of consciousness.

C. Conclusion

My work, as documented in this thesis, began as an exploration of methods by which to rigorously study consciousness. After some failure, I focused on how the nematode *C. elegans* senses light in the hope that this study might provide insight into the mechanistic basis of visual perception. Although it has not yet done that, I did discover that worms sense light likely through its generation of reactive oxygen species, such as hydrogen peroxide. Moreover, I

discovered a set of independent neural circuits that control the worm's behavioral response to light. Along the way, I developed software to facilitate my research, and this software is also discussed in this thesis.

PART 1:

CONSCIOUSNESS AND TRACE CONDITIONING

Chapter 2:

Philosophy of Consciousness

A. Introduction

Consciousness is a phenomenon of high priority because it is the passage through which we have all of our experiences. It is the essence of what we are. If we seek to understand ourselves, we must first understand the physical basis of consciousness. Furthermore, it is of great interest because it has resisted scientific analysis for centuries. Some philosophers agree. For example, Searle said, "In my view, the most important problem in the biological sciences today is the problem of consciousness" (Searle 2000). In the following sections I will provide my definition of consciousness, theories that have been offered for how neural activity corresponds to consciousness, and the approach I selected for the study of consciousness.

B. Definitions of consciousness and related terms

The word "consciousness" is used colloquially to refer to 2 different phenomena. In the first use, one can ask if someone is "conscious" or not. This refers to the state of consciousness and can be thought of as an arousal level. A "conscious" state contrasts with an "unconscious" state, such as when a person is in a dreamless sleep or gets knocked out. People are less responsive to stimuli in unconscious states than in conscious ones. In the second use of "consciousness," one can ask if someone is "conscious of" something or not. This refers to the contents of consciousness, and assumes that the organism is already in a state of consciousness. Currently, the contents of your consciousness are the words that you are reading, as well as the words you hear in your head as you read them. The contents of consciousness shift quickly over time as new stimuli appear, while the overall state of consciousness changes much more slowly. When something becomes a content of consciousness, a person is said to have a subjective

experience. These subjective experiences are what directly distinguish conscious from unconscious states from the first-person point-of-view.

Sensation is simply the detection of a stimulus, while perception is the process that occurs when a sensory signal becomes a content of consciousness. Sensation is not a sufficient condition for perception to occur. Consider the case where one is looking at a visual scene, and there is a very small change, such as a slight increase in an object's brightness. The change is very accurately detected by the retina, but such a change may not cause a change in the content of consciousness, and therefore remains imperceptible. Sensation is also not a necessary condition for perception to occur. Thoughts, hallucinations, imagination and dreams are examples of perception in the absence of sensation, also known as non-veridical perception. One must also consider whether a stimulus has the capacity to be perceived. Some stimuli that the body senses do not have the capacity to be perceived, such as the current molecular state of the bloodstream. The body is sensing and responding to the levels of oxygen, carbon dioxide and nutrients in the blood, the signals of which may even be relayed to parts of the brain, yet it is impossible to directly perceive this. Why some stimuli result in perception while others do not is a fundamental question in the study of consciousness.

The contents of consciousness are present with different intensities. One might be talking on the phone while driving, and the conversation might have a stronger presence in consciousness than the road ahead. When an ambulance drives by, this might cause a shift in focus, or attention, from the conversation back to the road. Attention is the process that selectively amplifies one content of consciousness over another. Even without a change in stimulus, attention can shift the perception of a complex stimulus from one feature to another.

One final term that requires a definition is awareness. Like "consciousness", awareness actually refers to two phenomena. In the first case, one can ask if someone is "aware" or not. This refers to a state of awareness, akin to a state of consciousness, and contrasts with a state of unawareness (e.g. sleep). In the second case, one can ask whether someone is "aware of" something. This refers to awareness as knowledge about that thing. It is the second case that I will focus on here. In the specific context of consciousness research, experimenters instruct subjects to report whether they experience a stimulus or not. So instead of observing perception directly, researchers observe perception indirectly through subjects' responses, and those responses depend on another indirection, that of the subject being aware, i.e. having knowledge, of what they perceive. It is conceivable that a person could have perception in the absence of awareness, and therefore fail to report perception when it actually occurs. Altogether, the scientific study of consciousness considers awareness of experience of a stimulus as a sufficient condition for the presence of perception, although the presence of perception does not guarantee the presence of awareness.

The perception I've described so far is perception of stimuli external to the body. Perception can also apply to internal stimuli, and these may in some cases correspond to the emotions that people experience. Additionally, a sense of self is a special type of perception where one perceives one's self as separate and distinct from everything else. Finally, free will is the perception that one is in control of one's actions and perhaps to some degree one's thoughts.

Consciousness can be described as a hierarchy of features. An animal that has the capacity for perception has the simplest form of consciousness. More "advanced" animals may have perception as well as a sense of self, without feeling that they are in control of their own actions. Even more advanced animals, such as humans, appear to possess perception, a sense of

self, and free will. These features of consciousness form a hierarchy, with perception a necessary condition for a sense of self, and both perception and a sense of self as necessary conditions for free will.

In what follows, I will use the word "consciousness" primarily to refer to perception.

C. Blindsight as an example

I hope that the explanation above is clear, and you now understand what I mean when I use the word "consciousness." However, if the meaning of consciousness is still unclear, perhaps the example of blindsight will provide greater insight.

Blindsight is a condition where a person claims to be blind but still retains visual ability (Cowey 2010, Weiskrantz..Marshall 1974). Blindsight is caused by damage to the primary visual cortex (V1), and since that damage is usually restricted to a single visual hemifield, the patient retains normal vision in half of their visual field. In this way, patients have lost experiential vision, or visual perception, in half of their visual field. In a typical experiment, a visual bar is shown to the subject's "blind" hemifield and the subject is asked if the bar is moving horizontally or vertically. At slow bar velocities, the subject will report that they can't perceive anything, so they don't know which way the bar is moving. However, if the experimenter asks the subject to answer regardless, the subject can report accurately nearly 90% of the time (Weiskrantz..Sahraie 1995). This kind of accuracy is limited to simple tasks, such as questions with only two possible answers. Additionally, an individual with bilateral damage and full-field blindsight has been shown to be able to navigate a room full of objects, albeit slowly (de Gelder..Pegna 2008).

The condition of blindsight demonstrates a difference between perception and information processing. After damage to primary visual cortex, the patient's brain is still capable of doing basic visual analysis. However, this analysis occurs without the concomitant experience of visual perception. Behavioral functions remain intact, but the subjective experience has been severely compromised. The example of blindsight demonstrates that subjective experience is not a necessary condition for behavioral performance, although it might intuitively feel that way. In fact, behavioral performance can persist in the absence of experience. In the specific case of blindsight, the question remains as to what exactly the primary visual cortex is doing that manifests as subjective experience in response to visual input.

D. The problem of consciousness

To emphasize, perception is the process by which a sensory signal becomes a content of the conscious state. Perceptions are the experiences that one has, such as experiencing the warmth of a fire on a cold day. One doesn't just sense the warmth but one also *perceives* it. Philosophers use the term qualia to refer to these subjective experiences.

The challenge is to explain how physical matter can produce experience of any kind at all. In other words, how do some configurations of matter (e.g. our brains) create experience, while other configurations of matter (e.g. chairs) do not, as far as we know? As Chalmers said:

> The really hard problem of consciousness is the problem of *experience*. When we think and perceive, there is a whir of information-processing, but there is also a subjective aspect. As Nagel (1974) has put it, there is *something it is like* to be a conscious organism. This subjective aspect is experience. When we see, for example, we *experience* visual sensations: the felt quality of redness, the experience of dark and light, the quality of depth in a visual field … But the question of how it is that these systems are subjects of experience is perplexing … It is widely agreed that experience arises from a physical basis, but we have no good explanation of why and how it so arises. Why should physical processing give rise to a rich inner life at all? It seems objectively unreasonable that it

> should, and yet it does. If any problem qualifies at *the* problem of consciousness, it is this one. (Chalmers 1995)

The primary problem is that we lack any reason for why experience exists at all, as it seems fairly straightforward to imagine animal life without consciousness. Nonetheless, we have consciousness. A secondary problem is that we lack rules that provide a correspondence between physical matter and the kind of subjective experience. Why do we experience light as perceptual vision and experience sound as perceptual audition, and how are these two perceptual spaces specified and kept distinct? Surely the answer must lie in the specific processing that the brain does to produce perceptual vision, while the brain does different processing to produce perceptual audition. The details of this distinction remain cryptic.

E. Philosophical positions on consciousness

Based on the current scientific worldview, it's quite unexpected that the brain produces consciousness at all. We have no "laws" for how consciousness can be generated from the biochemistry of physical matter, yet this is clearly what seems to be happening in the brain. So how consciousness arises from matter is an unanswered philosophical and scientific question.

In the final chapter of his book *Natural Fabrications*, Seager articulates 4 general views that one can adopt in trying to explain how physical matter might generate consciousness (Seager 2012). Some of these views rely on the concept of emergence. The idea of emergence is that in a sufficiently complex system high-level properties can "emerge" from the intricate low-level interactions that occur. A canonical example involves the weather, where macroscopic objects, such as a hurricane, emerge from interactions of microscale volumes of air of varying pressure and temperature. Another common example is that of an ant hill, where the entire colony seems

to organize itself as a superorganism to accomplish feats that individual ants cannot (Holldobler & Wilson 2008).

Seager distinguishes between 2 kinds of emergence. In conservative emergence, the macroscale properties that appear follow completely from microscale laws of physics. Another way to think about this is that if we had unlimited computing power and ran a simulation of the system with just the location and momentum of every microscale particle, and set the simulation in motion following the basic laws of physics, then the macroscale properties would emerge without having to add any additional macroscale rules. A hurricane is an example of conservative emergence. I also believe that many current scientists would agree that the macroscale phenomena they study, from the economy to neuroscience, can be thought of as conservative emergents.

This is not to say that the best way for a person to understand a hurricane is by doing an atomic simulation of one. It is often better to rely on concepts that are much higher than the microstates of particles in order to get a feel for what is happening (e.g. temperature and pressure), since our brains are good at conceptual hierarchies and poor at keeping track of lots of microstates. I argue that those intermediate levels of explanation are still the result of microstate interactions, nothing more.

Conservative emergence stands in contrast to radical emergence, which holds that certain macroscale properties do not follow from the basic laws of physics but require new macroscale laws to explain their existence. Another way to think about this is if we had unlimited computing power and we ran a simulation of a system incorporating just microscale features and laws, emergent properties of the real system would not emerge in the simulation. Additional rules at the macroscale would need to be included to simulate the radically emergent properties.

Given this background on emergence, Seager proposes 4 alternatives for how we might account for consciousness:

(1) The first view he calls "Watchful Waiting", and I call this the conservative emergence view of consciousness. This view holds that although we currently lack a viable theory for how consciousness is generated from matter (see the next section for some of these theories), this doesn't mean we won't figure it out eventually, using standard reductionist science. After all, in the early 20th century the phenomenon of life seemed impenetrable by science, so we invoked the theory of vitalism, an extra force, to account for life. But after a century of work science has now shown that life can be reduced to biochemistry in cells, nothing more. This view holds that something similar will happen with consciousness and that consciousness will be shown to be conservatively emergent from the brain. We are just missing key concepts that connect physical matter to experience, which we'll learn through the indefatigable scientific hunt.

(2) The second view he calls "Embracing Emergence", and I call this the radical emergence view of consciousness. This view holds that unlike other phenomena which are conservatively emergent, consciousness is a radically emergent phenomenon. Although our microstate simulation of the brain will generate all the expected behaviors of a person, it will not properly simulate consciousness without additional rules that apply at the macroscale.

(3) The third view he calls "Favoring Fundamentality", and I call this the panpsychism view of consciousness. This view holds that conscious experience is a basic property of matter, in addition to the basic physical properties. Not only does matter have

mass, charge and other primitive properties, it also has a class of proto-conscious properties that may be considered the underpinnings of consciousness. Under this view, even an atom has the necessary properties to generate subjective experience, by having an atomic amount of subjective experience itself. So consciousness as we know it is simply a conservative emergent of this new class of properties.

(4) Finally, the fourth view he calls "Modifying Metaphysics", and I call this the mysterian view of consciousness. This view holds that science itself is not telling us about reality as it is, but is just giving us useful concepts for manipulating reality for our practical benefit. Since science is not showing us the Truth and we don't have knowledge of Reality, understanding consciousness is not possible either.

As a scientist, I believe that one must consider these options if one chooses to study consciousness.

I believe that our work as scientists of consciousness is to identify those particular macroscopic phenomena that specifically generate consciousness. We must identify those precise features of neural activity that distinguish consciousness-generating neural activity from the rest of neural activity that does not generate experience.

F. Theories for the neural activity that corresponds to consciousness

Despite the problem that consciousness poses for explanations of how it comes into existence at all, neuroscientists have nonetheless developed theories for the kinds of neural activity that correspond with consciousness in the brain. It is important to be clear that none of these theories provides an *explanation* for how subjective experience can possibly emerge from physical matter; rather, these theories assume consciousness exists without explanation and

endeavor to identify the kinds of neural activity that generate consciousness as opposed to the kinds of neural activity that do not. This special neural activity has been called the neural correlate of consciousness (NCC) by Crick and Koch: "The NCC is the minimal set of neuronal events that gives rise to a specific aspect of a conscious percept" (Crick & Koch 2003).

The first, and perhaps most basic theory, which I will call population rate theory, contends that perception emerges when enough connected neurons exhibit a certain level of activity, or firing rate (Crick & Koch 2003). The level of activity in a network would correspond to the richness of the perception:

> Coalitions may vary both in size and in character. A coalition produced by visual imagination (with one's eyes closed) may be less widespread than a coalition produced by a vivid and sustained visual input from the environment … Coalitions in dreams may be somewhat different from waking ones. (Crick & Koch 2003)

Although Crick & Koch refer to a difference in "character", they do not provide further details. There is experimental evidence supporting the notion that levels of activity linearly correlate with visual object perception (Bar..Dale 2001, Grill-Spector..Malach 2000). In this proposal, different coalitions of neurons would account for distinct perceptions (Zeki & Bartels 1999). The notion that a certain level of coordinated neural activity corresponds to the level of perception would exclude animals from possessing the capacity for experience if their nervous systems were not of sufficient size or exhibited sufficient activity. If such a theory were true, one would question whether *C. elegans*, with only 302 neurons, has sufficient neural capacity for perception.

A second theory, which I will call synchrony theory, contends that it is not overall neural activity that is critical for perception to occur but that *synchronization* of neural activity must increase, even in the absence of a change in overall firing rate There is experimental evidence in humans that show that threshold stimulus trials that result in perception occur during phase

synchronization (Meador..Vachtsevanos 2002, Palva..Palva 2005). Additionally, synchrony occurring even before stimulus onset correlates with whether a stimulus is perceived or not (Nakatani..van Leeuwen 2005, Palva..Palva 2005). The frequency of activity that results in synchronization during perception varies from 4-50 Hz (Palva..Palva 2005), with synchrony most commonly observed in the gamma band (30-50 Hz) (Fries..Singer 1997). Synchrony may be critical not only within a brain region but also across brain regions (Srinivasan..Tononi 1999, Melloni..Rodriguez 2007). Of all the theories presented here, synchrony theory is currently motivating the largest number of neuroscientific investigations into consciousness.

A third theory, which I will call recurrence theory, holds that stimuli initially trigger a feedforward sweep of activity in the cortex, which is followed by recurrent feedback (Lamme 2006). This theory postulates that it is in fact the recurrent activation of cortex that is responsible for perception, and not the feedforward sweep. Some evidence supports this theory. For example, if recurrent activity is disrupted within a specific time window after stimulus presentation, visual perception is reduced (Pascual-Leone & Walsh 2001). Recurrent activity may also be called sustained activity: when a stimulus is presented only briefly, the recurrent activity occurs after 100 ms or so, even after the stimulus has been removed. Such sustained activity may also serve as a neural correlate of consciousness.

A final theory for neural activity that results in consciousness is called integrated information theory (Tononi 2004). This theory states that a system's capacity for consciousness is dictated by its capacity to integrate information. One can measure a system's capacity to integrate information by systematically dividing the system into subsets and measuring the effect that perturbing one subset has on the activity of the other subset. Generally speaking, systems where perturbations significantly affect the other subset's outputs are said to have higher levels

of information integration than systems where perturbations do not significantly affect the other subset's outputs. These analytical operations are mathematically defined. Overall, integrated information theory is an interesting way to measure a network's complexity. Since neural circuits have the properties of a network, the theory can also be applied to score the integrated information capacity of neural systems. The theory hypothesizes that these scores will correlate to the level of consciousness exhibited by the system.

G. My approach to studying consciousness in *C. elegans*

Studying consciousness in humans is advantageous because there is no doubt that humans are capable of consciousness, and it can be indirectly observed when subjects report on their perceptual states. However, humans pose significant disadvantages due to the high degree of biological complexity and limited tools that a researcher has available for causal analysis. To understand the mechanisms of consciousness, one would need to perturb elements of the nervous system and observe whether it affected the consciousness phenotype in some way. Such perturbation analysis is strikingly limited in humans, compared with other animals. So while the phenomenon of interest is clearly present in humans, rigorous analysis is limited by the methods available.

As one moves down the list of animals commonly used in research, from humans to monkeys to rodents to insects and finally to nematodes, there is definitely a reduction in complexity as well as an increase in causal tools and speed of experimentation. However, one becomes less certain of the capacity for consciousness. So there appears to be a trade-off between studying the phenomenon of interest (consciousness) and doing rigorous analysis.

I chose to focus on the organism with the simplest nervous system so that I could do the most rigorous and thorough analysis possible. This organism is the nematode *C. elegans*, also known as the "worm". About the size of an eyelash (1 mm long and 100 µm in diameter), the worm has only 1031 somatic cells in its entire body. Nearly a third of the cells are neurons, 302 to be exact. The entire connectome of the worm is known, and it is the only complete map of any nervous system (Albertson & Thomson 1976, White..Brenner 1986). The worm is transparent, so imaging neural activity inside the animal is simple and of excellent resolution.

But does the worm have the capacity for consciousness? How would one go about trying to answer this question? Based on the theories for how neural activity creates consciousness described above, one might be tempted to look for similar patterns of neural activity in the worm's nervous system. However, whether these theories actually account for, or even correlate with, consciousness remains speculation.

Instead, I chose a different approach. I searched the literature for behaviors that correlate with the capacity for consciousness in humans, with the hope that I could test *C. elegans* for the presence of the behavior. My rationale was that if *C. elegans* exhibited the behavior, and if the correlation between the behavior and consciousness was evolutionarily conserved, then this would serve as evidence for consciousness in *C. elegans*. Having identified an assay that correlated with consciousness, I could then study the molecular, anatomical and physiological basis of consciousness.

I found one behavior that correlates with awareness of stimuli contingencies in humans that I chose to pursue in the worm. This behavior is a specific kind of classical conditioning. In classical conditioning (think Pavlov's dog), a subject is presented with a conditioned stimulus (CS),which on its own does not elicit any innate response. A subject is also presented with an

unconditioned stimulus (US), which on its own elicits an innate response. After repeatedly pairing presentation of the CS followed by presentation of the US, a subject is said to have "learned" if the CS alone now elicits a behavioral response, called the conditioned response (CR). This is the standard classical conditioning method.

Researchers discovered that a specific kind of classical conditioning, called trace conditioning, correlates with subjects' awareness that the CS preceded and predicted the US (Clark & Squire 1998). In this experiment, subjects are given an eyeblink conditioning protocol, where the CS is a sound of a specific frequency and the US is a puff of air to the eye. After many trials, the subject learns to blink (the CR) after hearing the CS but slightly before the US will turn on. In one kind of experiment, called delay conditioning, the CS onset precedes the US, and both coterminate (Figure 2.1, left). Under these conditions, subjects will learn to blink, but when asked afterwards they won't necessarily know which sound predicted the air puff. In a slight variation of the experiment, called trace conditioning, the CS onset and offset precede the US onset, so that there is no temporal overlap between the two stimuli (Figure 2.1, right). Under these conditions, fewer subjects learn to blink, but when asked afterwards the subjects that learned will also be aware of which sound predicted the air puff.

These results showed that if a human successfully trace conditions, they are likely to be aware of the relationship between the stimuli. This awareness is associated with the perception of the stimuli and their temporal relationship, and therefore may function as a test for consciousness.

It is difficult to tell if animals without language have the capacity for awareness because it is difficult, though not impossible, to train them to respond in a specific manner dependent on their mental state. Might it be the case that if an animal trace conditions, it also has the capacity

for awareness of stimuli relationship? Rodents, and perhaps even flies, have been shown to trace condition, suggesting that these organisms might also be capable of awareness of the temporal relationship between stimuli (Han..Anderson 2003, Tully & Quinn 1985).

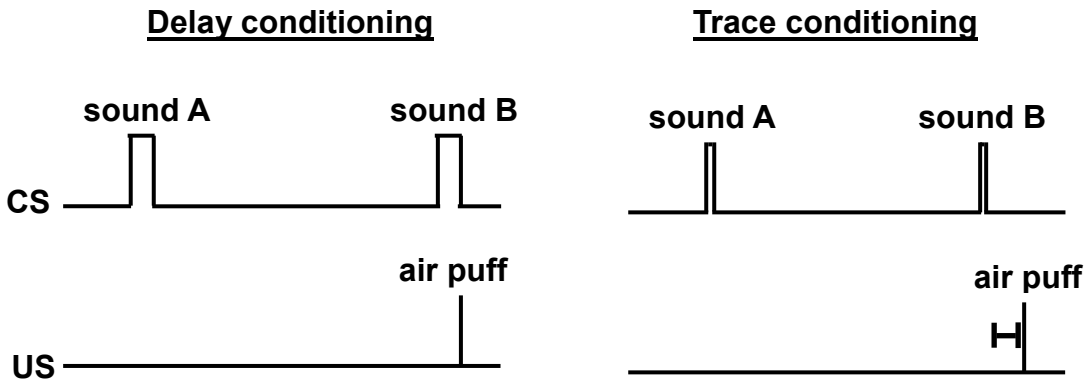

Figure 2.1: Trace conditioning might be a test for perception

Schematic showing the delay and trace conditioning protocols. The horizontal lines indicate the passage of time. Delay conditioning does not correlate with awareness of the temporal relationship between the CS and the US, while trace conditioning does correlate with awareness of the relationship. (Clark & Squire 1998)

Since previous work on learning in *C. elegans* did not involve such classical conditioning protocols, I tried to develop such an assay. I tried several different conditioned stimuli including the odors isoamyl alcohol (IA) and octanol (OCT) and oxygen gas (O_2), and unconditioned stimuli, including light and carbon dioxide (CO_2). I varied the number of trials, the duration of the stimuli, their relative timing, the inter-trial interval (ITI), and many other stimulus parameters. However, under no condition did I observe learning after either delay or trace conditioning protocols. These results are presented in Chapter 3.

Although I failed to show that *C. elegans* are capable of classical conditioning, I unexpectedly observed several novel behavioral responses while testing stimuli for learning. Most interestingly, I observed that bright short wavelength light inhibited the feeding rhythm of

the worm, in addition to causing avoidance which had already been described (Edwards..Miller 2008, Ward..Xu 2008). Studying a behavioral response to light intrigued me, because if I was able to understand the neural circuit that controlled this behavior, I might be able to search the *C. elegans* nervous system for patterns of neural activity that have been theorized to be important for perception (p. 35). By studying such a neural circuit in the context of the connectome, I would be in a position to look for recurrent, sustained, or synchronous activity, or perhaps even analyze integrated information, among groups of neurons functioning in the neural circuit. Might it be possible that when I shine light on the worms, they might actually perceive the light and truly "see"? So I set out to understand the molecular and cellular basis for the worm's feeding response to light. Unlike my attempts at classical conditioning, these efforts proved quite fruitful, and are discussed in Chapter 4.

Chapter 3:

Failure to Classically Condition *C. elegans*

A. Introduction

The mechanisms of consciousness are difficult to study. Although another person's subjective experience cannot be observed directly, we can indirectly observe consciousness by relying on a person's report of their subjective experience. However, understanding the mechanism that produced that report is impeded by the sheer complexity of the human brain as well the limited availability of tools for accurately and non-invasively manipulating neural activity. Better tools are available in model organisms, but these animals generally lack an ability to report on their subjective experience so one is less sure that one is studying consciousness. An exception is that one can train a primate to report on what they see (Cowey & Stoerig 1995). Trace conditioning, a type of learning, has been shown to correlate with awareness of a relationship between stimuli in humans, and I sought to test whether *C. elegans* was capable of this type of learning. In this chapter I will provide background on learning and evidence for a connection between conditioning and consciousness.. I will also discuss forms of learning that *C. elegans* are capable of, and provide behavioral results of the acute responses of worms to many stimuli. Finally, I show results of my attempts at classical conditioning by pairing these stimuli and looking for a change in the worm's response. Unfortunately, the worms were not able to condition under these circumstances.

B. Types of learning

Of all the capacities that distinguish humans from other animals, our expansive ability to learn seems to be the most defining. Learning is a change in output without a change in input, i.e. a change in behavior without a change in stimulus. Learned behaviors contrast with innate

behaviors, which are actions that do not rely on a history of stimulus presentation but are genetically and developmentally "pre-programmed" into the animal.

Learning can be partitioned into a hierarchy of categories (Figure 3.1). The simplest form of learning occurs when repeated presentation of a single stimulus alters the response to that stimulus. This first type is called non-associative learning. Non-associative learning can be

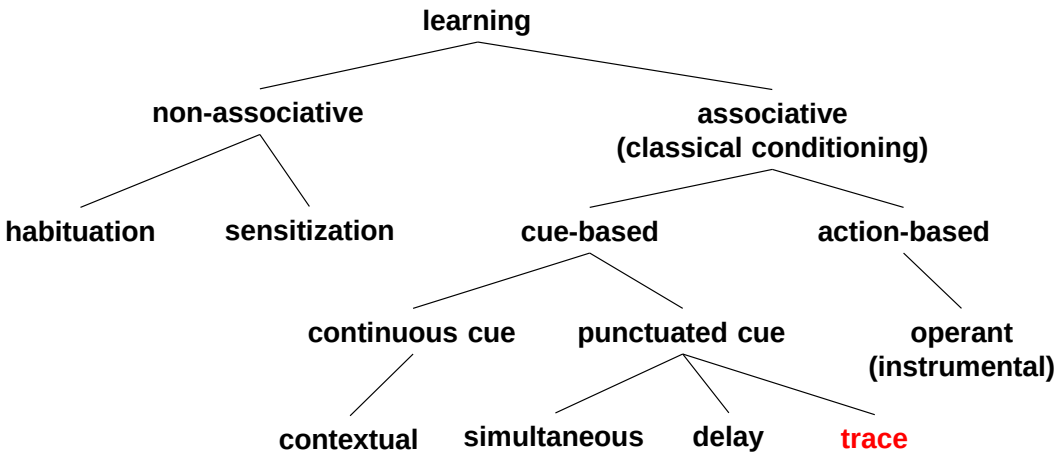

Figure 3.1: Categories of learning

Learning can be grouped into 2 categories: non-associative and associative, which can be further subdivided as shown. Trace conditioning is indicated in red because it is associated with awareness of stimulus relationship in humans and will be the focus of this chapter.

further divided into 2 categories: habituation occurs when the response to a stimulus decreases after repeated presentation, while sensitization occurs when the response to a stimulus increases after repeated presentation (Lipsitt 2006). One example of habituation would be the failure to notice or respond when a loud plane flies overhead, after living next to an airport for several weeks. Sensitization can also include a generalization of response to different stimuli after repeated presentation of the response-inducing stimulus.

The second category of learning is associative learning, also known as classical conditioning. In classical conditioning, an animal learns to associate the presence of one

stimulus with the presence of another (Pavlov 1906). As an aside, even non-associative learning can be considered a subset of associative learning, where the animal learns to associate a stimulus to the presence of no other stimulus (Cevik 2014). Associative learning can be further divided based on whether the predictive item is an external cue (cue-based learning) or an action taken by the animal itself (operant or instrumental conditioning).

Cue-based learning can be further divided based on the timing of the predictive cue (Kryukov 2012). In contextual conditioning, an animal learns that a specific context, that is a specific set of stimuli present continuously, predicts exposure to a conditioned stimulus. The classical example is contextual fear conditioning in rodents, where the rodent learns that when they are in a room that looks a certain way, e.g. has horizontal stripes on the wall, they will be shocked with electricity (Maren..Liberzon 2013). We know that the mouse has learned this relationship because they exhibit a new behavior after several trials of pairing the context with shock: they learn to freeze when placed in the room which has been associated with shock.

If the predictive cue only occurs for a brief moment, then conditioning can be further categorized based on the timing of the predictive cue relative to the predicted stimulus. At this point, it is worth defining some terms. The conditioned stimulus (CS) is the stimulus that usually does not elicit a response when presented. The unconditioned stimulus (US) is the stimulus that does elicit a response when presented. After the CS and US are presented in a paired manner (simultaneously or sequentially) one or more times, the animal is said to have learned if the animal now responds to presentation of the CS alone. This response is called the conditioned response (CR). In simultaneous conditioning, the CS and US are presented simultaneously. This won't be discussed further here. Instead, I will focus on delay and trace conditioning for the remainder of this chapter. In delay conditioning, the onset of the CS precedes the onset of the

US, but both coterminate (Figure 3.2, left). In trace conditioning, the onset and offset of the CS precedes the onset of the US (Figure 3.2, right).

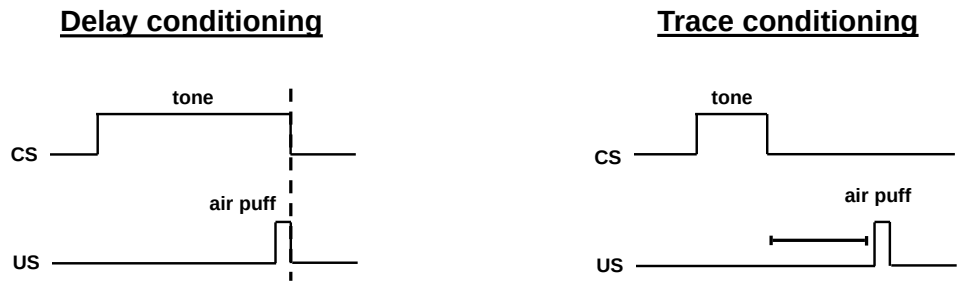

Figure 3.2: Timing in delay and trace conditioning

Schematic showing the timing for delay and trace conditioning. The important difference between these two protocols is the lack of overlap between the tone and the air puff in trace conditioning.

C. The connection between trace conditioning and consciousness

Having described several types of learning, I will now discuss one experiment that provides evidence for a connection between trace conditioning and consciousness (Clark & Squire 1998). In this experiment, participants watched a silent movie. While their attention was focused on the movie, they underwent an eyeblink conditioning protocol. The conditioned stimuli (CS) were 2 different sounds: a 1 Khz pure tone and a white noise static, both at a volume of 85 dB. For each subject, one of the two sounds was paired with a puff of air to the eye, which served as the unconditioned stimulus (US). The CS that was paired with the US was called the CS+, while the CS that was unpaired was called the CS-. This type of conditioning, where only one of several CSes precedes the US, is called differential conditioning. After several trials, subjects were said to have learned if they preferentially blinked after hearing the CS+ but not the CS-. After the conditioning protocol was completed, awareness was assessed using a questionnaire. Specifically, subjects were asked 17 true/false questions that sought to determine

their awareness of the temporal relationship between the stimuli, such as "I believe the air puff usually came immediately before the tone" and "I believe the tone predicted when the air puff would come on" (Clark & Squire 1999). If the subjects answered 75% of the questions correctly, they were deemed to be aware of the temporal relationship between the CSes and the US. The subjects underwent either delay or trace conditioning (Figure 3.3).

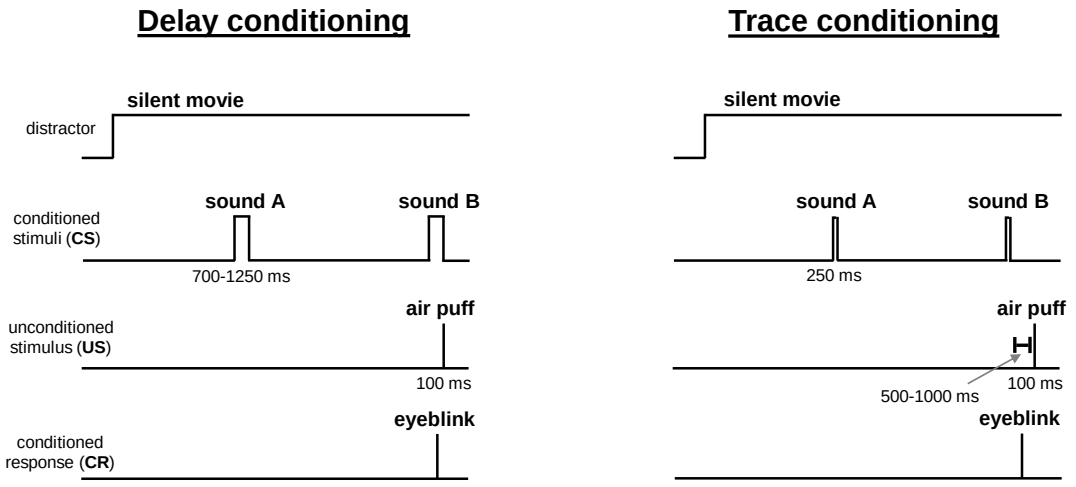

Figure 3.3: Schematic of experiment showing correlation between trace conditioning and awareness of stimuli contingencies

(Clark & Squire 1998)

The principal result from this experiment was as follows. Both subjects who were aware of the stimulus contingencies and those who were not successfully learned in the delay conditioning protocol. In contrast and strikingly, in the trace conditioning protocol, subjects who were aware on average learned while subjects who were not aware did not learn.

These results indicated that if a subject learned under trace conditioning, then they were also aware of what they had learned. To confirm this and see how well the correlation held (i.e. if an individual learned, were they guaranteed to be aware?), one of the authors of the study (Bob

Clark) graciously agreed to share the original data with me. I found that there was no correlation between learning and awareness for subjects in the delay condition, but that there was a significant correlation between learning and awareness in the trace condition (Figure 3.4). Moreover, I confirmed the previous result and found that on average, if a subject learned during trace conditioning, they were aware of the stimuli contingencies, while this was not true of delay conditioning (Figure 3.5).

The finding that trace conditioning correlates with awareness of stimuli contingencies has been replicated by the same group (Clark & Squire 1999, Clark..Squire 2001, Clark..Squire 2002, Manns..Squire 2000, Manns..Squire 2000, Manns..Squire 2001, Manns..Squire 2002) as well as another group (Papka..Woodruff-Pak 1997, Woodruff-Pak 1999). Additionally, electric shock has been used as the US in a fear conditioning paradigm to arrive at the same conclusion regarding trace conditioning (Weike..Hamm 2007, Knight..Bandettini 2003, Knight..Bandettini 2006). There is one group of researchers who agree that trace conditioning correlates with awareness but also claim that delay conditioning does as well (Lovibond & Shanks 2002, Marinkovic..Dawson 1989, Knuttinen..Disterhoft 2001).

Overall, after reading a substantial portion of the literature on the topic of delay and trace conditioning and awareness, I conclude that there is an ambiguity. It isn't clear that the trace conditioning task correlates with awareness because the trace interval requires a memory to be formed. Trace conditioning is more difficult than delay conditioning, in that fewer people learn to trace condition (Figure 3.5; $p < 0.05$, chi-squared test). Perhaps awareness is actually correlated with "difficult" learning tasks, and trace conditioning correlates with awareness because it is more "difficult" than delay conditioning?

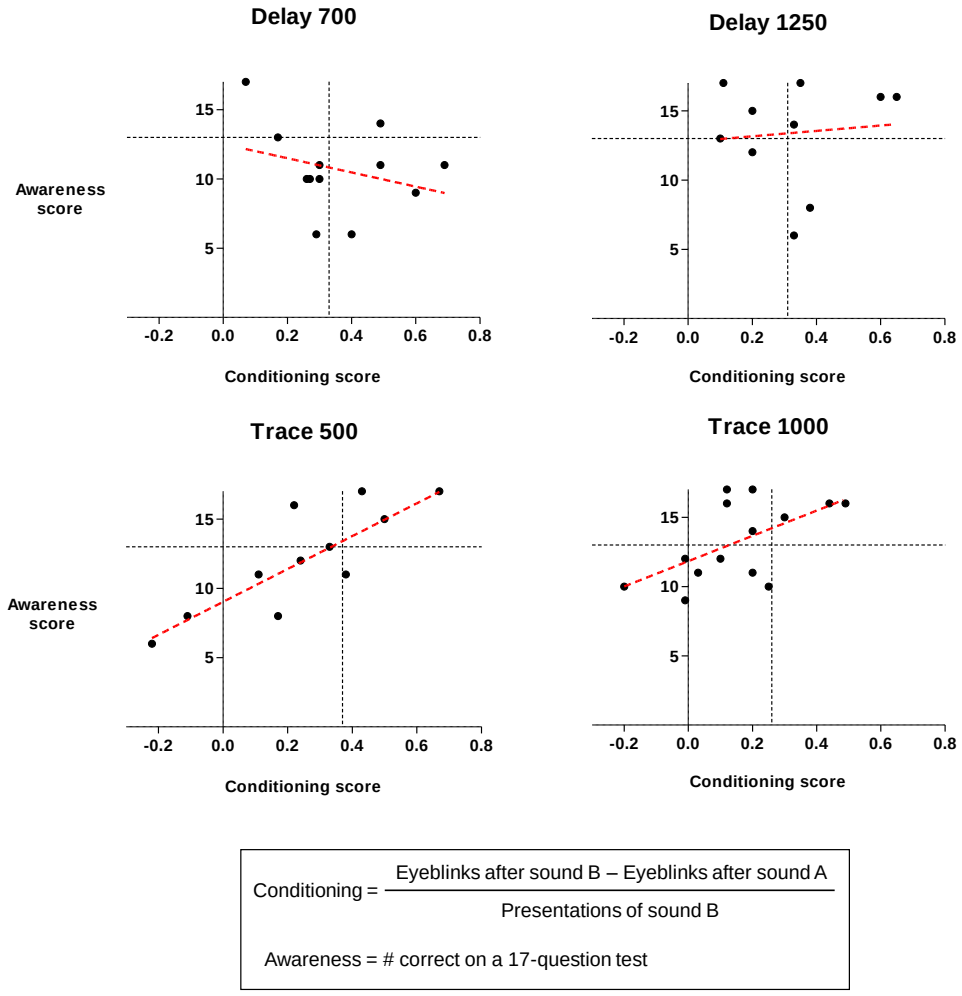

Figure 3.4: Trace but not delay conditioning correlates with awareness of stimuli contingencies

The x-axis indicates degree of learning, as assessed on the final block of trials. The y-axis indicates degree of awareness, as assessed by a questionnaire at the end of the experiment. Each dot represents one participant. The red dashed line is the regression of the data. For Delay 700 and 1250, the regression slope was not significantly different than 0. For Trace 500 and 1000, the regression slope was significantly different than 0 ($p < 0.05$). Delay 700 refers to a 700 ms delay from CS+ onset to US onset and Delay 1250 refers to a 1250 ms delay. Trace 500 refers to a 500 ms delay from CS offset to US onset and Trace 1000 refers to a 1000 s delay. Vertical and horizontal lines indicate thresholds used to declare whether a subject had learned or was aware, as used in Figure 3.5. My analysis of data from (Clark & Squire 1998).

	Awareness Score			
	Learned	n	Didn't Learn	n
Delay 700:	10.20	5	11.00	7
Delay 1250:	12.83	6	14.25*	4
Trace 500:	14.20*	5	10.57	7
Trace 1000:	15.67*	3	12.64	11

Figure 3.5: If learning occurs during trace conditioning then the subjects are aware of stimuli contingencies

Awareness score is the number correct on a 17-question test. Subjects classified as "learned" if last block learning performance was greater than 2 standard deviations from 0. * $p < 0.05$ and indicates that on average the group was aware of the stimuli contingencies. My analysis of data from (Clark & Squire 1998).

Much ongoing research is interested in identifying the brain areas and neural circuits that subserve delay and trace conditioning. Thus far, work has identified the cerebellum as critical for both delay and trace conditioning, and the hippocampus as required for trace conditioning (Clark & Squire 1998, Cheng..Desmond 2008). It is important to point out that just because an amnesiac patient with damage to the hippocampus does not trace condition does not mean that this person does not possess consciousness. I argues that trace conditioning is a sufficient, but not a necessary, condition for consciousness.

One caveat worth mentioning concerns toxiphobia and conditioned taste aversion. In these experiments, rats are given a specific taste (e.g. saccharin) and several hours later are given an injection of a toxic substance that makes them ill (e.g. lithium chloride) (Garcia..Koelling 1955, Yamamoto..Sakai 1994). Conditioned taste aversion has also been studied in humans (Bernstein & Webster 1980). Due to the long delay between the CS (taste) and the US (nausea or sickness), this protocol can be considered a form of trace conditioning. It is worth noting that

conditioned taste aversion can occur even if the US is provided under anesthesia (Bermudez-Rattoni..Garcia 1988), such that the animal does not experience exposure to the toxin. While the result is unexpected, the anesthesia experiment does not address the question of whether conditioned taste aversion correlates with contingency awareness in humans, as is the case for trace conditioning with the eyeblink protocol. It remains an open question as to whether conditioned taste aversion correlates with awareness of the relationship between stimuli.

Despite the controversy of whether delay conditioning correlates with awareness, scientists agree that trace conditioning correlates with awareness. My analysis also supports this view. To the extent that awareness of stimuli contingencies depends on conscious perception, trace conditioning could be a method for studying consciousness in organisms that, unlike humans, cannot easily report on their subjective experience. Furthermore, conditioning is a behavior that many organisms exhibit, from flies (Tully & Quinn 1985) to mice (Han..Anderson 2003). If I can show that *C. elegans* can trace condition, perhaps I will be able to indirectly study the neural mechanisms of consciousness in worms.

D. Review of *C. elegans* learning

C. elegans is capable of both non-associative and associative learning. However, as I will describe, none of the most well-studied paradigms corresponds with delay or trace conditioning, which led me to attempt to develop my own conditioning assay.

a. Plate-tap habituation

The most well-studied example of non-associative learning in *C. elegans* is called plate tap habituation. When worms are touched on their heads, they reverse their locomotion, and

when they are touched on their tails, they accelerate forward (Chalfie..Brenner 1985). In fact, if one taps the plate that the worms live in and essentially vibrates the whole worm, the worm reverses. Repeated tapping results in a reduction of reversals, and this habituation depends on the inter-stimulus time interval, with shorter intervals resulting more quickly in habituation than longer intervals (Rankin & Broster 1992, Giles & Rankin 2009, Rankin & Wicks 2000). Worms also habituate in response to nose touch (Hart..Kaplan 1999), and I have found that the worms also habituate their reversal response to light (Figure 3.8). In addition to habituation, worms are capable of sensitization of the plate tap response (Rankin..Chiba 1990). Finally, researchers have also shown that worms habituate to odorants that they are naively attracted to, and this is distinguished from olfactory learning (p. 55) by the fact that they can be dishabituated (Morrison..van der Kooy 1999, Bernhard & van der Kooy 2000, Nuttley..van der Kooy 2001, Pereira & van der Kooy 2012).

b. Thermotaxis learning: temperature ± food

In addition to non-associative learning, *C. elegans* is capable of associative learning. The learning comes in several forms, but the general idea is that worms are able to learn that stimuli can be associated with the presence or absence of food. Worms eat bacteria.

In the first demonstration of associative learning in *C. elegans*, researchers found that worms were attracted to the temperature at which they were grown. This behavior is called thermotaxis learning. If worms feed on bacteria and grow at a certain temperature from 16 to 25 °C, they learn to move towards that growth temperature when exposed to a temperature gradient (Hedgecock & Russell 1975). This preference can be modified, such that if worms are grown at one temperature and then shifted to a different temperature as adults, they will learn to prefer the

new temperature after several hours of feeding at the new temperature (Hedgecock & Russell 1975). Furthermore, worms avoid the growth temperature if they are kept at that temperature in the absence food (Hedgecock & Russell 1975). This work has been replicated and the neural and genetic mechanisms have been studied more recently (Mori & Ohshima 1995, Gomez..Nef 2001, Kimura..Mori 2004, Mohri..Mori 2005, Samuel..Murthy 2003, Kuhara..Mori 2002, Ishihara..Katsura 2002), although there is some controversy (Chi..Samuel 2007). My interpretation of these results is that worms learn to associate food with a specific temperature, and are attracted to a specific temperature because they expect to find food there.

c. Olfactory learning: odor ± food

Worms are innately attracted to certain small water-soluble compounds, such as sodium and chloride, (Ward 1973, Dusenbery 1974, Bargmann & Horvitz 1991) and certain odorants, such as benzaldehyde and isoamyl alcohol (Bargmann..Horvitz 1993). In the second demonstration of associative learning in *C. elegans*, researchers found that worms exposed to an initially attractive odorant for 30-90 minutes in the absence of bacteria became less attracted to the odorant than worms who were simply kept in the absence of bacteria (Colbert & Bargmann 1995, Colbert & Bargmann 1997). The authors called this learning adaptation, though I and others prefer the term olfactory learning. The learning can be specific to the odorant. As an example, training to isoamyl alcohol did not affect chemotaxis to other odorants, such as butanone (Colbert & Bargmann 1995). Olfactory learning has been replicated by others, with the same and additional odorants (Law..van der Kooy 2004, Nuttley..van der Kooy 2002, Atkinson-Leadbeater..van der Kooy 2004, Pereira & van der Kooy 2012, Morrison..van der Kooy 1999).

Researchers have also shown that the presence of food enhances the attractiveness of a simultaneously presented odor (Torayama..Katsura 2007). So the presence of food can function as a positive, or appetitive, unconditioned stimulus, while the absence of food can function as a negative, or aversive, unconditioned stimulus, when paired with an odorant. Nicotine has also been used as a positive US in the absence of food (Sellings..van der Kooy 2013).

d. Gustatory learning: water-soluble molecules ± food

In addition to using odorants as a conditioned stimulus (CS), researchers have shown that water-soluble molecules can also serves as the CS in *C. elegans* associative learning. This was first demonstrated using sodium chloride as the CS, and the protocol was similar to that for olfactory learning. Worms were kept in the presence of the ion and the absence of food, and this reduced the worm's attraction to the ion when compared with worms that were just kept in the absence of food (Saeki..Iino 2001). In this case, the conditioning is not very specific to sodium chloride but generalizes to other soluble molecules (Saeki..Iino 2001). The conditioning took multiple hours of CS-US co-presentation to achieve maximal effect (Saeki..Iino 2001), though it can be as short as 15 minutes under alternative assay conditions (Hukema..Jansen 2006). Researchers have replicated these findings and are actively dissecting the mechanism that controls salt chemotaxis learning (Tomioka..Iino 2006, Hukema..Jansen 2006, Ikeda..Iino 2008, Kano..Maricq 2008, Oda..Iino 2011, Beets..Schoofs 2012). In fact, it appears that worms learn to be attracted to the specific concentration of salt that is present during growth, similar to thermotaxis (Kunitomo..Iino 2013). Additionally, garlic has been used to condition the response to sodium and chloride ions instead of the absence of food (Wen..van der Kooy 1997).

Salt can also be used as the CS for appetitive learning, with food paired to increase the attraction of sodium or chloride ions (Wen..van der Kooy 1997).

e. Food learning: bacterial odor + sickness

This example of associative learning is perhaps the most ecologically realistic. Similar to aversive gustatory learning exhibited by mammals where food that later makes one sick is avoided, worms can learn to avoid species of bacteria that will make them sick and eventually kill them (Zhang..Bargmann 2005, Pujol..Ewbank 2001). Worms must be exposed to the pathogenic bacteria for at least 4 hours before learning to avoid the smell of the bacteria (Zhang..Bargmann 2005). The bacteria must be toxic: if it is mutated to be harmless, the worms do not learn to avoid them (Zhang..Bargmann 2005). The avoidance of pathogenic bacteria is an active area of research and has been replicated many times (Pradel..Ewbank 2007, Reddy..Kim 2009, Chang..Kim 2011).

This conditioning paradigm is complex because there are several stimuli driving behavior in opposite ways. Pathogenic bacteria are initially attractive to worms because it functions as food and provides a low-oxygen environment, which the worms prefer over the surrounding bacteria-free environment of higher oxygen (Reddy..Kim 2011, Gray..Bargmann 2004). The pathogenic bacteria are also aversive, because it is an area of higher carbon dioxide concentration and it eventually causes intestinal sickness. So although this paradigm is ecologically realistic, I find it difficult to study rigorously because the stimuli are entangled with each other and therefore difficult to isolate.

f. Protocols most similar to delay and trace conditioning

All 4 protocols for associative learning described above require minutes to hours of co-exposure of the CS and US. Of the types of learning previously described (Figure 3.1), they seem most similar to contextual conditioning, as the CS and US are present continuously during the training period. These protocols are certainly unlike delay and trace conditioning, the kinds of learning associated with awareness in humans and therefore my primary interest. I will describe my efforts to develop a delay/trace conditioning assay below, but a closer reading of the existing literature revealed that 2 groups have described assays similar to delay/trace conditioning.

In both cases, the researchers used a dunking protocol. In the first case, worms were trained to avoid sodium or chloride ions by dunking the worms in the CS+ (either sodium or chloride) solution (10 s) followed by dunking them in an aversive copper sulfate (US) solution (2 s), removing the worms to water for 1 minute, then dunking the worms in the CS- (chloride or sodium) solution (10 s) followed by dunking in water (2 s). Worms were kept in water for 1 min between trials. After six of these trials, worms were tested for the time it took to leave a spot of CS+ compared to the time it took to leave a spot of CS-, and it was found that worms left the CS+ more quickly than after US-only training and left the CS- more slowly than after US-only training (Wen..van der Kooy 1997). This exposure protocol might constitute delay conditioning or trace conditioning with 0 seconds between the end of the CS and beginning of the US. However, this experiment is not as clean as using sound or an air puff as stimuli, because the chemicals likely persist after dunking causing their exposure to overlap with the next stimulus. This concern is alleviated by the fact that learning was specific to the CS+ and not the CS-, so chemical persistence is likely to be short-lived (less than 1 min). Overall, this protocol appears

to be an example of delay conditioning in worms. This experiment has not been replicated by another publication.

In the second case, researchers used a mixture of 1-propanol and hydrochloric acid (HCl) to do simultaneous conditioning (Amano & Maruyama 2011). Worms were briefly (< 1 s) dunked in the mixture and then rested in water for 1-10 min between trials, up to 10 trials. Remarkably, worms learned to reduce their attraction to propanol after as little as 1 trial. In a trace conditioning design, brief exposure to propanol was followed 30 s later by brief exposure to HCl, worms rested for 10 min in water, then the cycle was repeated 5 times. Worms also reduced their attraction to propanol after such training, which resembles trace conditioning. Unexpectedly, it did not matter whether the propanol preceded the HCl, or vice versa. This poses problems to the interpretation that worms were learning that the CS predicted the presence of the US. This assay has not been replicated by another publication.

I was concerned that the chemical stimuli used in these reports of learning might persist despite washing, making it difficult to interpret either of these experiments as bona fide examples of trace conditioning. Therefore, I sought to identify a new assay for delay and trace conditioning.

E. Efforts at Classical Conditioning of *C. elegans*

a. General strategy

I took a structured approach to developing a delay/trace conditioning (temporal conditioning) assay in *C. elegans*. First, I identified all of the temporally-controllable stimuli that were known to elicit behavioral responses in *C. elegans*. These constitute the set of stimuli that I might use in a temporal conditioning experiment. Next, I created an N x N matrix of these

stimuli, where N is the total number of stimuli identified and the rows are CSes and the columns are USes. Any of these stimuli can conceivably be used as either a conditioned stimulus (CS) or an unconditioned stimulus (US) in a learning assay, so a cell in this table defines a unique pair of stimuli to be used for training. The diagonal is greyed out because an associative learning experiment cannot use the same stimulus as both the CS and US. The numbers indicate the experiment that I successfully completed, which will be described below. The matrix is presented as Figure 3.6.

b. Light as an unconditioned stimulus

I began by characterizing the worm's response to light, as a prerequisite before using light as an unconditioned stimulus (US). Ken Miller's lab had previously reported that light was aversive to worms (conference abstract). As I was characterizing the response to light, the first 2 papers documenting the behavioral response and identifying neural and molecular mechanisms were published (Ward..Xu 2008, Edwards..Miller 2008). I successfully replicated the reported avoidance of light, finding that worms reversed when light was shined on a worm's head (Figure 3.7). This response was strongest at the lowest wavelength of light that transmitted through the microscope (Figure 3.7); standard glass severely attenuates light with wavelength less than 350 nm. Additionally, I noticed that the response to light habituated (Figure 3.8), similar to the response to plate tap previously described (p. 53). Longer light exposure caused a stronger reversal response and habituation, so I expected that by reducing light exposure and thereby reducing the strength of the behavioral response, the habituation rate would also be reduced. Unexpectedly, this was not the case: Habituation was complete by trial 20 of light exposure, regardless of duration of light exposure (Figure 3.8). Also notable was that for ½ sec exposure

trials (green line), the first few trials appeared to sensitize the reversal response to light. This response still habituated.

CS \ US	IA AWA, AWC	But AWC^{on}	Pent AWC^{off}	Thia AWA, AWC	Benz AWC	Dia AWA	Pyr AWA	Oct ASH, ADL, AWB	Light on head	Light all over	Air Puff	Plate Tap	Heat laser diode	Electric shock	Electric field	CO_2 BAG	O_2 URX, AQR, PQR
IA	Stim								1		Habit	Habit.				2	
Butanon		Stim							Habit		Habit	Habit					
Pentadio			Stim						Habit		Habit	Habit					
Thiazole				Same stim					Habit.		Habit	Habit.					
Benz.					Stim				Habit.		Habit	Habit.					
Diacetyl						Stim			Habit.		Habit	Habit.					
Pyrazine							Stim		Habit.		Habit	Habit.					
Octanol								Stim	Habit.		Habit	Habit.				3	
Light on head									Same stim		Habit	Habit.	Same resp.			Same resp.	
Light all over									Habit.	Same stim	Habit	Habit.					
Air Puff									Habit.		Stim	Habit.					
Plate Tap									Habit.		Habit	Same stim.	Same resp.			Same resp.	
Heat									Habit.		Habit	Habit.	Same stim			Same resp.	
Electric shock									Habit.		Habit	Habit.		Same stim			
Electric field									Habit.		Habit	Habit.			Same stim		
CO_2									Habit.		Habit	Habit.	Same resp.			Same stim	
O_2									Habit.		Habit	Habit.				4	Stim

Figure 3.6: *C. elegans* stimulus matrix for learning

This matrix shows all of the combinations of stimuli I considered for temporal conditioning. Rows are CSes, columns are USes. The diagonal is dark grey because these cells represent the same stimulus being used as the CS and US and were not considered. The CSes and USes tested in experiments are shaded red. Pairs of stimuli are shaded orange and numbered in the order that the experiments were done. Light blue cells indicate that a stimulus habituates, which might not make it function well as a US. Light grey cells indicated that the stimuli generate the same response in naive worms (e.g. reversals), so they were also excluded. Empty white cells indicate pairs that are open for further study. If the sensory neuron is known for a stimulus, it is listed in the top row beneath the stimulus. Abbreviations: IA = isoamyl alcohol, But = butanone, Pent = pentadione, Thia = thiazole, Benz = benzaldehyde, Dia = diacetyl, Pyr = pyrazine, Oct = octanol.

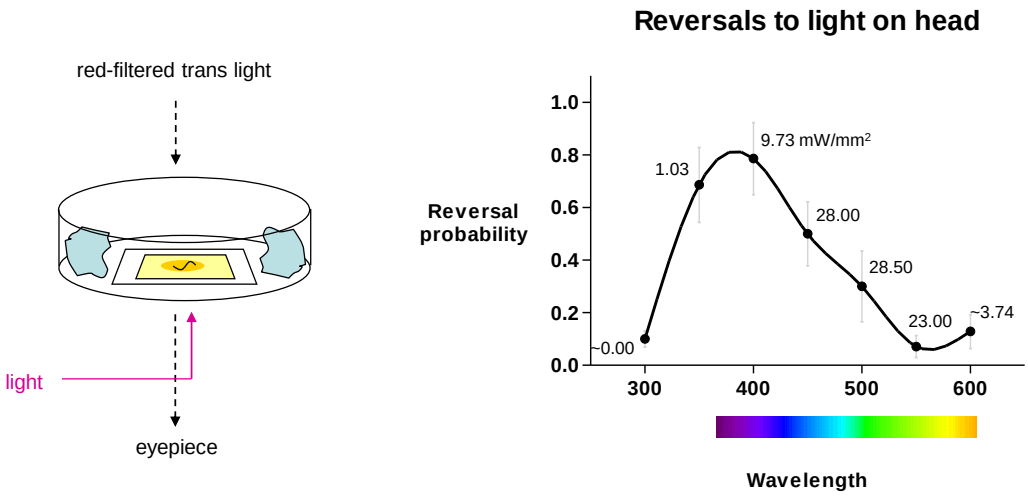

Figure 3.7: Light exposed to the head causes worms to reverse

Left, Experimental setup showing a single worm with bacteria on a thin agar pad on a coverslip. The cylinder surrounding the worm is a Petri dish. The light blue blobs are Kimwipes soaked in water to reduce drying of the pad; these are not necessary. Light of the specified wavelength was generated by a Xenon lamp (Polychrome). The behavioral response was observed via red-filtered transmitted light from a halogen lamp, which did not alter worm behavior.
Right, Fraction of worms that reversed in response to the specified wavelength and power of light. n = 7 worms, 10 trials per worm per wavelength, 1 min inter-trial interval. Each worm was exposed to a different duration of light, from 1/16 sec (no response) to 3 sec. A 40x objective was used. Worms are most sensitive to 350 nm light, as it elicited a response equivalent to that seen with ~10x more power at 400 nm.

While doing these experiments, I noticed that light not only caused reversals but also immediately inhibited worm feeding, as indicated by immediate stopping of the pumping rhythm. This was a novel response that had not been previously reported. This single observation ultimately determined my path forward (Chapter 5 and Chapter 6) after my attempts to condition worms failed.

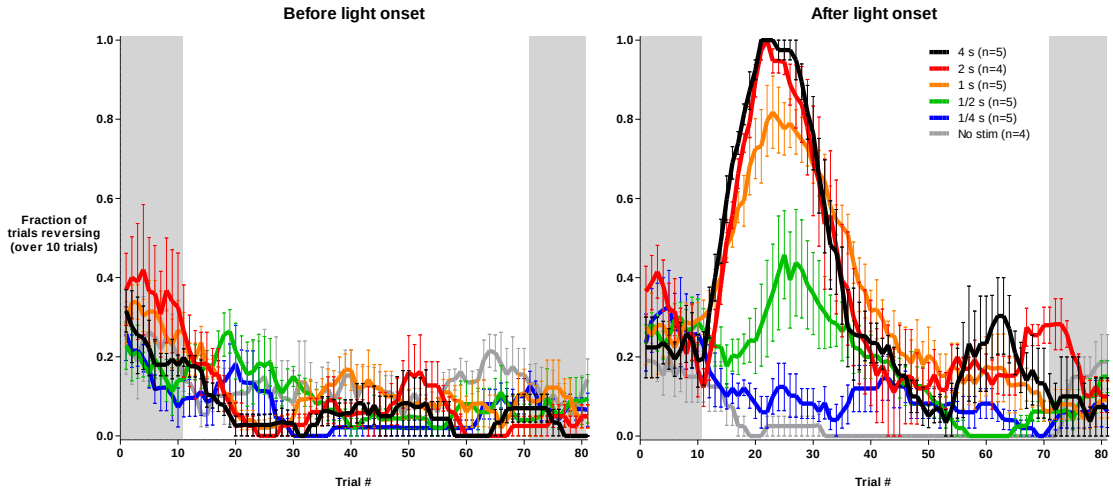

Figure 3.8: Light-induced reversals habituate

Worms stopped responding to light after ~20 trials. The number of trials to complete habituation was duration-independent. Left panel shows reversal fraction in 5 s before light onset, and right panel shows reversal fraction in 5 s after light onset. Light was 400 nm (4 mW/mm^2) with 1 min between trials. Different color lines correspond to different durations of light exposure, as indicated in the legend. Grey shading indicates trials without any light presented. Each point is the average of the preceding 10 trials. n = 4-5 worms per condition.

c. Air flow as an unconditioned stimulus

Short wavelength light appeared to function reliably as an inducer of reversals and held promise as a US. I also observed that a high-flow rate air (1 L/min) reliably induced worm reversals (Figure 3.9). Like with light and plate taps, repeated exposure to air flow resulted in a habituation of the reversal response (Figure 3.10).

The fact that both light and air flow habituated made me concerned that they would not work reliably as a US. If the learning took more than the number of trials before habituation, the US might stop being meaningful to the animal, which could explain why the animal did not learn. Nonetheless, I proceeded with using light as a US because it was convenient to control and did not risk drying out the worms, like the air flow did.

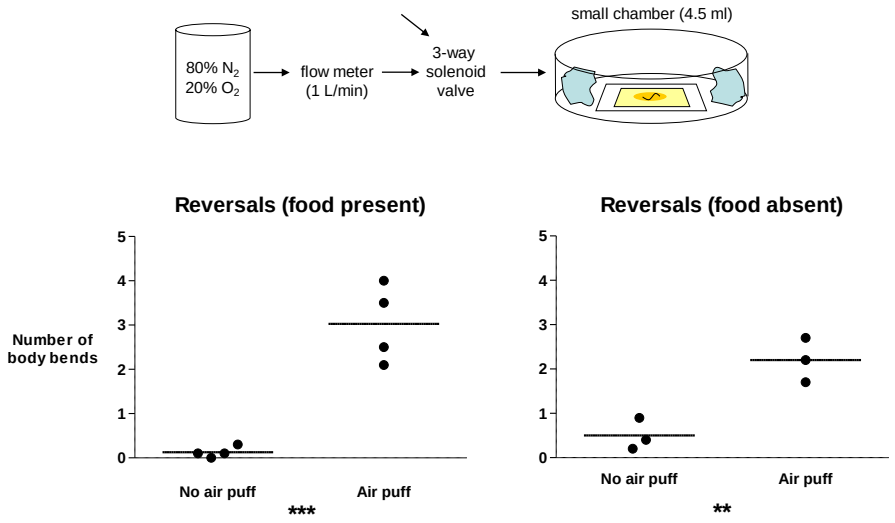

Figure 3.9: Air flow causes worms to reverse

Top, Experimental setup showing a gas tank (Airgas) with room air composition connected to a flow meter (Cole-Parmer) to control flow rate (1 L/min). A computer-controlled solenoid valve (Numatics MPG LS03L6F00B 12 VDC 0.65 W) was used to switch between no air flow and air flow. Custom Matlab software was written to control the solenoid. The headspace of the chamber was minimized to maximize the air flow exposed to the worm.
Bottom, Air flow caused worms to reverse, in the presence (left) or absence (right) of bacteria. n = 3-4 worms, 10 trials per worm per puff condition, 1 min inter-trial interval. *** $p < 0.001$, ** $p < 0.01$, t-test.

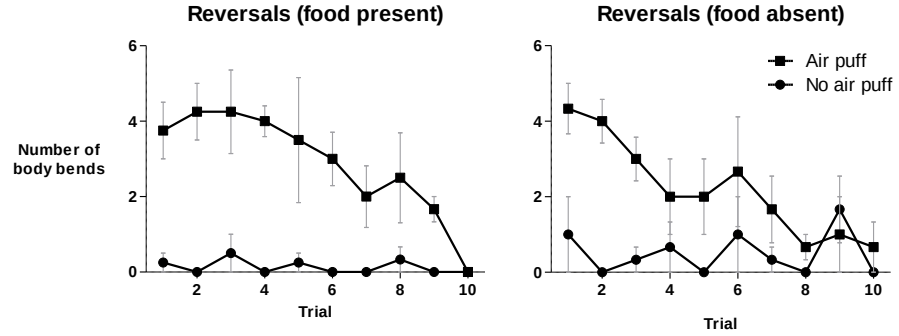

Figure 3.10: Air flow-induced reversals habituate

Worms stopped responding to repeated exposure to air flow after as few as 10 trials. This habituation is not influenced by the presence (left) or absence (right) of bacteria. Plate tap habituation usually occurred after 40 trials (data not shown). n = 3-4 worms, 10 trials per worm, 1 min inter-trial interval.

d. Isoamyl alcohol as a conditioned stimulus

The ideal conditioned stimulus (CS) is one that worms can sense but that on its own does not yield a significant behavioral response, which might interfere with conditioned response. I began my analysis using isoamyl alcohol (IA), which is known to be attractive to the worm (Bargmann..Horvitz 1993). I characterized worms' acute response to IA and found that worms detected 3 minute exposures to IA (Figure 3.11) by modulating their reversal rate (Figure 3.12, Figure 3.13), consistent with previous reports (Chalasani..Bargmann 2007, Luo..Samuel 2008). Specifically, IA slightly inhibited reversals on IA (10^{-3} dilution) onset and increased reversals on removal (10^{-5} to 10^{-3} dilution). I also replicated the effect of IA removal when diluted with mineral oil instead of water (data not shown). This result led me to believe that the worms were able to detect IA under these conditions, and so IA would be suitable as a CS.

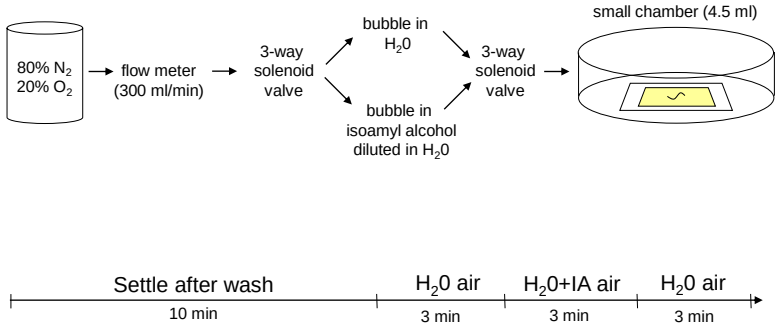

Figure 3.11: Protocol for assessing response to isoamyl alcohol (IA)

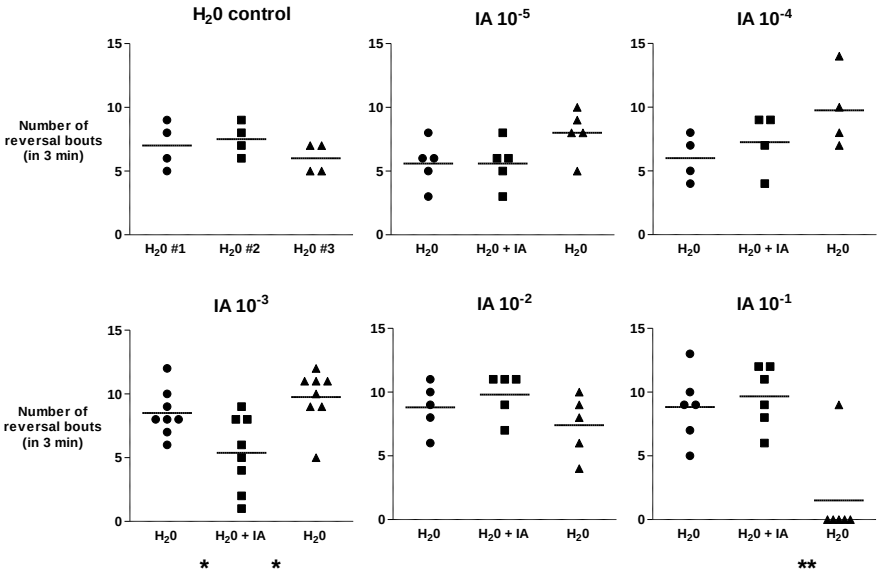

Figure 3.12: Isoamyl alcohol inhibits reversals

Exposure to 10^{-3} IA reduced reversals and removal of IA led to an increase in reversals. Exposure to 10^{-1} IA caused egg-laying and paralysis, which accounted for the reduction in reversals after removal of IA shown in the bottom right panel. Horizontal line indicates mean. ** $p < 0.01$, * $p < 0.05$, t-test.

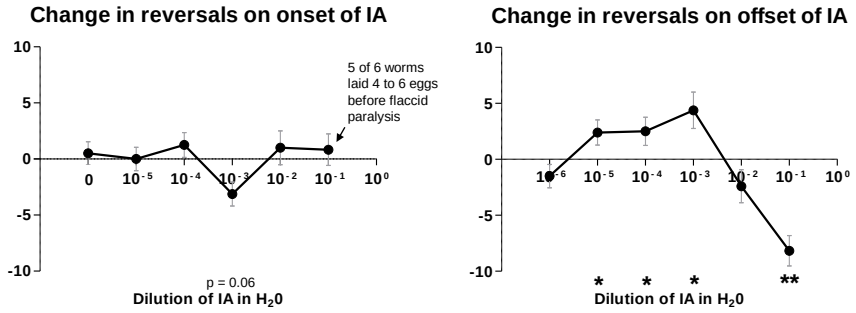

Figure 3.13: Dose response to isoamyl alcohol

Summary of results presented in Figure 3.12. n = 4-8 worms per point. Error bars are s.e.m.

Since temporal conditioning requires repeated pairing of CS and US in order for an association to be learned, I characterized the worm's response to repeated stimulations with

isoamyl alcohol (IA). I found that repeated presentation of IA (10^{-2}) led to an increase in the rate of reversals after IA removal in later trials, while repeated presentation of lower concentration IA (10^{-3}) did not (Figure 3.14). Therefore, IA (10^{-3}) was used as the conditioned stimulus in subsequent experiments. Note that because these experiments were only looking at the reversal rate in the 5 s following IA removal, the results are different than those shown in Figure 3.13 where the reversals were observed over a 3 min time window following IA removal.

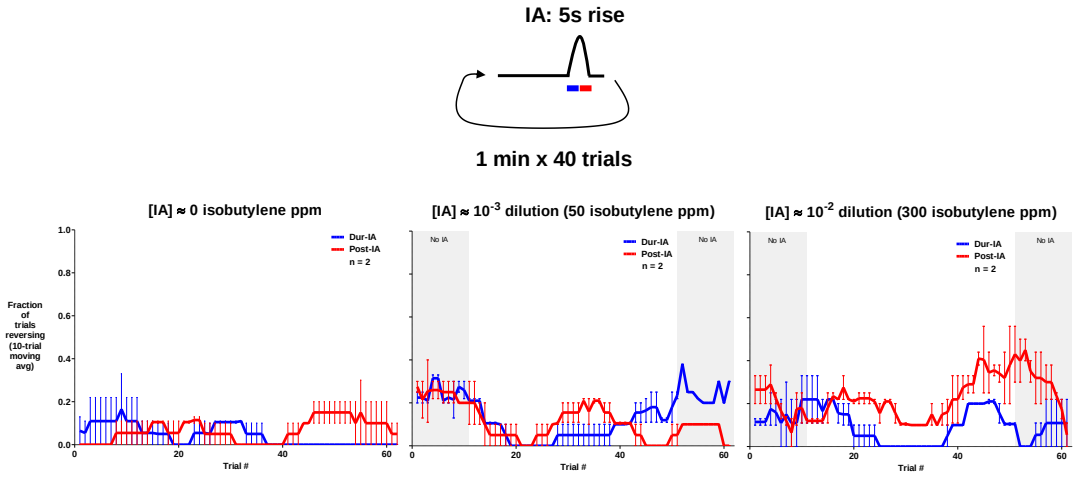

Figure 3.14: Isoamyl alcohol might sensitize its own response

Top, Timing protocol with 5 s of IA repeated 40 times with a 1 min inter-trial interval.
Bottom, Blue lines indicate reversals during the onset of IA. Red lines indicate reversals during the 5 s after IA removal. Increase after trial #40 might indicate sensitization of the response to IA. Gray bars indicate trials without IA exposure. Butylene ppm equivalents measured using photoionization detector (Photovac 2020ComboPro) and were used to confirm that odor was physically reaching the worm. Error bars are s.e.m.

e. Isoamyl alcohol paired with light

Having characterized the worm's response to isoamyl alcohol and light, I tested whether worms could learn that the smell of IA predicted the light (Figure 3.15). I tested several worms using a 5 s pulse of IA (10^{-3}) as the CS and a 2 s pulse of light (400 nm, 4 mW/mm^2) as the US (Figure 3.16). I also systematically varied the inter-trial interval (ITI), which is known to determine the duration of the associative memory that is formed (Figure 3.17). However, after

examining 7 worms, I did not observe any evidence of learning. If the worms were learning, I would expect to see an increase in the reversal rate in response to IA on later trials, which I did not observe.

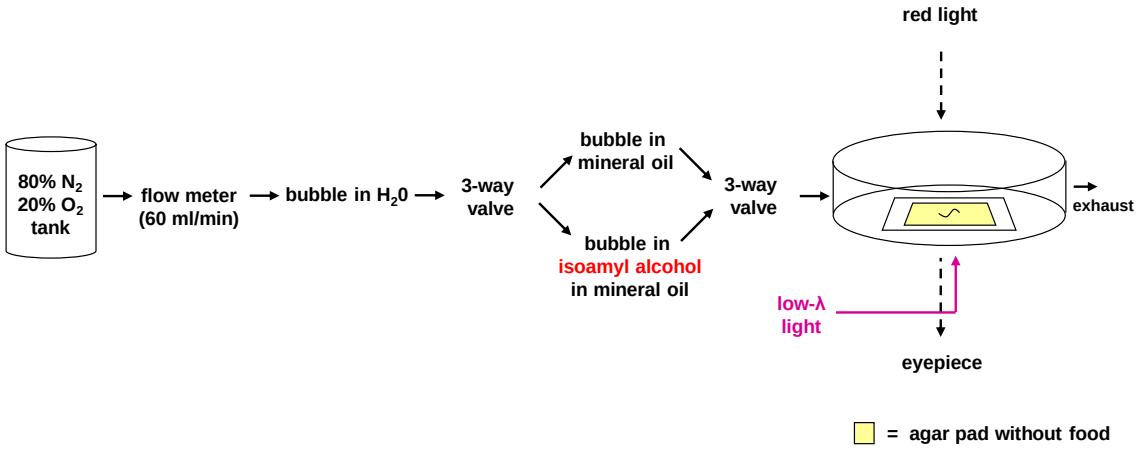

Figure 3.15: Experimental design for single-worm odor + light conditioning

The worms may not have learned for several reasons. First, it was possible that under these conditions a 5 s pulse of IA was not sensed by the worm. This could be addressed by imaging the AWC sensory neuron that senses IA and confirming that it responds (Chalasani..Bargmann 2007). Additionally, one could vary the duration of the IA pulse before light onset; I only tested a 5 s pulse, but perhaps it would be worth testing longer pulses to guarantee that the worms were sensing the IA. Second, it might take more than 5 s for the worm to exhibit a learned response to IA, so there might be a learned response that is being masked by the presentation of light. This concern could be addressed by measuring learning using probe trials that lacked light presentation, rather than relying on precession of the response. I use probe trials in subsequent experiments. Third, the response to light might habituate too quickly to support learning. One could try a different US from the matrix which doesn't habituate. I will

show that I found that the response to CO_2 does not habituate, so CO_2 may make a better US than light (p. 78). Alternatively, I could try conditioning habituation defective mutants, such as *hab-1*. A fourth and final reason that might explain why the worms did not learn is that the worms can't learn an association between this specific pair of stimuli, isoamyl alcohol and light). In subsequent experiments I try different pairs of stimuli.

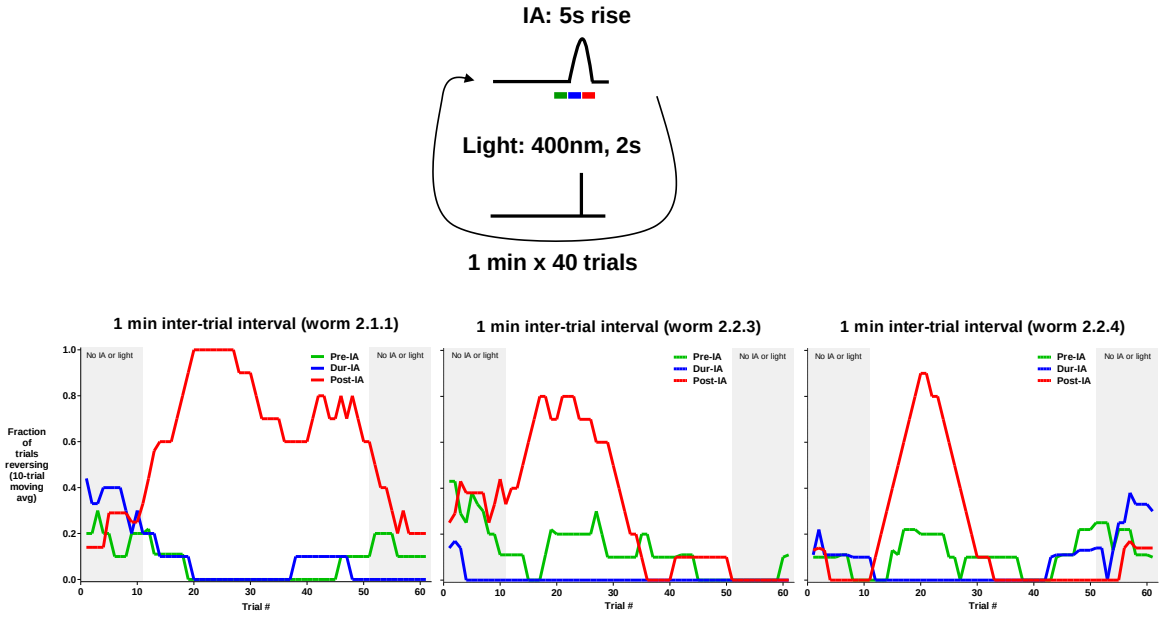

Figure 3.16: Worms fail to learn to associate isoamyl alcohol with light

Top, Delay conditioning protocol with worms exposed to 5 s of IA (10^{-3}) coterminating with 2 s of light (400 nm, 4 mW/mm^2) to the head. Colored lines below IA trace correspond to the timing of observation for the curves in the bottom portion of the figure.
Bottom, Reversal response observed during different periods of the experiment. Each chart is the response of a single worm. Green line indicates reversals in the 5 s before IA onset, blue line indicates reversals in the 5 s during IA exposure, and red line indicates reversals in 5 s after light onset. Lines are a 10-trial moving average. All worms robustly responded to light. No worms showed a substantial increase in the blue line, which would have indicated learning. The first worm showed partial habituation to light, while the second and third worms showed complete habituation. Grey shading indicates control trials without any stimulus.

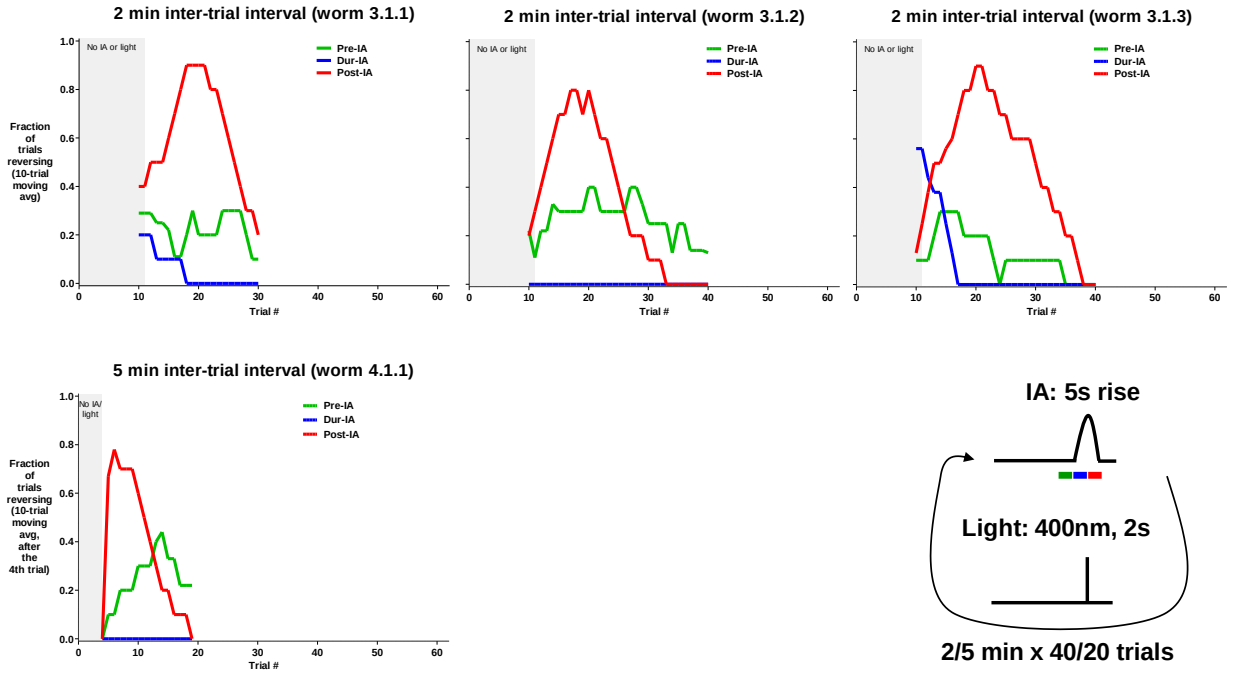

Figure 3.17: Longer inter-trial intervals do not cause learning

Increasing the ITI from 1 min (Figure 3.16) to 2 or 5 min did not induce learning. All 4 animals show clear habituation to light. Lines and shading as described in Figure 3.16.

The single-worm assay was tedious and inefficient, as I could only collect one data series during each experiment. I designed and implemented a multi-worm tracker (called WormWatcher) that recorded videos of worm locomotion and extracted the locomotion of a population of worms, providing hundreds of data series per experiment rather than just one. This software is described in detail in Chapter 8.

f. Isoamyl alcohol as a conditioned stimulus (wormtracker)

Using my new wormtracker (Chapter 8), I reassessed the response of worms to isoamyl alcohol, using an experimental setup shown in Figure 3.18. Unexpectedly, the wormtracker observed that worms responded to the odor of mineral oil (Figure 3.19), the dilutant I used in

previous single-worm isoamyl alcohol (IA) conditioning experiments. Since worms responded to mineral oil in the absence of IA, I sought to assess whether worms responded to another dilutant, water. In fact, worms showed little to no response to air bubbled in water (Figure 3.20). Therefore, I used water in subsequent experiments as the dilutant for odorants including IA.

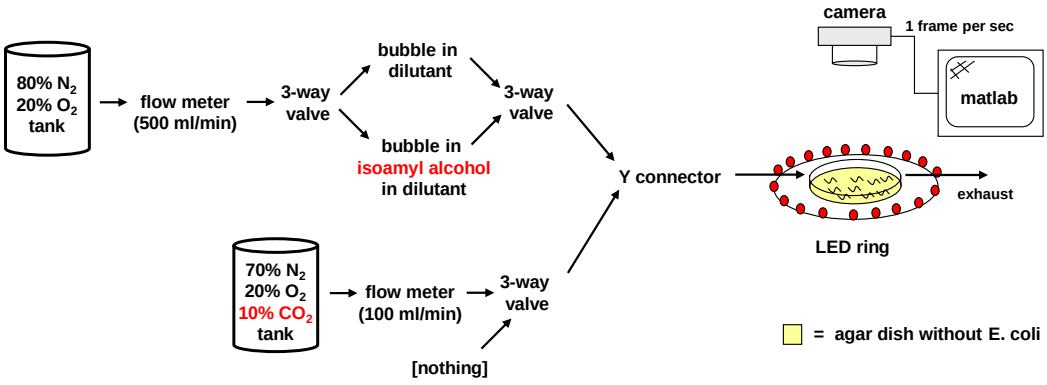

Figure 3.18: Experimental design for recording the locomotion of worms in response to various stimuli

Worms reliably accelerated in response to 1 s of IA (10^{-4}) diluted in water (Figure 3.21). Removal of IA caused a reduction in worm speed. I tested various concentrations and durations of IA to identify one most suitable for use as a CS. Higher concentrations, up to 10^{-2}, resulted in more reliable and larger accelerations (Figure 3.22, Figure 3.23). Speed remained elevated for the first 10 s of IA, after which it declined even in the continuing presence of IA (Figure 3.24, Figure 3.25).

The effect of varying IA concentration and duration on the worm's locomotion speed is summarized in Figure 3.26 and Figure 3.27.

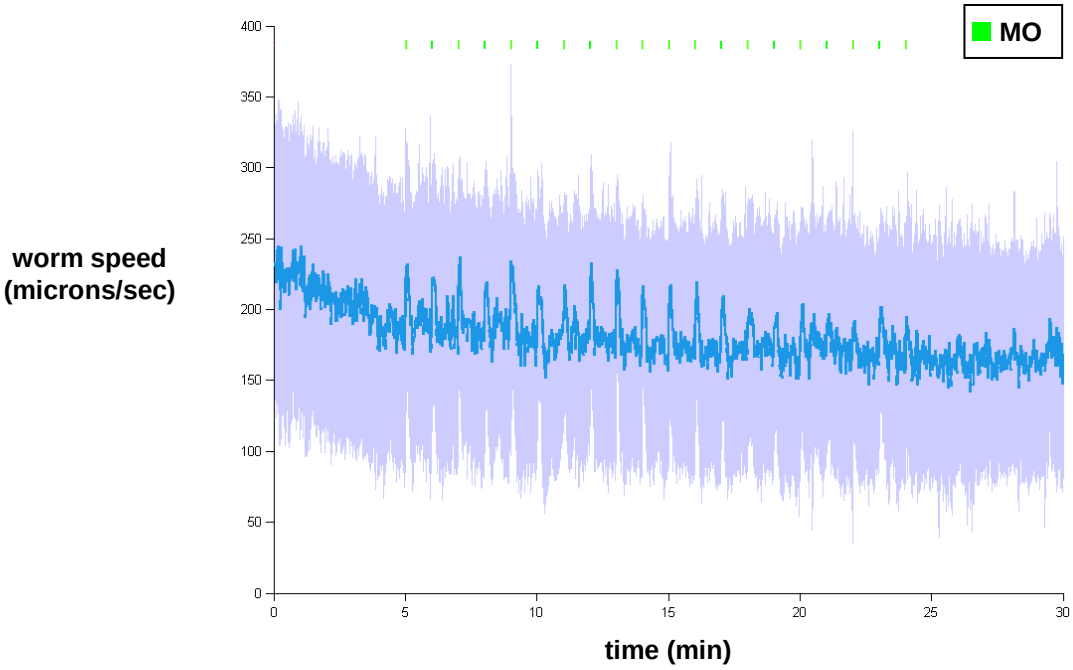

Figure 3.19: Mineral oil odor causes worms to accelerate

Worms increased their speed after exposure to 1s of undiluted mineral oil odor (green lines). When not being exposed to mineral oil odor, worms were exposed to the same flow rate of air. n = 55-133 worms, 500 ml/min flow rate, 20 trials, 1 min ITI, no bacteria present. Error shading is s.d.

The experiments using the wormtracker to asses the worm's response to isoamyl alcohol were conducted in the absence of bacteria. The presence or absence of bacteria may influence the worm's ability to learn. One might speculate that in the absence of bacteria, worms might be so focused on finding bacteria that they ignore novel stimuli that they encounter. Alternatively, one might speculate that in the presence of bacteria, worms might be so content feeding that they ignore novel stimuli that they encounter. To prepare for either case, I measured the worm's response to IA in the presence of food. Interestingly, worms exhibited acute slowing while in the presence of food (Figure 3.28), the opposite response than was observed in the absence of food.

After the studying the worm's behavioral response to isoamyl alcohol, I decided to use 10^{-4} dilution in water with durations of less than 10 s as a conditioned stimulus in learning experiments.

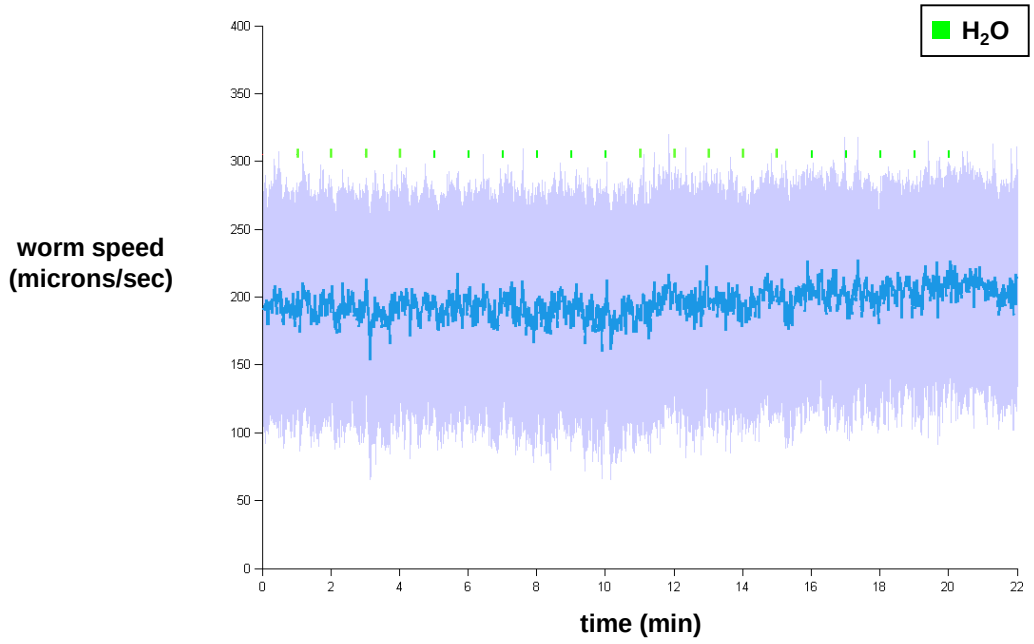

Figure 3.20: Air bubbled in water does not affect worm locomotion

Worms did not respond to 1s of air bubbled in water (green lines). n = 54-161 worms, 500 ml/min flow rate, 20 trials, 1 min ITI, no bacteria present. Error shading is s.d.

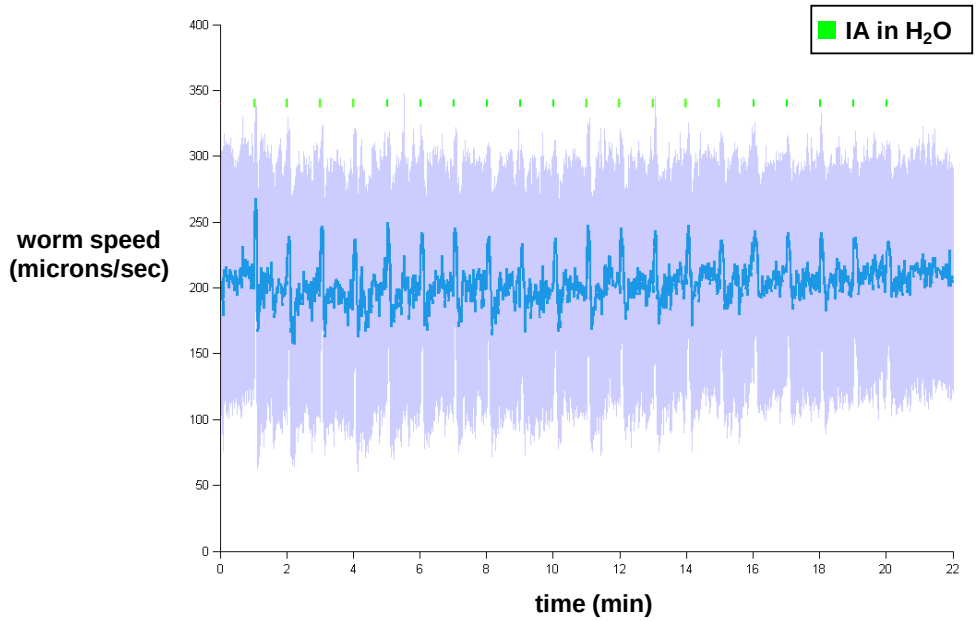

Figure 3.21: Isoamyl alcohol (IA) odor causes worms to accelerate

Worms increased their speed in response to 1 s IA (10^{-4}, green lines) and decreased their speed past baseline in response to removal of IA. n = 177-168, 500 ml/min flow rate, 20 trials, 1 min ITI, no bacteria present. Error shading is s.d.

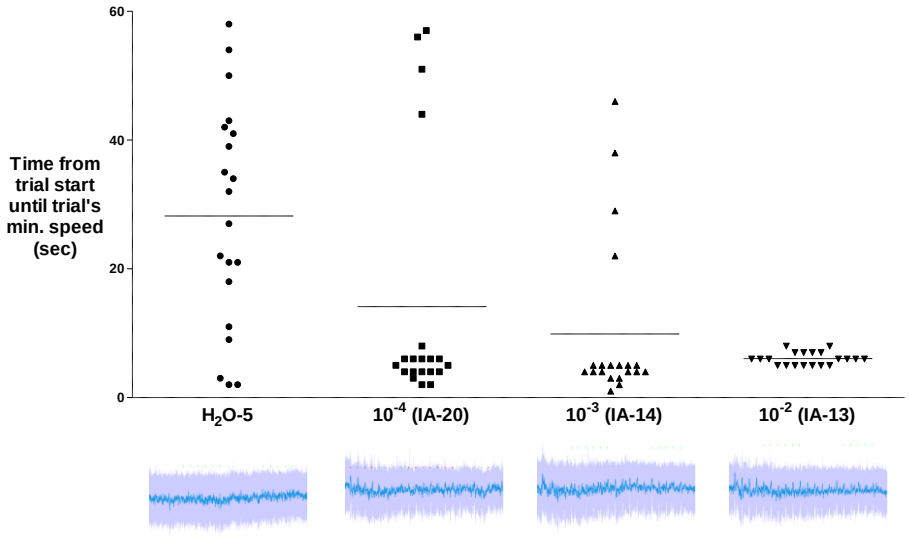

Figure 3.22: Higher concentrations of isoamyl alcohol cause more reliable responses

Reliability was measured as the latency from stimulus onset to minimal speed in the trial. Horizontal line indicates the mean latency. Source traces are shown in the bottom row. 500 ml/min flow rate, 20 trials, 1 min ITI, no bacteria present. Error shading is s.d.

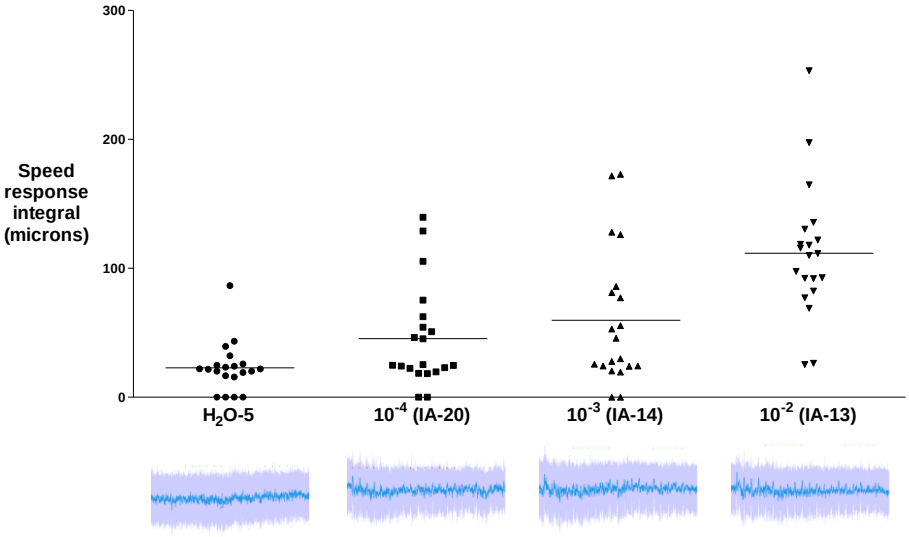

Figure 3.23: Higher concentrations of isoamyl alcohol cause larger accelerations

Accelerations were measured by the taking integral of the odor-induced speed increase. Horizontal lines indicate the mean integral. Source traces are shown in the bottom row. 500 ml/min flow rate, 20 trials, 1 min ITI, no bacteria present. Error shading is s.d.

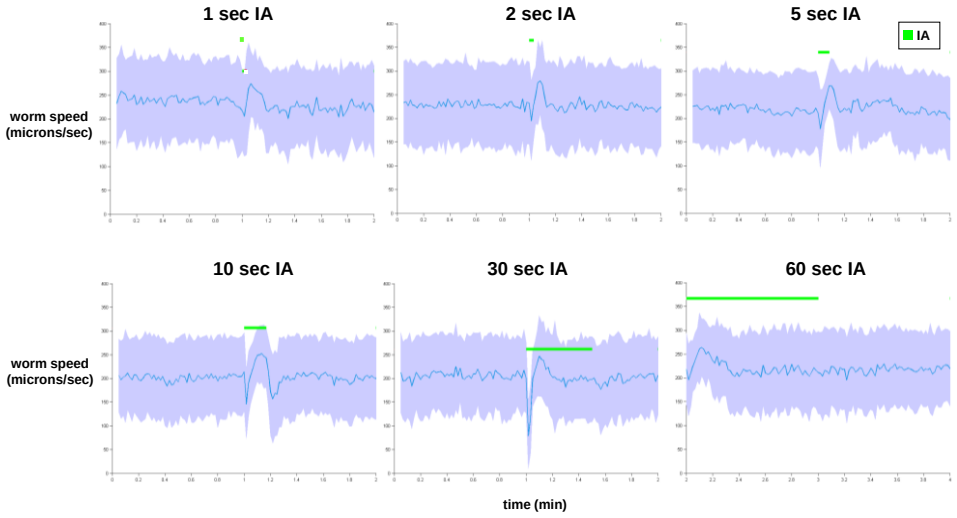

Figure 3.24: Prolonged isoamyl alcohol exposure causes worms to return to baseline speed

Worms reduces their response to IA (10^{-4}) after prolonged exposure. 500 ml/min flow rate, no bacteria present. Error shading is s.d.

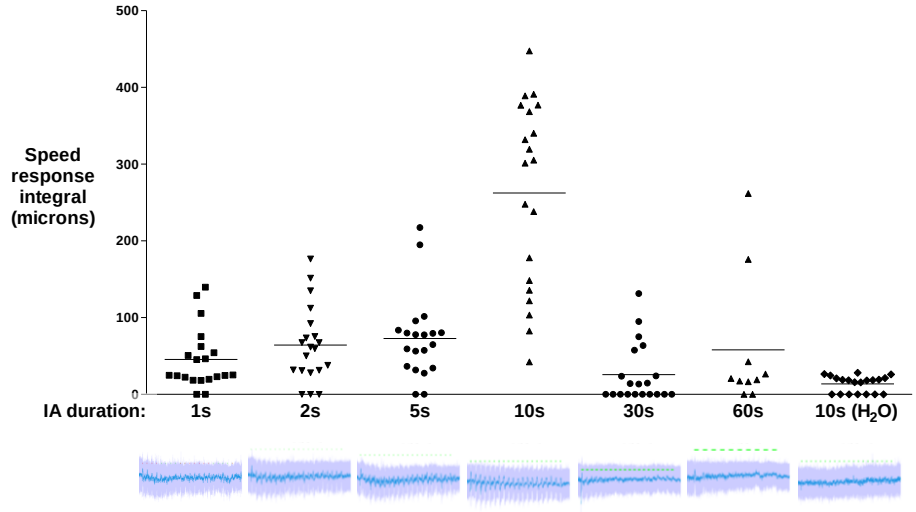

Figure 3.25: Repeated presentation of varying durations of isoamyl alcohol

Worms responded most strongly to 10 s of IA (10^{-4}). Horizontal lines indicate the mean integral. Source traces are shown in the bottom row. 500 ml/min flow rate, 10-20 trials, 1-2 min ITI, no bacteria present. Error shading is s.d.

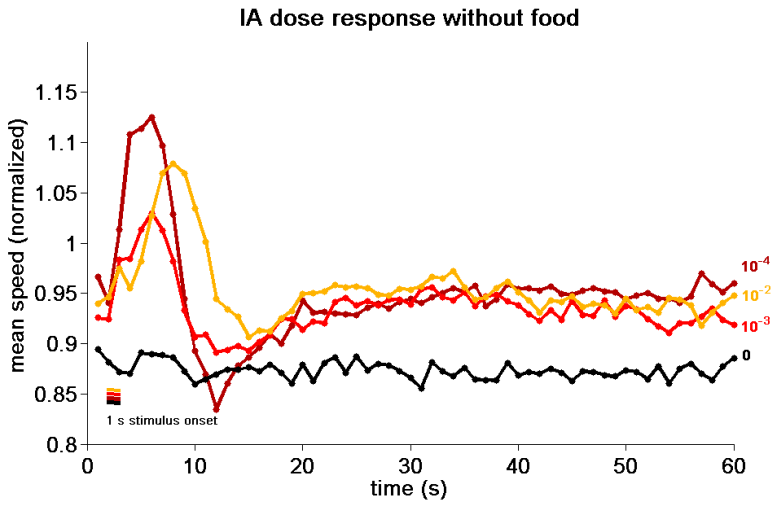

Figure 3.26: Dose response to isoamyl alcohol

Worm response to varying concentrations of 1s of IA, normalized to the worm's speed before the first stimulus exposure. Each curve is the average of 20 trials from one experiment like that shown in Figure 3.21.

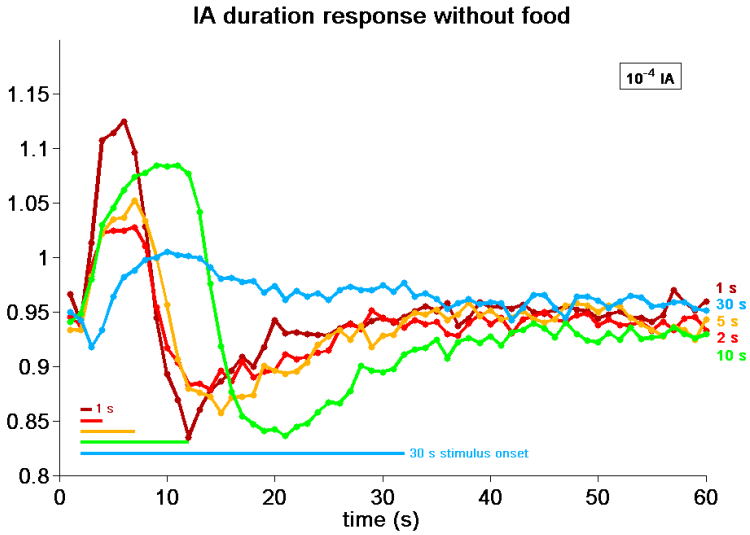

Figure 3.27: Duration response to isoamyl alcohol

Worm response to varying durations of IA (10^{-4}), normalized to the worm's speed before the first stimulus exposure. Each curve is the average of 20 trials from one experiment like that shown in Figure 3.21. Longer durations resulted in an amplitude decrease because the response attenuated over 20 trials, whereas the response to shorter durations did not.

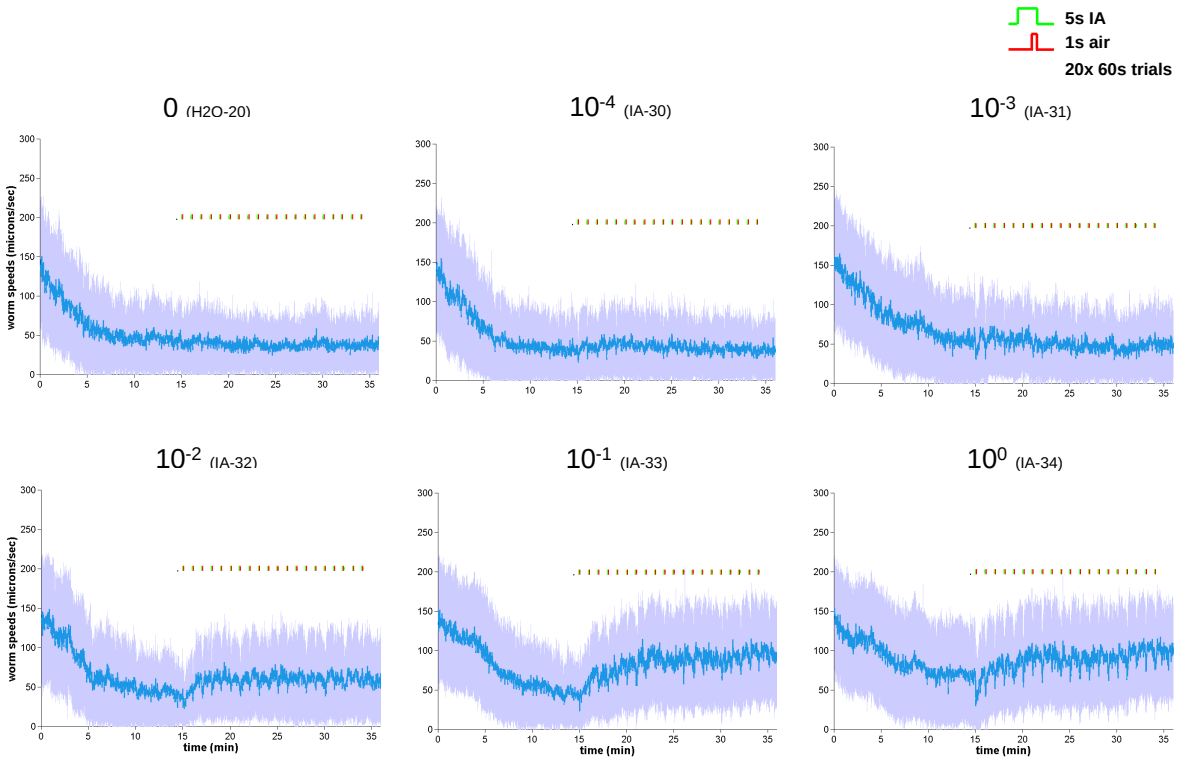

Figure 3.28: Isoamyl alcohol causes worms to slow on food

Worms slowed in response to 5 s of IA (green lines) coterminating with a control 1 s air increase (red lines, 100 ml/min). 500 ml/min air flow, 20 trials, 1 min ITI, bacteria present. Error shading is s.d.

g. Carbon dioxide as an unconditioned stimulus

Repeated presentation of light and air flow led to habituation, which might interfere with the worm's ability to learn. Carbon dioxide (CO_2) causes an avoidance response similar to light (Hallem & Sternberg 2008), and Niels Ringstad, a former postdoc in our lab, discovered a physiological response to CO_2 in the BAG neuron (Hallem..Ringstad 2011). Equipped with CO_2 tanks, I measured the worm's response to CO_2 using the wormtracker to assess whether it was suitable as an unconditioned stimulus in learning experiments.

Worms responded to CO_2 by slowing (Figure 3.29) and unlike the response to light, the response to CO_2 did not habituate after 30 trials (Figure 3.30). Moreover, worms have jerky

forward-backward movement in response to CO_2 (Figure 3.31). Closer examination by eye showed that CO_2 paralyzed worms through a wave of body muscle contraction that travelled from the tail to the mid-body and later from the mid-body to the head. This was reflected in the change in worm size measured by the tracker (Figure 3.32). CO_2 response latency was dependent on flow rate (Figure 3.33) but not CO_2 duration (data not shown). CO_2 response amplitude was partially dependent on flow rate (Figure 3.34) but not CO_2 duration (data not shown).

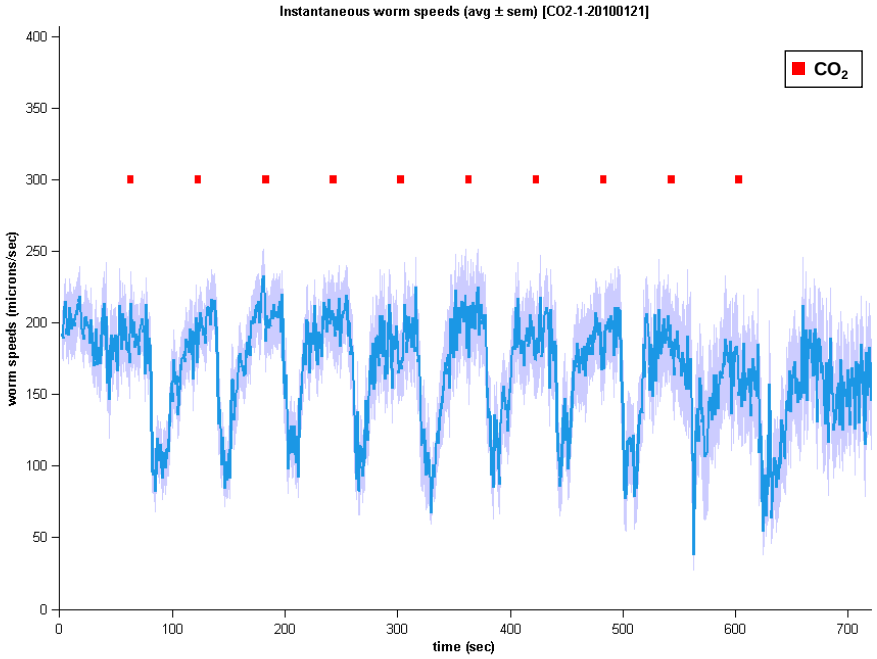

Figure 3.29: Carbon dioxide (CO_2) causes worms to slow

Worms slowed in response to 5 s of CO_2 (10%, red lines). n = 6-23, 50 ml/min flow rate, 10 trials, 1 min ITI, no bacteria present. Error shading is s.e.m.

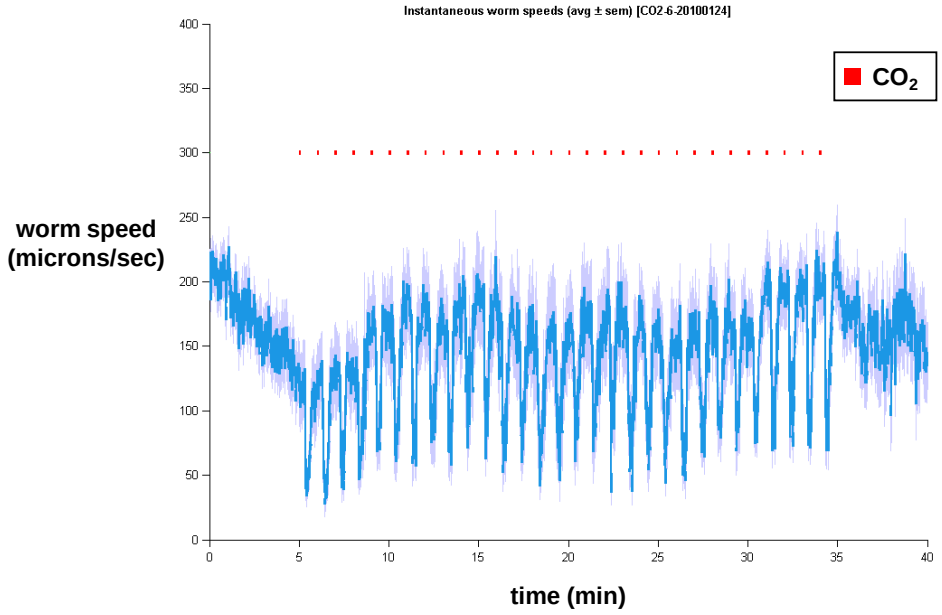

Figure 3.30: CO_2-induced slowing does not habituate

Worms reliably slowed in response to 5 s of CO_2 (10%, red lines). n = 9-53, 60 ml/min flow rate, 30 trials, 1 min ITI, no bacteria present. Error shading is s.e.m.

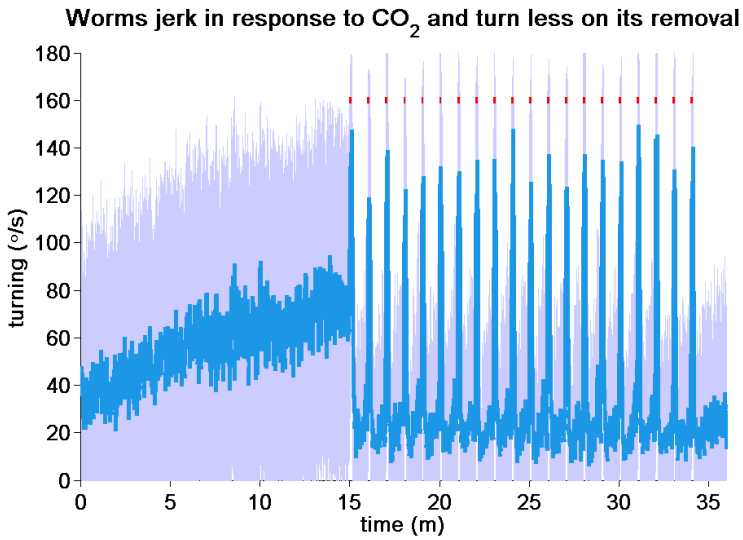

Figure 3.31: CO_2 induces a brief reversal

Worms jerked backwards then forwards in response to 5s of CO_2 (100%, red lines). n = 41-83, 500 ml/min flow rate, 20 trials, 1 min ITI, no bacteria present. Error shading is s.d.

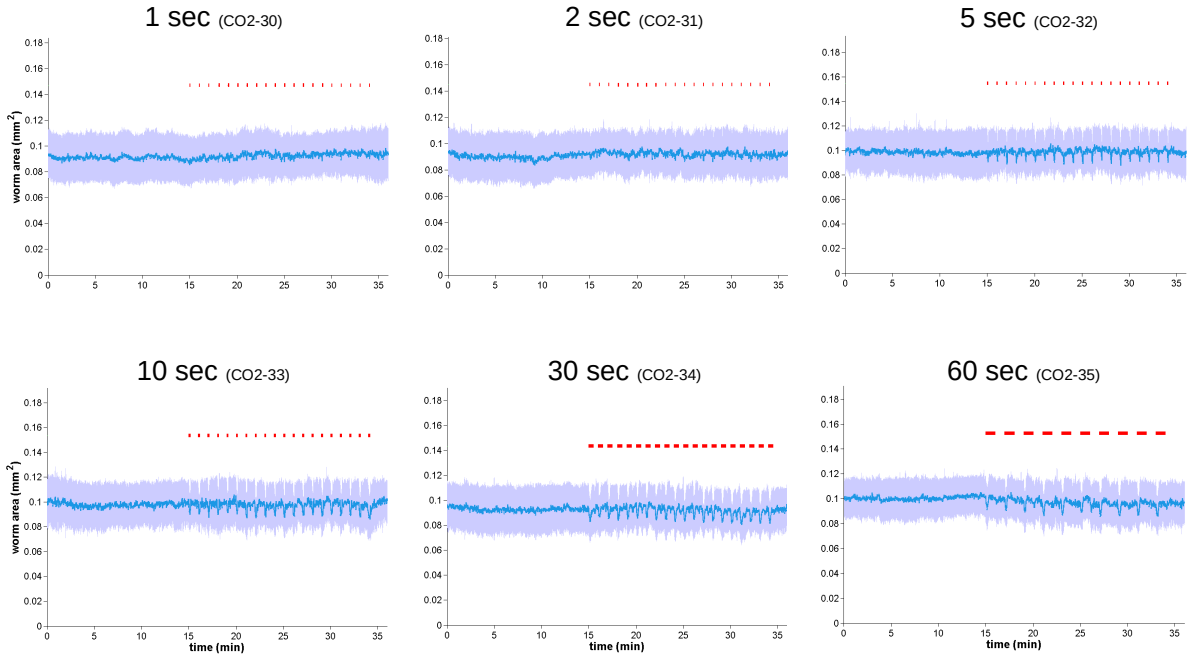

Figure 3.32: CO_2 causes worms to shrink

Worms reduced their projected area in response to varying durations of CO_2 (100%, red lines). 500 ml/min flow rate, 20 trials, 1 min ITI, no bacteria present. Error shading is s.d.

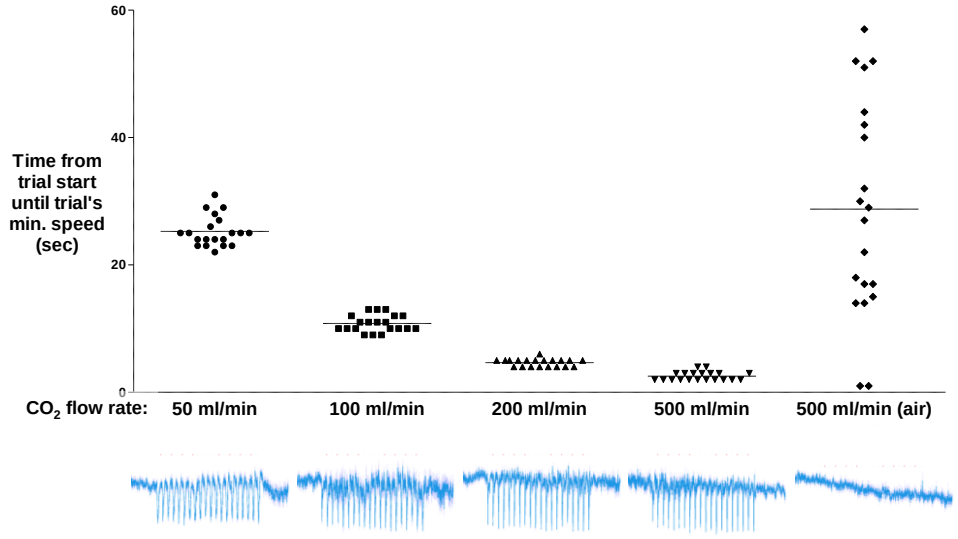

Figure 3.33: Higher flow rate reduces the response latency to CO_2

Worms responded more quickly to 5 s of CO_2 (10%) at higher flow rates. Horizontal lines are means. Source traces are shown in the bottom row. 500 ml/min flow rate, 20 trials, 1 min ITI, no bacteria present. Error shading is s.e.m.

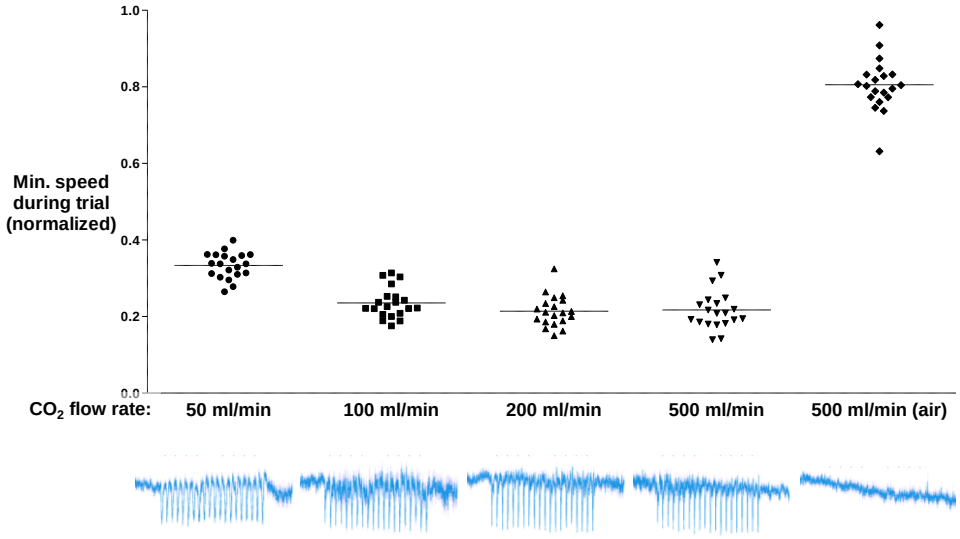

Figure 3.34: Higher flow rate increases the response amplitude to CO_2

Worms responded with a slightly larger response to 5 s of CO_2 (10%) at high flow rates. Lower speed is a larger amplitude. Horizontal lines are means. Source traces are shown in the bottom row. 500 ml/min flow rate, 20 trials, 1 min ITI, no bacteria present. Error shading is s.e.m.

All experiments for CO_2 described were done in the absence of bacteria. Since food is a critical component of the worm's environment, I tested the response to CO_2 in the presence of bacteria. Worms showed a similar slowing in response to CO_2 in the presence of food (Figure 3.35). Additionally, CO_2 increased locomotion speed after its removal, and the worms appeared agitated. This may have also occurred in the absence of food but was masked by a higher baseline speed.

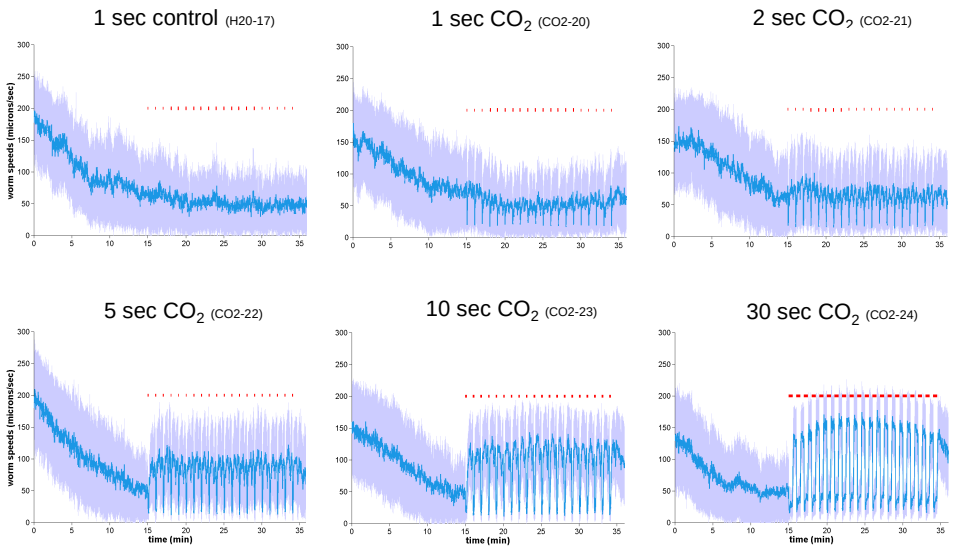

Figure 3.35: CO_2 causes worms to slow and its removal causes worms to accelerate on food

Worms responded to varying durations of CO_2 (17%, red lines) in the presence of food. CO_2 concentration was increased compared to previous experiments because lower concentrations led to weaker responses on food (data not shown).500-600 ml/min flow rate, 20 trials, 1 min ITI. Error shading is s.d.

I tested the response to several additional concentrations of CO_2 in the presence of food. Longer durations of CO_2 (17%) caused slowing followed by acceleration that increased speed to 3x the baseline (Figure 3.36). Similar results were observed for higher concentrations of CO_2 (100%) (data not shown). Worms recovered their baseline speed when exposed to CO_2 for multiple minutes (Figure 3.37). Notably, undiluted CO_2 (100%) caused a secondary response following the primary slowing (Figure 3.38). I speculate that this response is due to synchronization of the defecation cycle, because it appeared that the body contraction induced by CO_2 reset the defecation cycle. Synchronized shrinking due to defecation could conceivably result in a reduction of speed.

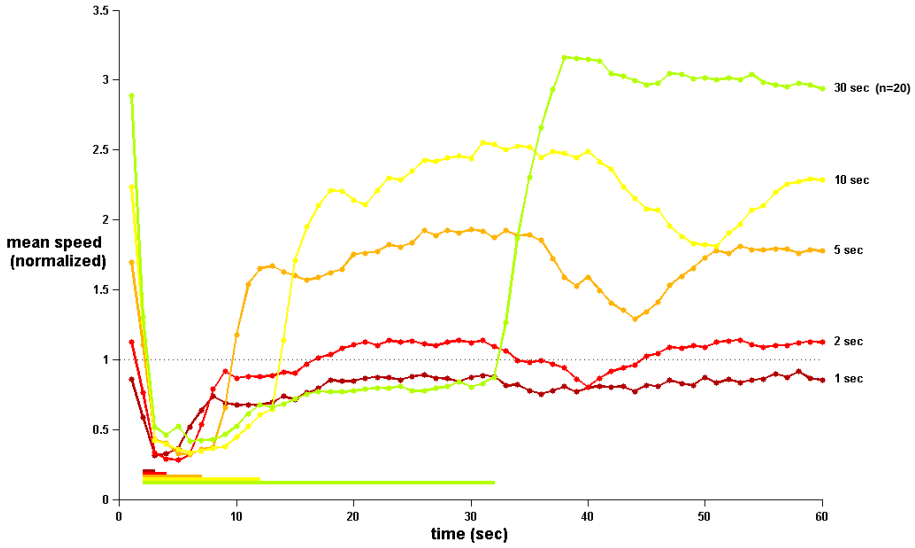

Figure 3.36: Duration response to CO_2 on food

Worm response to varying durations of CO_2 (17%), normalized to the worm's speed before the first stimulus exposure. Each curve is the average of 20 trials from one experiment like that shown in Figure 3.35. Curves with the first timepoint greater than 1 indicate that the stimulus increased the pre-stimulus locomotion speed after the first trial

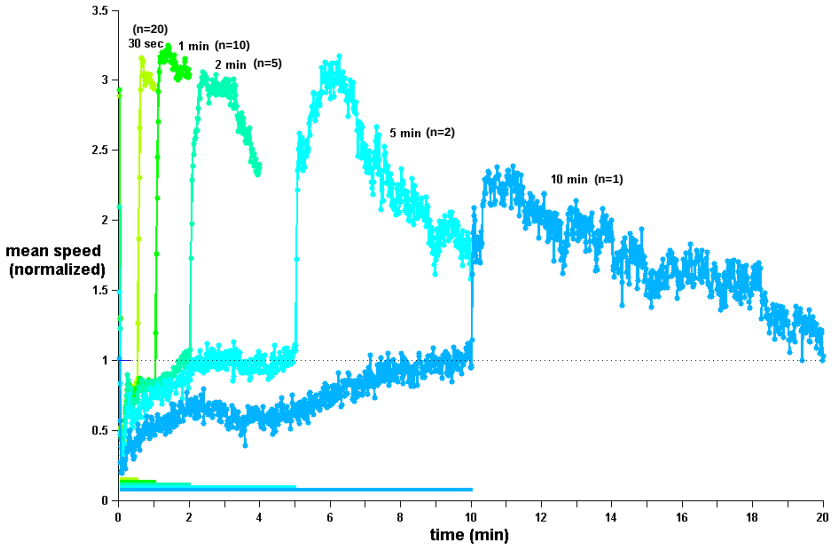

Figure 3.37: Worm recover their speed after minute-scale exposure to CO_2

Worm response to varying durations of CO_2 (17%), normalized to the worm's speed before the first stimulus exposure. Each curve is the average of 20 trials from one experiment like that shown in Figure 3.35. 2 min or longer exposure resulted in a recovery to baseline speeds until CO2 removal, after which speeds rapidly increased.

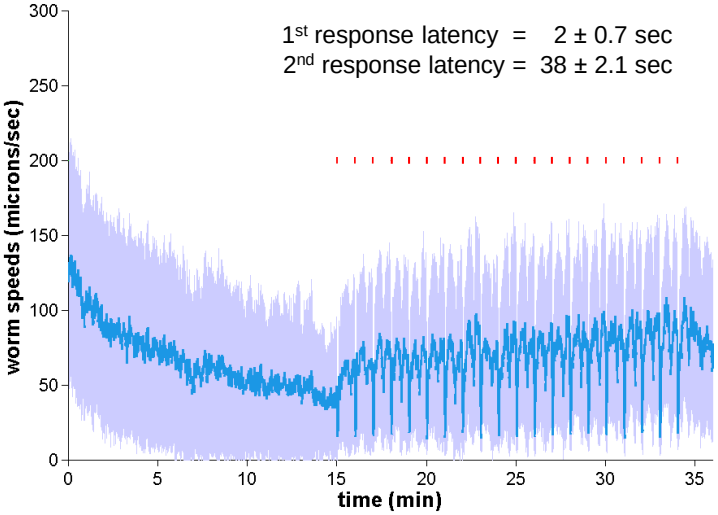

Figure 3.38: Concentrated CO_2 causes a secondary slowing response

Worms showed a secondary slowing 38 s after CO_2 (100%, red lines) presentation. This effect was also observed using lower concentrations of CO_2 (17%). I speculate that this slowing is due to synchronized defecation. 500-600 ml/min flow, 20 trials, 1 min ITI, bacteria present. Error shading is s.d.

While I uncovered a series of unexpected responses to CO_2, the most relevant result for conditioning experiments was that the slowing response to CO_2 did not habituate after repeated CO_2 exposure.

h. Isoamyl alcohol paired with carbon dioxide

Worms were exposed to isoamyl alcohol (10^{-4}, 3 s) with carbon dioxide (2%, 1 s) in a delay conditioning paradigm. After 20 trials of pairing, I failed to see any new response to probe trials of IA alone; the worms continued to show weak accelerations, which is the same response as naive worms (Figure 3.39). Varying the inter-trial interval (ITI) also had no effect (Figure 3.40). Increasing the number of trials also had no effect (Figure 3.41).

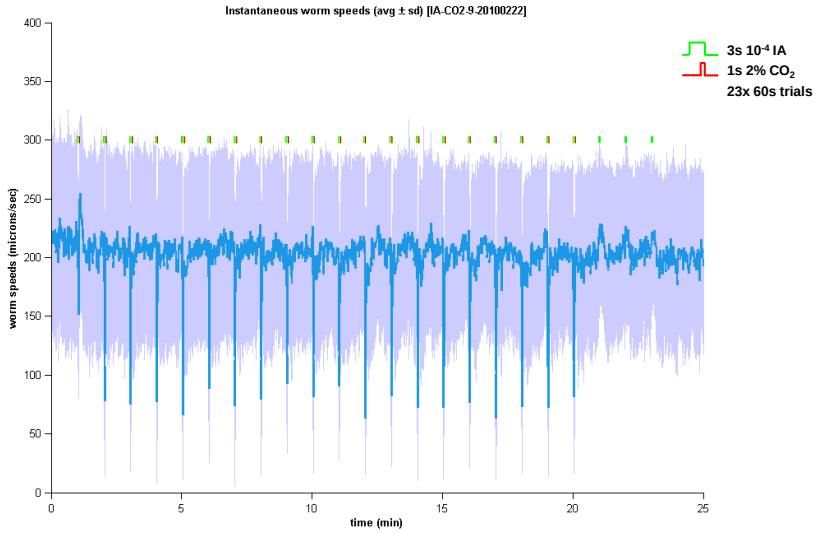

Figure 3.39: Delay conditioning with isoamyl alcohol and CO_2 fails to induce learning

Worms were exposed to a delay conditioning protocol of 3s of IA (10^{-4}, green lines) coterminating with 1 s of CO_2 (2%, red lines), as diagrammed in the upper right corner. Training was followed by 3 probe trials where IA was presented alone. Worms responded to IA alone with a brief acceleration similar to the response of naive worms (Figure 3.21). 500-600 ml/min flow, 20 training trials, 1 min ITI, no bacteria present. Error shading is s.d.

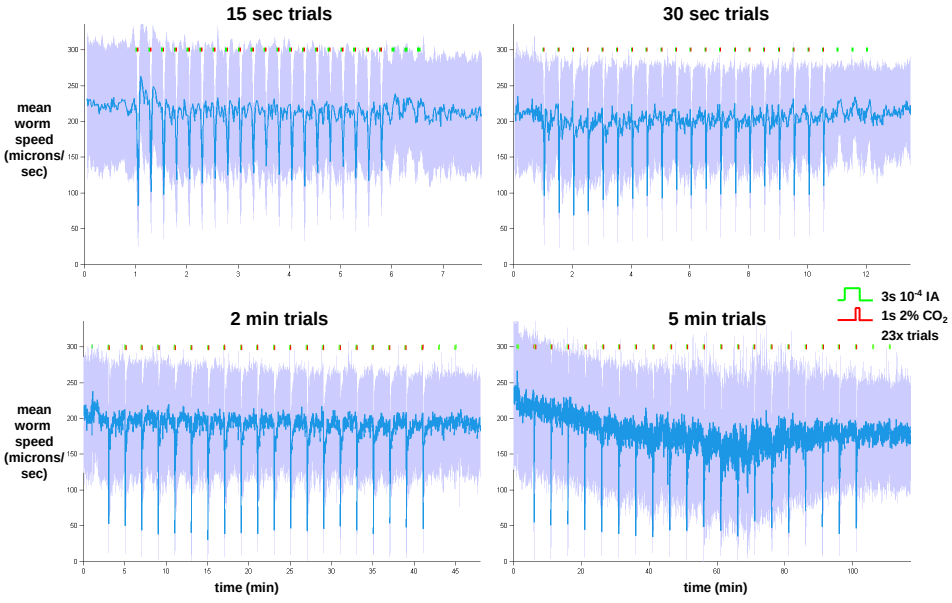

Figure 3.40: Varying the inter-trial interval (ITI) does not cause learning

Worms were exposed to the same protocol as in Figure 3.39 but with shorter or longer ITIs. Worms still failed to show an altered response to probe trials. Error shading is s.d.

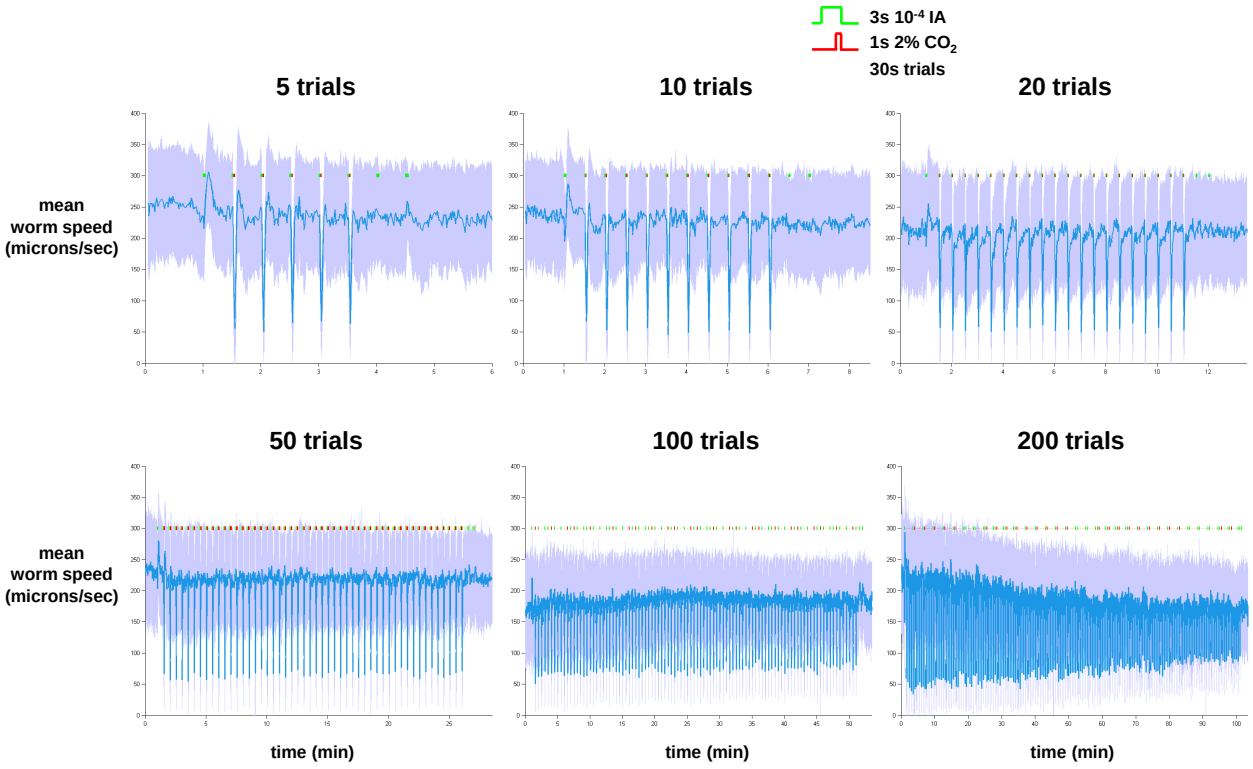

Figure 3.41: Varying the number of trials does not cause learning

Worms were exposed to the same protocol as in Figure 3.39 but with varying number of trials and a 30 s ITI. Worms still failed to show an altered response to probe trials. Error shading is s.d.

I next exposed worms to a trace conditioning protocol, with trace intervals of either 0 s or 1 s. Again, no learning was observed (Figure 3.42). In addition to not altering their acute response to IA, worms also failed to change their preference for IA as assayed by chemotaxis (data not shown).

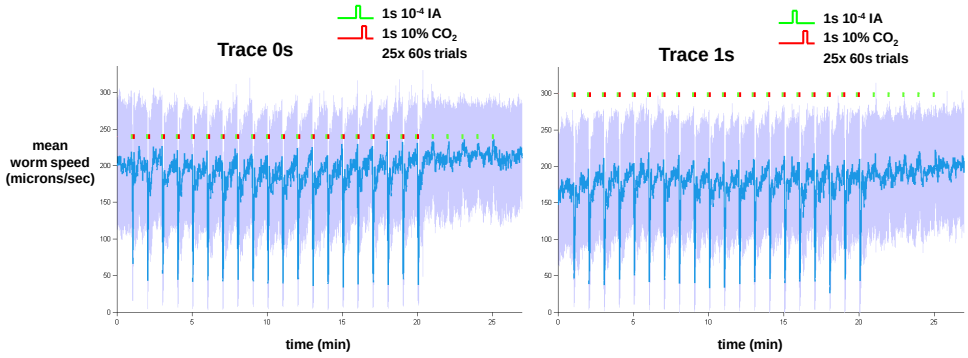

Figure 3.42: Trace conditioning with IA and CO_2 failed to elicit learning

Worms were exposed to a trace conditioning protocol of 1 s of IA (10^{-4}, green lines) followed after a trace interval with 1 s of CO_2 (10%, red lines). Worms did not modify their response to 5 IA-only probe trials. 500-600 ml/min flow, 20 training trials, 1 min ITI, no bacteria present. Error shading is s.d.

Conditioning experiments pairing isoamyl alcohol with carbon dioxide could have failed for several reasons. First, it is possible that worms cannot learn in environments which lack food. However, even in an environment with bacteria, worms failed to learn (Figure 3.43). Second, the US might not be strong enough, as previous research showing carbon dioxide-induced contextual conditioning in rats used 100% CO_2 as the US (Mongeluzi..Abrahamsen 1996). This concern was also addressed in Figure 3.43 where worms were exposed to 100% CO_2 as the US, but the animals still failed to condition. Third, the environment might have been too cold for the worms to learn, because the air flow reduced the temperature of the environment (data not shown). However, warming of the air flow did not result in learning (data not shown). Fourth, the CS itself might be too distracting. In monkey and rodent experiments, animals are often habituated to the CS before conditioning. I have not addressed this concern. Fifth, the worms might not be capable of learning this specific association between IA and CO_2. This seemed the most likely outcome, so I tested different pairs of stimuli under the wormtracker.

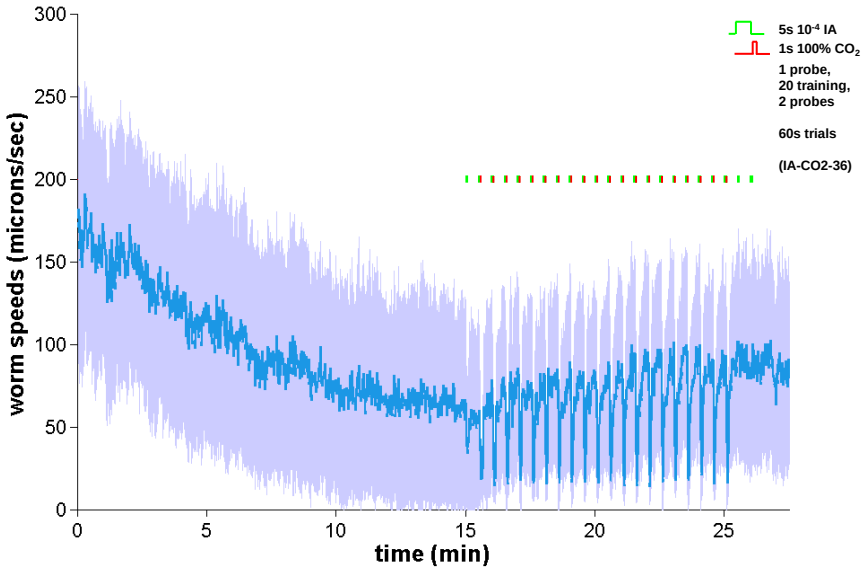

Figure 3.43: Delay conditioning fails with a strong US and in the presence of food

Worms were exposed to a delay conditioning protocol with 5 s of IA (10^{-4}, green lines) coterminating with 1 s of CO_2 (100%, red lines). Even in the presence of bacteria, worms did not alter their response to 2 IA-only probe trials. 500-600 ml/min flow, 20 training trials, bacteria present. Error shading is s.d.

i. Air flow avoidance (wormtracker)

The air flow that carried the odor and gas stimuli had a cooling effect on the worm's environment (data not shown). While varying the air flow rate, I found that worms avoided high flow rate air streams with strongest avoidance observed at 500 ml/min (Figure 3.44). Interestingly, this avoidance was dependent on the temperature of the air stream, as warming the air flow reduced avoidance (Figure 3.45). Thermsensory mutants (*ttx-1*) and mechanosensory mutants (*mec-1, mec-2, mec-3, mec-4*) showed grossly wild-type responses to cold high-flow rate air (data not shown), suggesting that the response to air flow functions independently of known temperature and mechanosensation pathways.

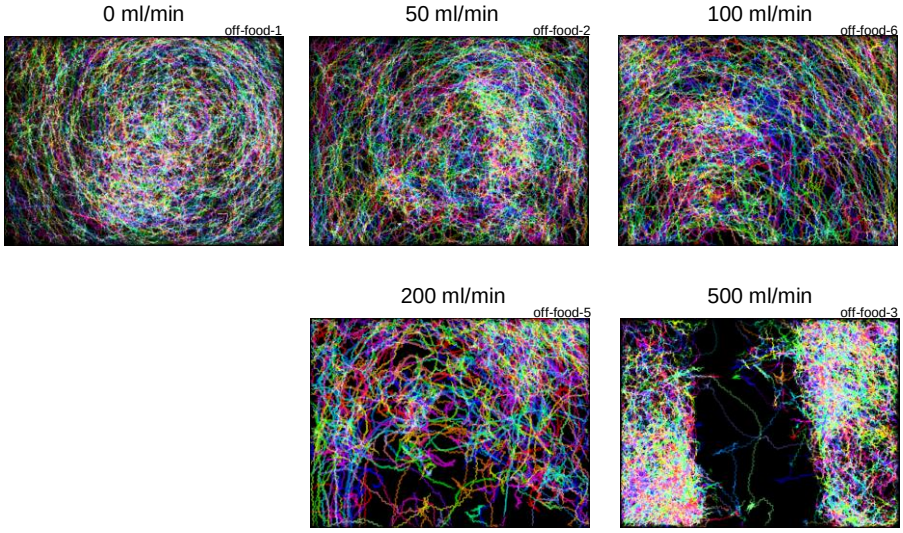

Figure 3.44: Air flow causes worms to avoid

Worms were presented with varying rates of air flow while being observed by the wormtracker. Worms begin to avoid at 200 ml/min and clearly avoid at 500 ml/min. The air flow entrance and exit are at the bottom and top of the frame, respectively. Each worm's path is color-coded. Black regions indicate areas avoided by the worms. Assay conducted for 30 min in the absence of food.

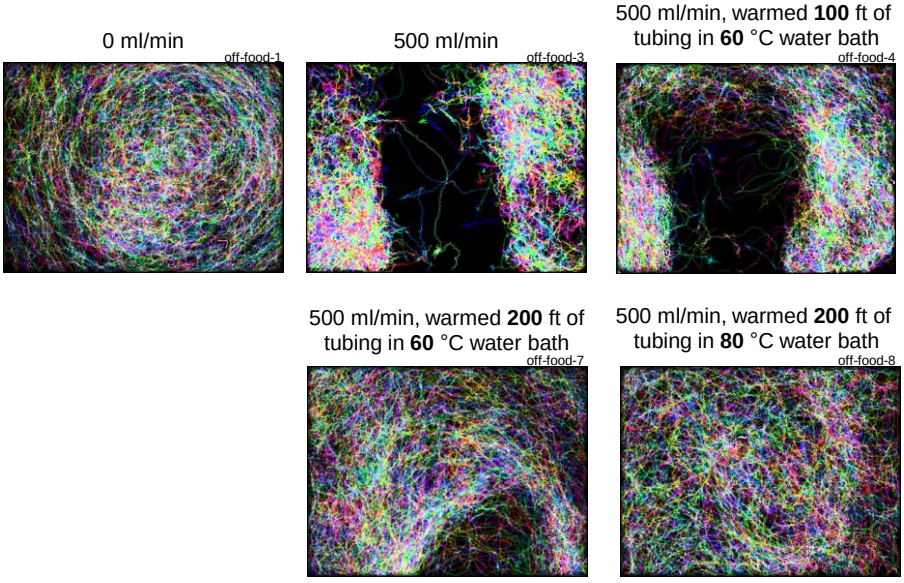

Figure 3.45: Warming the air flow prevents worms from avoiding

Worms were presented with air flow (500 ml/min) that was warmed to varying degrees. Warming reduced the air flow avoidance phenotype until it was completely abrogated. The air flow entrance and exit are at the bottom and top of the frame, respectively. Each worm's path is color-coded. Black regions indicate areas avoided by the worms. Assay conducted for 30 min in the absence of food.

j. Octanol as a conditioned stimulus

Since the attractive odor isoamyl alcohol did not work as a CS, I tried an aversive odor, octanol (OCT), instead (Bargmann..Horvitz 1993). While AWC is the neuron primarily responsible for detecting isoamyl alcohol (Chalasani..Bargmann 2007), ASH and other sensory neurons are required for the avoidance of octanol (Troemel..Bargmann 1995, Chao..Hart 2004). Perhaps by using a stimulus that functioned through a different neural circuit, the worms would be able to learn.

In the absence of food, 10% octanol (diluted in water) did not have a strong effect on worm speed but appeared to reduce turning rate (Figure 3.46). In the presence of food, the

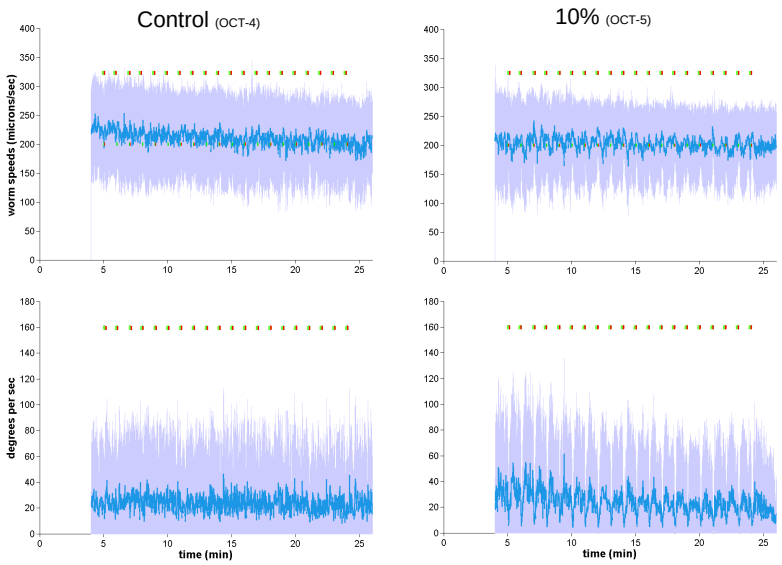

Figure 3.46: Octanol (OCT) causes worms to move in a straighter line

Top, Worms showed a very weak response to octanol in their speed.
Bottom, Worms showed a more significant response to octanol in their turning. 5 s of octanol (10%, green lines) resulted in drops in turning. Red lines indicate a control puff of air. 500 ml/min flow, 20 trials, 1 min ITI, no bacteria present. Error shading is s.d.

overall magnitude of the response to octanol was small except when undiluted, which caused worms to slow (Figure 3.47). As the duration of octanol was increased, worms responded in a

more complex manner: 10 s exposures resulted in habituation while 30-60 s exposures caused an increase in speed (Figure 3.48). A summary of the dose response is given in Figure 3.49, and a summary of the duration response is given in Figure 3.50.

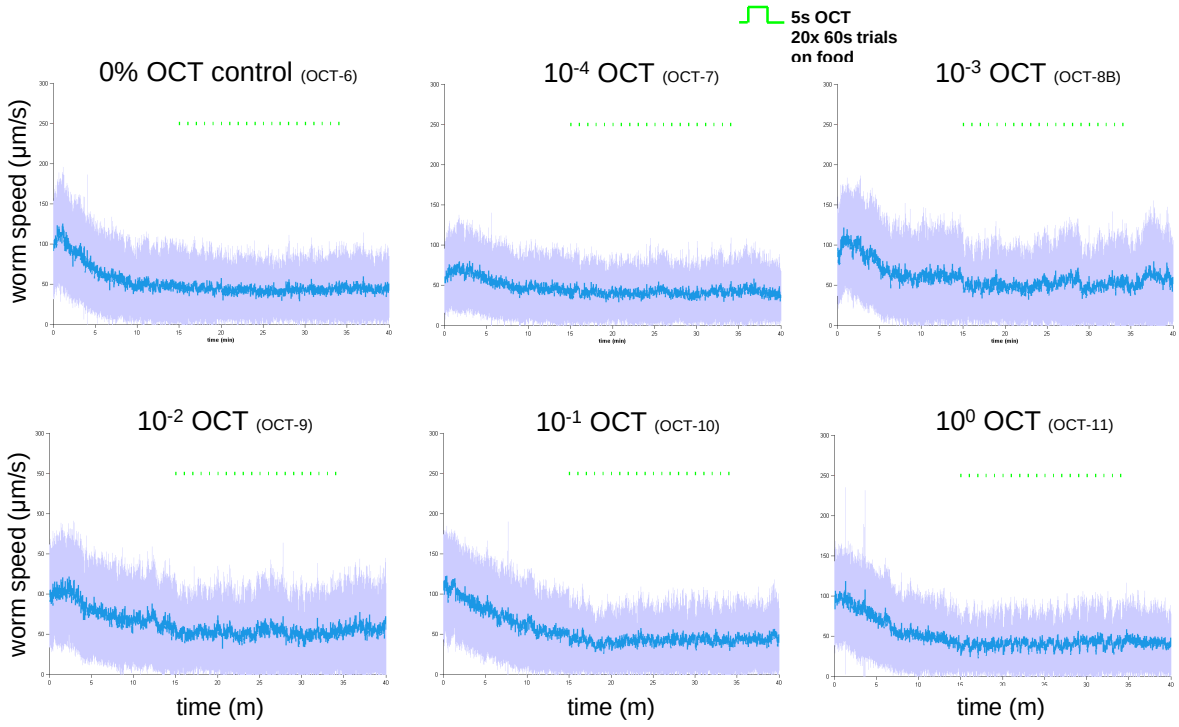

Figure 3.47: Octanol causes worms to slow on food

Worms did not respond to 5 s of OCT (varying concentrations, green lines), except to undiluted OCT, which caused slowing. 500 ml/min flow, 20 trials, 1 min ITI, no bacteria present. Error shading is s.d.

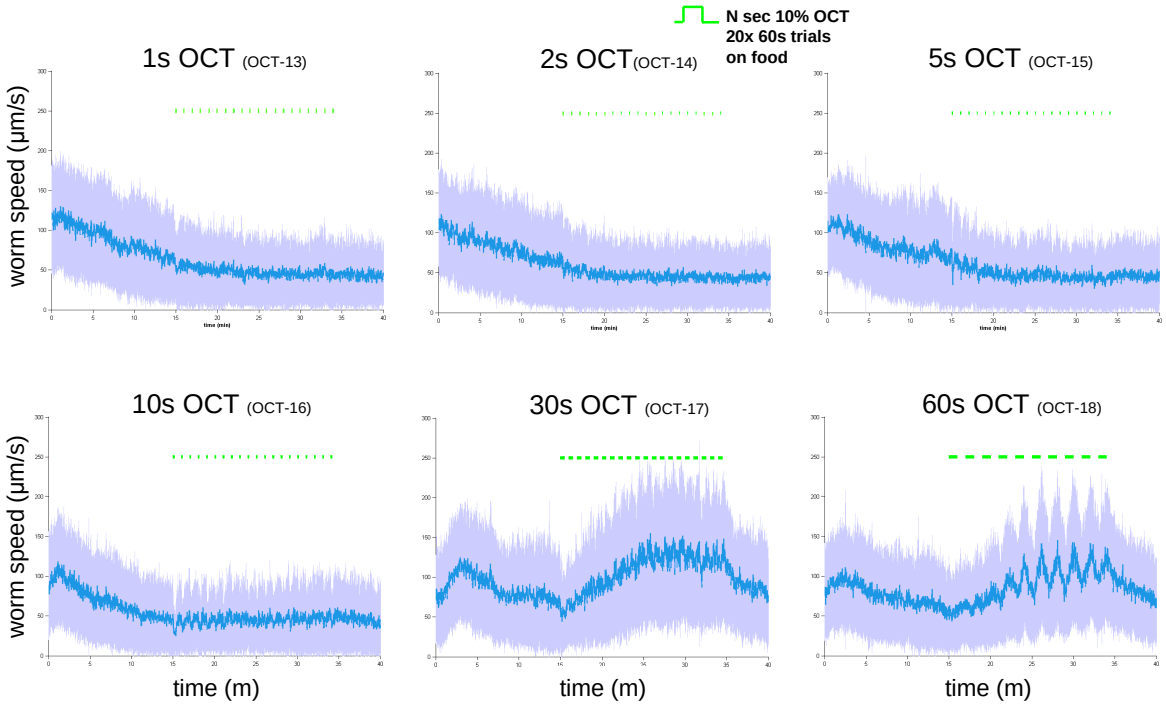

Figure 3.48: Longer durations of octanol increases worm speed

Worms responded to longer durations of OCT (10%, green lines) by increasing their overall speed. 500 ml/min flow, 20 trials, 1 min ITI, no bacteria present. Error shading is s.d.

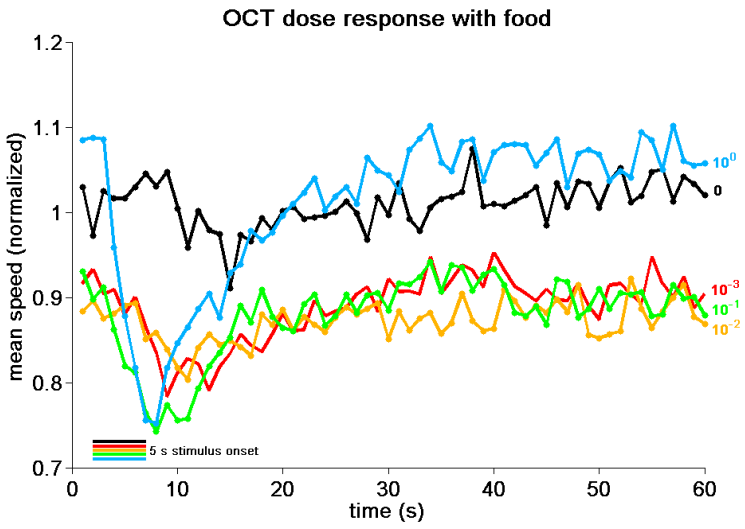

Figure 3.49: Dose response to octanol on food

Worm response to varying concentrations of 5 s of OCT, normalized to the worm's speed before the first stimulus exposure. Each curve is the average of 20 trials from one experiment like that shown in Figure 3.47.

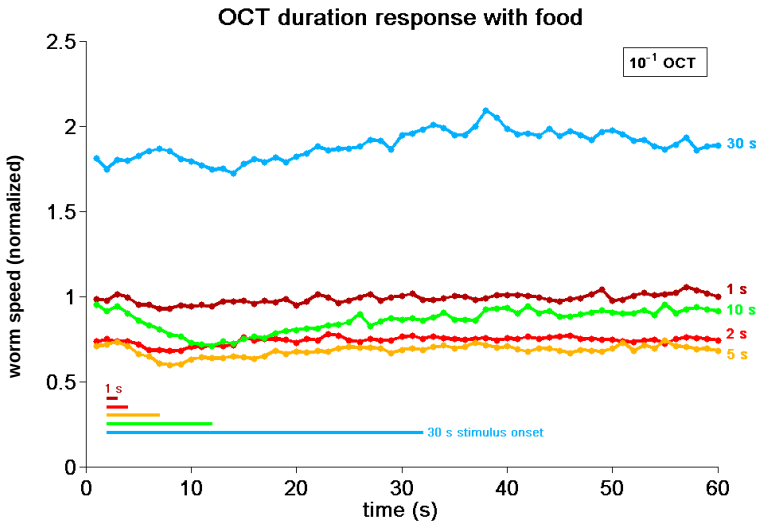

Figure 3.50: Duration response to octanol on food

Worm response to varying durations of OCT (10%), normalized to the worm's speed before the first stimulus exposure. Each curve is the average of 20 trials from one experiment like that shown in Figure 3.48. Longer durations increased speed above 1 due to higher speeds on trials after the first trial.

k. Octanol paired with carbon dioxide

Delay conditioning experiments using octanol as a CS paired with carbon dioxide as the US failed to result in learning. Worms did not respond in a non-naive manner after as many as 200 trials of pairing (Figure 3.51), nor did they learn after a variety of trial durations ranging from 8 s to 10 min (Figure 3.52).

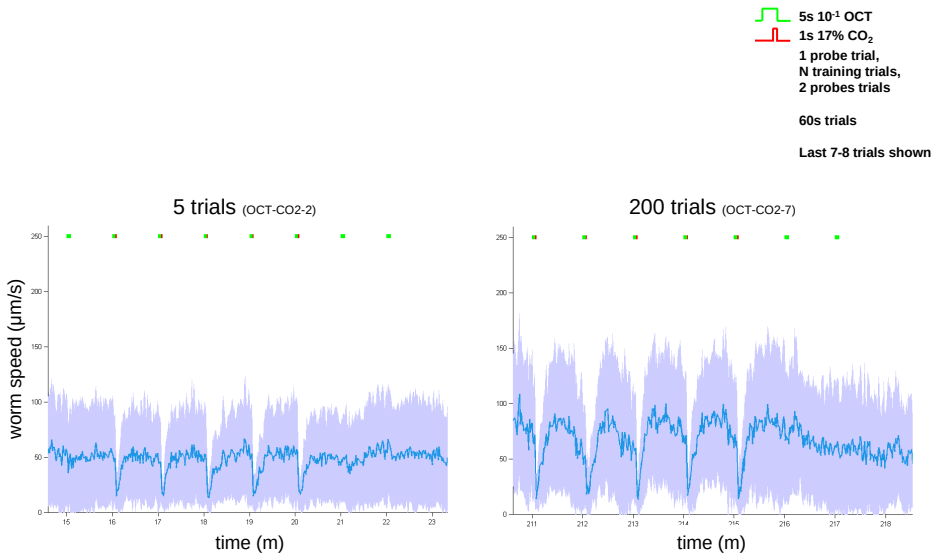

Figure 3.51: Delay conditioning with octanol and CO_2 fails even after 200 trials

Worms were exposed to a delay conditioning protocol of 5 s of OCT (10%, green lines) coterminating with 1 s of CO_2 (17%, red lines). Neither 5 (left) nor 200 (right) trials of pairing resulted in learning as measured by 2 post-training OCT-only probe trials. Only the 1st 7-8 trials from each experiment are shown. 500-600 ml/min flow, 5-200 training trials, 1 min ITI, bacteria present. Error shading is s.d.

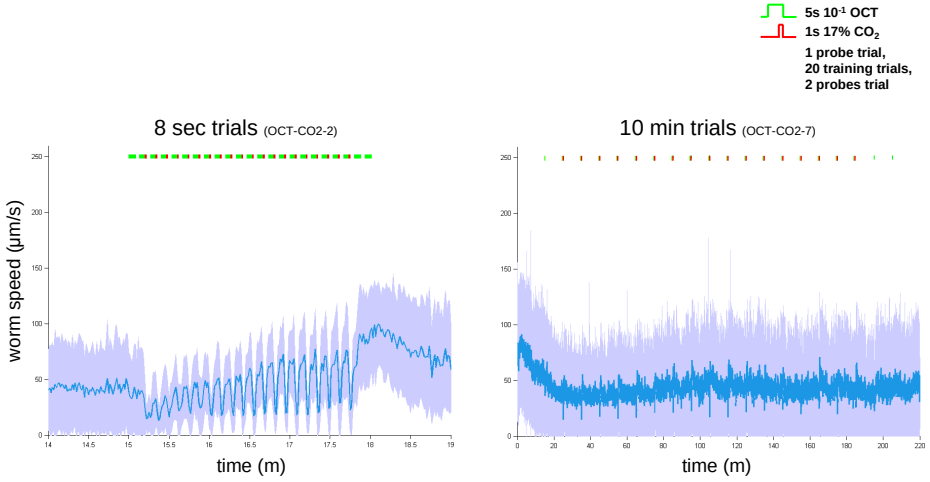

Figure 3.52: Varying the inter-trial interval does not result in learning

Worms were exposed to a delay conditioning protocol of 5 s of OCT (10%, green lines) coterminating with 1 s of CO_2 (17%, red lines) of varying ITIs. Worms failed to learn as demonstrated by no new response on 2 OCT-only probe trials. 500-600 ml/min flow, 20 training trials, bacteria present. Error shading is s.d.

l. Oxygen as a conditioned stimulus

Worms failed to learn after using both attractive (isoamyl alcohol) and aversive (octanol) odorants as conditioned stimuli. Both of these odorants are detected by distinct sensory neurons. As a final attempt at conditioning, I used oxygen gas (O_2) as a conditioned stimulus.

Worms exhibit a preference for specific concentrations of O_2 (4-10%) (Gray..Bargmann 2004). O_2 is detected by the AQR, PQR and URX sensory neurons, distinct from those that detect IA and OCT (Zimmer..Bargmann 2009). To determine the O_2 concentration to use as a conditioned stimulus, I recorded the response to O_2 using the wormtracker (Figure 3.53). In these experiments, worms were kept in an environment lacking O_2 (100% nitrogen) and then provided with pulses of O_2. Lack of O_2 is known to cause significant changes in worm development and locomotion (Padilla..Hajeri 2012); however, I speculated that worms could tolerate brief periods without O_2 (5-15 min) without entering an altered metabolic state.

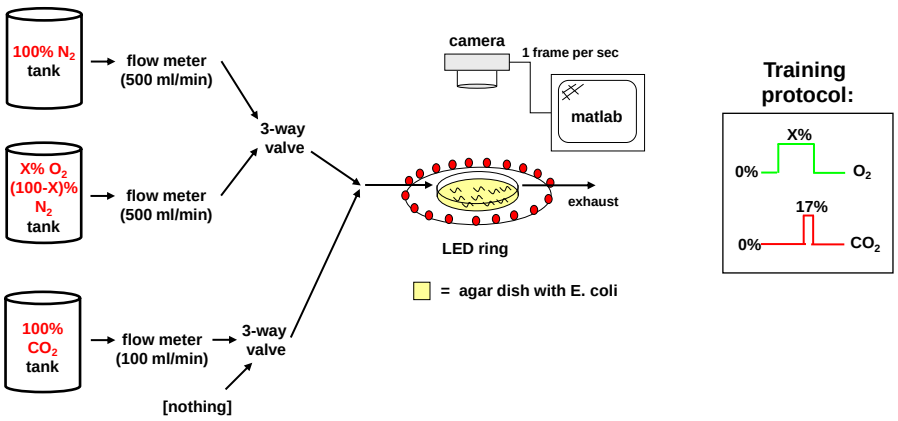

Figure 3.53: Experimental design for pairing oxygen (O_2) with carbon dioxide (CO_2)

Worms accelerated in response to an increase in O_2 (Figure 3.54), similar to the O2-ON response observed by Dengke Ma. a postdoc in our lab (Ma..Horvitz 2012). This acceleration

was proportional to the duration of restoration of O_2 (Figure 3.55). A dose response summary is provided in Figure 3.56, and a duration response summary is provided in Figure 3.57.

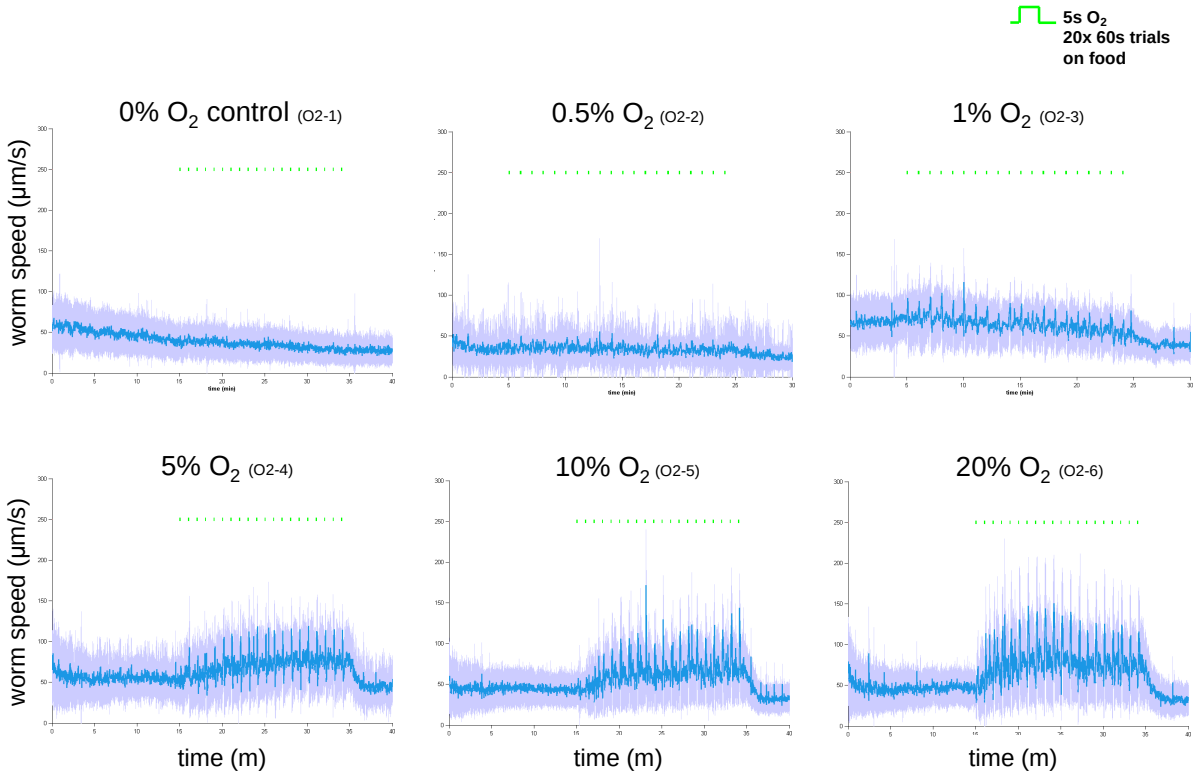

Figure 3.54: O_2 causes worms to accelerate

Worms accelerated in response to 5 s of O_2 of varying concentration (green lines). 500 ml/min flow, 20 trials, 1 min ITI, bacteria present. Error shading is s.d.

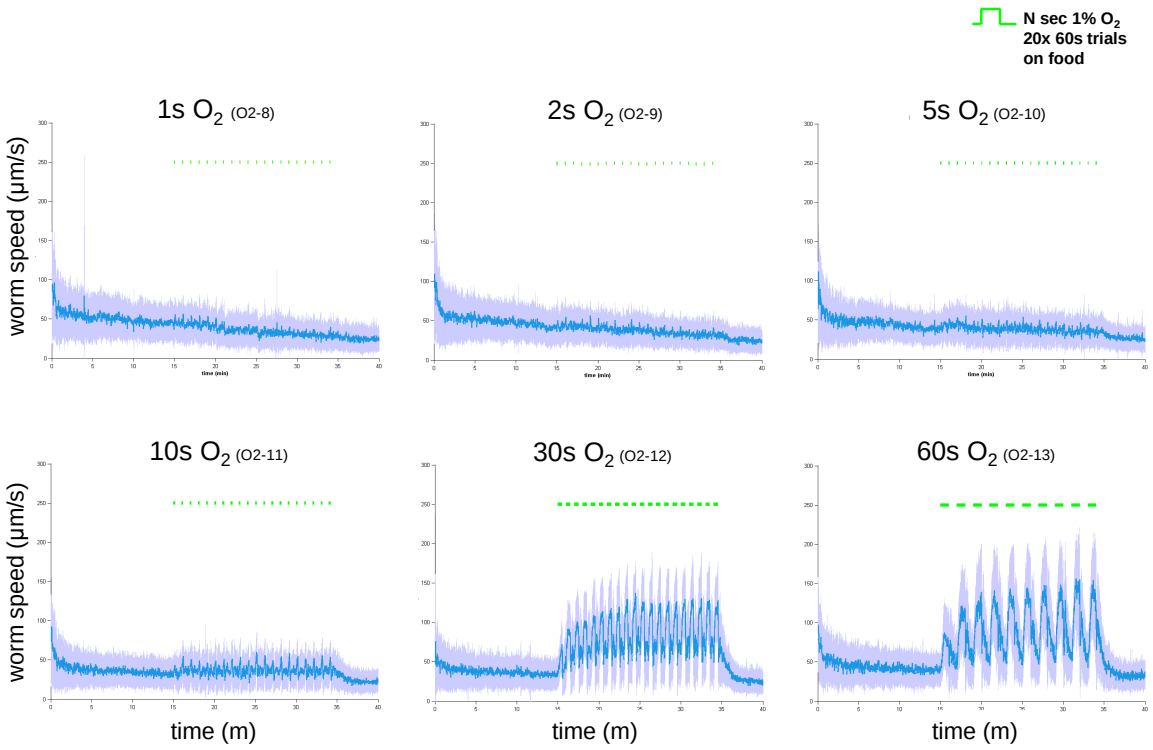

Figure 3.55: Longer durations of O_2 cause larger accelerations by worms

Worms accelerated the most in response the longest durations of O_2 (1%, green lines). 500 ml/min flow, 20 trials, 1 min ITI, bacteria present. Error shading is s.d.

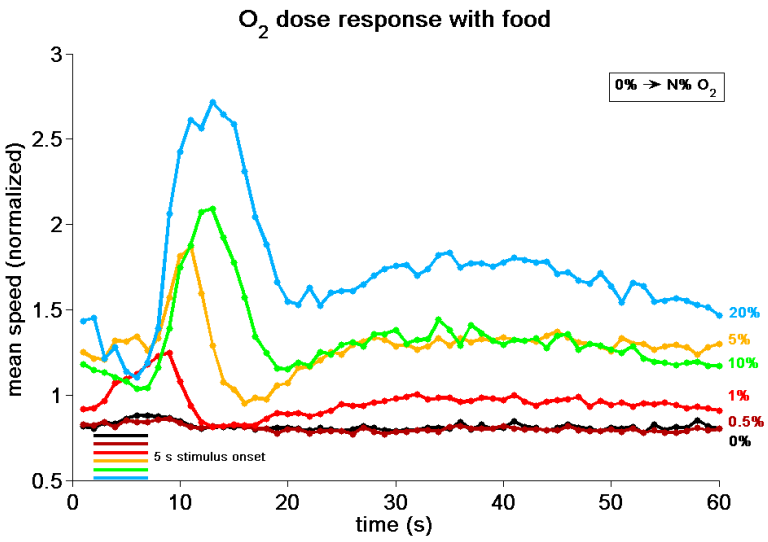

Figure 3.56: Dose response to O_2 on food

Worm response to varying concentrations of 5 s of O_2, normalized to the worm's speed before the first stimulus exposure. Each curve is the average of 20 trials from one experiment like that shown in Figure 3.54.

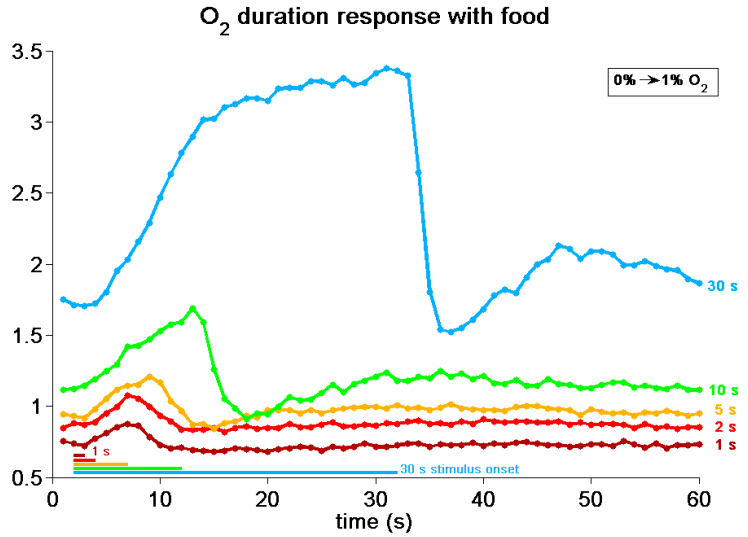

Figure 3.57: Duration response to O_2 on food

Worm response to varying durations of O_2 (1%), normalized to the worm's speed before the first stimulus exposure. Each curve is the average of 20 trials from one experiment like that shown in Figure 3.55. 30 s of O_2 increased initial speed above 1 due to an increase in speed after the first trial.

m. Oxygen paired with carbon dioxide

Having characterized the worm's response to O_2 change using the wormtracker, I sought to use O_2 (1%) as a conditioned stimulus, paired with CO_2 as the unconditioned stimulus. Unfortunately, worms did not learn under a variety of trial repetitions (Figure 3.58) or trial durations (Figure 3.59).

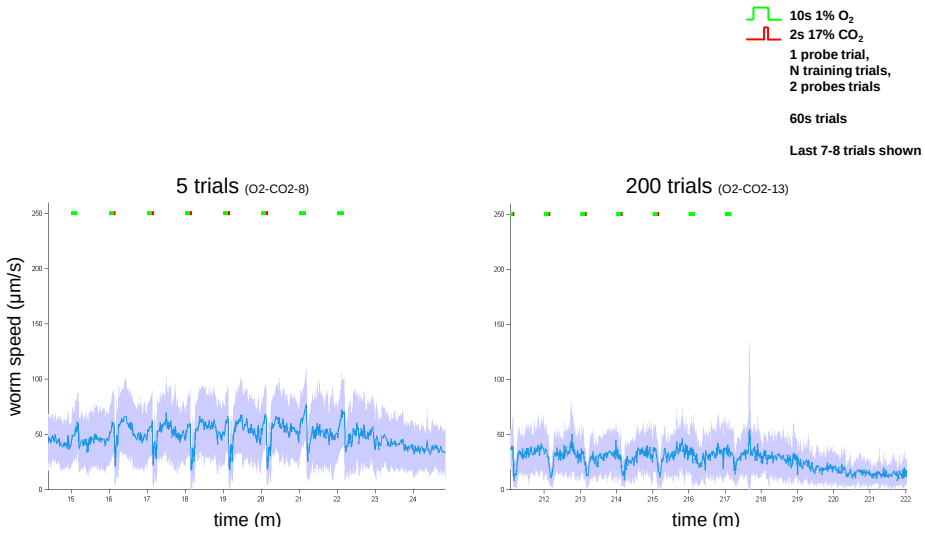

Figure 3.58: Delay conditioning with O_2 and CO_2 fails even after 200 trials

Worms were exposed to a delay conditioning protocol of 10 s of O_2 (1%, green lines) coterminating with 2 s of CO_2 (17%, red lines). Neither 5 (left) nor 200 (right) trials of pairing resulted in learning as measured by 2 post-training O_2-only probe trials. Only the 1st 7-8 trials from each experiment are shown. 500-600 ml/min flow, 5-200 training trials, 1 min ITI, bacteria present. Error shading is s.d.

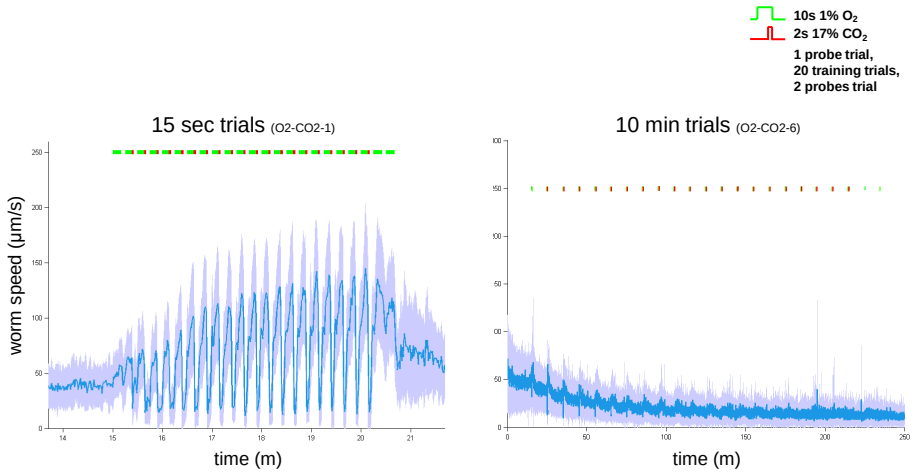

Figure 3.59: Varying the inter-trial interval does not result in learning

Worms were exposed to a delay conditioning protocol of 10 s of O_2 (1%, green lines) coterminating with 2 s of CO_2 (17%, red lines) of varying ITIs. Worms failed to learn as demonstrated by no new response on 2 O_2-only probe trials. 500-600 ml/min flow, 20 training trials, bacteria present. Error shading is s.d.

F. Conclusion and future directions

In conclusion, I was unable to get worms to either delay or trace condition using a variety of stimuli. I paired the attractive odorant isoamyl alcohol (IA) with aversive light, IA with CO_2, the aversive odorant octanol (OCT) with CO_2, and the attractive gas O_2 with CO_2. I did not observe learning with any of these pairings. I also tested whether the presence or absence of food might affect learning, and I did not observe any effect. At this point, there is no evidence supporting the presence of consciousness in the worm.

If one were to continue trying to temporally condition worms, I would first attempt to replicate the previously reported dunking experiments (Wen..van der Kooy 1997, Amano & Maruyama 2011). Alternatively, one could try additional stimulus pairs taken from the stimuli matrix (Figure 3.6).

I was very discouraged by these negative results for learning in *C. elegans*. On a positive note, these experiments enabled me to observe a variety of previously unreported behavioral responses to stimuli, including

1. Inhibition of feeding by light
2. Habituation of the reversal response to light
3. Slowing by CO_2
4. Body contraction and inhibition of defecation by CO_2
5. Avoidance of cold high-flow air
6. Habituation of the reversal response to air flow
7. Acute acceleration by isoamyl alcohol (off food)
8. Paralysis and egg-laying by isoamyl alcohol (off food)
9. Acute deceleration by isoamyl alcohol (on food)
10. Acute deceleration by octanol (on food)
11. Acute acceleration by O_2

Of these 11 behavioral responses, I was attracted to the response to light because it could be studied efficiently. The behavior was immediately visible in individual animals in an assay that only took a few seconds. Moreover, visual perception is the form of subjective experience I'm most fascinated with, and studying the light response of the worm might lead me to studying their capacity for visual perception, if present.

PART 2:

LIGHT, HYDROGEN PEROXIDE AND *C. ELEGANS*

Chapter 4:

Introduction to Light and *C. elegans*

A. History of light and *C. elegans*

The fact that *C. elegans* avoids light is a relatively recent discovery. The earliest worm experiments used ultraviolet light to assess survival, not behavior (Hartman & Herman 1982). The authors identified 9 mutants (*rad* from "radiation sensitive") with reduced brood size in response to a sub-lethal dose of 254 nm UVC light (5 J/m^2, administered at the rate of 1 J/m^2/s which is equivalent to 1 W/m^2 or 0.001 mW/mm^2, which is the units I use in my experiments):

Gene	Synonyms	Description
rad-1	*lem-3*	Functions in DNA damage response
rad-2	*smk-1*	Regulates the innate immune, UV and oxidative stress functions of DAF-16/FOXO
rad-3	*xpa-1*	Core nucleotide excision repair factor for the repair of UV-induced DNA lesions
rad-4		Uncloned locus that affects meiotic nondisjunction of the X chromosome
rad-5	*clk-2*	Ortholog of the telomere length-regulating protein Tel2p
rad-6		Uncloned locus
rad-7		Uncloned locus that acts in a pathway with *rad-3*
rad-8		Ortholog of the dehydrogenase/reductase mitochondrial protein RTN4IP1
rad-9		Uncloned locus

Figure 4.1: Mutants with reduced brood size in response to UV light

(Hartman & Herman 1982)

Many of these genes are conserved in mammals and are involved in the response to DNA damage and general stress. The authors also found absence of egg production after 25 J/m^2 of 270 nm and 50,000 J/m^2 of 315 nm light (Keller..Rupert 1987). In my own experiments, I've found that worms die after 2,000,000 J/m^2 of 436 nm light. These data show that low-wavelength light causes the greatest damage to the worm, as is also found when exposing *E. coli* and other organisms to light.

The first published work to look at the worm's behavioral response to light found that worms increase reversals in response to 520-600 nm light at 0.12 J/m^2/s (0.00012 mW/mm^2) but did not respond to lower wavelengths down to 420 nm at the same power (Burr 1985). The reversal response is subtle (an increase from 12% to 20%) and within the range I see in non-stimulated wild-type worms. Furthermore, the light came from a lantern slide projector and was 4 orders of magnitude weaker than the light others and I have used in more recent behavioral experiments (0.1 – 20 mW/mm^2 from a mercury lamp). Due to the low power and weak response, I don't place any stock in these findings.

With the rise of fluorescence imaging and the prevalence of green fluorescent protein (GFP), worm researchers noticed that worms avoid the GFP excitation light (470 nm). The power at 470 nm that causes worm avoidance is roughly 1 mW/mm^2, 10,000x the power used by Burr. Researchers noticed that light applied to the worm's head induces reversals, while light applied to the tail induces accelerations. Whole-body illumination generally induces accelerations. By screening for mutants that fail to avoid whole-body illumination of 405 nm at 5 mW/mm^2 or 436 nm at 1.5 mW/mm^2, researchers isolated mutations in 3 genes they named *lite-1, lite-2* and *lite-3* (Edwards..Miller 2008). *lite-1* encodes a 7- or 8-transmembrane protein most homologous to the *Drosophila* gustatory receptor *Gr28b*. The *Drosophila* gustatory receptor class comprises at least 56 members: *Gr64a* and *Gr5a* sense most or all sugars (Dahanukar..Carlson 2007) and *Gr21a* and *Gr63a* sense carbon dioxide (or bicarbonate ion) (Jones..Vosshall 2007). Ectopic expression of *lite-1* in muscle induces light-dependent contraction, and the authors interpreted this result to suggest that *lite-1* might be a light receptor (Edwards..Miller 2008). Consistent with the survival results mentioned previously, worm behavior is most sensitive to 350 nm UVA and worms show no avoidance to 550 nm green light.

The authors posited that this response might be an avoidance of sunlight, which includes 0.02 mW/mm^2 of 350-375 nm light, which is sufficient power to cause avoidance in worms via a mercury arc lamp. Finally, *lite-1* site-of-action remains mysterious, as the neurons that express it, AVG and PVT, are not required for light avoidance.

Researchers have also identified neural and molecular components underlying head-light-induced reversals. Using 340 nm light at 0.7 mW/mm^2, researchers found that 7 pairs of amphid sensory neurons (ASH, ASI, ASJ, ASK, AWB, AWC, ADL) are required for light-induced reversals (Ward..Xu 2008). Subsets of these neurons are also partially required (ASH, ASJ, ASK, AWB), but none of these neurons is required individually or in triplet combinations, as assessed by laser ablation. By patching on to ASJ, the authors found that light induces an inward current in ASJ. The authors then identified molecules acting in ASJ for this response. They found that *lite-1* is both necessary and sufficient for both ASJ's and ASK's response to light (Liu..Xu 2010). *lite-1* mutants also fail to reverse in response to head-directed light, and this can be partially rescued by expressing *lite-1* solely in either ASJ or ASK. The G_α proteins GOA-1 and GPA-3 act downstream of LITE-1 to activate the guanylate cyclases DAF-11 and ODR-1. This activation is inhibited by the phosphodiesterases PDE-1,2,5 acting redundantly. The guanylate cyclases generate cGMP which open the cyclic nucleotide-gated (CNG) channels TAX-2 and TAX-4 to depolarize ASJ. Furthermore, *tax-2* is sufficient in ASJ, ASK or AWB to rescue the light avoidance defect of *tax-2* mutants. Finally, ectopic expression of *lite-1* in the ASI neuron can generate a light-dependent inward current that requires all of the downstream machinery of *daf-11*, *tax-2*, and *tax-4*. Overall, this molecular pathway is very reminiscent of light-sensing and signal transduction in mammalian photoreceptor cells, with rhodopsin replaced by LITE-1.

Gene	Synonyms	Description
lite-1	*gur-2*	Gustatory receptor ortholog of *Drosophila Gr28b*, putative UV light sensor GPCR
goa-1		G protein alpha subunit G_o
gpa-3		G protein alpha subunit
daf-11		Transmembrane guanylate cyclase that localizes to ciliated endings, soma and dendrites
odr-1	*gcy-10*	Guanylate cyclase that localizes to ciliated endings
pde-1		Cyclic nucleotide phosphodiesterase related to CaM-dependent phosphodiesterase
pde-2/5		Phosphodiesterases
tax-2		Orthologous to rod photoreceptor cyclic nucleotide-gated channel beta subunit
tax-4		Orthologous to rod photoreceptor cyclic nucleotide-gated channel alpha subunit

Figure 4.2: Genes involved in head light-induced reversals

(Liu..Xu 2010)

Neuron	Function
ASJ	Sensory neuron for light and hydrogen peroxide; promotes exit from dauer
ASK	Sensory neuron for light and ascarosides; promotes local search after food removal
ASH	Sensory neuron for aversive stimuli, including metals, odorants and osmolarity
AWB	Sensory neuron for aversive odorants, such as high isoamyl alcohol, nonanone and benzaldehyde
ASI	Sensory neuron; inhibits dauer entry and promotes dietary restriction-induced longevity
ADL	Sensory neuron for aversive stimuli, including octanol, high isoamyl alcohol, and metals
AWC	Sensory neuron for attractive odors such as isoamyl alcohol and benzaldehyde; promotes turning

Figure 4.3: Neurons involved in head light-induced reversals

Italics indicates a weak requirement for that neuron. (Ward..Xu 2008)

Following the discovery of LITE-1 in worms, fruit fly researchers reported that *Drosophila* larvae (maggots) also avoid shortwave light (Xiang..Jan 2010). 360 nm light at 0.05

mW/mm^2 is the minimal light power necessary to elicit a partial avoidance response, and the response is absent at 525 nm light at 32 mW/mm^2. The authors identified class IV dendritic arborization neurons (ddaC) that cover the entire body wall as light-sensitive neurons required for the light avoidance behavior. The dendritic neurons themselves require nearly the same power as the behavior for activation (0.1 mW/mm^2 at 340 nm). These neurons rely on the LITE-1 homolog Gr28b.b and the transient receptor potential channel TrpA1 to spike in response to light. Thus, light-sensitive neurons outside the Bolwig organ mediate light avoidance (Xiang..Jan 2010).

The light necessary to elicit the minimal avoidance response for both *C. elegans* and *Drosophila* could feasibly be produced by the sun. The sun produces 0.02 mW/mm^2 over 350-375 nm, and *C. elegans* increases its speed by 50% in response to this light produced by a mercury lamp (Edwards..Miller 2008). *Drosophila* can avoid 5 seconds of 0.05 mW/mm^2 light at 360 nm (Xiang..Jan 2010). Avoiding sunlight has been speculated to encourage worms and flies to stay within their rotting substrates, limiting UV damage and thereby promoting survival.

B. Light and hydrogen peroxide are linked

Both *Drosophila* and *C. elegans* sense light via gustatory receptors, so might it be the case that light first produces a small molecule that is then sensed by a gustatory receptor? Not only can high-energy light produce conformational changes in chromophores bound within proteins (e.g. retinal in rhodopsin), light can also generate reactive oxygen species (ROS) such as hydrogen peroxide (H_2O_2). For example, antibodies irradiated with 312 nm UV light generate H_2O_2 (Wentworth..Lerner 2001). H_2O_2 is also generated by ligand-receptor binding with hematopoietin receptor and epidermal growth factor receptor (EGFR) (DeYulia..Golde 2005).

H_2O_2 either diffuses into the cell or is transported by an aquaporin transporter (Bienert..Jahn 2006) and modifies proteins by oxidizing cysteine and methionine residues (Giorgio..Pelicci 2007). H_2O_2 is also a byproduct of mitochondrial respiration and can be generated and degraded in many additional ways intracellularly (Veal..Morgan 2007). H_2O_2 can oxidize protein tyrosine phosphatases (PTPs) and thereby release receptor tyrosine kinases (RTKs) from inhibition (Knebel..Herrlich 1996). All in all, H_2O_2 can play a multitude of roles in cell signaling and toxification.

What if H_2O_2 itself is the stimulus for light-induced avoidance behaviors, and light is just a convenient lab method for producing H_2O_2? One aspect of the behavior that I've been studying (the acute inhibition of feeding by light) requires nearly an order of magnitude more light than that produced by sunlight (0.2 mW/mm^2 at 350 nm) and elicits what appears to be regurgitation or vomiting in addition to avoidance. I can understand why the worm would avoid light as it is lethal, but why also vomit during the process? In fact, there exist strains of the pathogenic bacteria *Streptococcus* and *Enterococcus* that can kill *C. elegans* by producing lethal amounts of H_2O_2 (Jansen..Schnabel 2002, Bolm..Chhatwal 2004, Moy..Ausubel 2004). If the worm ingests these toxic bacteria, it seems reasonable that it should detect the H_2O_2, vomit up the bacteria it has already eaten, and leave the area.

However, it should also be noted that previous research has tested aspects of the H_2O_2 hypothesis. The ASJ neuron depolarizes not only to light but also to 1 mM H_2O_2; however, this response persisted in the absence of *lite-1* (Liu..Xu 2010). Given my finding that *gur-3*, a *lite-1* homolog, mediates the light response and H_2O_2 response of I2, a pharyngeal neuron, I hypothesize that the H_2O_2 response of ASJ might be mediated by *gur-3*. Additionally, the *Drosophila* ddaC neuron shows a slight but insignificant activation in response to 10 μM H_2O_2

(Xiang..Jan 2010). I suspect that this concentration is too low to elicit a response, and a higher concentration should be tested.

In conclusion, only 3 papers have been published on the worm's avoidance response to light, and none has commented on the feeding inhibition that I have studied. The putative light sensor LITE-1 functions similarly in the fly to mediate light avoidance of larvae. Amphid sensory neurons depolarize in response to light via a G protein-mediated generation of cGMP, similar to how our photoreceptor neurons respond to light. While sunlight may elicit aspects of the light response, I speculate that other aspects might be elicited by environmental sources of harmful hydrogen peroxide.

Chapter 5:

Signal Transduction of Light and H_2O_2 by Gustatory Receptor Paralogs

Submitted for publication

Authors: Nikhil Bhatla & Bob Horvitz

A. Abstract

Animals sense light and process this signal to produce environment-dependent behaviors. Molecular light-sensing relies on the absorbance of a photon by the chromophore retinal, which is detected by the opsin family of photoreceptor proteins. Interestingly, the nematode *Caenorhabditis elegans* and the fruit fly *Drosophila* melanogaster avoid UV light using the protein LITE-1/GR28B.B, which is a member of a family of gustatory receptors. Here we show that in addition to promoting an avoidance behavior by C. elegans, light inhibits feeding behavior. We identify the I2 pharyngeal neurons as cellular light sensors required for this behavior. Hydrogen peroxide elicits behavioral and cellular responses strikingly similar to those caused by light. The sensing of both light and hydrogen peroxide are mediated by the LITE-1 and GUR-3 proteins, both putative gustatory receptors, as well as by the conserved antioxidant enzyme peroxiredoxin PRDX-2. Our results suggest that the LITE-1/GUR-3 family of receptors likely detects light through its generation of hydrogen peroxide or of another redox product.

B. Introduction

Sensing and responding to light is critical for organisms to survive and flourish. Plants move toward the sustaining energy of the sun (Whippo 2006), while animals use photosensor arrays to provide input to neural circuits for vision-dependent behaviors (Land & Fernald 1992). At the molecular level, photoreception depends on the chemical modification of a chromophore by light, such as isomerization around a double bond, formation or rupture of a covalent bond, or electron transfer (Moglich..Moffat 2010). This chemical modification is then detected by a photoreceptor protein: animals rely on opsins (Terakita 2005) and in some cases cryptochromes

(Fogle..Holmes 2011, Chaves..Ahmad 2011), while plants and bacteria have a broader range of photoreceptor proteins (Moglich..Moffat 2010, Christie..Getzoff 2012, Wu..Shi 2012).

Recent work has identified a new class of proteins that function in photoreception. Both the nematode *Caenorhabditis elegans* and larvae of the fruit fly *Drosophila melanogaster* avoid UV light through the action of a member of the gustatory family of G protein-coupled receptors (GPCRs) called LITE-1 or GR28B.B, respectively (Edwards..Miller 2008, Liu..Xu 2010, Xiang..Jan 2010). How LITE-1/GR28B.B detects light is not known. Here we show that *C. elegans* inhibits feeding in response to light, that the pharyngeal I2 neurons function as cellular light sensors, and that hydrogen peroxide elicits similar behavioral and cellular responses. Detection of light and hydrogen peroxide relies on LITE-1 and GUR-3, a related gustatory receptor homolog, as well as on the peroxiredoxin PRDX-2. These results suggest that the LITE-1/GUR-3/GR28B.B family of receptors responds to light by detecting the product of an oxidation reaction triggered by light.

C. Light inhibits feeding

C. elegans ingests bacteria through its pharynx. In a process similar to filter feeding, the pharynx sucks in surrounding liquid, retains larger particles such as bacteria and transports them to the grinder (Fang-Yen..Samuel 2009). This feeding process is called "pumping" and can be observed with a dissecting microscope (120x magnification). Each pump involves a posterior-directed contraction of the grinder followed by an anterior-directed relaxation (Figure 5.1a). At room temperature (22-23 °C) and in the presence of bacterial food, worms pump between 4 and 5 times per second (4-5 Hz). We scored feeding in real-time by eye. We found that exposure to violet light severely disrupted this feeding rhythm (Figure 5.1b, c) and confirmed this finding by

analyzing high-frame-rate videos (86 fps, Figure 5.2a). We used 436 nm violet light (13 mW/mm^2) as the light stimulus, unless stated otherwise. The pumping response can be divided into three phases: pumping immediately stops in response to light (the "acute" response, 0-3 s after light onset); pumping then increases while the light is maintained (the "rebound" response, 5-10 s after light onset); and pumping remains suppressed even after light is removed (the "sustained" response, 0-10 s after light removal) (Figure 5.1c, Figure 5.3).

To determine the spectral sensitivity of the pumping response to light, we varied both the wavelength and power of light. The pumping response was elicited by the shortest wavelength of light that we could deliver through our microscope (350 nm UVA, 0.2 mW/mm^2), and can be elicited by higher power light of longer wavelengths (500 nm green, 6 mW/mm^2) (Figure 5.1d-h). Similar spectral and power sensitivity has been reported for the locomotory avoidance of *C. elegans* to light (Edwards..Miller 2008, Ward..Xu 2008). The pumping response is unlikely to be caused by a temperature increase, because long wavelength light increases temperature more than short wavelength light (Edwards..Miller 2008, Ward..Xu 2008, Xiang..Jan 2010) and we observed the strongest behavioral response to short wavelength light.

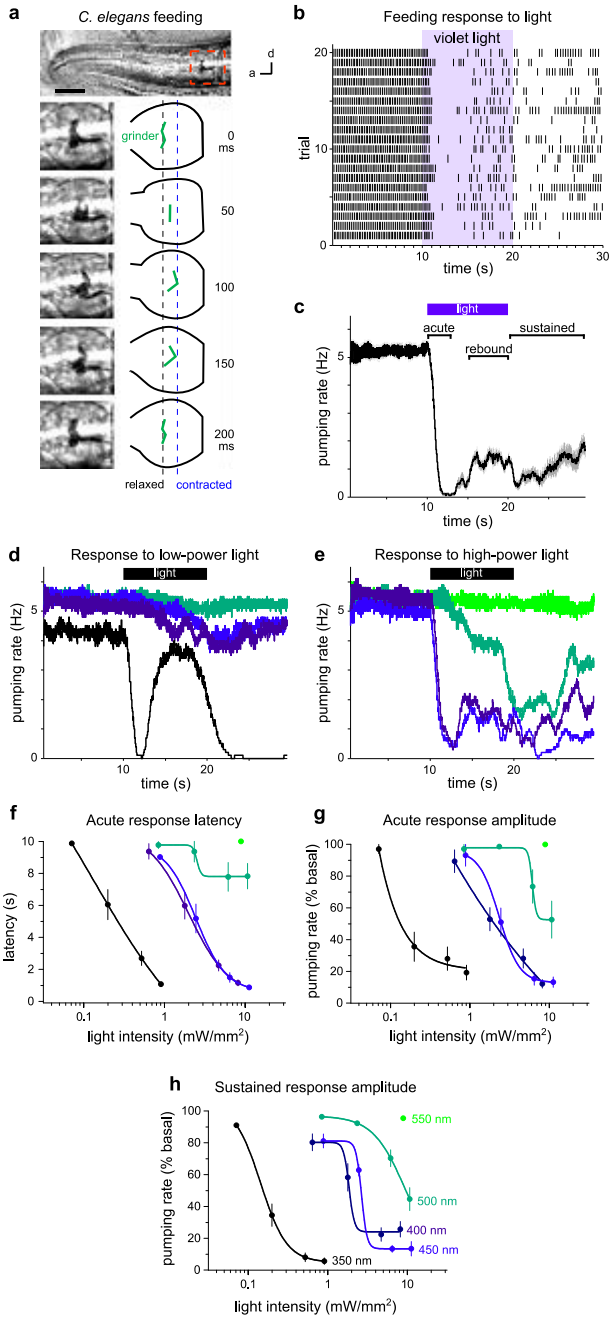

Figure 5.1: Shortwave light inhibits *C. elegans* feeding

a, Top: Adult *C. elegans* head. Bottom: The posterior bulb of the pharynx, showing one pump of the grinder. d = dorsal, a = anterior. Scale bar = 20 µm.

b, Raster plot of pumps (each tick represents a pump), one trial per row, before, during and after light exposure. Light was 436 nm at 13 mW/mm^2.

c, Moving average of data shown in **b**, with the acute, rebound and sustained responses to light labeled.

d, Pumping responses to 350 (UVA), 400 (violet), 450 (blue) and 500 nm (green) light of 0.6-0.9 mW/mm^2.

e, Pumping responses to 400, 450, 500 and 550 nm (green) light of 8-11 mW/mm^2.

f, Spectral sensitivity of the acute response latency, defined as the time from light onset to first missed pump (see Methods).

g, Spectral sensitivity of the acute response amplitude, defined as the minimum of the pumping rates after light onset normalized to the baseline pumping rate (see Methods).

h, Spectral sensitivity of the sustained response amplitude, defined as the pumping rate after light removal normalized to the baseline pumping rate (see Methods).

d-h Shorter wavelength light is more potent than longer wavelength light for eliciting the pumping response to light. Colors of lines in **d-h** indicate wavelengths of light, as labeled in **h**. n = 10-20. Light shading around traces and error bars indicate standard error of the mean (s.e.m.).

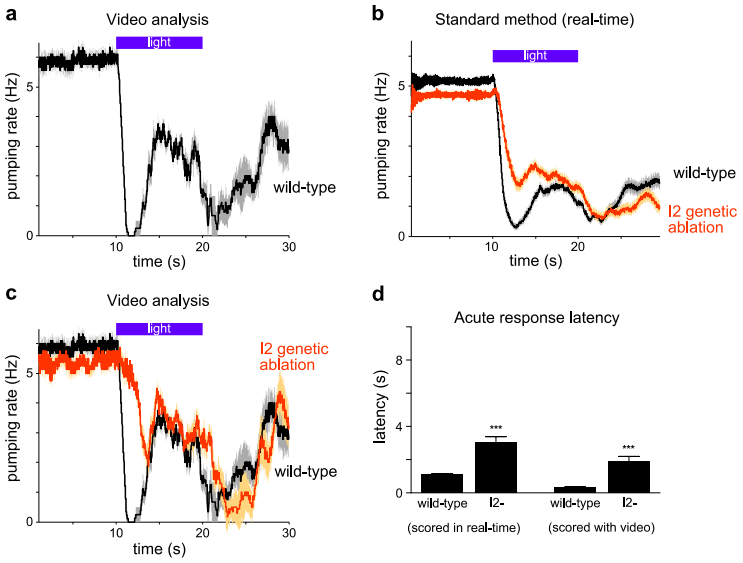

Figure 5.2: Real-time scoring of pumping is equivalent to video analysis of pumping

a, Pumping response to light of wild-type animals scored by reviewing high-frame rate-video (86 fps). The acute, rebound, and sustained phases of the response are visible, as in Figure 5.1c. n = 9.
b, Genetic ablation by expression of the transgene $P_{flp\text{-}15}$*::csp-1b* caused a delay in the pumping response similar to that observed after I2 laser ablation (Figure 5.4b). These worms were scored by eye in real-time. n = 60.
c, Pumping response to light of I2-ablated animals ($P_{flp\text{-}15}$*::csp-1b*) scored by reviewing high-frame-rate video. The latency defect is similar to that in **b** and Figure 5.4c. n = 8.
d, Quantification of acute response latency for the wild type and I2 genetic ablation by eye and by video analysis.
Light is 436 nm at 10-13 mW/mm^2. Light shading around traces and error bars indicate standard error of the mean (s.e.m.). *** $p < 0.001$, t-test.

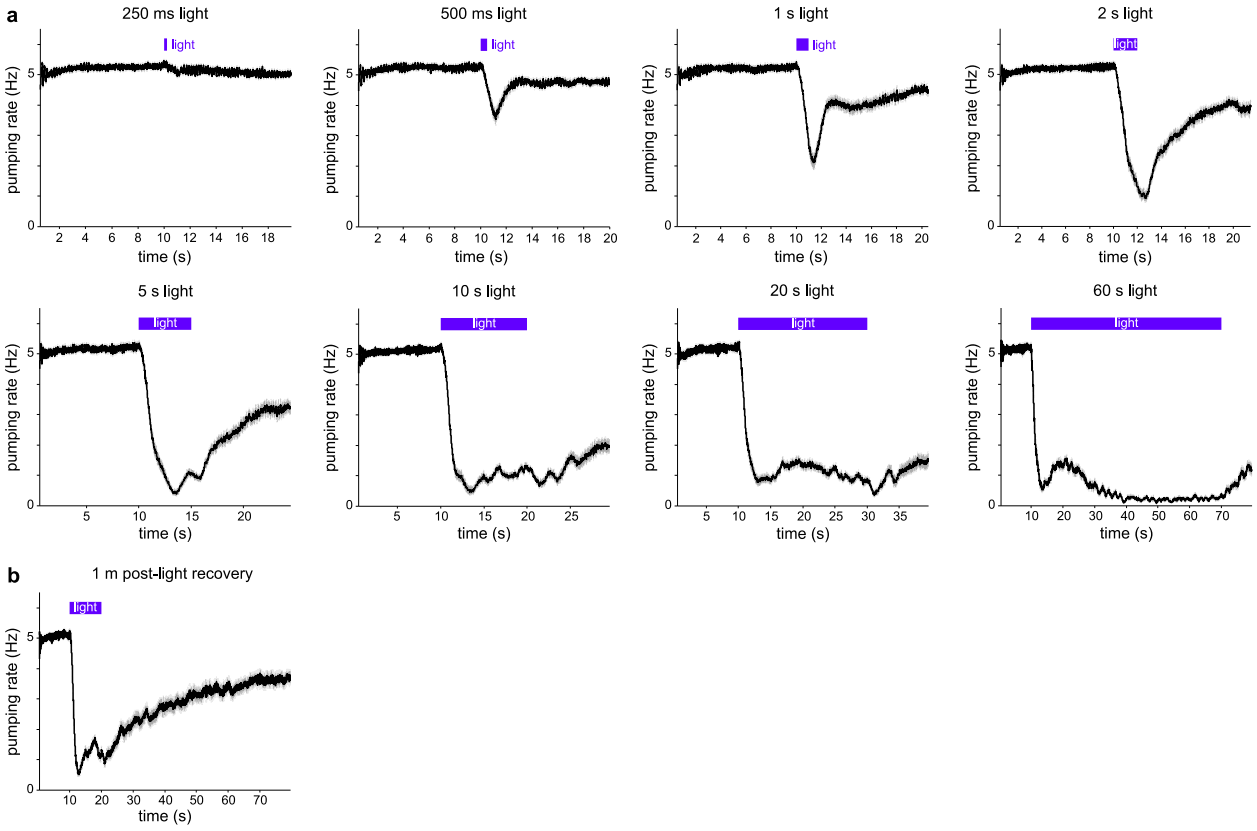

Figure 5.3: Effect of varying the duration of light and the recovery period

a, Pumping response to light for durations of 0.25-60 s.
b, Pumping response observed for 60 s after light removal.
n = 60.

D. The pharyngeal I2 neurons can sense light

To identify neurons that control the inhibition of feeding behavior in response to light, we used laser microsurgery to individually kill all 14 neuron classes in the pharynx (Albertson & Thomson 1976) (Figure 5.4a). We found that killing the I2 neuron pair delayed the acute pumping response by more than 1 s, indicating that I2 promotes speed of the acute response (Figure 5.4b, c). Ablation of I2 also significantly reduced the amplitude of the acute response (Figure 5.4d). Cell-specific genetic ablation of I2 using the caspase CSP-1B (Denning..Horvitz 2013) confirmed these findings (Figure 5.2b, d). Furthermore, the analysis of pumping using

high-frame-rate videos confirmed that real-time scoring by eye had sufficient accuracy to score the latency defect in I2-ablated worms (Figure 5.2c, d).

To determine if the I2 neuron transduces a light-dependent signal, we generated transgenic *C. elegans* strains that express the genetically-encoded calcium sensor GCaMP3 (Tian..Looger 2009) using a promoter that expresses specifically in I2 and PHA, a neuron in the tail (P_{flp-15} (Kim & Li 2004)). I2 showed a rapid and robust increase in GCaMP3 fluorescence in response to light, both in the neurites and the soma (Figure 5.4e). The GCaMP3 response appeared most quickly and most strikingly in the posterior neurite of I2, which began responding within 200 ms and peaked around 600 ms with a 300% fluorescence increase (Figure 5.4f). Using spatially-restricted light exposure and neurite-ablation experiments, we found that the posterior neurite is the compartment most sensitive to light and likely contributes to the responses seen in the anterior neurite (Figure 5.5). To test whether the spectral sensitivities of the I2 calcium and the pumping responses are similar, we varied the wavelength of light used to stimulate I2. Like the behavioral response, the response of I2 was most strongly elicited by the shortest wavelength of light (350 nm; Figure 5.4g).

Three lines of evidence indicate that the I2 neuron senses light without any neural intermediary. First, mutants that lack synaptic signaling because of a putative null mutation in *unc-13/*UNC13, an evolutionarily conserved protein required for synaptic release (Richmond..Jorgensen 1999), showed a robust calcium response to light (Figure 5.4h, i). By contrast, *unc-13(s69)* mutants showed nearly no pumping response to light (Figure 5.6). In addition, mutants that lack dense-core vesicle release because of a putative null mutation in *unc-31(u280)*, a conserved protein orthologous to human CADPS/CAPS (Speese..Martin 2007), showed an I2 response to light very similar to that of the wild type, reducing the likelihood of

signaling to I2 via humoral mechanisms (Figure 5.4i). Second, in the absence of all pharyngeal neurons except I2, MC and M4 (MC and M4 are required for normal pumping rate and growth), the I2 neuron still responded to light, thus precluding a requirement for predicted gap junction input to I2 from I1 and M1 (Albertson & Thomson 1976) (Figure 5.4j). Third, the 200 ms latency of the I2 response is similar to that of sensory neurons in *C. elegans*, such as the BAG neurons (Hallem..Ringstad 2011) (N. Ringstad, personal communication). Taken together, these data indicate that I2 is the neural sensor for the fast inhibitory component of the light-induced pumping response.

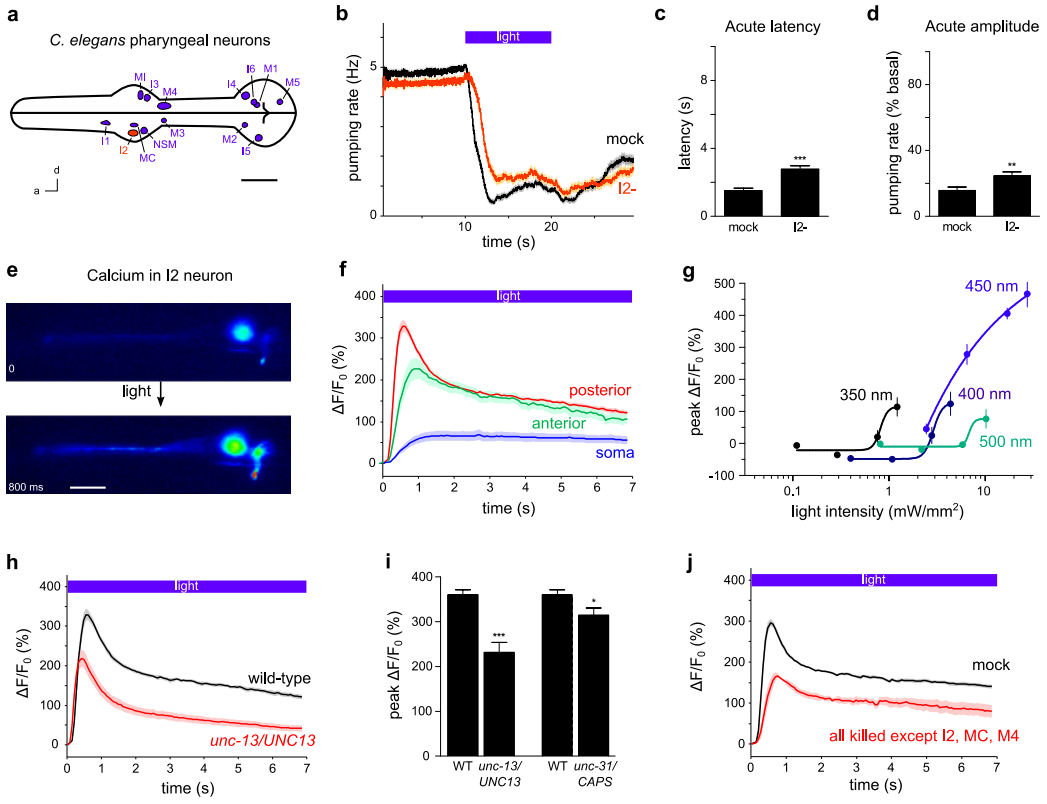

Figure 5.4: The I2 neurons directly sense light

a, Map of pharyngeal neuron nuclei; if a neuron class is paired, only a single neuron is shown. d = dorsal, a = anterior. Scale bar = 20 µm.
b, I2 ablation delayed the pumping response to light. n ≥ 72 trials.
c, Quantification of acute pumping response latency defect of I2-ablated worms.
d, Quantification of acute pumping response amplitude defect of I2-ablated worms.
e, Example of adult I2 calcium response (GCaMP3) to light (485 nm, 26 mW/mm^2). Scale bar = 10 µm.
f, Calcium increased in all three compartments of I2 in response to light. n = 20.
g-j, The posterior neurite of I2 was analyzed.
g, I2 was more sensitive to shorter wavelengths of light, though longer wavelengths could elicit a robust response at higher power. n = 10.
h, Mutants of *unc-13/UNC13(s69)*, which are defective in synaptic signaling, still showed an increase in I2 calcium in response to light. n ≥ 21.
i, Quantification of peak calcium response in I2 in *unc-13* and *unc-31/CAPS(u280)* animals. n ≥ 20.
j, I2 responded to light after ablation of all pharyngeal neurons except I2, MC and M4 (n = 3).
*** p < 0.001, ** p < 0.01, * p < 0.05, t-test. Light shading around traces and error bars indicate s.e.m.

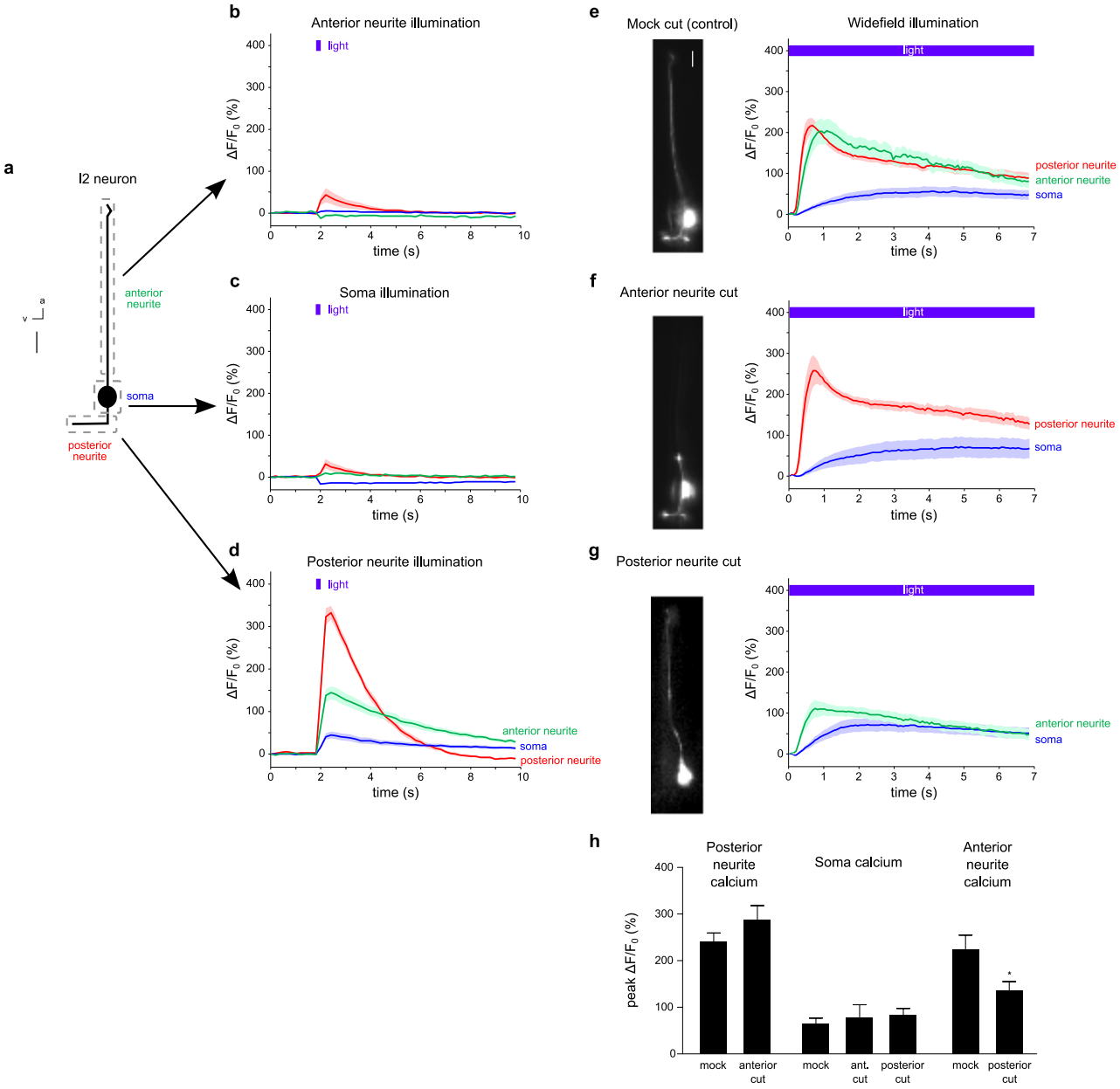

Figure 5.5: The posterior neurite is the most light-sensitive compartment of I2

a, Diagram of the I2 neuron exposed to spatially-restricted illumination. Dashed gray boxes indicate three areas of illumination. Scale bar = 5 µm.
b, I2 responded weakly after anterior neurite illumination.
c, I2 responded weakly after soma illumination.
d, I2 responded strongly after posterior neurite illumination. n = 11. The small declines in signal in **b** and **c** were a consequence of anterior neurite and soma bleaching, respectively.
e, An intact I2 neuron responded normally to light (control). n = 13.
f, An I2 neuron with a cut anterior neurite responded normally to light. n = 7.
g, An I2 neuron with a cut posterior neurite responded weakly to light. n = 15. Red trace is posterior neurite response, blue is soma response, and green is anterior neurite response.

h, Quantification of the calcium response in different compartments after ablating the anterior or posterior neurite. Cutting the posterior neurite reduced the response in the anterior neurite but did not eliminate it.
Light shading around traces and error bars indicate s.e.m. *** $p < 0.05$, t-test.

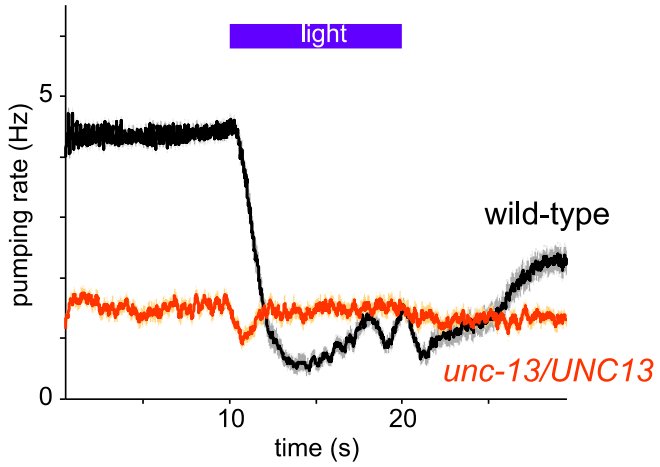

Figure 5.6: *unc-13* mutants are nearly completely defective in the pumping response to light

n = 40.

E. The gustatory receptor homolog *gur-3* functions in I2 for light-sensing

Rhodopsin is the light-sensing protein that functions in eyes. However, *C. elegans* lack eyes, and its genome does not encode rhodopsin homologs (Bargmann 1998). To identify molecular components in the light transduction pathway in I2, we first examined mutants of *lite-1*, a gustatory receptor homolog required for light avoidance (Edwards..Miller 2008, Liu..Xu 2010). *lite-1(ce314)* mutants exhibited a partial defect in the acute response and a strong defect in the sustained response to light (Figure 5.7a, h). However, the I2 neuron responded normally to light in *lite-1* mutants, suggesting that a different molecular sensor functions in I2 (Figure 5.7b, k). Furthermore, genetic ablation of the I2 neuron in *lite-1* mutants significantly enhanced the pumping defect, indicating that I2 and *lite-1* likely function in parallel (Figure 5.7c, h). Next, we tested additional genes known to function downstream of *lite-1* (Ward..Xu 2008, Liu..Xu

2010). Mutants of the G proteins *goa-1(n1134)* and *gpa-3(pk35),* guanylyl cyclases *daf-11(m47)* and *odr-1(n1936),* and phosphodiesterases *pde-1,2,3,5* had a grossly normal feeding response to light (Figure 5.8a-d). Mutants of the cGMP-gated ion channels *tax-2(p671),* critical for the light-induced response of the ASJ neuron (Ward..Xu 2008), also had a normal feeding response to light (Figure 5.8e, h). Mutants of another cGMP-gated ion channel, *tax-4(p678),* exhibited a latency defect like that of I2-ablated worms, although the physiological response of I2 was not affected in these mutants (Figure 5.8f, g, h). These results indicate that *lite-1* functions in the pumping response to light outside of the I2 neuron, through genes other than those required for the response of the ASJ neuron to light.

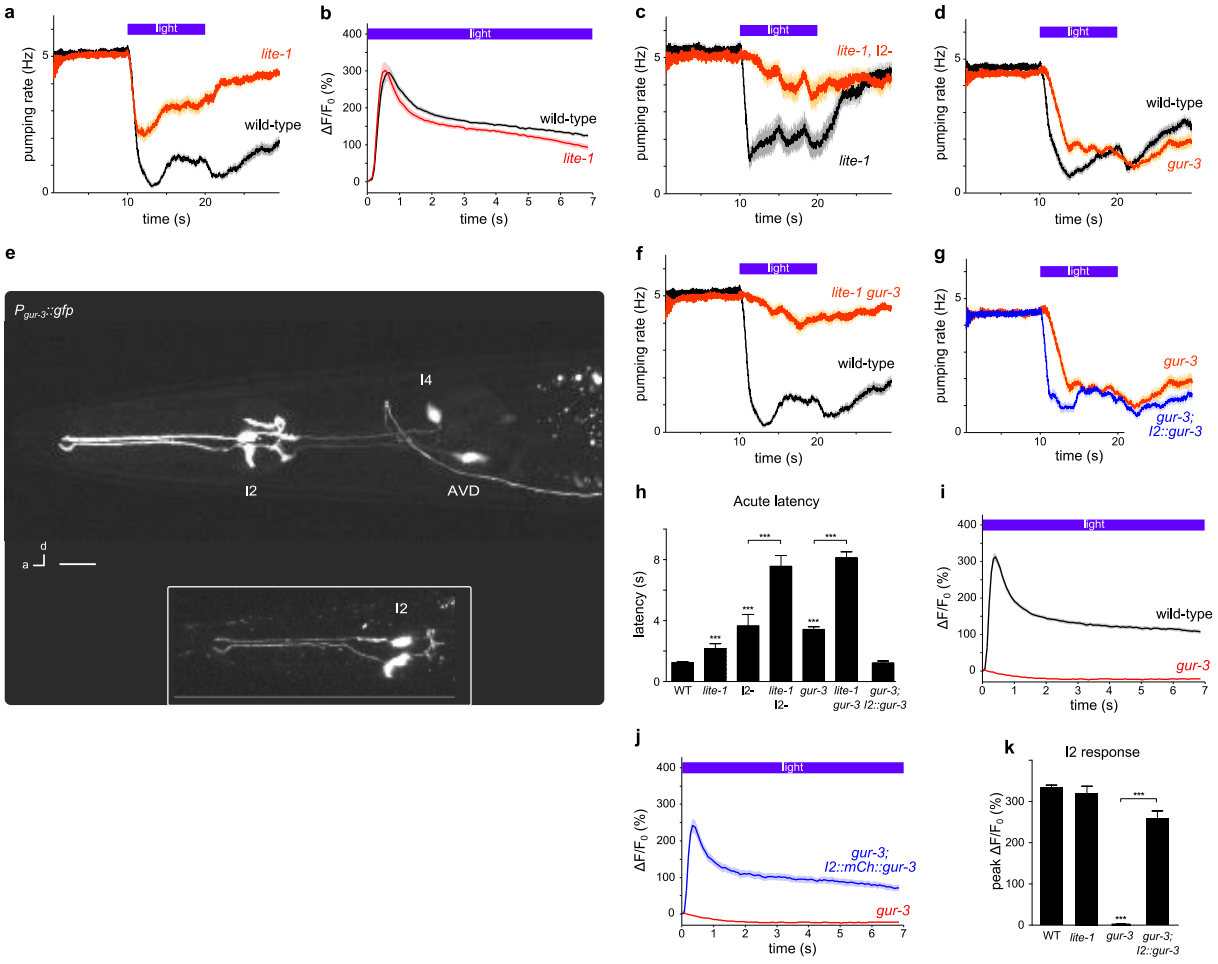

Figure 5.7: Light activates I2 through its gustatory receptor homolog GUR-3

a, Mutants of *lite-1(ce314)* had defects in the acute and sustained pumping responses to light. n = 60.
b, Mutants of *lite-1* had a normal calcium response to light in I2. n ≥ 20.
c, Genetic ablation of I2 in *lite-1* mutants caused a nearly complete defect in the pumping response to light. n = 20.
d, Mutants of *gur-3(ok2245)* had a delayed pumping response to light. n = 60.
e, *gur-3* is expressed in I2, I4 and AVD, as indicated by a $P_{gur\text{-}3}$*::gfp* transgene. Variable PVC expression in the tail is not shown. Inset: mCherry-tagged *gur-3* was localized in all three compartments of I2 (soma, anterior neurite, posterior neurite). Scale bar = 10 µm.
f, *lite-1 gur-3* double mutants had nearly no pumping response to light, substantially enhanced over the single mutants. n = 60.
g, I2-specific *gur-3* expression restored normal pumping response latency in *gur-3* mutants. n = 60.
h, Quantification of acute response latency for traces shown. n ≥ 20.
i, Mutants of *gur-3* were completely defective in the I2 response to light. n ≥ 22.
j, I2-specific *gur-3* expression restored the I2 response to light in *gur-3* mutants. n = 24.
k, Quantification of the peak response of I2 to light. n ≥ 20.
b, i-k, The posterior neurite of I2 was analyzed. *** p < 0.001, t-test. Statistical tests compared mutants to the wild type, unless drawn otherwise. "I2" in transgene refers to $P_{flp\text{-}15}$. "I2-" refers to genetic ablation using *nIs569*. Light shading around traces and error bars indicate s.e.m.

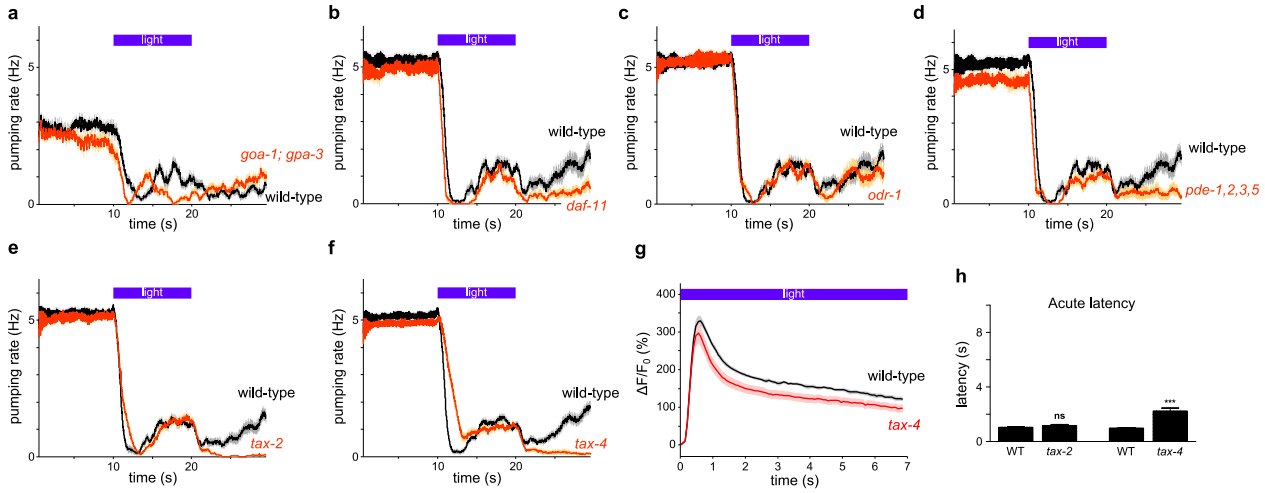

Figure 5.8: Genes that function downstream of *lite-1* are generally not required for the feeding response to light

a, Mutants of the G proteins *goa-1* and *gpa-3* had a grossly normal feeding response.
b, Mutants of the guanylyl cyclase *daf-11* had a grossly normal feeding response.
c, Mutants of the guanylyl cyclase *odr-1* had a grossly normal feeding response.
d, Mutants of the phosphodiesterases *pde-1,2,3,5* had a grossly normal feeding response.
a-d, n = 20.
e, Mutants of the cGMP-gated ion channel *tax-2(p671)* had a slight latency defect, but that defect was not significant. n = 40.
f, Mutants of the cGMP-gated ion channel *tax-4(p678)* exhibited a latency defect. n = 60.
g, Mutation of *tax-4* results in a grossly normal calcium response in I2. n ≥ 20.
h, Quantification of acute response latency of *tax-2* and *tax-4*.
*** p < 0.001, ns = not significant, t-test. Light shading around traces and error bars indicate s.e.m.

To identify genes that function in the I2 pathway, we tested other members of the *lite-1* family of receptors (Figure 5.9). While mutants of *egl-47(n1081)* and *gur-4(ok672)* had a normal light-induced pumping response (data not shown), mutants of *gur-3(ok2245)*, the closest *lite-1* paralog, exhibited an increased latency similar to that of I2-ablated worms (Figure 5.7d, h). The *ok2245* mutation deletes 1,208 bases, inserts two bases immediately after the first exon and is predicted to result in a premature stop codon. Another deletion mutant, *ok2246*, also exhibited an increased latency in its response to light (data not shown). Strikingly, *lite-1 gur-3* double mutants were nearly completely defective in all phases of the pumping response to light (Figure 5.7f, h), indicating that the *lite-1* and *gur-3* pathways function together to control essentially the

entire response. Genetic ablation of I2 in the *gur-3* mutant did not enhance the pumping defect, indicating that I2 and *gur-3* likely function in the same pathway (Figure 5.10). To identify candidate cells in which *gur-3* might function, we examined the expression pattern of *gur-3* using a transcriptional reporter ($P_{gur\text{-}3}$*::gfp*) and observed expression in the I2, I4 and AVD neurons (Figure 5.7e), with variable expression in the PVC neuron (data not shown). I4 has no published function, while AVD is a command motor neuron for stimulus-dependent reversal and PVC is a command motor neuron for stimulus-dependent forward acceleration (Chalfie..Brenner 1985). To test whether *gur-3* acts in I2 for the pumping response to light, we generated a transgenic strain that expressed a fluorescence-tagged GUR-3 specifically in I2 ($P_{flp\text{-}15}$*::mCherry::gur-3*) (Figure 5.7e, inset). I2-specific expression of *gur-3* rescued the latency defect of *gur-3* mutants (Figure 5.7g, h), indicating that *gur-3* functions cell-autonomously in I2.

Since *gur-3* is required for I2 function in light-induced feeding inhibition, we examined whether *gur-3* is required for the I2 calcium response. We found that *gur-3* mutants completely lacked the I2 calcium response to light and that this response was restored by I2-specific expression of *gur-3* (Figure 5.7i-k), indicating that *gur-3* functions in I2 upstream of its calcium response.

To assess whether *gur-3* can endow a neuron with light-sensing ability, we examined its effect when expressed in a neuron that normally does not express *gur-3*. Because our GCaMP3 transgene was also expressed in the PHA tail neuron, we noticed that PHA also responds to light, albeit with a longer latency than that of I2 (1.4 s; Figure 5.11a). This response depended entirely on *lite-1* (Figure 5.11b). In the absence of *lite-1*, *gur-3* expression in PHA was able to restore its response to light (Figure 5.11c). This finding establishes that GUR-3 misexpression can make cells light-responsive.

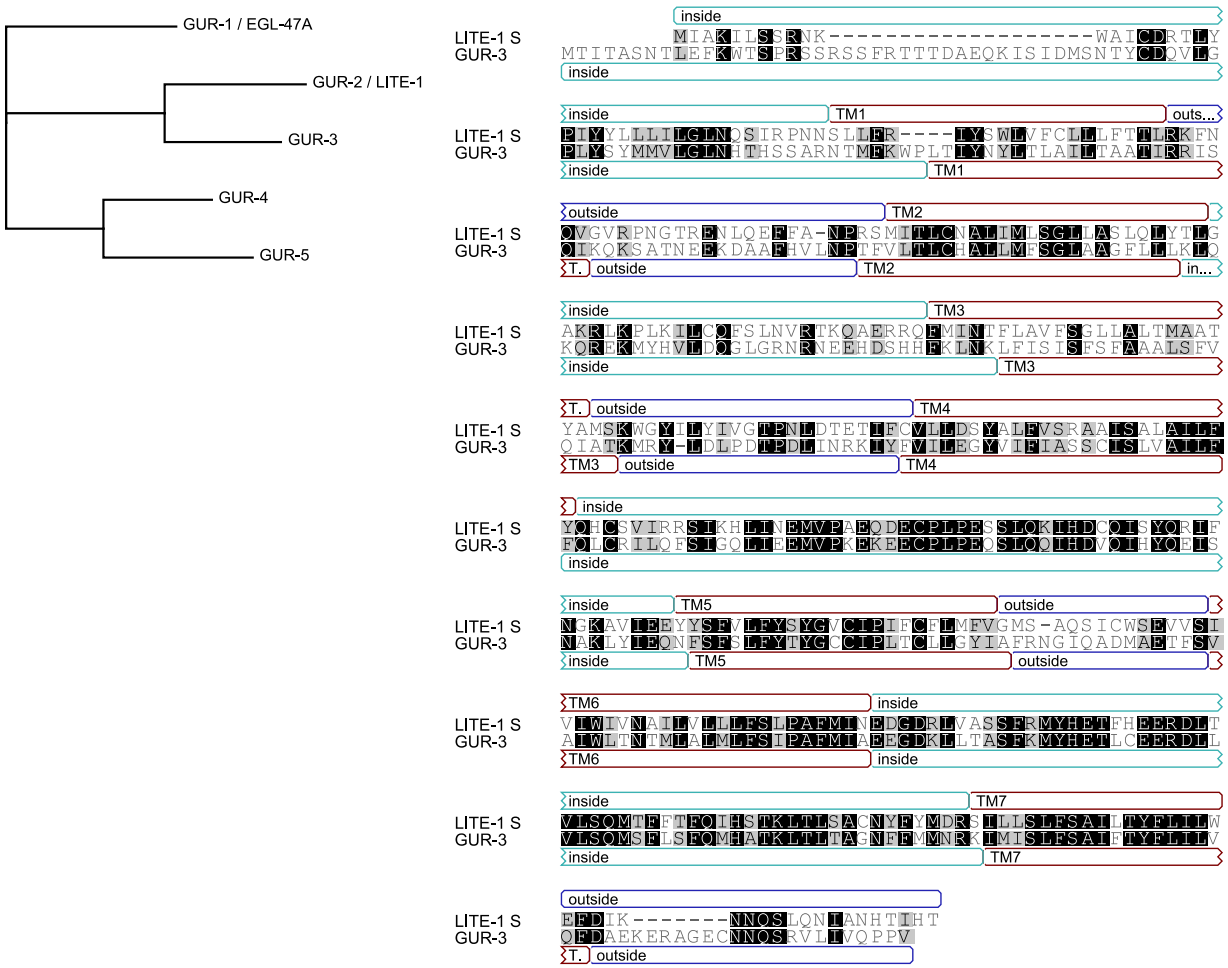

Figure 5.9: The presumptive gustatory receptor family in *C. elegans*

Five paralogs of the *Drosophila* gustatory receptor family are present in the worm genome. The tree was generated using Geneious (Biomatters), and the alignment was generated using ClustalW. A black box indicates amino acid identity, and a grey box indicates amino acid similarity, as defined by a Blosum55 score matrix with a threshold of 1. Amino acid sequences are from WormBase. LITE-1S has been described (Liu..Xu 2010). Transmembrane predictions are from TMHMM (http://www.cbs.dtu.dk/services/TMHMM/). LITE-1S and GUR-3 are 41% identical.

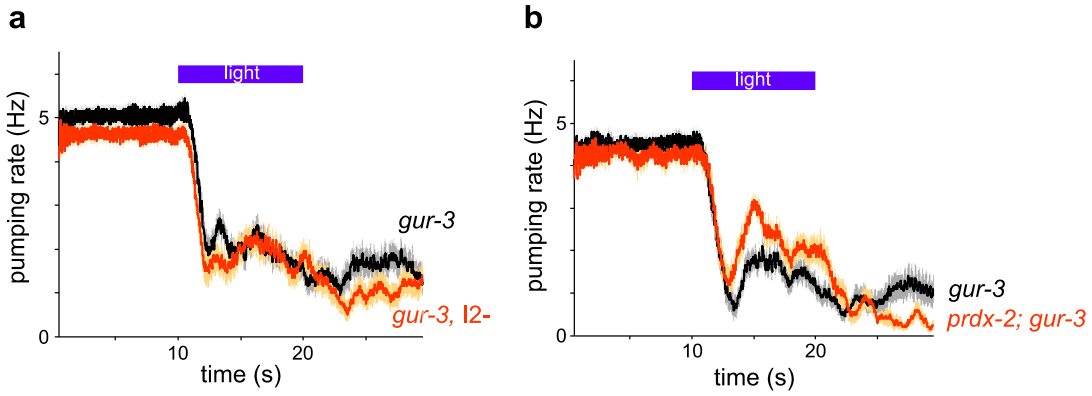

Figure 5.10: The I2 neuron, *gur-3* and *prdx-2* likely function in the same pathway

a, Genetic ablation of I2 in *gur-3(ok2245)* mutants did not enhance the defect of *gur-3* single mutants.
b, *prdx-2; gur-3* double mutants exhibited a latency defect similar to that of *gur-3* single mutants. n = 20. Light shading around traces indicates s.e.m.

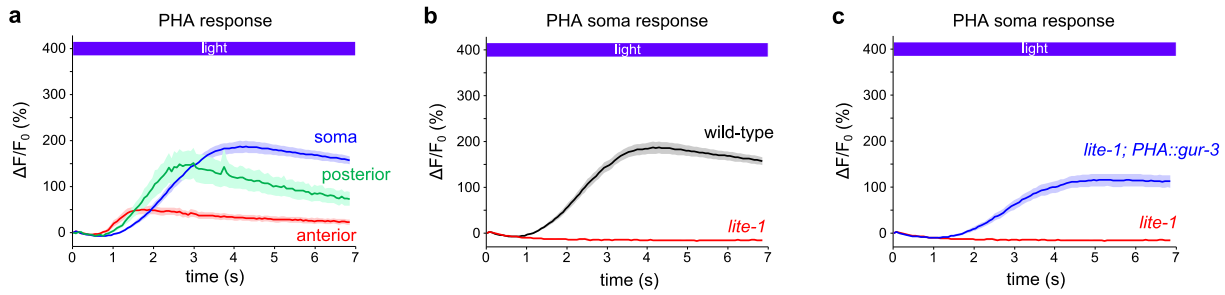

Figure 5.11: *gur-3* misexpression in PHA causes PHA to respond to light

a, Calcium increased in all three compartments of PHA in response to light (485 nm, 26 mW/mm^2) using the $P_{flp\text{-}15}$*::gcamp3* transgene. n = 13.
b, The PHA response required *lite-1*. n ≥ 13.
c, PHA-specific *gur-3* expression ($P_{flp\text{-}15}$*::mCherry::gur-3*) restored the light-induced PHA calcium response in *lite-1* mutants. n ≥ 14. Light shading around traces indicates s.e.m.

F. Hydrogen peroxide elicits similar responses via identical mechanisms

The light used in these experiments was substantially brighter (4x-100x) than sunlight ( ). We found that sunlight was also able to inhibit feeding (Figure 5.12), although not as effectively as the bright light used in the experiments described above. Since light can generate

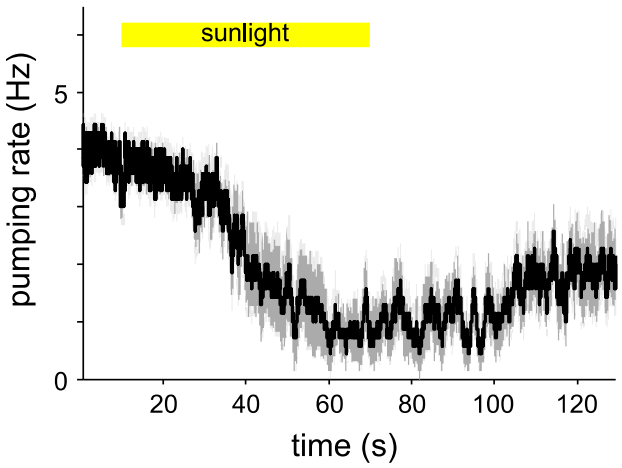

Figure 5.12: Sunlight inhibits feeding

Pumping of wild-type worms during exposure to direct sunlight for indicated interval (60 s). Sunlight power was measured to be 0.006 mW/mm^2 over 359-371 nm. n = 7. Light shading around traces and error bars indicate s.e.m.

hydrogen peroxide in water (Richardson 1893, Bedford 1927, Blum 1932), especially in the presence of biological photosensitizers such as riboflavin, tryptophan and tyrosine (McCormick..Eisenstark 1976, Wang & Nixon 1978), we hypothesized that *C. elegans* might be responding to hydrogen peroxide when exposed to light. When we provided worms with vapor from hydrogen peroxide liquid (9 M), they exhibited a behavioral response strikingly similar to that elicited by light: they stopped pumping and reversed their locomotion to avoid the source of H_2O_2 (Figure 5.13a, f, g). Dosage analysis of the response to liquid hydrogen peroxide revealed that H_2O_2 inhibited feeding at concentrations as low as 10 µM and caused avoidance at concentrations as low as 10 mM (Figure 5.13f, g). 100 µM to 1 mM hydrogen peroxide is toxic to C. elegans (Jansen..Schnabel 2002), and light can generate 1 µM to 15 mM hydrogen peroxide in solution, depending on photosensitizer concentration and exposure duration (McCormick..Eisenstark 1976, Wang & Nixon 1978, Imlay 2008). Taken together, the sensitivity of *C. elegans* to hydrogen peroxide appears likely to be physiologically relevant.

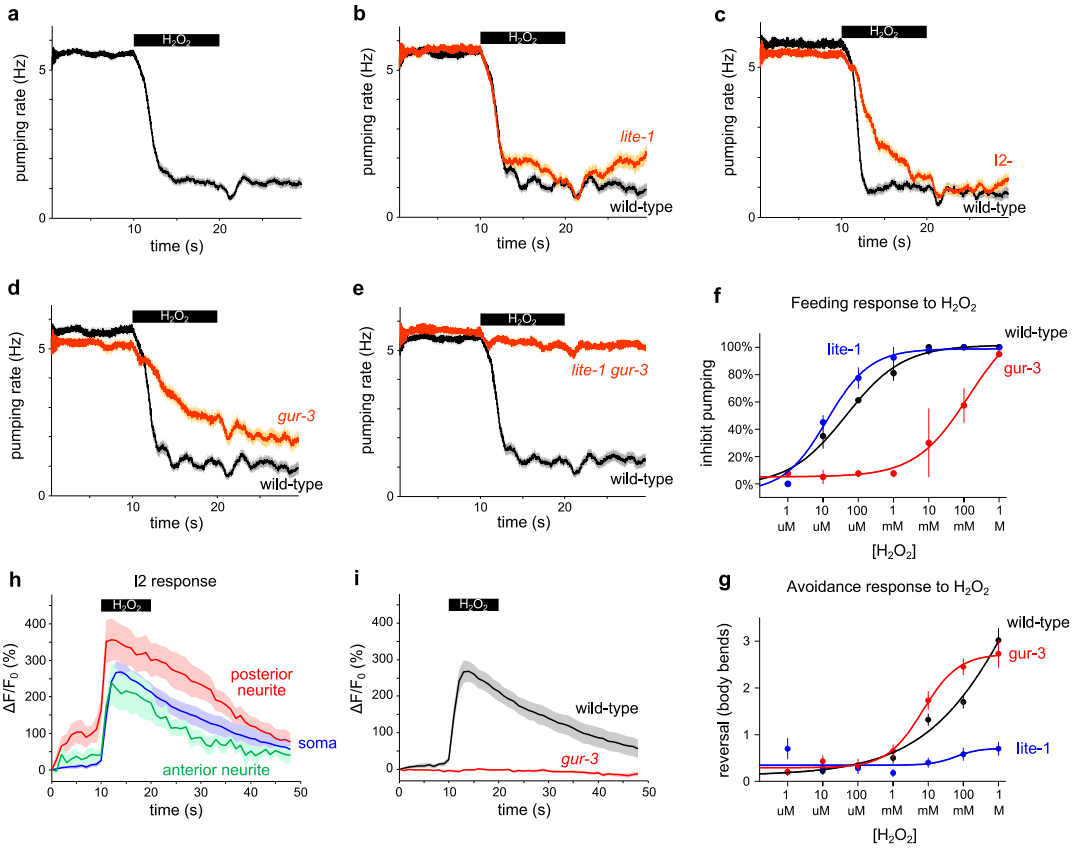

Figure 5.13: Hydrogen peroxide is sensed through the same pathway as light

a, Vapor emitted by hydrogen peroxide (9 M) inhibited feeding by wild-type worms.
b, *lite-1* mutants inhibited feeding like wild-type worms.
c, Genetic ablation of I2 resulted in an acute latency defect in response to H_2O_2 vapor.
d, *gur-3* mutants exhibited an acute defect in response to H_2O_2 vapor.
e, *lite-1 gur-3* double mutants were nearly completely defective in the feeding response to H_2O_2 vapor. **a-e,** $n \geq 60$.
f, Dose response curve to liquid H_2O_2 indicating that concentrations as low as 10 µM inhibited feeding of wild-type worms. *lite-1* mutants showed no defect, while *gur-3* and I2-ablated worms showed a reduced sensitivity to hydrogen peroxide.
g, Dose response curve to liquid H_2O_2, indicating that concentrations as low as 10 mM induced reversals of wild-type worms. *lite-1* mutants were severely defective, and *gur-3* mutants were not defective. **f, g,** $n \geq 20$.
h, All three compartments of I2 responded to H_2O_2 vapor (9 M).
i, The I2 neuron failed to respond in *gur-3* mutants. Plot shows I2 soma only, but all three compartments failed to respond in *gur-3* mutants. **h,i,** $n = 10$.
Light shading around traces and error bars indicate s.e.m.

We sought to determine whether *lite-1* or the I2 pathway, including *gur-3*, was responsible for the inhibition of pumping in response to hydrogen peroxide. As with light, *lite-1* mutants failed to avoid hydrogen peroxide (Figure 5.13g). However, they continued to inhibit

pumping in response to hydrogen peroxide (Figure 5.13b, f). Worms lacking the I2 neurons exhibited a latency defect strikingly similar to that observed in response to light (Figure 5.13c). *gur-3* mutants also exhibited a defective acute response to hydrogen peroxide (Figure 5.13d). Furthermore, the *lite-1 gur-3* double mutant was nearly completely defective in the feeding response to hydrogen peroxide (Figure 5.13e), indicating that *lite-1* also functions in the feeding response to hydrogen peroxide.

We imaged calcium in I2 using GCaMP3 to determine if the neuron acutely responded to hydrogen peroxide vapor. As with light, the I2 neuron showed an acute increase in calcium in response to hydrogen peroxide (Figure 5.13h). As with light, *gur-3* was required for the I2 calcium increase in response to hydrogen peroxide (Figure 5.13i). Taken together, these results indicate that light- and hydrogen peroxide-sensing rely on the same signal transduction mechanisms.

G. The antioxidant enzyme peroxiredoxin *prdx-2* functions in I2 for sensing light

Given a possible role for hydrogen peroxide in the mechanism of light-sensing, we next tested antioxidant genes that might function in this response. Peroxiredoxins are an evolutionarily conserved family of antioxidant enzymes that contain a redox-active cysteine directly oxidized by hydrogen peroxide (Rhee..Bae 2012, Neumann..Manevich 2009, Hofmann..Flohe 2002, Wood..Karplus 2003, Wood..Poole 2003). The *C. elegans* genome encodes three peroxiredoxins: *prdx-2*, *prdx-3* and *prdx-6*. While *prdx-3(gk529)* and *prdx-6(tm4225)* mutants were normal in their response to light (data not shown), the *prdx-2(gk169)* mutant had a delayed acute response similar to that caused by *gur-3* mutation and I2 ablation

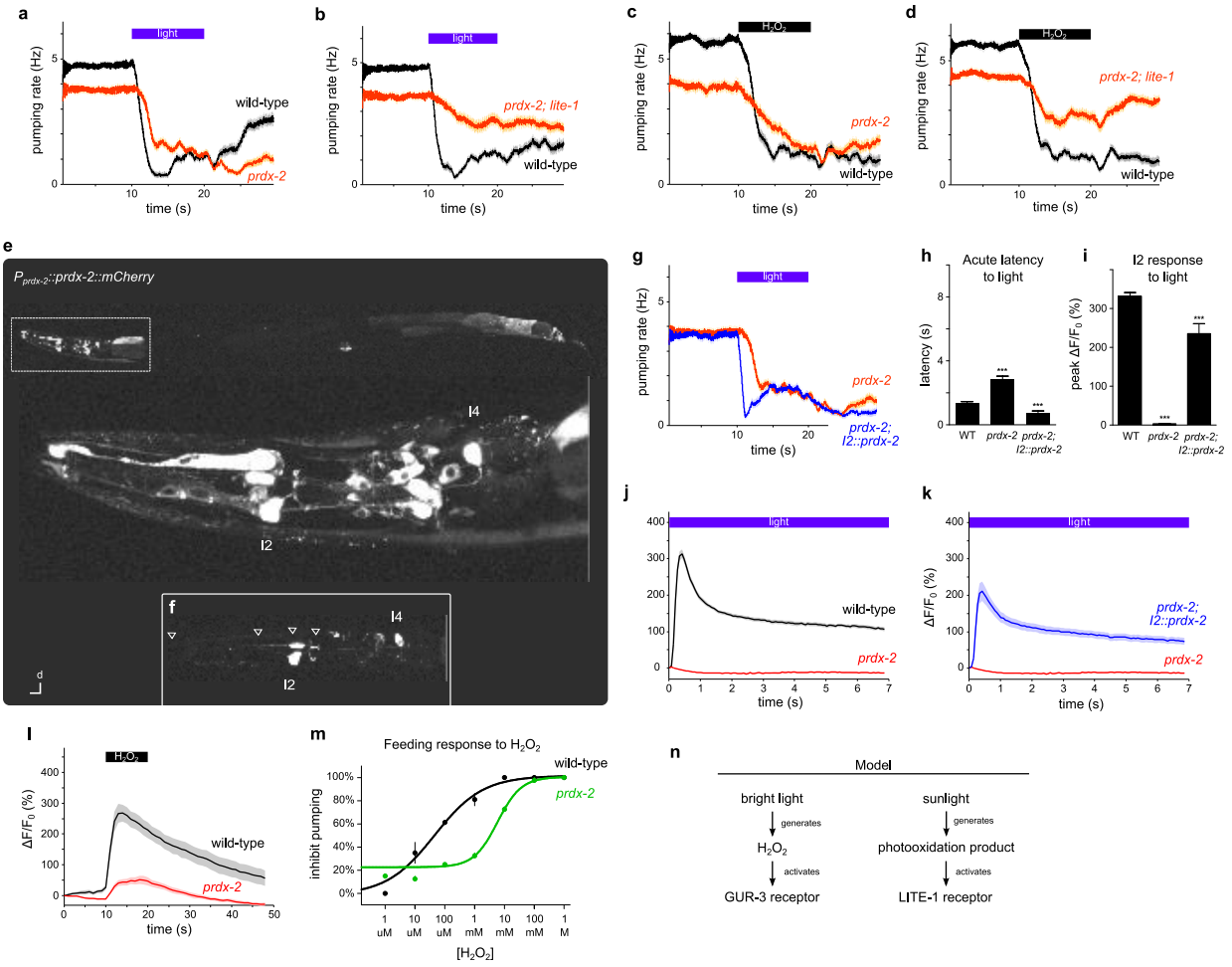

Figure 5.14: Light activates I2 through its peroxiredoxin PRDX-2

a, *prdx-2(gk169)* mutants had a delayed pumping response to light. **b,** *prdx-2; lite-1* double mutants had nearly no pumping response to light, substantially enhanced over the single mutants. **c,** *prdx-2* mutants were defective in the acute pumping response to hydrogen peroxide. **d,** *prdx-2; lite-1* double mutants were defective in both the acute and sustained phases of the pumping response to hydrogen peroxide. **a-d,** $n \geq 60$. **e,** *prdx-2* showed a broad expression pattern, as indicated by a functional P_{prdx-2}*::prdx-2::mCherry* transgene with mosaic transmission: I2 and I4, intestinal cells, muscles, epithelial cells, and additional unidentified neurons. The head is magnified in the middle of the panel to show the multitude of neurons and other cells that expressed *prdx-2*, including I2 and I4. **f,** Inset: mCherry-tagged *prdx-2* was localized in all three compartments of I2. Arrowheads point to two parts of the anterior neurite, the soma, and the posterior neurite. Scale bar = 50 µm (top), 12 µm (middle), 25 µm (inset). **g,** I2-specific *prdx-2* expression restored normal pumping response latency in *prdx-2* mutants. n = 60. **h,** Quantification of acute response latency to light of wild-type, *prdx-2* and I2-specific *prdx-2* rescued animals. **i,** Quantification of the peak response of I2 to light. $n \geq 22$. **i-k,** The posterior neurite of I2 was analyzed. **j,** Mutants of *prdx-2* were completely defective in the I2 response to light. $n \geq 22$. **k,** I2-specific *prdx-2* expression restored the I2 response to light in *prdx-2* mutants. $n \geq 23$. **l,** Mutants of *prdx-2* were substantially defective in the I2 soma response to hydrogen peroxide vapor (9 M). **m,** *prdx-2* mutants were defective in the pumping response to hydrogen peroxide liquid. **n,** Model for how hydrogen peroxide and light might interact with the GUR-3 and LITE-1 receptors. *** $p < 0.001$, t-test. Statistical tests compared mutants to the wild type and rescued animals to mutants. Light shading around traces and error bars indicate s.e.m.

(Figure 5.14a). *C. elegans* PRDX-2 is 72% identical to human PRDX1 and PRDX2.1. Like the *lite-1 gur-3* double mutant, the *prdx-2; lite-1* double mutant was severely defective in the feeding response to light, substantially enhanced over either single mutant (Figure 5.14b). The *prdx-2; gur-3* double mutant did not enhance the latency defect of the *gur-3* single mutant, indicating that *prdx-2* and *gur-3* likely function in the same pathway (Figure 5.10). As with light, the *prdx-2* mutant was defective in the acute response to hydrogen peroxide vapor (Figure 5.14c), and the *prdx-2; lite-1* double mutant was severely defective in all aspects of the pumping response to hydrogen peroxide (Figure 5.14d). *prdx-2* mutants were also defective in the response to liquid hydrogen peroxide, though not as severely as *gur-3* mutants (Figure 5.14m). Examination of the expression pattern of *prdx-2* using a rescuing translational reporter ($P_{prdx\text{-}2}$*::prdx-2::mCherry*) revealed expression in a broad set of tissues: I2, I4 and intestine (as previously reported (Isermann..Bruchhaus 2004)), as well as expression in muscle (pharyngeal muscle 1, vulval muscle, body wall muscle), epithelial cells (e1, e3), and many neurons in the head and tail (Figure 5.14e, f). To test whether *prdx-2* acts in I2 for the pumping response to light, we generated a transgenic strain that expresses *prdx-2* cDNA specifically in I2 ($P_{flp\text{-}15}$*::prdx-2 cDNA*). I2-specific expression of *prdx-2* rescued the latency defect of *prdx-2* mutants (Figure 5.14g, h), indicating that *prdx-2* functions in I2 for the pumping response to light.

Since *prdx-2* is required for the function of I2 in light-induced pumping inhibition, we examined whether *prdx-2* is also required for the I2 calcium response. We found that *prdx-2* mutants completely lacked the I2 calcium response to light and that this response was restored by I2-specific expression of *prdx-2* (Figure 5.14i-k). *prdx-2* mutants also showed a defective I2 response to hydrogen peroxide (Figure 5.14l). Taken together, these results show that the

conserved antioxidant *prdx-2* functions in I2 to facilitate its response to both light and hydrogen peroxide.

H. Discussion

By analyzing feeding behavior by the eyeless *C. elegans*, we have identified a sensory pathway that is shared for the detection of light and hydrogen peroxide. We found that the presumptive G protein-coupled taste receptor GUR-3 acts in light and H_2O_2 signal transduction and functions in the I2 neuron to endow it with light- and H_2O_2-sensitivity. *gur-3* is homologous to *C. elegans lite-1* and *Drosophila Gr28b.b*, both of which were previously known to be required for light-avoidance behavior (Edwards..Miller 2008, Xiang..Jan 2010). In addition, we showed that *lite-1* functions in the worm's feeding response to light and the feeding and avoidance responses to hydrogen peroxide.

In *Drosophila*, gustatory receptors have been shown to detect a variety of chemicals, including sugars (*Gr5a* and *Gr64a*) (Chyb..Carlson 2003, Dahanukar..Carlson 2007), bitter compounds (*Gr66a*) (Moon..Montell 2006), and carbon dioxide (*Gr21a* and *Gr63a*) (Jones..Vosshall 2007, Kwon..Carlson 2007). Light can generate hydrogen peroxide in water, and this effect is enhanced with photosensitizers known to be present in biological systems (Richardson 1893, Bedford 1927, Blum 1932, McCormick..Eisenstark 1976, Wang & Nixon 1978, Hockberger..White 1999). We propose a model in which members of the LITE-1/GUR-3 family of presumptive gustatory receptors function as redox sensors, not as direct light sensors (Figure 5.14n). The physiological function of GUR-3 is likely to be as a hydrogen peroxide sensor, since it mediates feeding inhibition in response to low concentrations of H_2O_2 (10 µM). Under bright light, however, GUR-3 can also function indirectly as a light sensor by sensing the

hydrogen peroxide produced by light. On the other hand, the physiological function of LITE-1 is unlikely to be as a hydrogen peroxide sensor, since it mediates avoidance in response to much higher concentrations of H_2O_2 (10 mM). Since LITE-1 is required for avoiding sunlight-level intensities of light (Edwards..Miller 2008, Ward..Xu 2008, Liu..Xu 2010, Xiang..Jan 2010), we propose that LITE-1's physiological function is to detect a redox product produced by light other than hydrogen peroxide. Overall, these studies demonstrate a novel mechanism by which light can be sensed.

We also identified a role for the PRDX-2 peroxiredoxin in light- and H_2O_2-sensing. Peroxiredoxins are enzymes directly oxidized by hydrogen peroxide (Rhee..Bae 2012, Neumann..Manevich 2009, Hofmann..Flohe 2002, Wood..Karplus 2003, Wood..Poole 2003). While it is conceivable that peroxiredoxin acts as an oxidation sensor and signals the presence of light and H_2O_2, we favor a model in which peroxiredoxins do not function in acute signaling but rather function to reduce an oxidized compound produced in the sensory pathway for light and H_2O_2, such as an oxidized ligand or receptor. In this way PRDX-2 could maintain the system's sensitivity to light and H_2O_2 by reducing an oxidized signaler.

Prolonged exposure to light will kill the worm (Ward..Xu 2008), so avoiding light is an effective survival strategy. But why should the worm interrupt its feeding as well? Based on our work, we hypothesize that light generates H_2O_2 or another redox product that is toxic to the worm. Sensing that it is in a harsh environment, the worm stops feeding to prevent ingestion of this toxic compound. Occasionally we observed bubbles emerging from the worm’s mouth during the pumping rebound response. This observation suggests that not only does the worm stop ingestion, but it also reverses the flow of liquid in the pharynx, using a gag reflex to expel a toxic compound and preserve the integrity of its internal organs.

I. Methods

a. Strains

The following worm strains were used:

N2 (“wild-type”)
MT21421 *nIs569[P_{flp-15}::csp-1b cDNA, P_{ges-1}::gfp]*
MT21650 *nIs575[P_{flp-15}::gcamp3; lin-15(+)]; lin-15(n765)*
MT21772 *unc-13(s69); nIs575; lin-15(n765)*
MT21644 *nIs575; unc-31(u280); lin-15(n765)*
MT20722 *lite-1(ce314)*
MT20515 *goa-1(n1134); gpa-3(pk35)*
MT4589 *odr-1(n1936)*
DR47 *daf-11(m47)*
TQ1828 *pde-1(nj57) pde-5(nj49); pde-3(nj59); pde-2(tm3098)*
PR671 *tax-2(p671)*
PR678 *tax-4(p678)*
MT21570 *nIs575; lite-1(ce314) lin-15(n765)*
MT2248 *egl-47(n1081)*
RB845 *gur-4(ok672)*
MT21783 *gur-3(ok2245)*
MT21793 *lite-1(ce314) gur-3(ok2245)*
MT21910 *lin-15(n765); nEx2065[P_{gur-3}::gfp, lin-15(+)]*
MT21785 *nIs575; gur-3(ok2245) lin-15(n765)*
MT22166 *gur-3(ok2245) lin-15(n765); nEx2144[P_{flp-15}::mCherry::gur-3, lin-15(+)]*
MT22201 *nIs575; gur-3(ok2245) lin-15(n765);*
nEx2173[P_{flp-15}::mCherry::gur-3, $P_{unc-122}$::dsRed]
MT21791 *lite-1(ce314) nIs569*
MT21790 *gur-3(ok2245) nIs569*
VC1151 *prdx-3(gk529)*
FX04225 *prdx-6(tm4225)*
VC289 *prdx-2(gk169)*
MT21898 *prdx-2(gk169); lite-1(ce314)*
MT22174 *prdx-2(gk169); lin-15(n765); nEx2078[P_{prdx-2}::prdx-2::mCherry, lin-15(+)]*
MT22177 *prdx-2(gk169); lin-15(n765); nEx2155[P_{flp-15}::prdx-2 cDNA, lin-15(+)]*
MT21899 *prdx-2(gk169); nIs575; lin-15(n765)*
MT22186 *prdx-2(gk169); nIs575; lin-15; nEx2162[P_{flp-15}::prdx-2 cDNA, $P_{unc-122}$::dsRed]*
MT22080 *prdx-2(gk169); gur-3(ok2245)*

b. Molecular biology

We used the following primers to amplify DNA for generating transgenes by standard cloning and PCR fusion procedures. For PCR fusion, the appropriate overlapping region was appended to these primers. For cDNA, wild-type mixed-stage poly-A RNA was used as template.

P_{flp-15}: TGAACTTTCCTCATTTCCCCTTCGTTC,
GACGAGGTGTATGTGGGAGACC
csp-1b cDNA: ATGCCGAGAACGGACGCC,
TTACATCGACCTTGAAAAGTGCCAT
P_{gur-3}: GCCTGATGGAACACACTTCCAAC,
CAACGTATTCGACGCTGTTATCGTC
gur-3: ATGACGATAACAGCGTCGAATACGTT,
GTTTACCCCGTCTCTATTTCCGCTTTG
P_{prdx-2}*::prdx-2*: TGAAGCATTTGCAAGAAAGCTCGAC,
GTGCTTCTTGAAGTACTCTTGGCTTTC
prdx-2 cDNA: ATGTCGAAAGCATTCATCGGAAAGC,
CGGTTATCAAGCAATTTCATGAATTTCAGAATTTC

The molecular lesion of *gur-3(ok2245)* was identified by Sanger sequencing. The deletion lies in the interval including GTAAGTTCACTGGAATGAAC to TGTTTCCTATTAGTATGGTG, which covers from the first base after the first exon to the 4th intron. The sequence TT is inserted in this interval. We used the following primers for genotyping (L = left, OL = outer left, IL = inner left, OR = outer right, IR = inner right):

gur-3(ok2245): L: ATGACGATAACAGCGTCGAATACGTT
OR: GAAACTAGTTCGTTTTTAGGAAATTGAGACTGTC
IR: CAAAAACCATGTATTCTTTGTGCGATTTTCATG
prdx-2(gk169): OL: CATGTCTCTCGCTCCAAAGGTGC
OR: GTGATGGGTCGATGATGAAGAGTCC
IL: CGCTCTCCAATTTTGCCAATGTATTTC
IR: GCCTTGAACTCCTCAGCACGG

c. Behavioral response to light

Worms were maintained at 20 °C. 40-80 larval stage 4 (L4) or young adult worms were picked the night before to a 6 cm Petri dish filled with nematode growth medium (NGM) seeded

with OP50 *E. coli* bacteria [1]. Worms were assayed the next day at 22.5 °C or room temperature as 1-day-old adults. For the response to light, pumping was scored by eye using a stereo dissecting microscope set to 120x magnification and illuminated with a halogen transmitted light source (Zeiss Lumar and KL 2500 LCD, 3100 K). Custom Matlab software (Supplementary Software) recorded the timing of pumps as indicated by manual key presses and controlled by a shutter (via Zeiss EMS-1 controller) that presented and removed mercury arc epi-illumination (HBO 100). The epi-illumination irradiated the whole body of the worm with a spot diameter of approximately 2 mm. The assay began with a baseline period of 10 s, followed by 10 s of arc illumination, followed by 10 s without arc illumination. We used a modified CFP filter set (Zeiss Lumar 47 HE CFP 486047) to illuminate 436 ± 13 nm violet light at an intensity of 13 mW/mm^2, and we observed pumping with a long-pass GFP emission filter. Each worm was tested once, unless its neurons had been ablated with a laser. After ablation, each worm was assayed 1-4 times with at least several minutes allowed for recovery between assays. For the response to sunlight, we took the worms outside on a clear, sunny day in the month of October (13-16 °C). The sun's intensity was measured to be 0.005 mW/mm^2 from 359-370 nm, which is near the ASTM G17303 global tilt reference [2] of 0.008 mW/mm^2. At the start of the assay, the dissecting microscope was oriented so that the optics mounting pole cast a shadow on the worm. After 10 s the microscope was rotated so that the worms were exposed to direct sunlight for 60 s. Then the microscope was rotated back to the shadow position for the remaining 60 s. To assess the spectral sensitivity of the pumping response, we used a different setup. Worms were placed on an NGM agar pad on a coverslip and observed using an inverted microscope with a 20x air objective (Zeiss Axiovert S 100). Monochromatic arc illumination emitted 350, 400, 450, 500, and 550 ± 8 nm light onto the worms, and intensity was varied (Till Photonics Polychrome V,

150 W xenon bulb). A custom dichroic mirror was manufactured to reflect light across this range and transmit wavelengths greater than 600 nm (Chroma). Custom Matlab software controlled the Polychrome light source, and pumping was assayed by eye with the same protocol as used with the dissecting microscope. Discrete pumping events were averaged using a 1 s forward moving average to generate average traces. Light power was measured using a laser power meter (Coherent FieldMate). Light avoidance was qualitatively scored if a worm either increased its speed or reversed in response to light.

d. Behavioral response to hydrogen peroxide

The pumping response to H_2O_2 vapor was scored in a manner similar to that used to score the pumping response to light. Pumping was scored by eye using the custom software described above. H_2O_2 vapor was administered from a pulled glass needle loaded into a nanoliter injector (World Precision Instruments Nanoliter 2000, Micro4 controller). 30% H_2O_2 (8.82 M) was loaded into the needle. After 10 s, the needle was brought to the head of the worm, and after 10 s, it was removed. For the behavioral response to H_2O_2 liquid, drops of varying concentrations (1 µM - 1 M) diluted in M9 were placed near the head of the worm while it was feeding on food. The drop flowed to cover part of the head such that H_2O_2 was sucked into the pharynx. The pumping response to H_2O_2 liquid was scored by observing whether pumping was inhibited in the following 10 s. The avoidance response to H_2O_2 liquid was scored as the number of smooth reversal body bends beginning immediately following the placement of the drop. All observations were made by eye using a macroscope (Wild Makroskop M420).

e. Behavioral statistics

For the pumping response, the acute response latency for a single trial is the time of the first missed pump relative to the onset of light. Notationally, t_i is the time of the i^{th} pump, l_i is the latency between the i^{th} and $i+1^{th}$ pump, and $\bar{l}$ is the mean latency for a set of pumps. To calculate the acute response latency, we calculated $\bar{l}_{pre-light}$ for the first 10 s prior to light onset and compared that to the latencies (l_j) observed during the following 10 s of light, in temporal order. For the first $l_j > 2\bar{l}_{pre-light}$, the acute response latency was calculated as

$$acute\ response\ latency = t_j - t_{light\ on} + \bar{l}_{pre-light}$$

where t_j is the time of the last pump with a pre-light latency and $t_{light\ on}$ is the time that light was turned on. The acute response amplitude is the rate of pumping in the first 3 s following the first missed pump normalized to the pre-light pumping rate. More formally, acute response amplitude was calculated as

$$acute\ response\ amplitude = \frac{n_{post-miss}/3}{n_{pre-light}/10}$$

where $n_{post-miss}$ is the number of pumps in the 3 s after the acute response latency after light onset and $n_{pre-light}$ is the number of pumps during the first 10 s of the experiment prior to light exposure. The sustained response amplitude is the rate of pumping in the 10 s after light removal divided by the rate of pumping in the 10 s before light onset. Amplitude measurements are represented as percentages.

f. Laser ablation

We used a pulsed nitrogen laser to conduct laser microsurgery of individual pharyngeal neurons (Laser Science, Inc. VSL-337 attached to a Zeiss Axioplan)[3]. The laser passed through

a dye cell containing coumarin ([5 mM] in methanol), which shifted the wavelength from 337 nm to 435 nm. Worms were immobilized by 10 mM sodium azide and mounted on an agar pad between a coverslip and slide and examined through a 100x oil objective. Control animals experienced the same handling, except they were not exposed to the laser. In general, ablations were done on larvae of stage 1 or 2 (L1 or L2) and cells were identified based on nucleus location as observed by Nomarski differential interference contrast optics. Worms were placed on NGM plates following ablation for recovery. The next day, larvae were remounted to examine whether the intended ablation was successful. We confirmed that the cell either looked damaged, appeared as a refractile corpse, or was absent, compared to mock-ablated controls. For ablations in which we cut the anterior or posterior neurite of I2, cutting was confirmed by observing an absence of GCaMP3 fluorescence where the neurite is normally located and presence in the soma. On the following, day adults were assayed for their pumping or I2 calcium response to light by exposing them to bright violet light (436 nm, 13 mW/mm^2) as described above.

g. Calcium imaging

To study the calcium response of the I2 neuron, we generated a transgenic strain expressing GCaMP3 specifically in I2 and PHA, a neuron in the tail (*Pflp-15::gcamp3*). To assay the response to light, worms were immobilized using the friction provided by 0.10 µm polystyrene beads (Polysciences, Inc. #00876) on 10% agarose in M9 (Kim..Fang-Yen 2013). The slide was imaged using an inverted microscope (Zeiss Axiovert S 100) with a monochromatic xenon light source set to emit at 485 nm (Till Photonics Polychrome V). Via a 40x air objective, an electron multiplying charge coupled device (EMCCD) camera recorded the

changes in I2 or PHA fluorescence (Andor iXon+). In our standard assay, the worm was simultaneously imaged and stimulated with 26 mW/mm^2 blue light for 7 s, and videos were recorded at full resolution (1002x1004), 15 fps (temporal resolution of 66 ms), and 8-bit pixel depth. For the I2 spectral analysis, the power of 485 nm light was reduced (2 mW/mm^2) so that it failed to stimulate the I2 response. A specific wavelength was presented for 2 s, followed by low-power imaging light, which allowed us to record the response of I2 to different wavelengths. For spatial analysis, we used a laser-scanning confocal microscope (Zeiss LSM 510) to selectively stimulate regions of the head with the 488 nm emission from a 25 mW argon laser. Videos were recorded at low resolution (128x128) so that a high frame rate could be sustained (5 fps). A 40x water objective was used. Worms were imaged for 2 s at 2% laser power, then a region of interest (ROI) was stimulated for 0.16 s (axon), 0.12 s (soma), or 0.62 s (dendrite) at 100% laser power, followed by imaging for 8 s. Duration of exposure for ROIs varied as their areas varied, with each pixel in each ROI exposed for the same duration. The same software was used for analysis. To assay the response to H_2O_2, worms were glued to NGM agar pads (Meridian Surgi-lock 2oc). The exposure time per frame was increased (200 ms, 5 fps). Worms were exposed to the vapor of 30% H_2O_2 (8.82 M) loaded into a glass needle, as described for the behavioral assay above. After 10 s, the needle was lowered near the nose of the worm, and after 10 s was removed. To analyze calcium-imaging videos, video frames were aligned using Fiji's StackReg plug-in. Videos were analyzed for changes in fluorescence using manually drawn ROIs in a custom Matlab program. The fluorescence change in each compartment (anterior neurite, soma, posterior neurite) was calculated as

$$\frac{\Delta F}{F_0}(t) = \frac{F(t) - F_{bg}(t)}{F(0) - F_{bg}(0)} - 1$$

where F is the mean pixel value in an ROI and F_{bg} is the mean pixel value in a background ROI to control for bleaching. F/F_0 is represented as a percentage.

h. Expression analysis

Gene expression was examined using transgenes with either the promoter fused to a fluorescent protein or the full gene product fused to a fluorescent protein. For $P_{gur\text{-}3}$*::gfp*, $P_{flp\text{-}15}$*::mCherry::gur-3*, and $P_{prdx\text{-}2}$*::prdx-2::mCherry*, 40 optical sections (each 1 µm thick) were taken using a laser-scanning confocal microscope (Zeiss LSM 510), and a maximum axial projection was used to generate a single image.

Chapter 6:

Independent Neural Circuits Coordinate a Behavioral Sequence in *C. elegans*

In preparation for publication

Authors: Nikhil Bhatla, Rita Droste, Anne Huang, Bob Horvitz

A. Abstract

Neural cells are specialized for the rapid and spatially-targeted signaling required for effective coordination of behavior. In the presence of food, the nematode *Caenorhabditis elegans* feeds at a high rate, and exposure to UV light immediately alters this feeding rhythm. By studying the worm's feeding response to light, here we identify a pattern of neural function in which neurons appear to act independently to control sequential phases of a behavior. In the first phase, light rapidly inhibits feeding, with the I2 neuron sensing light and releasing glutamate likely onto pharyngeal muscle, where it is received by the AVR-15 glutamate-gated chloride channel. In the second phase, the inhibition of feeding is maintained via a circuit that includes the extrapharyngeal neuron RIP and pharyngeal neurons I1 and MC. Finally, in the third phase, light stimulates pharyngeal contractions via the M1 neuron. These three circuits appear to be independent, because eliminating one circuit does not cause a disruption in the behavioral effects controlled by the other two circuits. We conclude that what initially appeared to be a simple reflex is instead a sequence of behavioral responses coordinated by independent neural circuits, suggesting a motif we term "parallel temporal tiling."

B. Introduction

Animals are easily distinguished from other types of life by their ability to rapidly coordinate motor behavior. Simple reflexes, such as the crayfish tail-flip escape (Edwards..Krasne 1999), allows the animal to avoid aversive conditions, and more complex motor sequences, such as the stereotyped song of the zebra finch (Fee..Hahnloser 2004) and vocal communication by humans (Kuhl 2004), facilitate social behavior. Motor coordination relies on the proper functioning of neural circuits, and neural circuit malfunction can lead to loss

of motor control, such as that exhibited in Parkinson's disease (Stern..Ilson 1983). While reflex arcs serve as the neural mechanism for simple reflexes (Lundberg 1979), we have a poor understanding of how neural circuits direct motor sequences of greater complexity.

To gain insight into the neural control of motor sequences, we selected a behavioral response in the nematode *C. elegans* for further study. *C. elegans* is an ideal system for analyzing neural circuits because (a) its nervous system is numerically simple, with only 302 neurons, and (b) its connectome (the set of all connections between all neurons) has been described (Albertson & Thomson 1976, White..Brenner 1986, Bhatla 2011). Moreover, neural circuits in *C. elegans* and other invertebrates can be understood in a "gap-free" manner: sensory neurons can be identified and the transmitted signal can be observed as it is transferred from neuron to neuron until it reaches muscle (Chalfie..Brenner 1985, Chalasani..Bargmann 2007, Piggott..Xu 2011, Kocabas..Ramanathan 2012, Olsen & Wilson 2008, Ruta..Axel 2010). Such an end-to-end understanding is far more difficult to achieve in neural systems of greater complexity, such as in mammals. We relied on single-cell ablation techniques (Fang-Yen..Avery 2012), neural activity imaging (Tian..Looger 2009), and the numerical simplicity and connectome of *C. elegans* to analyze how the nervous system coordinates the sequence of behaviors that constitute the worm's response to light.

We previously observed that UV light interrupts the feeding rhythm of the worm and concluded that light likely generates a redox product that is toxic to the worm (p. 115). In an effort to reduce toxic exposure caused by light, the worm inhibits feeding and avoids the light. We showed that the I2 neuron acts as a sensor of light and hydrogen peroxide and reduces the latency of feeding inhibition in response to light (p. 115). Here, we identify glutamate as the neurotransmitter secreted by I2 and show that the AVR-15 glutamate receptor functions in

pharyngeal muscle to control feeding, suggesting that the neural circuit in which I2 functions is monosynaptic. Furthermore, we identify four neuron classes that appear to function in two additional neural circuits to control later aspects of the feeding response to light. The RIP and I1 neurons likely function through the pacemaker neuron MC to promote the amplitude of feeding inhibition, suggesting that the neural circuit in which they function is polysynaptic. Finally, the M1 neuron stimulates pharyngeal contractions, likely to expel material from the pharynx. These components appear to function independently to control different aspects of the behavioral response. These results suggest that the motor sequence induced by light is controlled by neural circuits that implement "parallel temporal tiling," a motif where neurons independently control separate temporal phases of a behavioral sequence.

C. The I2 neuron secretes glutamate and the AVR-15 glutamate receptor functions in pharyngeal muscle

C. elegans ingests bacterial food through its pharynx, where it crushes the bacteria and transports it into its intestine for further digestion and nutrient absorption. The feeding process can be quantified by recording the frequency of grinder movement (called a "pump"), which can be viewed under a dissecting microscope. In the presence of food, worms pump between 4 and 5 times per second (4-5 Hz). The pharyngeal nervous system consists of only 20 neurons in 14 classes, and systematic laser ablation previously identified the M4 (Avery & Horvitz 1987), MC (Avery & Horvitz 1989) and M3 (Avery 1993) motor neurons as being critical for different aspects of normal feeding. Interested in how additional neurons might modify the feeding rhythm in response to a stimulus, we focused on studying the effect that light has on the feeding rhythm (p. 115). Short wavelength light (436 nm, 13 mW/mm^2) alters feeding in three distinct

phases. First, pumping rapidly stops in response to light (the "acute" response, 0-3 s after light onset). Second, pumping subsequently increases in the presence of light (the "rebound" response, 5-10 s after light onset). Third, pumping remains reduced even after light is removed (the "sustained" response, 0-10 s after light removal) (Figure 6.1a). We previously identified the I2 neuron as being activated by light to reduce the latency of the acute response (p. 115), and we sought additional components functioning in this pathway.

To provide insight into the source of calcium for I2 activation, we tested mutants that disrupt calcium influx. We tested mutants of voltage-gated calcium channels (VGCCs): *egl-19* (α_1 subunit, L-type) (Jospin..Allard 2002), *unc-2* (α_1 subunit, N/P/Q-type) (Mathews..Snutch 2003), *cca-1* (α_1 subunit, T-type) (Steger..Avery 2005), *unc-36* ($\alpha_2\delta$ subunit) (Huang..Bargmann 2007) and *tag-180* ($\alpha_2\delta$ subunit); non-specific cation channels: *unc-77/NALCN* (Yeh..Zhen 2008) and *nca-2/NALCN* (Jospin..Schuske 2007); and endoplasmic reticulum channels: *unc-68/RYR* (Maryon..Anderson 1996) and *itr-1/ITPR* (Baylis..Sattelle 1999). All mutants exhibited a normal acute response to light, though several had rebound and sustained responses different than that of the wild type (Figure 6.1b,c,e,f, Figure 6.2). We focused our attention on the acute response, because loss of I2 results in an acute response defect (Figure 6.8b). To examine these mutants in a more sensitive assay, we tested their calcium response to light in I2. Although most mutants had a normal I2 calcium response to light, we found that mutants carrying nonsense alleles of *unc-2(e55)* and *unc-36(e251)* exhibited a partial defect: the response was delayed by ~400 ms (~200 ms for wild-type vs. ~600 ms for *unc-2*) and the response peak was ~50% that of the wild type (Figure 6.1g, h, j, k). To see if the partial defects could be enhanced, we generated an *unc-36; unc-2* double mutant. The *unc-36; unc-2* double mutant was no more defective in the I2 calcium response than the *unc-2* single mutant (Figure 6.1i-k), suggesting that *unc-2* and *unc-36*

function in the same pathway for the calcium response of I2. Interestingly, the *unc-36; unc-2* double mutant did show a higher latency for the acute feeding response (Figure 6.1d-f). Taken

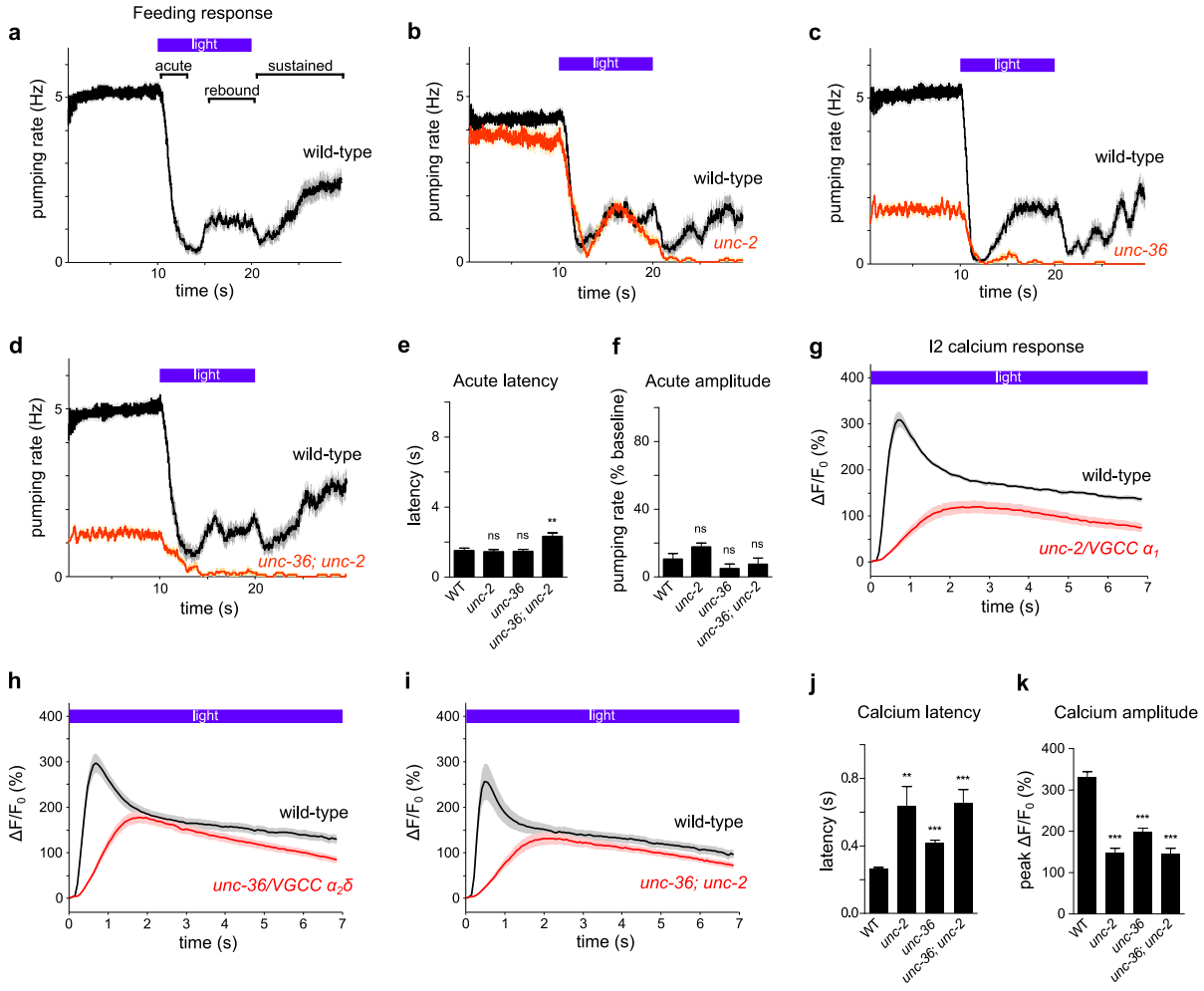

Figure 6.1: The UNC-2 and UNC-36 voltage-gated calcium channels are partially required for the light-induced calcium response of I2

a, Pumping response to light of the wild-type, with the acute, rebound, and sustained responses labeled.
b, *unc-2(e55)* mutants showed a normal acute pumping response to light.
c, *unc-36(e251)* mutants showed a normal acute pumping response to light.
d, *unc-36; unc-2* double mutants were enhanced over the single mutants and exhibited a latency defect in the acute pumping response.
e, Quantification of the acute response latency.
f, Quantification of the acute response amplitude. $n \geq 19$.
g, *unc-2* mutants were partially defective in the calcium response of I2.
h, *unc-36* mutants were partially defective in the calcium response of I2.
i, *unc-36; unc-2* mutants were not enhanced over the single mutants in the calcium response of I2.
j, Quantification of the latency of the calcium response.
k, Quantification of the peak calcium response.
*** $p < 0.001$, ** $p < 0.01$, ns = not significant, t-test. Light shading around traces and error bars indicate s.e.m.

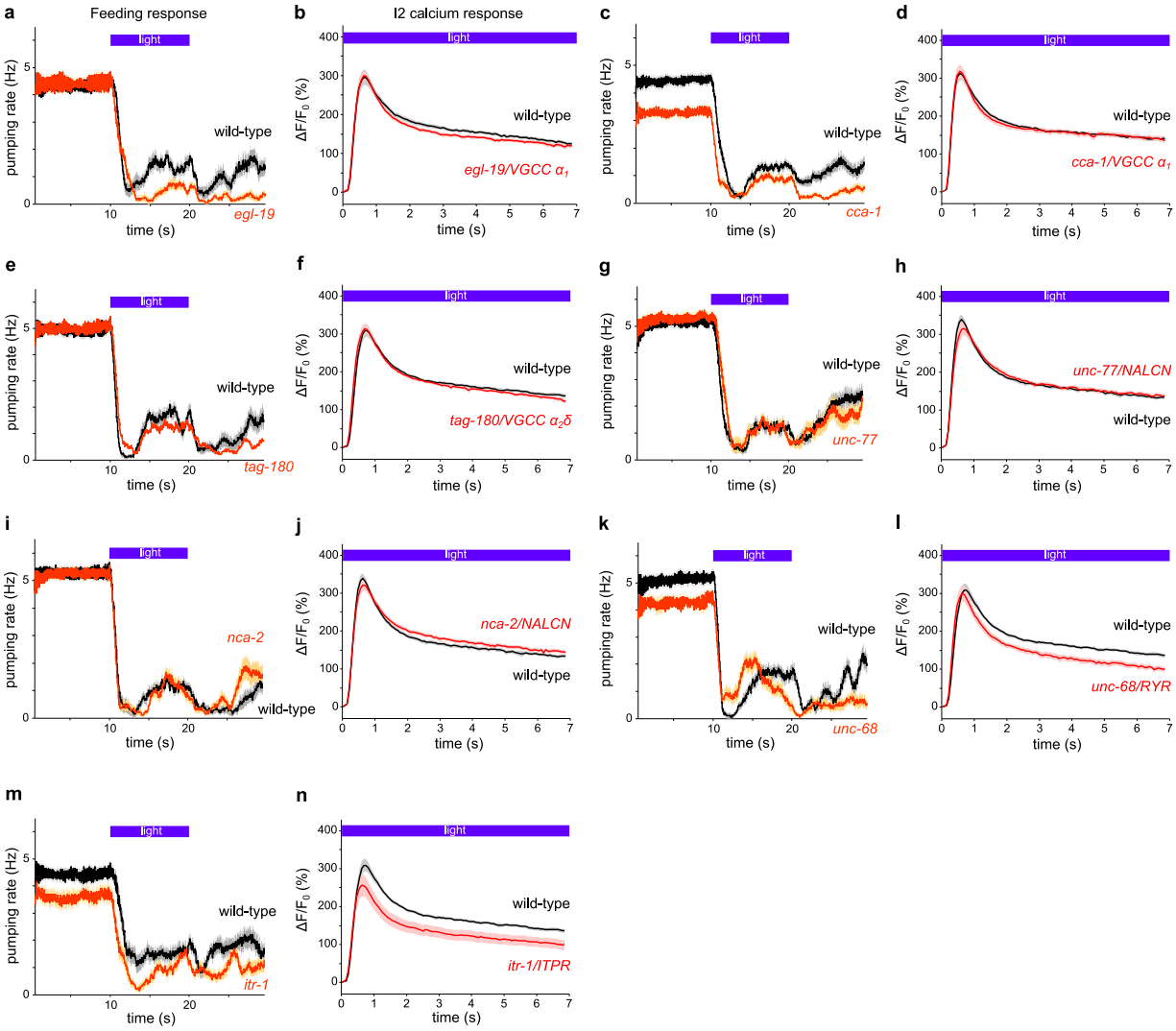

Figure 6.2: Calcium channel mutants that exhibited a normal acute pumping response and a normal I2 calcium response to light

a, *egl-19(n582)/VGCC* mutants showed a normal acute pumping response to light.
b, *egl-19* mutants showed a normal calcium response in I2.
c, *cca-1(ad1650)/VGCC* mutants showed a normal acute pumping response to light.
d, *cca-1* mutants showed a normal calcium response in I2.
e, *tag-180(ok779)/VGCC* mutants showed a normal acute pumping response to light.
f, *tag-180* mutants showed a normal calcium response in I2.
g, *unc-77(gk9)/NALCN* mutants showed a normal acute pumping response to light.
h, *unc-77* mutants showed a normal calcium response in I2.
i, *nca-2(gk5)/NALCN* mutants showed a normal acute pumping response to light.
j, *nca-2* mutants showed a normal calcium response in I2.
k, *unc-68(e540)/RYR* mutants showed a grossly normal acute pumping response to light.
l, *unc-68* mutants showed a normal calcium response in I2.
m, *itr-1(sa73)/ITPR* mutants showed a grossly normal acute pumping response to light.
n, *itr-1* mutants showed a grossly normal calcium response to light. $n \geq 20$.
All calcium data reflect the calcium change in the posterior neurite of I2. Light shading around traces indicate s.e.m.

together, *unc-2* and *unc-36* are partially required for the I2 calcium response to light.

To identify the neural circuit in which I2 functions, we sought to determine the neurotransmitter that I2 secretes. Like mammalian neurons, worm neurons signal via the primary neurotransmitters glutamate (Lee..Avery 1999), GABA (Schuske..Jorgensen 2004) and acetylcholine (Rand 2007) as well as the biogenic amines serotonin and dopamine; functions have also been shown for the trace amines octopamine and tyramine (Chase & Koelle 2007). While most neurotransmitter mutants showed a grossly normal feeding response, mutants defective in glutamate neurotransmission due to mutation in a vesicular glutamate transporter (*eat-4/VGLUT*) were defective in the acute response to light (Figure 6.3a, Figure 6.4). Specifically, mutants carrying a deletion in *eat-4(ky5)* exhibited a severe defect in the latency and amplitude of the acute response (Figure 6.3e, f). To show that this defect was caused by the mutation in *eat-4*, we assayed a strain carrying a genomic *eat-4* transgene (*njEx378[*$P_{eat\text{-}4}$*::eat-4::gfp]*) (Ohnishi..Mori 2011). This transgene fully rescued the defect of *eat-4* mutants (Figure 6.3b, e, f). We also tested multiple alleles of *eat-4* and found a similar defect (data not shown), indicating that mutation of *eat-4* caused the acute response defect observed in *eat-4* strains.

To determine whether *eat-4* is expressed in the I2 neuron and might function there, we examined transgenic worms carrying a translational fusion of *eat-4* driven by its endogenous 5.5 kb promoter (*njEx378*) (Ohnishi..Mori 2011). We observed *eat-4* expression in the I2 neuron (Figure 6.3c), indicating that I2 is likely glutamatergic. To demonstrate a function for *eat-4* in I2, we used an I2-specific promoter (Kim & Li 2004) to generate a transgenic strain that expressed *eat-4* cDNA specifically in I2 (*P*$_{flp\text{-}15}$*::eat-4 cDNA::gfp*). We found that I2-specific expression of *eat-4* partially rescued the acute latency and amplitude defects of *eat-4* worms

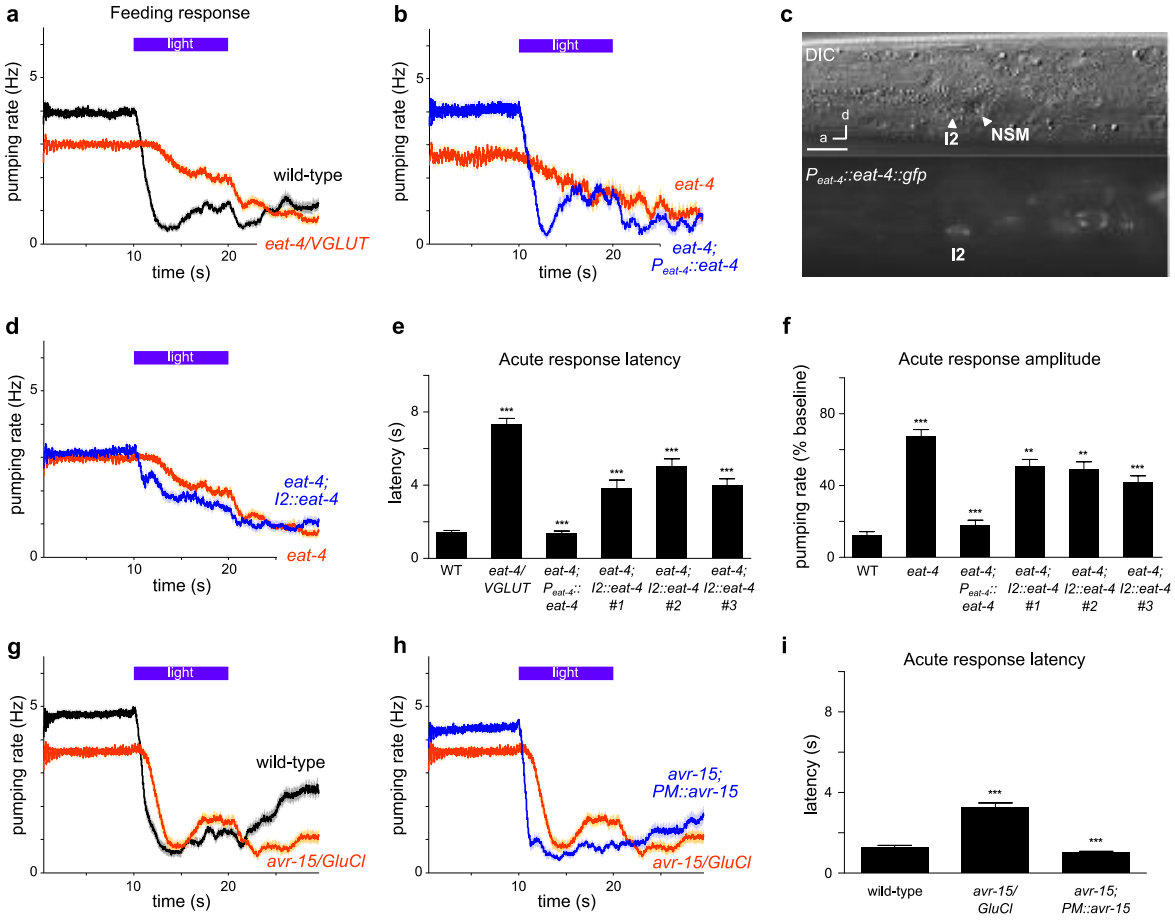

Figure 6.3: The I2 neuron secretes glutamate to rapidly block muscle contraction

a, Mutants of *eat-4/VGLUT(ky5)* were defective in the acute response to light.
b, Expression of a genomic *eat-4* fragment (*njEx378*) completely rescued the defective acute response of *eat-4* mutants.
c, Top: DIC image of an L4 worm head. Bottom: Expression pattern of *eat-4* as indicated by a transgene carrying *njEx378[P_{eat-4}::eat-4 cDNA::gfp]*. Expression was observed in the I2 neuron but not in the nearby NSM neuron. Scale bar = 10 µm. d = dorsal, a = anterior.
d, I2-specific *eat-4* expression using the P_{flp-15} promoter partially restored the acute pumping response to light in *eat-4* mutants.
e Quantification of acute response latency of wild-type, *eat-4* and rescued animals. Numbers indicate independent integrated transgenic lines.
f, Quantification of acute response amplitude of wild-type, *eat-4* and rescued animals.
g, Mutants of *avr-15/GluCl(ad1051)* had a delayed pumping response to light.
h, Pharyngeal muscle-specific *avr-15* expression restored normal pumping response latency in *avr-15* mutants. PM = pharyngeal muscle.
i, Quantification of acute response latency of wild-type, *avr-15* and pharyngeal muscle-specific *avr-15* rescue. n = 20-60 for all behavioral assays.
*** $p < 0.001$, ** $p < 0.001$, t-test. Statistical tests compared mutants to wild-type and rescued animals to mutants. Light shading around traces and error bars indicate s.e.m. "I2" promoter = P_{flp-15}, "PM" promoter = P_{myo-2}.

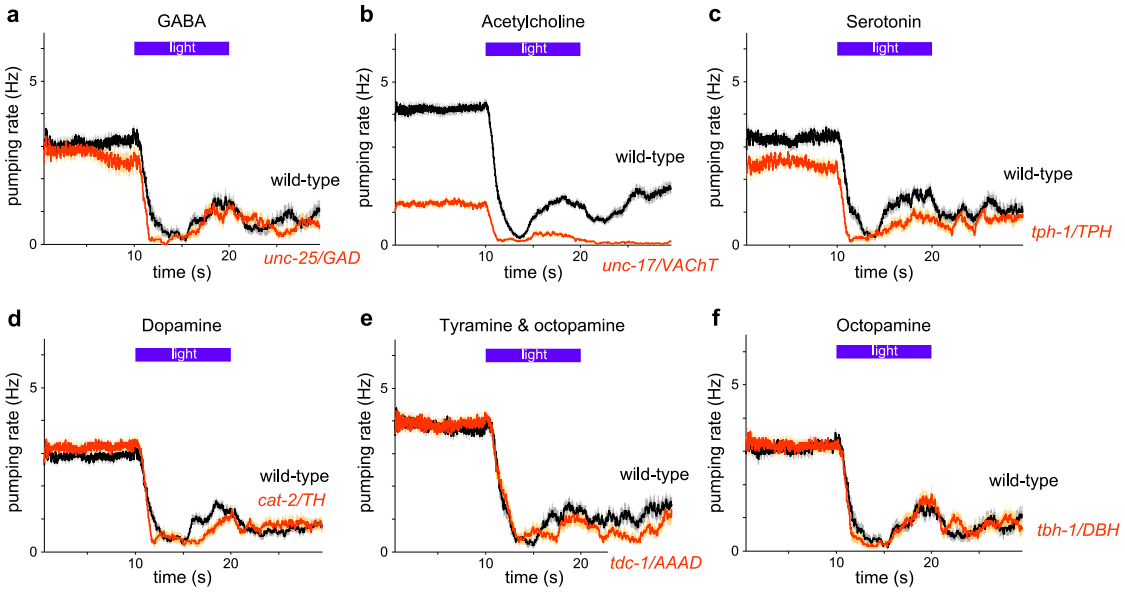

Figure 6.4: Neurotransmitter mutants that exhibited a normal acute response to light

a, *unc-25/GAD(e156)* mutants defective in GABA synthesis showed a normal pumping response to light.
b, *unc-17/VAChT(e245)* mutants defective in acetylcholine transport showed a normal acute response to light.
c, *tph-1/TPH(n4622)* mutants defective in serotonin synthesis showed a normal pumping response to light.
d, *cat-2/TH(e1112)* mutants defective in dopamine synthesis showed a normal pumping response to light.
e, *tdc-1/AAAD (n3420)* mutants defective in tyramine synthesis showed a normal pumping response to light.
f, *tbh-1/DBH(n3722)* mutants defective in octopamine synthesis showed a normal pumping response to light.
n ≥ 20. Some of these experiments were done at 20 °C instead of 22.5 °C. Light shading around traces indicate s.e.m.

(Figure 6.3d-f). This result indicates that I2 secretes glutamate in response to light and that additional glutamatergic neurons might also function in the acute response, since the defect of *eat-4* mutants is more severe than the defect caused by I2 ablation (Figure 6.8b).

Next we sought to identify the glutamate receptor that functions downstream of the I2 neuron for the acute response to light. The *C. elegans* genome encodes 19 glutamate receptors: AMPA-type cationic receptors (*glr-1* through *glr-8*) (Brockie..Maricq 2001), NMDA-type

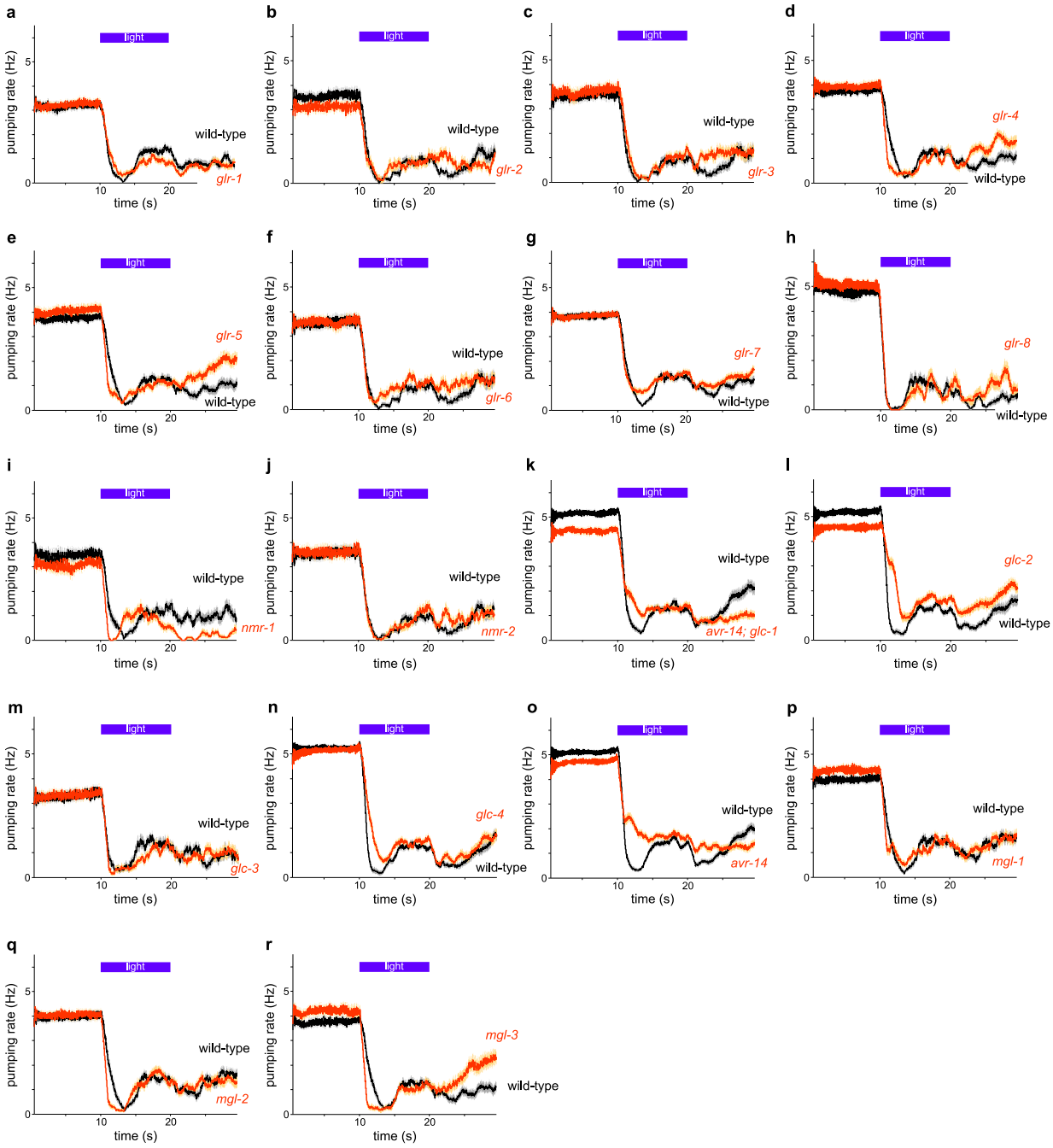

Figure 6.5: The feeding response of glutamate receptor mutants

a, *glr-1(n2461)* mutants had a normal pumping response to light.
b, *glr-2(ak10)* mutants had a normal pumping response to light.
c, *glr-3(ak57)* mutants had a normal pumping response to light.
d, *glr-4(tm3219)* mutants had a grossly normal pumping response to light.
e, *glr-5(tm3506)* mutants had a grossly normal pumping response to light.
f, *glr-6(ak56)* mutants had a normal pumping response to light.
g, *glr-7(tm2827)* mutants had a grossly normal pumping response to light.
h, *glr-8(gk283043)* mutants has a normal pumping response to light.
i, *nmr-1(ak4)* mutants has a grossly normal pumping response to light.

j, *nmr-2(ak10)* mutants had a normal pumping response to light.
k, *avr-14(ad1302); glc-1(pk54)* mutants had a defective amplitude in the acute response to light. Since *avr-14* single mutants also had an acute response defect of similar effect size (see **o**), we attributed the defect in this strain to the *avr-14* mutation.
l, *glc-2(gk179)* mutants had a latency defect in the acute response to light.
m, *glc-3(ok321)* mutants had a normal pumping response to light.
n, *glc-4(ok212)* mutants had a latency defect in the acute response to light.
o, *avr-14(ad1302)* mutants had an amplitude defect in the acute response to light.
p, *mgl-1(tm1811)* mutants had a normal pumping response to light.
q, *mgl-2(tm355)* mutants had a grossly normal pumping response to light.
r, *mgl-3(tm1766)* mutants had a grossly normal pumping response to light.
$n \geq 20$. Some of these experiments were done at 20 °C instead of 22.5 °C. Light shading around traces indicate s.e.m.

cationic receptors (*nmr-1*, *nmr-2*) (Brockie..Maricq 2001), chloride-channel receptors (GluCls: *glc-1* through *glc-4*, *avr-14*, *avr-15*) (Cully..Arena 1994), and metabotropic receptors (*mgl-1* through *mgl-3*) (Dillon..O'Connor 2006). We tested mutants for all glutamate receptors and found defective acute responses in *avr-14(ad1032)*, *glc-2(gk179)*, *glc-4(ok212)* and *avr-15(ad1051)* (Figure 6.5). Here we focus on *avr-15*. *avr-15* mutants exhibited a defect in the latency of the acute response similar to that of I2-ablated worms (Figure 6.3g, i). *avr-15* is expressed in pharyngeal muscle and functions downstream of the M3 neuron for grinder relaxation during pumping (Dent..Avery 1997). To determine whether *avr-15* functions in pharyngeal muscle for the response to light, we generated a transgenic strain that expresses *avr-15* cDNA specifically in pharyngeal muscle (Okkema..Fire 1993) ($P_{myo\text{-}2}$*::avr-15 cDNA*). We found that it completely rescued the latency defect of *avr-15* mutants (Figure 6.3h, i), indicating that *avr-15* functions in pharyngeal muscle to reduce the latency of the acute response to light.

Our findings that I2 secretes glutamate and that a glutamate receptor functions in muscle suggests that I2 signals directly to muscle after being activated by light. However, the described connectome of *C. elegans* does not include a synapse from I2 to pharyngeal muscle but identified synapses to five neurons (NSM, I4, M1, I6 and MC) and gap junctions with two partners (M1 and I1) (Figure 6.6a) (Albertson & Thomson 1976). If these neurons function as signaling posts

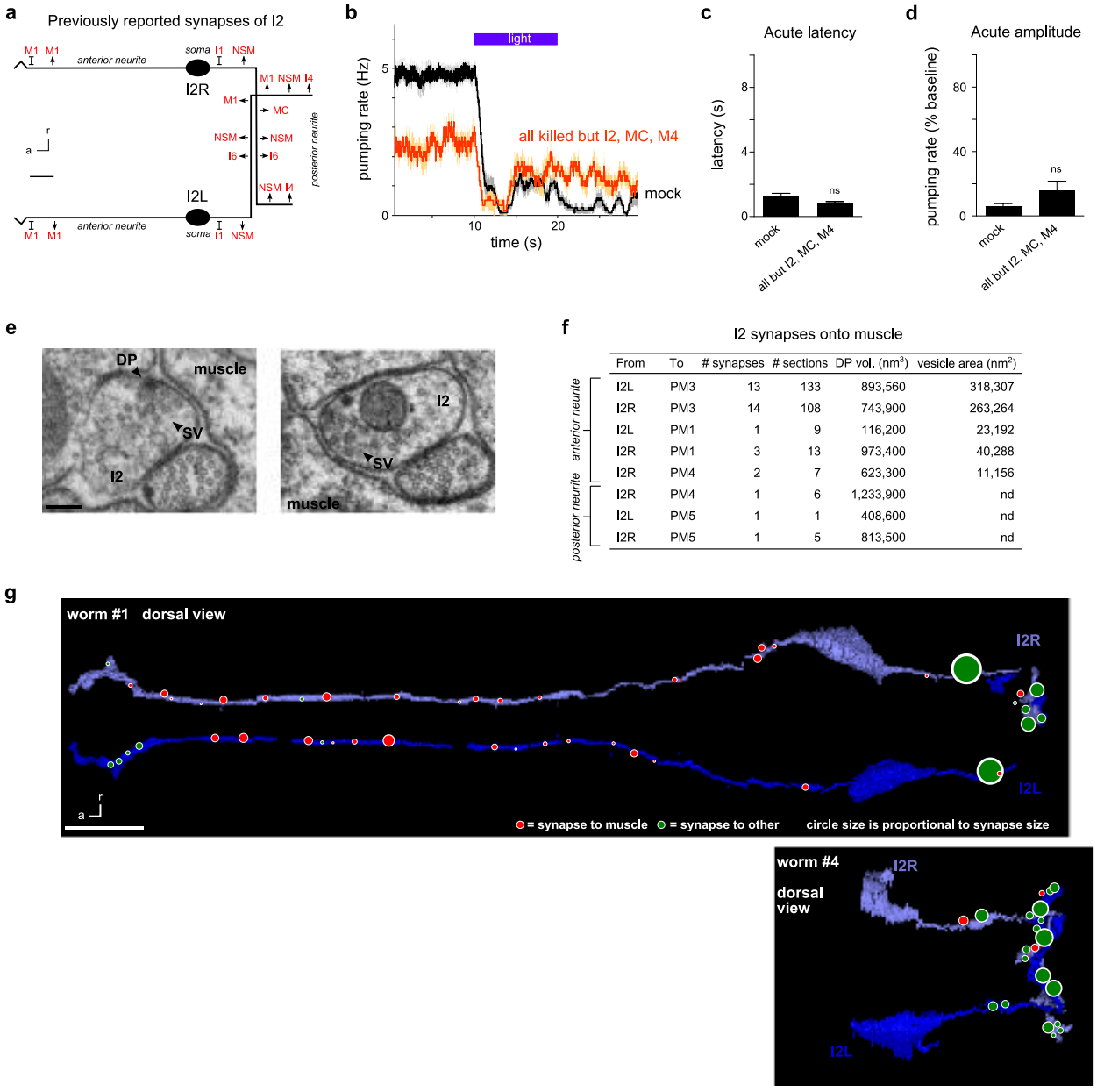

	From	To	# synapses	# sections	DP vol. (nm^3)	vesicle area (nm^2)
anterior neurite	I2L	PM3	13	133	893,560	318,307
	I2R	PM3	14	108	743,900	263,264
	I2L	PM1	1	9	116,200	23,192
	I2R	PM1	3	13	973,400	40,288
	I2R	PM4	2	7	623,300	11,156
posterior neurite	I2R	PM4	1	6	1,233,900	nd
	I2L	PM5	1	1	408,600	nd
	I2R	PM5	1	5	813,500	nd

Figure 6.6: The I2 neuron likely inhibits pharyngeal muscle directly

a, Schematic of I2 synapses previously identified (Albertson & Thomson 1976).
b, Laser ablation of all pharyngeal neurons except I2, MC and M4 did not affect the latency of the acute response. n = 2-4 worms, 6-12 trials.
c, Quantification of the acute response latency.
d, Quantification of acute amplitude.
e, Electron micrographs of two synapses from the anterior neurite of I2 to pharyngeal muscle. DP = dense projection, SV = synaptic vesicles. Scale bar = 100 nm.
f, Table showing measurements for all of the synapses identified between I2 and pharyngeal muscle (PM).

g, Morphological reconstruction of parts of four I2 neurons in two worms. Red circles indicate synapses onto muscle, and green circles indicate synapses onto other cells. Circles are scaled to synapse size. See Figure 6.7 for non-muscular synapse statistics and morphological reconstruction of the entire anterior pharynx. Dorsal view. Scale bar = 5 µm. nd = not determined. ns = not significant, t-test. Light shading around traces and error bars indicate s.e.m.

between I2 and muscle, ablating them together in single animals would be expected to phenocopy I2 ablation. We killed all pharyngeal neurons except I2, M4 and MC in individual animals. Although these worms had reduced baseline pumping, they exhibited a normal acute response to light (Figure 6.6b-d). MC was retained so that animals maintained baseline pumping greater than 1 Hz (Avery & Horvitz 1989). The absence of an effect on the acute response after removing nearly all of the synaptic partners of I2 supports the possibility that I2 signals directly with muscle, as suggested by our site-of-action analysis of *eat-4* and *avr-15*.

To further explore this possibility, we sought to identify additional synapses from I2 by reconstructing the pharynx using transmission electron micrographs of serial sections (ssTEM). We identified an area as a synapse if it contained two or more synaptic or dense-core vesicles near the plasma membrane, or a clear pre-synaptic dense projection even in the absence of any vesicles. We confirmed the previous finding of synapses onto NSM, I4 and I6, which had an average dense projection volume of nearly 1,500,000 nm^3 per synapse. Additionally, we found 13-14 synapses from the I2 neuron opposite to pharyngeal muscle 3 (PM3) and a smaller number of synapses onto pharyngeal muscles 1 (PM1), 4 (PM4) and 5 (PM5) (Figure 6.6e-g, Figure 6.7). The synapses onto pharyngeal muscle had smaller dense projections (mean volume of ~80,000 nm^3 per synapse) and were more broadly distributed, which might explain why they were not classified as synapses previously. The presence of synapses from I2 to PM3 were confirmed in a second worm (data not shown). Taken together, these results suggest that synapses from I2 directly onto pharyngeal muscle could be the sites of neurotransmission in response to light.

a

I2L chemical synapses

	Recipient	# syn. (Albertson)	# syn. (this work)	# sections	DP vol.(nm^3)	vesicle area (nm^2)
anterior neurite	PM3VL	0	13	133	893,560	318,307
	e3VL	0	14	138	700,800	332,999
	I1L	0	4	23	361,000	84,068
	PM1	0	1	9	116,200	23,192
	M1	1	1	15	0	42,168
posterior neurite	NSMR	3 (L+R)	4	39	8,838,700	nd
	I4	2	5	30	6,881,600	nd
	NSML	3 (L+R)	5	22	4,306,800	nd
	I6	1	2	17	3,918,000	nd
	M3L	0	1	5	798,300	nd
	PM5	0	1	1	408,600	nd
	M1	2	0	0	0	nd
	MCL	1	0	0	0	nd

I2R chemical synapses

	Recipient	# syn. (Albertson)	# syn. (this work)	# sections	DP vol.(nm^3)	vesicle area (nm^2)
anterior neurite	PM1	0	3	13	973,400	40,288
	PM3VR	0	14	108	743,900	263,264
	PM4VR	0	2	7	623,300	11,156
	e3VR	0	11	80	405,900	180,552
	I1R	0	3	19	106,300	36,492
	M1	1	2	24	0	59,184
posterior neurite	NSML	3 (L+R)	8	43	12,315,104	nd
	I6	1	2	18	4,849,204	nd
	NSMR	3 (L+R)	2	12	3,614,000	nd
	I4	2	3	14	2,569,900	nd
	M3R	0	1	6	2,380,100	nd
	PM4	0	1	6	1,233,900	nd
	M3L	0	1	5	813,500	nd
	PM5	0	1	5	813,500	nd
	BM	0	1	2	503,700	nd
	MCL	1	0	0	0	nd

b

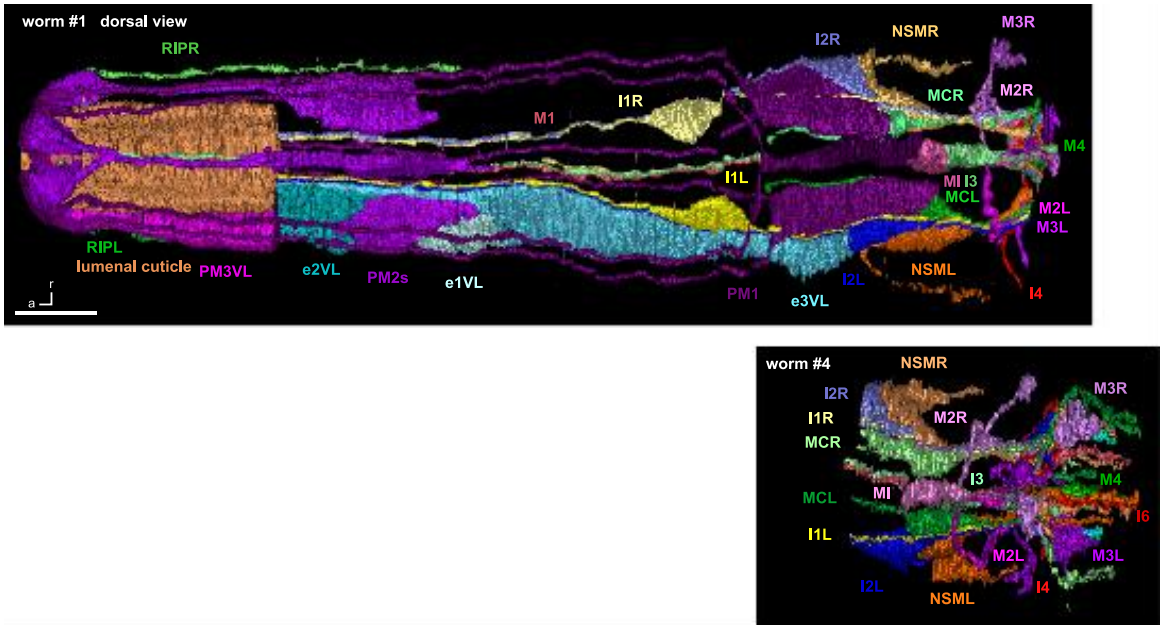

Figure 6.7: Synapses of the I2 pharyngeal neural and morphologies of all pharyngeal neurons and additional cells in the corpus

a, All synapses observed by reconstructing the left (I2L) and right (I2R) I2 neurons using transmission electron micrographs of serial sections (ssTEM). The anterior neurites, soma and part of the posterior neurites were reconstructed from one worm, and the soma and posterior neurites were reconstructed from a second worm, as shown in **b**. The anterior synapses were confirmed by sparsely sampling a third worm (data not shown). nd = not determined.
b, Morphological reconstruction of the anterior half of the pharynx, including part of the extrapharyngeal RIP anterior neurites. Ventral lateral (VL) epithelial cells and pharyngeal muscles are shown; only part of pharyngeal muscle 3 (PM3) and the lumenal cuticle are shown. Renderings are dorsal view. Scale bar = 5 µm.

D. The I1, RIP and MC neurons function in parallel with I2 to promote acute response amplitude

To identify additional neural circuits that control subsequent phases of the feeding response to light, we used laser microsurgery to systematically kill all 14 neuron classes individually in the pharynx (Figure 6.8a). Although ablation of most neurons did not affect the pumping response to light (Figure 6.9), we found that ablation of the I1 pair of neurons reduced the amplitude and increased the latency of the acute response (Figure 6.8c, i, j). This indicates that I1 promotes the amplitude of acute inhibition. I1 ablation also caused a defect in the sustained response. This role is consistent with a previously reported inhibitory function for I1, that of promoting ivermectin-induced lethality (Dent..Avery 2000). Given the distinct pumping curves of I2-ablated worms compared with I1-ablated worms (Figure 6.8b, c), we hypothesized that these neurons might function in parallel neural circuits. Supporting this view, double ablation of I1 and I2 in the same animal caused a significant enhancement of the latency and amplitude defects of either single ablation (Figure 6.8d, i, j). To assess whether other pharyngeal neurons might also be involved, we ablated all pharyngeal neurons except I1, I2, MC and M4. These animals retained a normal acute response to light (Figure 6.8e, i, j), making it unlikely that any other pharyngeal neurons play a critical role in the acute response. MC and M4 were retained in these experiments so that worms would grow to adulthood (Avery & Horvitz 1987) and exhibit a normal rate of pumping (Avery & Horvitz 1989).

To gain further insight into how light evoked inhibition of feeding, we sought additional neurons functioning in the I1 circuit. The *C. elegans* nervous system can be described as two neural networks connected by a single bridge: the main neural network with 280 neurons connects to the pharyngeal neural network with 20 neurons through gap junctions between the

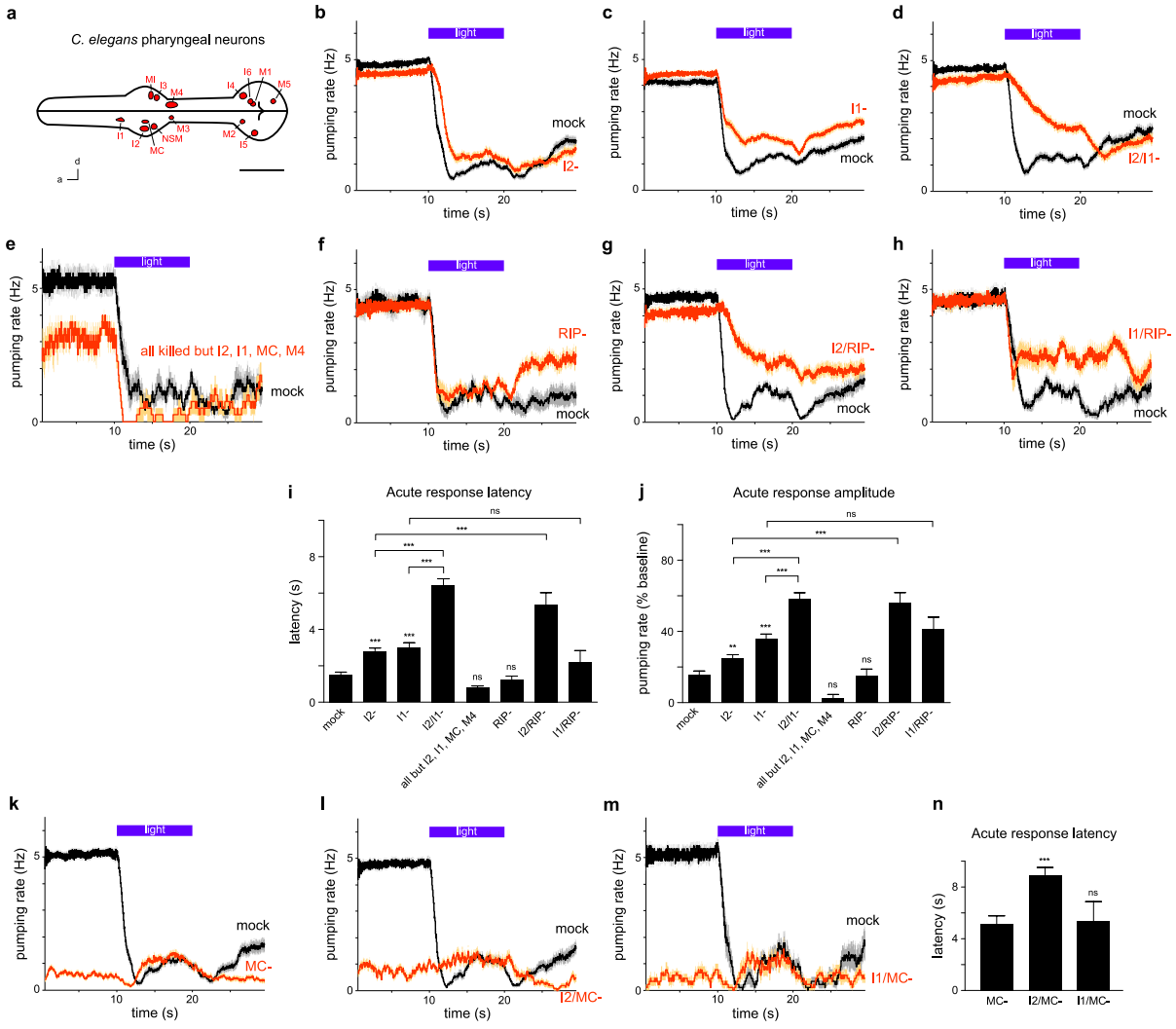

Figure 6.8: The I1, RIP and MC neurons define a neural pathway that controls the amplitude of acute inhibition in response to light

a, Map of pharyngeal neuron nuclei; if a neuron class is paired, only a single neuron is shown. d = dorsal, a = anterior. Scale bar = 20 µm.

b, I2 ablation increased acute response latency and decreased acute response amplitude. n ≥ 72 trials, 32 worms. Reproduced from p. 122.

c, I1 ablation decreased acute response amplitude, increased acute response latency, and decreased the sustained response. n ≥ 111 trials, 74 worms.

d, I/I12 double ablation enhanced the acute response defects of both single ablations. n ≥ 75 trials, 25 worms.

e, Ablation of all pharyngeal neurons except I2, I1, MC and M4 did not affect the acute response. n ≥ 4 trials, 4 worms.

f, RIP ablation did not affect the acute response and decreased the sustained response. n ≥ 14 trials, 6 worms.

g, I2/RIP double ablation enhanced the acute response defects of I2 ablation. n ≥ 26 trials, 9 worms.

h, I1/RIP double ablation did not enhance the acute response defects of I1 ablation. n ≥ 15 trials, 6 worms.

i, Quantification of the latency of the acute response.

j, Quantification of the amplitude of the acute response.
k, MC ablation resulted in grossly normal acute and rebound responses and an enhanced sustained response. $n \geq 49$ trials, 20 worms.
l, I2/MC double ablation exposed a severe acute response defect not seen in MC ablation. $n \geq 17$ trials, 11 worms.
m, I1/MC double ablation did not expose a severe acute response defect. $n \geq 9$ trials, 9 worms.
n, Quantification of the latency of the acute response. Comparison with mock-ablated animals was not done because of the substantial difference in baseline pumping rate.
*** $p < 0.001$, ** $p < 0.01$, ns = not significant, t-test. Light shading around traces and error bars indicate s.e.m.

RIP and I1 neuron pairs (Albertson & Thomson 1976). To determine whether RIP is involved in the feeding response to light, we used laser ablation to eliminate cell function. Single ablation of RIP did not affect the acute response, though it reduced the sustained response (Figure 6.8f, i, j). Since I1 ablation enhanced the defect of I2 ablation, we suspected that I2 ablation might serve as a sensitized background in which to observe more subtle functions for neurons in the I1 circuit. Like worms missing I1 and I2, worms lacking RIP and I2 showed a significant enhancement in the latency and amplitude defects of I2-ablated worms (Figure 6.8g, i, j). Given the similarity between these phenotypes and the structure of the nervous system, we speculate that RIP acts upstream of I1 to transmit a light-induced signal into the pharynx. Consistent with RIP acting in the same pathway as I1, ablation of RIP and I1 together did not enhance the defect of I1-ablated animals (Figure 6.8h-j). As a conclusion, our results suggest that a signal from the main neural network is transmitted to the RIP interneuron, where it is relayed to I1 to inhibit feeding in response to light. I1 appears to play a more significant role than RIP and therefore might have additional inputs and/or intrinsic activity.

To identify cells functioning downstream of I1, we examined its connectivity within the pharynx (Albertson & Thomson 1976). I1 was not reported to synapse directly with muscle. I1 synapses with several neurons including the MC neuron, which is the primary neuron that promotes normal pumping rate via direct synapses onto pharyngeal muscle

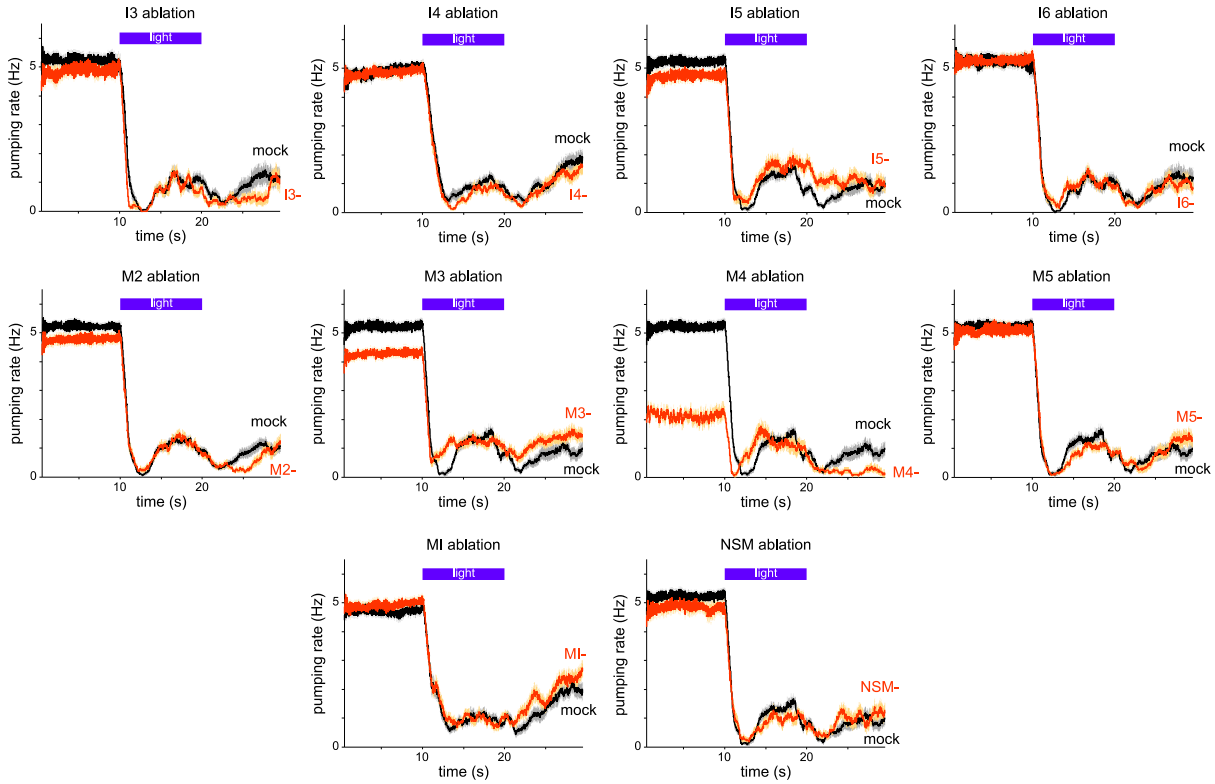

Figure 6.9: Individual laser ablation of most pharyngeal neurons did not affect the feeding response to light

Pumping response to light after ablations as indicated. n ≥ 18 trials, 7 worms.

(Avery & Horvitz 1989, McKay..Avery 2004). We hypothesized that MC might function downstream of I1. Initial characterization showed that MC-ablated worms had grossly normal acute and rebound responses (Figure 6.8k). Using logic similar to that used to identify a role for RIP, we sought to identify a function for MC in the I1 circuit by ablating it in the sensitized I2-ablated background. In fact, worms lacking MC and I2 exhibited essentially no acute response to light, and the acute response latency was significantly enhanced over MC-ablated worms (Figure 6.8l, n). I1 ablation in addition to MC ablation did not alter the response to light of MC-ablated worms (Figure 6.8m, n), suggesting that I1 and MC function in the same pathway. Altogether, these results suggest that a neuron from the main neural network transmits a light-

induced signal into the pharyngeal neural network via the RIP neuron, where it is relayed from I1 to MC to promote the amplitude of acute inhibition.

E. The M1 neuron controls the rebound response

Our results so far indicate that two neural circuits control the acute phase of the feeding response to light. These neural circuits appear to act in parallel, as loss of one enhances the defect caused by loss of the other. Our systematic neuronal ablations revealed an additional neuron that appears to function independently of these first two circuits, to control a separate phase of the motor sequence. Specifically, M1 ablation reduced the rebound response (Figure 6.10a, b), which occurs when prolonged light stimulates pharyngeal contractions after the acute phase of inhibition. Ablation of M1 did not affect the latency or amplitude of the acute response (Figure 6.10c, d). M1 directly synapses onto pharyngeal muscle (Albertson & Thomson 1976). Taken together, these results indicate M1 specifically promotes the rebound response to light.

To determine whether M1 might function downstream in the I2 or I1 circuits, we sought to understand the effect that I2 and I1 might have on the rebound response. However, the acute response defects caused by loss of I2 or I1 made it difficult to assess the presence of the rebound response, so we sought a new assay to probe M1 function. Instead of observing worms freely moving on an agar plate, we immobilized worms using high friction (Kim..Fang-Yen 2013). We noticed that pharyngeal pumping is completely inhibited under these conditions (data not shown). Importantly, when immobilized worms were exposed to the light used for calcium imaging (485 nm, 26 mW/mm^2), pumping was induced at a low rate (Figure 6.10e). We named this the "immobilized response" to light. We hypothesized that the mechanism that underlied the immobilized response was similar to the mechanism for the rebound response. To test this

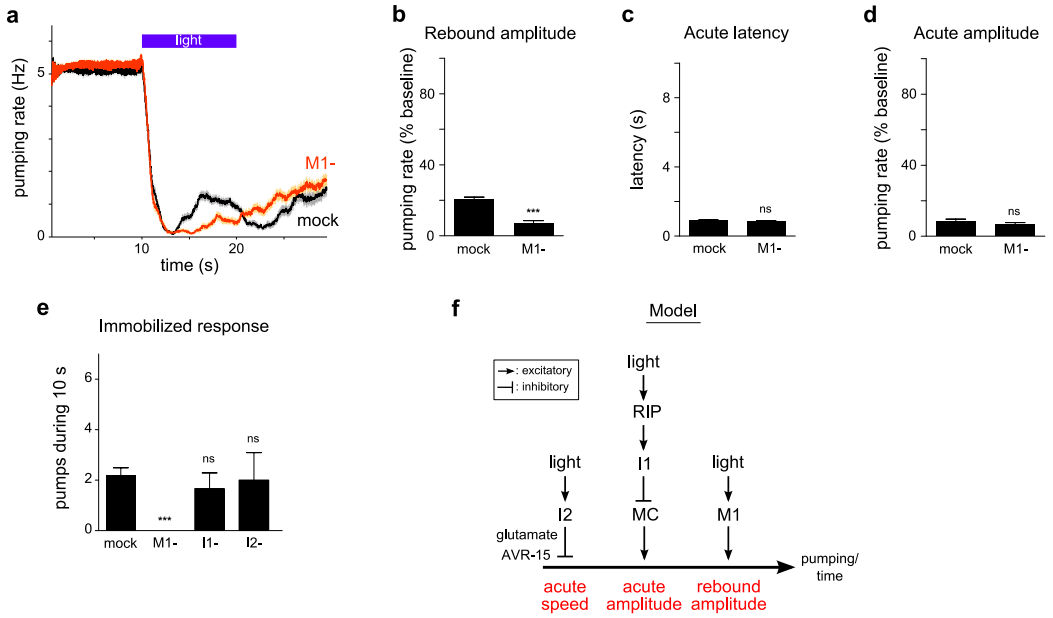

Figure 6.10: The M1 neuron promotes the rebound response

a, M1 ablation blocked the rebound response while leaving the acute response intact. $n \geq 62$ trials, 31 worms.
b, Quantification of rebound response amplitude.
c, Quantification of acute response latency.
d, Quantification of acute response amplitude.
e, M1 ablation completely abrogated the induction of pumping in response to light while worms were immobilized. I1 and I2 ablation did not affect the immobilized response.
f, Model for parallel temporal tiling in a neural circuit. The light signal is transmitted through three separate neural circuits, and each pathway independently controls a different phase of the behavioral response.
*** $p < 0.001$, * $p < 0.05$, ns = not significant, t-test, except for **e** which used a Mann-Whitney test. Light shading around traces and error bars indicate s.e.m.

hypothesis, we ablated the M1 neuron and found that the immobilized response was completely abrogated, suggesting that the immobilized response is mechanistically analogous to the rebound response (Figure 6.10e). Having identified a new assay for M1 function, we next sought to determine whether I2 or I1 functions in the immobilized response. Loss of I2 or I1 did not affect the immobilized response, in contrast to loss of M1 (Figure 6.10e). This result indicates that M1 acts in third circuit independent from the I2 and I1 circuits.

We suspect that the rebound response is like a gag reflex, as we occasionally observed bubbles being emitted from the pharynx after the onset of light (9 of 40 trials). Animals in which M1 had been ablated did not emit bubbles (0 of 53 trials).

F. Discussion

By studying a stimulus-induced behavior in the pharynx of *C. elegans*, we have been able to analyze the neural circuits that control a complex motor sequence. While the worm nervous system is small (302 neurons), its pharyngeal neural network is even smaller (20 neurons), making it amenable to the strategy of systematic laser microsurgery used here. We have identified 4 pharyngeal neuron classes (7 neurons) and 1 non-pharyngeal neuron class (2 neurons) that function to control different aspects of the feeding response to light. Light immediately inhibits feeding, and the latency of this acute inhibition is reduced by the I2 pharyngeal neuron (p. 115). Here we find that the I2 neuron secretes glutamate, and that the glutamate-gated chloride channel AVR-15 functions in pharyngeal muscle for the acute response. Electron microscopy coupled with combination ablations suggest that I2 signals directly to pharyngeal muscle, forming a monosynaptic circuit. The voltage-gated calcium channel subunits UNC-2 and UNC-36 are partially responsible for the influx of calcium in I2 in response to light. Additionally, we identify a neural circuit consisting of the nonpharyngeal neuron RIP and the pharyngeal neurons I1 and MC which acts in parallel with I2 to promote the amplitude of the acute response to light. Finally, a third circuit which includes the pharyngeal neuron M1 controls the rebound response, where light stimulates pumping after initially inhibiting it.

The pumping response to light is biologically relevant because light can be lethal to the worm (Ward..Xu 2008). Light can generate reactive oxygen species such as hydrogen peroxide (Wang & Nixon 1978), which are toxic to the worm (Jansen..Schnabel 2002). We speculate that the worm senses that it is ingesting toxic material and immediately inhibits feeding using a sensor embedded in the pharynx, the I2 neuron (p. 115). By its proximity to pharyngeal muscle, I2 can control pumping with very low latency. In a second pathway, the redox product might be sensed outside of the pharynx in the main nervous system (Ward..Xu 2008), and this signal might be relayed via the connection between the RIP extrapharyngeal neuron and the I1 pharyngeal neuron. Once pumping is successfully inhibited, we speculate that there is a subsequent response that protects the animal from additional deleterious effects. Toxic products may have already been ingested, and the worm might be better off if it expels such material from its pharynx and intestine via a gag reflex. The M1 pharyngeal neuron might promote the proposed efflux from the pharynx, as described below.

Based on this model (Figure 6.10f), we can make certain predictions. Our functional data coupled with the structural connectome suggest that I1 acutely inhibits pumping through the MC neuron. Since MC normally promotes pharyngeal pumping as a pacemaker neuron (Avery & Horvitz 1989), we speculate that I1 might inhibit pumping by inhibiting activity of the MC neuron. Robust pumping inhibition is thereby achieved via two prongs. In the first prong, I2 directly silences pharyngeal muscle. To strengthen the inhibition of muscle contraction, I1 silences MC, the neuron whose primary function is to promote muscle contraction. This two-pronged strategy might function more reliably to inhibit pumping than either single-pronged strategy alone.

To implement a reflex sequence like the pumping response to light, at least three different circuit designs are possible. In a "solo" design, light would cause a single neuron to vary its output over time to modulate the pumping rate, perhaps based on an internal timing mechanism or feedback from downstream targets. In the simplest case of a "serial" or "chain" design, each neuron in a single chain of neurons would control a different phase of the response. If one neuron were lost, the behavioral outcome of all downstream neurons would also be lost. This is the design proposed to control the sequence in a zebra finch's song (Long..Fee 2010). Finally, in a "parallel" design, each neuron would function independently of the rest and control a separate phase of the response, which would persist even if other neurons were lost. Interestingly, evolution seems to have arrived at a parallel design for the pumping response to light, with circuits defined by the I2, I1 and M1 neurons. These three circuits constitute an example of "parallel temporal tiling" (Figure 6.10f). The neural circuit motif is "temporal" because each neural circuit controls a separate time window of the behavioral sequence. The motif is "tiling" because the behavioral effects of the neural circuits span the entire time period during which light is provided, without any gaps or loss of neural control. This modular design might make it simpler for new circuits to be inserted into existing behaviors, without compromising the benefits provided by previously existing neural circuits. More complex behaviors in other animals may also rely less on serial mechanisms and more on parallel mechanisms.

G. Methods

a. Strains

The following worm strains were used:

N2 ("wild-type")
MT21650 *nIs575[P_{flp-15}::gcamp3; lin-15(+)]; lin-15(n765)*

MT21635 *nIs571[P $_{flp-15}$::gcamp3; lin-15(+)]; lin-15(n765)*
MT1212 *egl-19(n582)*
MT21639 *nIs575; egl-19(n582); lin-15(n765)*
CB55 *unc-2(e55)*
MT21652 *nIs575; unc-2(e55) lin-15(n765)*
JD21 *cca-1(ad1650)*
MT21787 *nIs575; cca-1(ad1650) lin-15(n765)*
CB251 *unc-36(e251)*
MT21637 *nIs571; unc-36(e251); lin-15(n765)*
VC550 *tag-180(ok779)*
MT21653 *tag-180(ok779; nIs575; lin-15(n765)*
VC12 *unc-77(gk9)*
MT21900 *nIs575; unc-77(gk9); lin-15(n765)*
VC9 *nca-2(gk5)*
MT21901 *nIs571; nca-2(gk5); lin-15(n765)*
CB540 *unc-68(e540)*
MT21651 *nIs575; unc-68(e540); lin-15(n765)*
JT73 *itr-1(sa73)*
MT21766 *nIs575; itr-1(sa73); lin-15(n765)*
MT21780 *nIs571; unc-36(e251); unc-2(e55) lin-15(n765)*
CB156 *unc-25(e156)*
CB933 *unc-17(e245)*
MT14984 *tph-1(n4622)*
CB1112 *cat-2(e1112)*
MT10548 *tdc-1(n3420)*
MT11374 *tbh-1(n3722)*
MT6308 *eat-4(ky5)*
IK883 *eat-4(ky5); njEx378[P$_{eat-4}$::eat-4::gfp; P$_{ges-1}$::NLS::gfp]*
MT21211 *eat-4(ky5); lin-15(n765); nIs529[P$_{flp-15}$::eat-4 cDNA::gfp; lin-15(+) #1]*
MT21212 *eat-4(ky5); lin-15(n765); nIs530[P$_{flp-15}$::eat-4 cDNA::gfp; lin-15(+) #2]*
MT21213 *eat-4(ky5); lin-15(n765); nIs531[P$_{flp-15}$::eat-4 cDNA::gfp; lin-15(+) #3]*
MT6305 *glr-1(n2461)*
VM1390 *glr-2(ak10)*
VM1846 *glr-3(ak57)*
FX3239 *glr-4(tm3239)*
FX3506 *glr-5(tm3506)*
VM685 *glr-6(ak56)*
FX2877 *glr-7(tm2877)*
VC20465 *glr-8(gk283043)*
VM487 *nmr-1(ak4)*
VM6310 *nmr-2(ak7)*
DA1384 *avr-14(ad1302); glc-1(pk54)*
VC350 *glc-2(gk179)*
XA7400 *glc-3(ok321)*
JD31 *glc-4(ok212)*
DA1371 *avr-14(ad1302)*

FX1811 *mgl-1(tm1811)*
FX355 *mgl-2(tm355)*
FX1766 *mgl-3(tm1766)*
JD105 *avr-15(ad1051)*
MT22171 *avr-15(ad1051); lin-15(n765); nEx2149[P_{myo-2}::avr-15A cDNA; lin-15(+)]*
OH4887 *otIs182[P_{inx-18}::gfp]*
PS3504 *syIs54[P_{ceh-2}::gfp, unc-119(+)]; unc-119(ed4)*
MT17641 *nIs264[P_{gcy-10}::4xNLS::gfp, lin-15(+)]; lin-15(n765)*
MT17912 *nIs282[P_{gcy-10}::4xNLS::gfp, lin-15(+)]; lin-15(n765)*
NL2334 *pkIs1273[P_{gpa-16}::gfp]*
MT21198 *nEx1997[P_{gpa-16}::gfp; P_{unc-54}::rfp]*

b. Molecular biology

We used the following primers to amplify DNA for generating transgenes by standard cloning procedures. For cDNA, wild-type mixed-stage poly-A RNA was used as template.

P_{flp-15}: TGAACTTTCCTCATTTCCCCTTCGTTC,
GACGAGGTGTATGTGGGAGACC
eat-4 cDNA: ATGTCGTCATGGAACGAGGCTTG,
CCACTGCTGATAATGCGGATTTTCC
P_{myo-2}: GTGTTGTGTATAGTGTACGAGAAAATGGAG,
TTCTGTGTCTGACGATCGAGGGT
avr-15A cDNA: ATGATAGGTCGATTGCGGAGAGG,
CGTACTGATGGCCACACCGTATTG

c. Behavioral response to light

This assay was conducted as previously described (p. 142). Briefly, pumping was scored by eye using a stereo dissecting microscope set to 120x magnification and illuminated with a halogen transmitted light source (Zeiss Lumar and KL 2500 LCD, 3100 K). Custom Matlab software (Supplementary Software) recorded the timing of pumps as indicated by manual key presses and controlled by a shutter (via Zeiss EMS-1 controller) that presented and removed mercury arc epi-illumination (HBO 100). We used a modified CFP filterset (Zeiss Lumar filter set 47 HE CFP 486047) to illuminate 436 ± 13 nm violet light at an intensity of 13 mW/mm^2. After ablation, each worm was assayed 1-4 times.

d. Behavioral statistics

Behavioral statistics were calculated as previously described (p.145). Briefly, the acute response latency is the time of the first missed pump relative to the onset of light. The first missed pump is determined by identifying the first time interval between pumps that exceeds twice the pre-light pumping rate for that animal. The acute response amplitude is the rate of pumping in the first 3 s following the first missed pump divided by to the pre-light pumping rate. The rebound response amplitude is the rate of pumping in the last 5 s of light exposure divided by the pre-light pumping rate.

e. Laser ablation

We used a pulsed nitrogen laser to conduct laser microsurgery of individual pharyngeal neurons (Laser Science, Inc. VSL-337 attached to a Zeiss Axioplan), as previously described (Bargmann & Avery 1995, Fang-Yen..Avery 2012). Briefly, Worms were immobilized by 10 mM sodium azide and mounted for viewing through a 100x oil objective. In general, ablations were done on larvae of stage 1 or 2 (L1 or L2), either using a cell-specific GFP reporter or based on nucleus location. Ablation of the M4 neuron was done on larvae stage 3 (L3), as the worms were more likely to grow to adulthood when ablated at this later stage. Ablations were confirmed the following day. On day 3 adults were assayed for their pumping response to light.

f. Calcium imaging

We assayed the calcium response to light of the I2 neuron as previously described (p. 146). Briefly, worms were immobilized using high friction (Kim..Fang-Yen 2013). In our standard

assay, the worm was simultaneously imaged and stimulated with 26 mW/mm^2 485 nm blue light for 7 s and videos were recorded at 15 fps. Videos were analyzed for changes in fluorescence using manually drawn regions-of-interest (ROIs) in a custom Matlab program. The latency of the calcium response was determined as the time from light onset to a calcium response greater than or equal to 20%.

g. Expression analysis

To observe gene expression of $P_{eat\text{-}4}$*::eat-4::gfp* in the I2 neuron, images were recorded using an upright microscope (Zeiss Axioskop 2) and a CCD camera (Hamamatsu ORCA-ER).

h. Electron microscopy

Adult N2 worms were loaded into a Type A carrier coated with 1-hexadecene and filled with a slurry of OP50 *E. coli*, then covered with a Type B carrier (Hall..Nguyen 2012). The sandwich was placed into the specimen holder and frozen using a high pressure freezer (Abra HPM010). Samples were substituted with 1% OsO_4, 0.2% uranyl acetate in 95% acetone::5% methanol at -90 °C for 110 h, warmed to -20 °C over 14 h, held at -20 °C for 16 h and warmed to 0 °C over 3.3 h (RMC FS-2500) (Fetter 2013). Samples were washed three times with acetone at 0 °C and three times at room temperature before stepwise infiltrated with Eponate 12 resin (Ted Pella) and polymerized at 65 °C. Individually embedded worms were thin-sectioned and imaged with a transmission electron microscope (JEOL JEM-1200 ExII) and CCD camera (AMT XR1241) at multiple resolutions (5,000x, 10,000x, 40,000x). Section thickness varied between 40-50 nm, with the 5,000x images spanning 30 x 30 µm. Images were cropped to remove captions, automatically aligned using TrakEM2 (Cardona..Douglas 2012) in Fiji, and then the

alignment was manually corrected. Cells in the anterior pharynx were manually traced. Synapses from the I2 neuron were annotated if more than two vesicles were present near the membrane or a clear membrane density was present in the absence of vesicles. Synapses were traced to provide the density volume and vesicle area statistics. Synapse size was calculated as the sum of the density volume and the vesicle volume, with an average vesicle diameter observed of 30 nm. Most synapses are polyadic, and the synapse size is accounted as being applied to all outputs equally.

PART 3:

SOFTWARE FOR SCIENCE

Chapter 7:

Introduction to Software for Science

A. The importance of scientific software

Every day software becomes a more integral part of society, and I believe that every day software is becoming an even more critical part of science. In fact, I now see a lack of specialized software as being one of the main bottlenecks restraining scientific discovery. Every aspect of the science that I do depends on software, and not just off-the-shelf software but also software I wrote that is specialized for the task at hand.

B. Types of scientific software

Scientific software comes in many forms, and I have identified 4 different categories of scientific software. The first category I call experimentation software. This is software that enables the scientist to do new kinds of experiments that they wouldn't be able to do without the software. My efforts at classical conditioning wouldn't have been feasible without my development of WormWatcher, a stimulus control and worm-tracking software (Chapter 8). Additionally, my assay studying the worm's feeding response to light would have been less sensitive without WormLips, software I developed for microscope control and for recording feeding events in real-time by eye (Chapter 9). Without using custom software, I would not have been able to make the discoveries that I did. As an example, the latency defect caused by loss of the I2 pharyngeal neuron is a subtle phenotype. Without accurate quantification of feeding timing provided by WormLips, I doubt I would have noticed the reliable though subtle effect that loss of I2 causes. Without this software, I would not have been able to study the phenomenon in as efficient and quantitative a manner. Experimentation is also limited by molecular reagents and physical devices, but the difference with software is that someone skilled in the art possesses a much more generalized skill. A software engineer can develop software to help advance nearly

any scientific experiment, while hardware and wetware skills are more specialized and therefore less generally applicable to different realms of science. For example, molecular biology skills are not very useful it you are working on human brain EEG experiments, but software skills remain useful because they enable automation of stimulus protocols which allow creative and new experiments to be conducted while scanning the human brain.

The second category of scientific software is analysis software. After conducting an experiment, it is critical that one analyzes the data in a way that can reveal insight into the phenomenon being studied. Matlab is an excellent environment in which to write custom analysis code, and both WormWatcher and WormLips are Matlab programs. One area in which analysis software is currently lacking is analysis of whole genome sequences (WGS). Although a significant amount of software exists, and we rely on an instance of Maqgene to do our WGS analyses in the Horvitz lab (Bigelow..Hobert 2009), in general analysis software is not as simple to use as it could be and it doesn't conduct all of the relevant analyses (e.g. deletion identification).

The third category of scientific software is organization software. This is the category that I think is most critically required for the advancement of knowledge. How can new results be appreciated without understanding them in the context of prior work? Every day new data are published, and the current method of organization, that of papers in journals, is in no way sufficient as a conceptually accessible form of organization. Moreover, there are existing datasets that have been published in paper format that would benefit from the interactional design of the Web. In this vein, I took two of the most impressive datasets, the neural connectome and cell lineage of *C. elegans*, and wrapped them inside interactive tools for browsing and navigating their graph and tree structures. These webapps are called the *C.*

elegans Neural Network (Chapter 10) and the *C. elegans* Cell Lineage (Chapter 11). Additionally, I have manually curated nearly 400 papers to extract neuron-specific findings, such as the effects of ablating a neuron, what stimuli the neuron responds to, and what genes function in the neuron for cell- and organism-level phenotypes. Built in to the Neural Network, this method of organizing knowledge makes it much more efficient to understand what is known about a specific neuron than having to prowl through the literature. Knowledge should be organized conceptually, not publishinally, and software will serve as the critical bridge for this organizational transformation.

The fourth and final category of scientific software is visualization software. Certainly visualizations can be a form of analysis and organization, but there is also a class of visualizations that are primarily used for presentation. An example is my Exon-Intron Graphic Maker (Chapter 12). When I joined the lab, I noticed that people often made elegant graphics that visualized a gene's structure, including the exons, introns and sites of mutation. However, this was tediously done by hand in a generalized graphics software, such as Adobe Illustrator or Photoshop. So I wrote a custom webapp which substantially reduced the time it took to accurately construct such graphics. Software that can help visualize data for presentation purposes is critical for the efficient and effective communication of results.

In conclusion, there is a great need for customized software to solve the new analytical, organizational, and visual challenges that are presented by conducting new experiments and collecting new kinds of data. Ideally, every biologist and neuroscientist would also be a software specialist.

Chapter 8:

WormWatcher: Software for Worm Tracking and Stimulus Control

A. Background

Wormtrackers are software that record videos of the locomotion of *C. elegans*. Wormtrackers are either specialized for single-worm tracking or multi-worm tracking. Single-worm trackers observe an individual worm at high spatial resolution (10-20x objective) and high temporal resolution (1+ fps). Worms are kept in a Petri dish on a stage which must be automatically controlled by the tracking software to keep the worm in the field-of-view, given the high spatial resolution and limited field-of-view of standard microscopes. Several single-worm tracking software packages have been developed (Pierce-Shimomura..Lockery 1999, Baek..Schafer 2002, Geng..Schafer 2004, Feng..Schafer 2004, Cronin..Sternberg 2005, Hoshi & Shingai 2006). The Sternberg and Schafer trackers are useful for high-resolution body posture analysis, such as identifying omega bends (Huang..Schafer 2006).

While single-worm trackers can analyze the behavior of individual worms at high spatial resolution, they are not designed for the analysis of a population of worms simultaneously. Multi-worm trackers record videos of multiple worms (up to several hundred) at low spatial resolution (1-2x magnification). Their main advantage is the ability to analyze large populations of worms and thereby accelerate the speed of data collection and analysis. Many multi-worm trackers have been developed, including the Parallel Worm Tracker (http://wormsense.stanford.edu/tracker/) (Ramot..Goodman 2008), and the Multi-Worm Tracker (Swierczek..Kerr 2011). A good review of both single- and multi-worm trackers is available in WormBook (Husson..Gottschalk 2012).

In the Horvitz lab, Dan Omura and Damon Clark from the Samuel lab developed a multi-worm tracker to study the worm's slowing in response to food (Omura..Horvitz 2012). However, this system had some significant limitations. First, because it used a frame-subtraction technique

to identify moving pixels as worms, it failed to identify worms that were extremely sluggish or paralyzed. This led to overestimation of the speed of a population of worms if some of them moved little or not at all. This method to identify worms is also used by the Parallel Worm Tracker. Second, this tracker only analyzed worm speed, not other behaviors such as turning or reversals. Third, this tracker was somewhat buggy, and occasionally refused to analyze videos. Fourth, this tracker stored videos in RAM, and was thereby limited to recording videos of at most 2 h. For my experiments with delay and trace conditioning, I needed to record behavior for 4 hours or more if I wanted to expose the worms to many trials of training.

B. WormWatcher: A multi-worm tracker

To address the issues described above, I wrote a wormtracking software within the Matlab environment. Dubbed "WormWatcher", this multi-worm tracker exhibits significant advantages over existing trackers. First, it identifies candidate worms by analyzing individual frames of an image, not relying on image subtraction like other wormtrackers. In this way it can identify worms that are paralyzed. Second, it takes many measurements of the worms, including speed, angle, angle change (turning), and size. There is also preliminary support for detecting the direction of locomotion. Third, WormWatcher records videos direct to the hard drive, allowing for videos of significantly longer lengths. We have successfully recorded 24 h videos with WormWatcher.

WormWatcher will be available at http://wormweb.org. The system relies on lighting projected from the side of the worms, such that the image produced is a bright worm on a dark background. This approach was developed by Dan Omura. A diagram of the entire experimental setup, including the wormtracker, is shown in Figure 8.1.

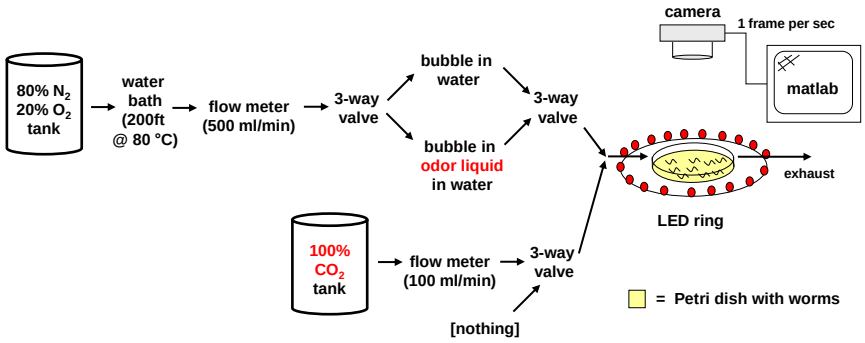

Figure 8.1: Experimental design of the wormtracker with a gas control system

C. How it works

The system records sequential frames at 1 fps to a video file. After the experiment is complete, a second program analyzes the video to identify worms and take measurements of their locomotion. These data are then plotted and the analysis is saved.

To identify worms in a video frame, the program begins by identifying candidate objects in each individual frame. It does this without frame subtraction in the following way:

1. Get the background image by "opening" it (erode + dilate).
2. Increase contrast by subtracting the background image from a denoised version of the current image.
3. Identify a threshold for separating foreground from background objects using Otsu's method (Otsu 1979).
4. Set. all background pixels to 0 by subtracting this threshold from the current image.
5. Label connected components that remain as candidate objects.

This process is illustrated visually in Figure 8.2.

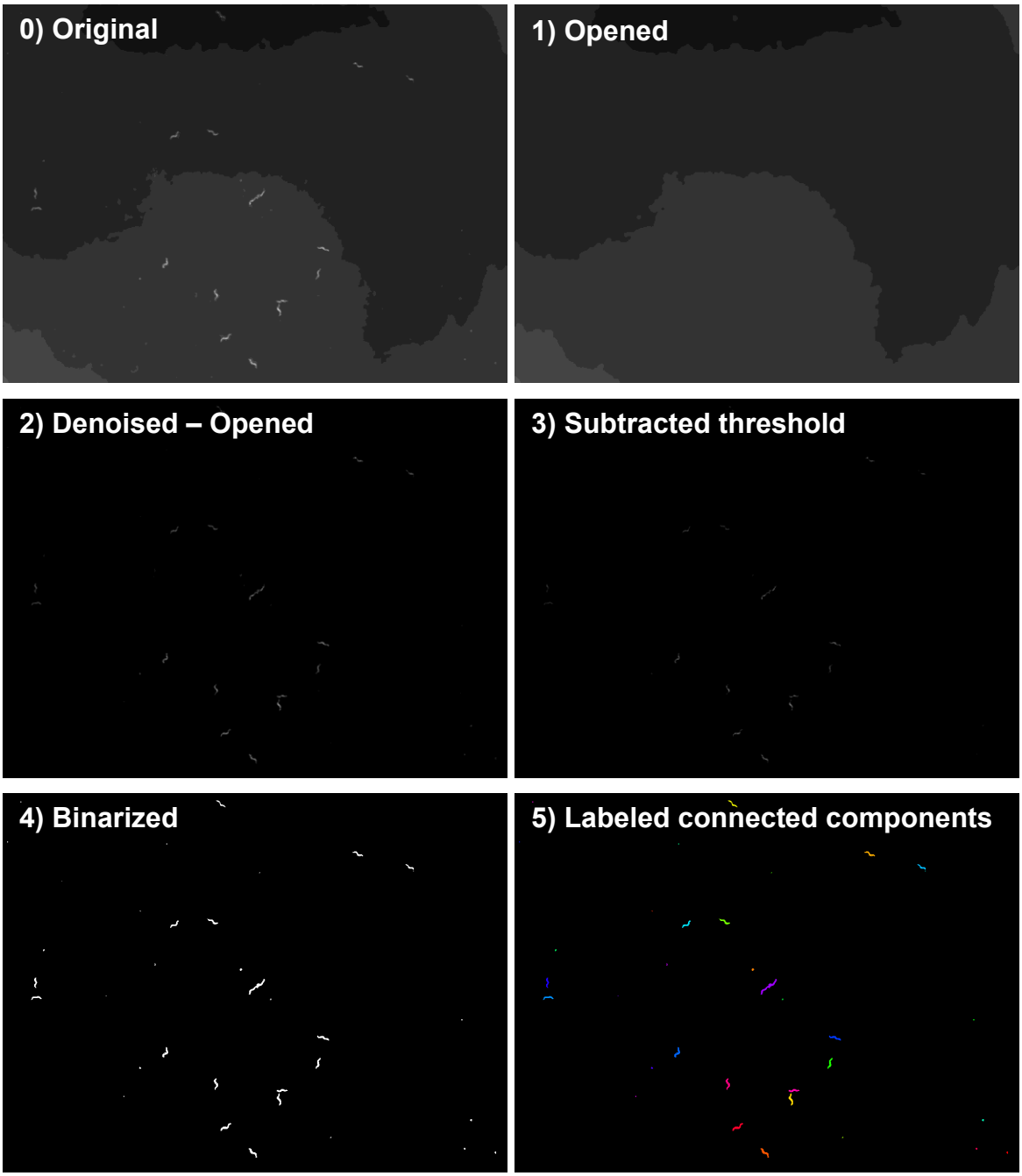

Figure 8.2: Object identification algorithm of WormWatcher

Once foreground objects have been identified, WormWatcher uses several heuristics to identify worms in each frame. If the worm is smaller than a user-specified minimum size, the object is ignored. Next, an object is identified as a worm if it is "curvy", i.e. if its solidity or

convexArea / area is greater than a threshold value (e.g. 1.44). This is perhaps the most critical heuristic in the entire program. Importantly, once an object is labeled as a worm in any frame of a video, every temporally-connected object (i.e. objects that overlap in sequential frames) are also considered worms. This means that an object only needs to pass the curvy threshold once in an entire video for it to be labeled as a worm throughout the video.

Another important feature of a multi-worm tracker is how it handles worm collisions. Generally, WormWatcher identifies an object as a collision if 2 worms previously occupied that space. 2 worms separate from a collision if a single object becomes 2 objects in a later frame. When a collision occurs, the object is not considered a worm and so is not included in statistics until it breaks up again, at which point it is considered 2 new worms, disconnected from the previous 2 worms that collided. More specifically, WormWatcher uses the following algorithm to deal with collisions:

1. Find the objects that overlap the current object in the previous frame
2. If no objects overlap, then add it as a new object to the pan-frame list of objects (this accounts for new worms crawling into the field of view).
3. If exactly 1 object overlaps, then
    a. For the overlapping object in the previous frame, check to see how many objects it overlaps with in the current frame
    b. If it overlaps with exactly 1 object, then mark the current object as the same object as the previous frame's object
    c. If it overlaps with more than 1 object, 2 worm may be separating from a collision:

i. Check the next frame to see if the objects are still separated in that frame

ii. If they are, then mark the current object as a new object in the object list

iii. If they aren't, then mark the current object as the same object as the previous frame's object. This helps to account for noisy videos where a single object breaks up into multiple objects on sequential frames, only to be rejoined on the following frame.

4. If more than 1 object overlaps and they're both worms, mark the current object as a new, non-worm object, due to 2 worms colliding

WormWatcher not only records videos, but also controls hardware during a recording. This feature was critical for the learning experiments (Chapter 3). The software can use the output of a parallel port as a digital control interface for hardware. In this way, WormWatcher controlled the valves used to expose worms to odors and gases at specified times (Chapter 3).

D. Outputs

Once all of the worms in a video are automatically identified and their movement across frames analyzed, WormWatcher produces an analysis file containing these results. These statistics include the total number of worms observed in a video, the average number of worms per frame, the average instantaneous worm speed, the average worm area, and the fraction of time all worms spent reversing. The program also produces graphs that show the number of worms over time in each frame, the average instantaneous worm speeds over time (Figure 8.3), the average instantaneous worm area (size) over time (Figure 8.4), the average worm heading

over time, the average worm turning rate over time (Figure 8.5), a histogram of mean worm areas, a histogram of worm "ages" (age is the number of frames the worm was continuously observed for), a histogram of all mean worm speeds, a histogram of all instantaneous worm speeds, and the fraction of worms reversing over time. A reversal is annotated if a worm's velocity changes by more than 140 degrees over 1 second. The "forward" direction is the one in which a worm spends most of its time proceeding while the "reverse" direction is the other direction.

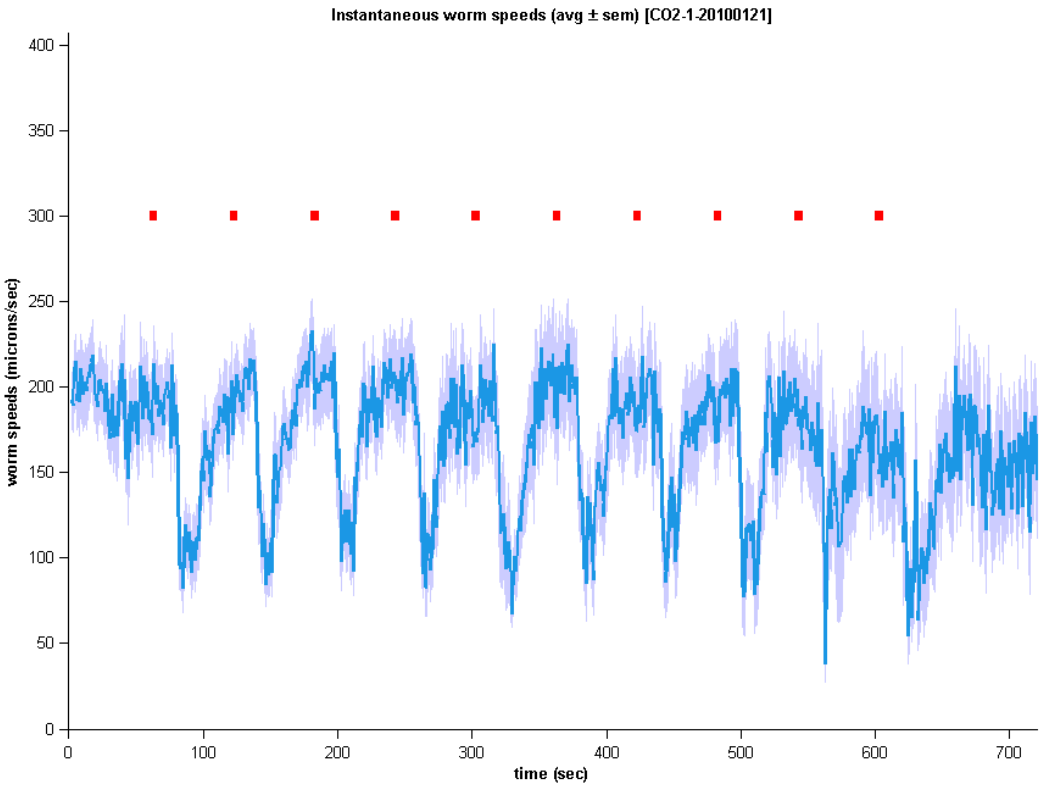

Figure 8.3: Graph produced by WormWatcher showing the change in worm speed over time

This example shows the drop in speed in response to brief repeated pulses of carbon dioxide (red marks). Error shading is s.e.m.

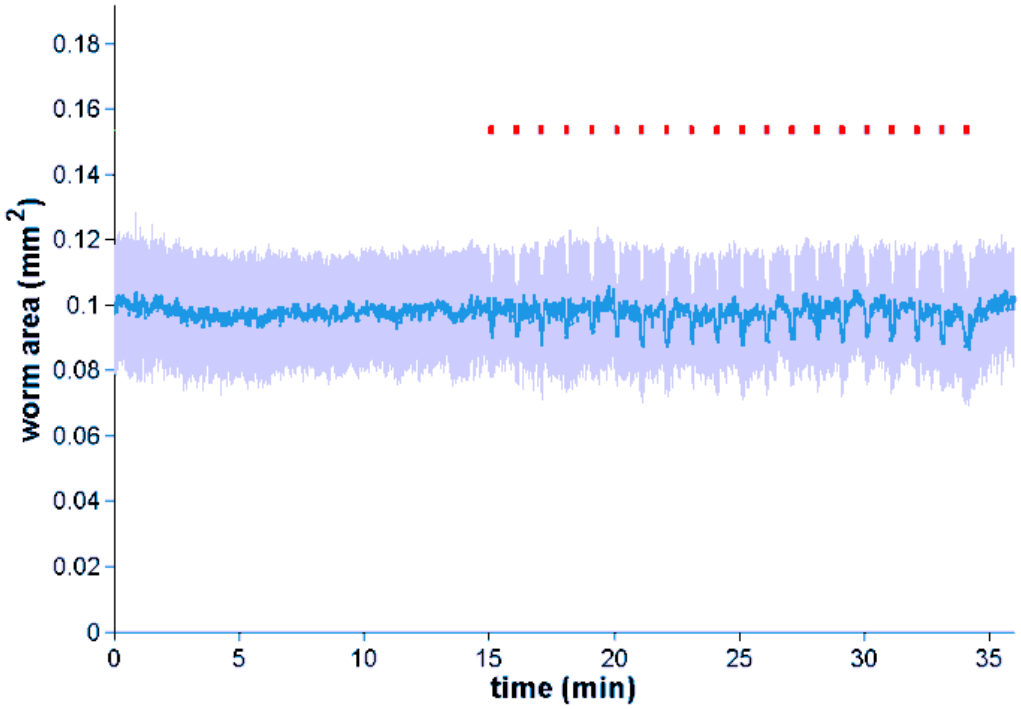

Figure 8.4: Graph produced by WormWatcher showing the change in worm size over time

This example shows that worms shrink in response to carbon dioxide (red marks). Error shading is s.d.

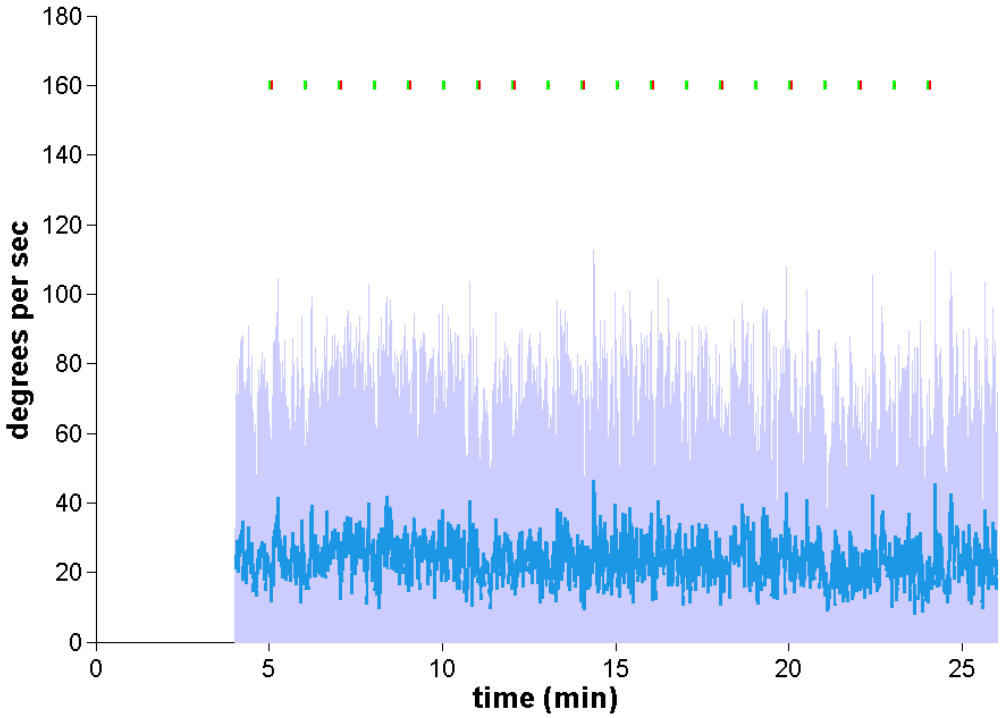

Figure 8.5: Graph produced by WormWatcher showing worm turning over time

In this experiment no change in turning was observed, and worms turned an average of about 20 degrees during the entire experiment. Error shading is s.d.

Additionally, the program produces an annotated video which marks every worm, as well as their historical tracks. This video is useful for confirming that the program identified worms accurately. A "heat map" of the worms' locations is also generated (Figure 8.6).

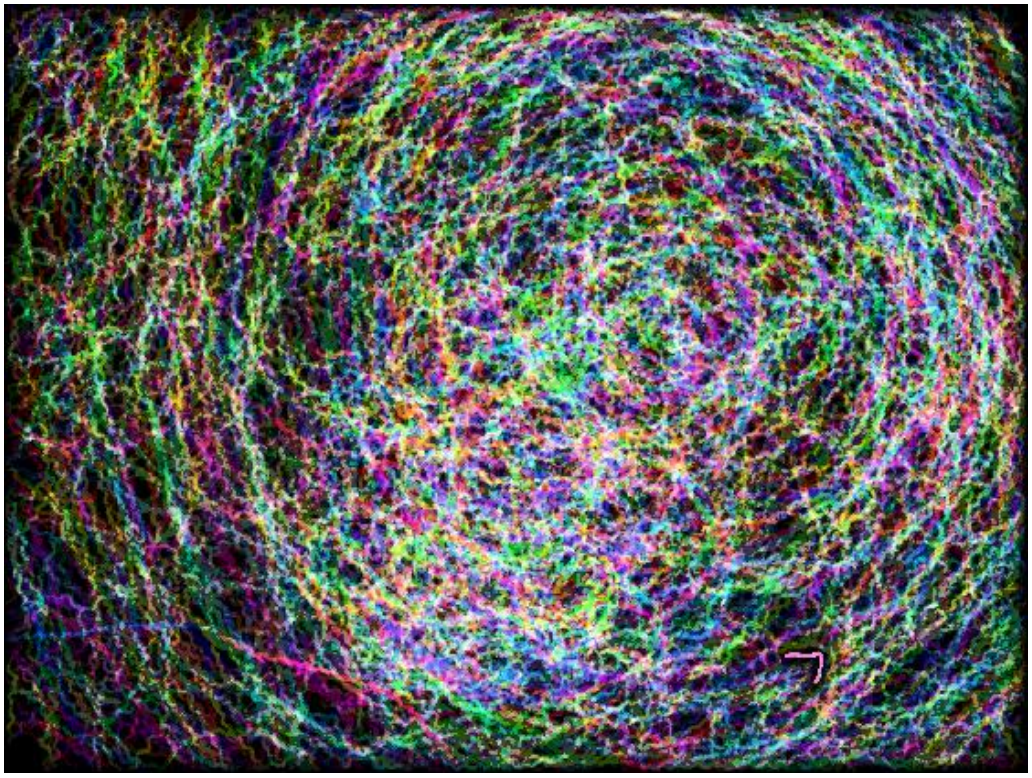

Figure 8.6: Heat map produced by WormWatcher showing worm tracks

Each worm makes a track selected from a small set of different colors. In this experiment, worms moved around the plate for 30 min and did not show any location preference.

E. Limitations

WormWatcher has 2 limitations, which may be significant depending on your application. First, it only records at a rate of 1 frame per second (fps), which limits its ability to notice high-speed changes. Second, it cannot perform realtime analysis and adapt the stimuli in a closed loop, limiting the types of experiments that can be controlled by WormWatcher. Both of these limitation have been addressed in the Multi Worm Tracker (Swierczek..Kerr 2011), and this tracker is recommended if high temporal resolution or real-time analysis is required for your application.

F. Conclusion

In conclusion, WormWatcher is a new addition to the multi-worm tracker family. It identifies worms without background subtraction, intelligently handles collisions, and produces a plethora of graphs and visualizations. WormWatcher is open-source and will be available at http://wormweb.org.

The software can also be extended to other species of worms. For example, I have modified the original WormWatcher to analyze the locomotion of Planaria. This software is being used by members of the Reddien lab to study Planarian behavior.

Chapter 9:

WormLips: Software for Real-time Event Scoring and Stimulus Control

To quantitatively study the effect of light on *C. elegans* feeding (Chapter 5 and Chapter 6), a real-time method for scoring pumping rates over time was required. After making the qualitative observation that pumping was inhibited by light, I developed a Matlab-based software tool for recording pumping in real-time as well as for controlling a microscope's light shutter. The bulk of experiments were conducted on the Zeiss Lumar stereo dissecting scope. This microscope, and all modern computerized Zeiss microscopes, can be controlled by a Windows PC via the MicroToolbox (MTB), a software library available from Zeiss. This toolbox allows control of all microscope features, including epifluorescent light shutter control.

Using this toolbox, I developed software called WormLips, which I used to study the *C. elegans* light-induced pump stop. Variations of this software also control the Polychrome light source as well as LED drivers from ThorLabs.

In addition to hardware control, WormLips records pumping in real-time as indicated by a human observer watching the worm through the microscope and pressing the Enter key with each pump. In the standard experiment (Figure 9.1), the transmission halogen lamp is on to enable observation of the worm (120x). The experiment begins with the first press of the Enter key. For the first 10 s, pumping is recorded. For the second 10 s, the shutter is opened to allow bright light from an arc lamp to hit the worm, which causes it to inhibit pumping. For the final 10 s, the shutter is closed again and the sustained response is observed and recorded.

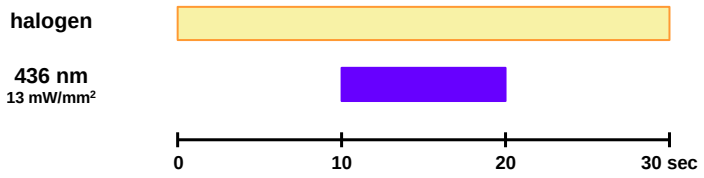

Figure 9.1: Timing of standard experiment with light inhibiting pumping

As output, WormLips generates a graph showing a 1 s moving average of the rate of pumping, with the light stimulation period marked (Figure 9.2).

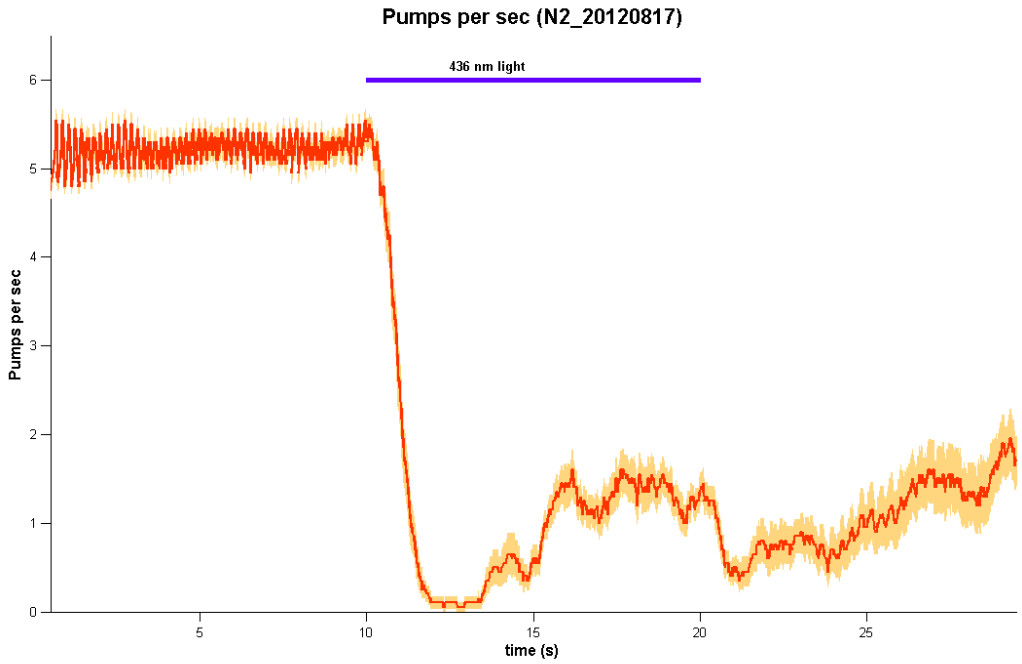

Figure 9.2: Output of WormLips

In this experiment, light was presented for 10 s from 10 s to 20 s, as indicated by the violet line. Error shading is s.e.m.

WormLips is open-source and will be available at http://wormweb.org.

Chapter 10:

C. elegans Neural Network: Webapp for Connectome Navigation and Knowledge Organization

The connectome is the set of connections among all neurons in a nervous system. At this point the term refers to anatomical connections, but the general concept applies to all functional connections. The concept of the "connectome" is getting a lot of attention lately, with some arguing that it will be as fundamental to neuroscience as whole genome sequences are to molecular biology (Sporns..Kotter 2005). Others argue that the connectome, while useful, will simply complement the standard functional approaches that are needed to understand brain function (Bargmann & Marder 2013). The main issue remains as to whether it will even be technically feasible to reconstruct the connectome of a vertebrate brain.

The very first, and to date only, connectome that has been assembled is that of the *C. elegans* nervous system. This set of more than 10,000 connections among 302 neurons was generated by electron microscopic (EM) reconstruction of several individual worms (Albertson & Thomson 1976, White..Brenner 1986). Even equipped with this dataset, the function of most neurons in the worm remain unclear, and even though we know the functions of some neurons their roles in neural circuits remain cryptic. At best, the connectome has provided the *C. elegans* research community with a map which can be used to generate specific hypotheses about functional connectivity. As an example, the hypothesis that RIP and I1 would be involved in the worm's pumping response to light was due to information provided by the connectome (Chapter 6): these neurons form the only anatomical connection between the pharyngeal nervous system and the main nervous system.

However, actually exploring the *C. elegans* connectome has been quite difficult and tedious. The two papers that uncovered the connectome are long, in total almost 400 pages. The connections of each individual neuron is laid out on a single page with a diagram, some EM

images, and a brief qualitative description. It is impractical to try to answer more complex questions of the connectome, such as what the shortest path is between two neurons.

To make the connectome more accessible and more efficient to use, I developed the *C. elegans* Neural Network, an interactive visualization of the connectome available as a web application at http://wormweb.org. A screenshot of the application is shown in Figure 10.1. The webapp has the following features:

1. Click on neurons to re-center them and see what other neurons they're connected to/
2. Specify a start neuron and an end neuron to find the shortest paths between 2 neurons
3. Zoom in and out to view neurons more than 1 degree away
4. View all connections in the visible portion of the network (which ends up looking like a dense spiderweb) by checking the "Show more connections on the graph" checkbox under "Options"
5. View and search the network of individual neurons. By default, neuron classes (i.e. pairs of neurons) are displayed, but this is a simplification, and the individual neuron network is a more accurate representation of the true network.
6. View functional data for the neuron of interest, which I have curated from the papers I have read. This includes gene expression, physiology, loss-of-function (e.g. laser ablation) phenotypes and gain-of-function (e.g. cell-specific gene rescue) phenotypes for the neuron of interest. Each datum is supported by evidence in the form of a figure or quote from the original paper and includes a link to the paper itself (Figure 10.2).
7. Search for cells that express a specific gene. One can also search for cells that express a given gene that are synaptically upstream from cells that express another gene.

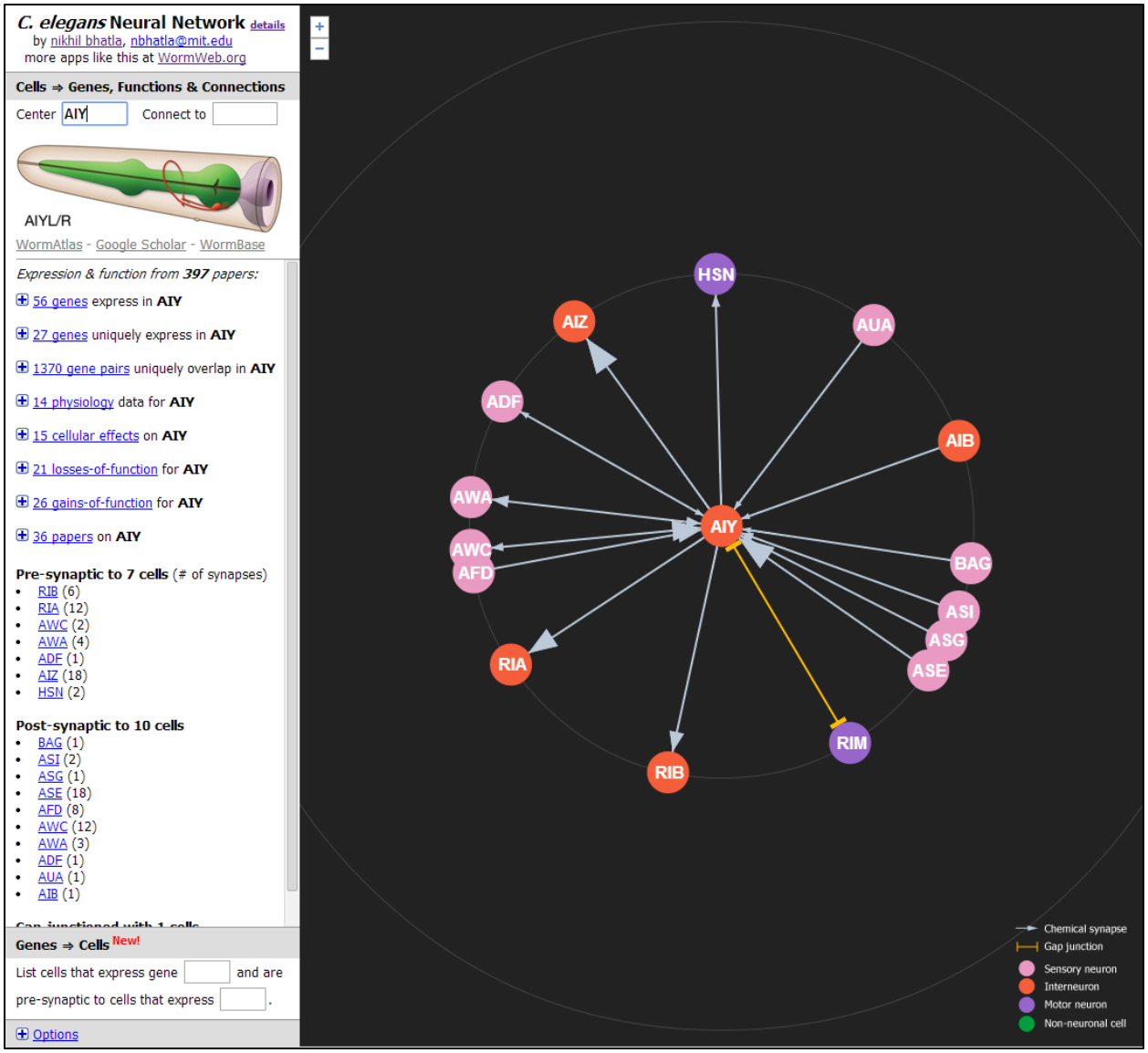

Figure 10.1: Web interface of the *C. elegans* Neural Network

The neurons connected with a target neuron are visualized on the right. Pink neurons are sensory neurons, red neurons are interneurons, and purple neurons are motor neurons. Arrows indicate a chemical synapse, while orange bar lines indicate a gap junction. On the left, one can find the set of shortest paths between 2 neurons. A cartoon of the neuron's placement and morphology is also provided. Below that are curated functional data, such as gene expression, physiology, loss-of-function and gain-of-function data on the target neuron. In the lower left corner, one can search for cells that express a specific gene and are connected with other cells that express another gene.

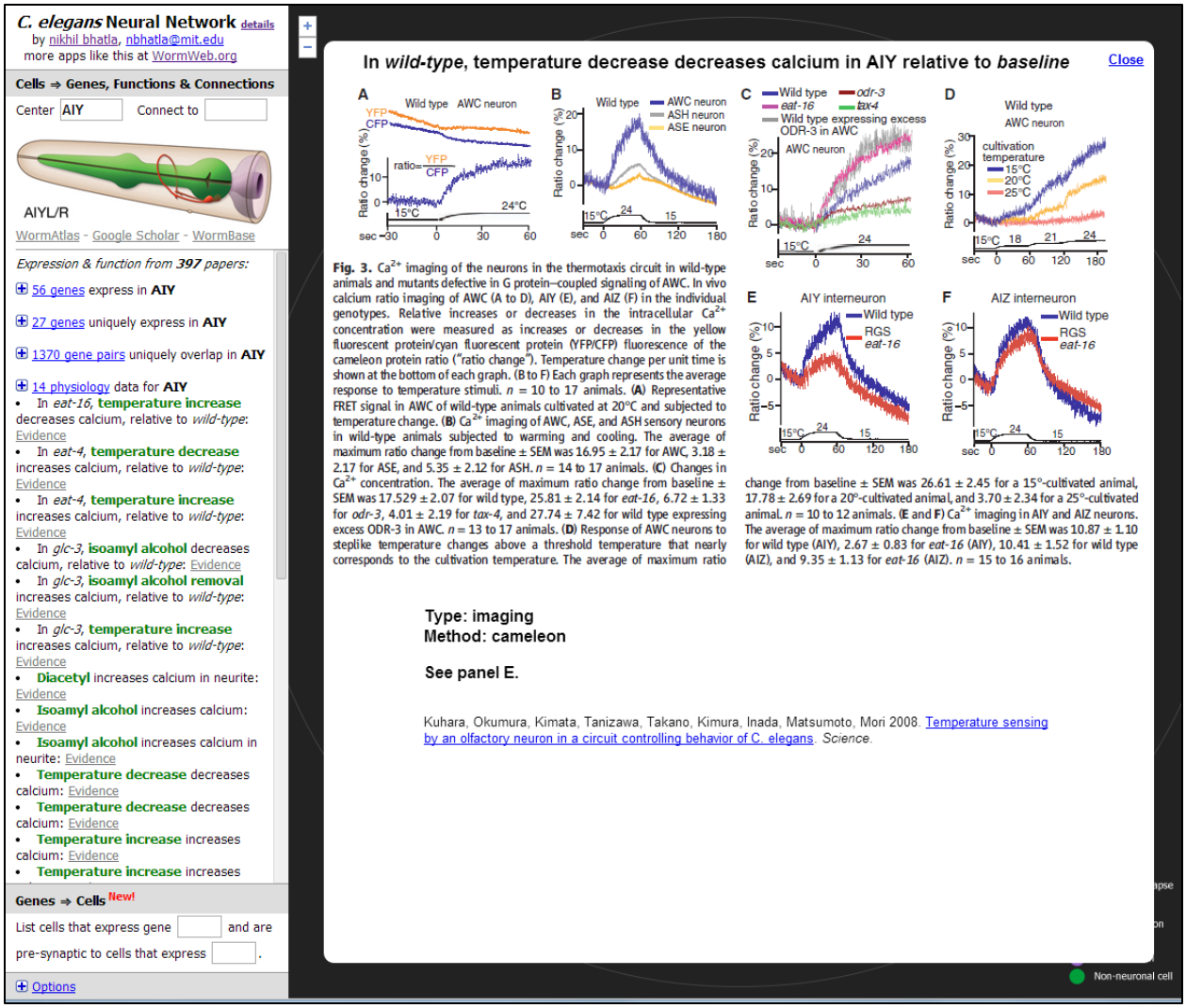

Fig. 3. Ca^{2+} imaging of the neurons in the thermotaxis circuit in wild-type animals and mutants defective in G protein–coupled signaling of AWC. In vivo calcium ratio imaging of AWC (A to D), AIY (E), and AIZ (F) in the individual genotypes. Relative increases or decreases in the intracellular Ca^{2+} concentration were measured as increases or decreases in the yellow fluorescent protein/cyan fluorescent protein (YFP/CFP) fluorescence of the cameleon protein ratio ("ratio change"). Temperature change per unit time is shown at the bottom of each graph. (B to F) Each graph represents the average response to temperature stimuli. n = 10 to 17 animals. (**A**) Representative FRET signal in AWC of wild-type animals cultivated at 20°C and subjected to temperature change. (**B**) Ca^{2+} imaging of AWC, ASE, and ASH sensory neurons in wild-type animals subjected to warming and cooling. The average of maximum ratio change from baseline ± SEM was 16.95 ± 2.17 for AWC, 3.18 ± 2.17 for ASE, and 5.35 ± 2.12 for ASH. n = 14 to 17 animals. (**C**) Changes in Ca^{2+} concentration. The average of maximum ratio change from baseline ± SEM was 17.529 ± 2.07 for wild type, 25.81 ± 2.14 for *eat-16*, 6.72 ± 1.33 for *odr-3*, 4.01 ± 2.19 for *tax-4*, and 27.74 ± 7.42 for wild type expressing excess ODR-3 in AWC. n = 13 to 17 animals. (**D**) Response of AWC neurons to steplike temperature changes above a threshold temperature that nearly corresponds to the cultivation temperature. The average of maximum ratio change from baseline ± SEM was 26.61 ± 2.45 for a 15°-cultivated animal, 17.78 ± 2.69 for a 20°-cultivated animal, and 3.70 ± 2.34 for a 25°-cultivated animal. n = 10 to 12 animals. (**E** and **F**) Ca^{2+} imaging in AIY and AIZ neurons. The average of maximum ratio change from baseline ± SEM was 10.87 ± 1.10 for wild type (AIY), 2.67 ± 0.83 for *eat-16* (AIY), 10.41 ± 1.52 for wild type (AIZ), and 9.35 ± 1.13 for *eat-16* (AIZ). n = 15 to 16 animals.

Figure 10.2: The *C. elegans* Neural Network can display evidence for the physiological response of a neuron

The database includes:

- 302 individual neurons in 118 classes
- 1 neuron-like cell class (XXX)
- 7 pharyngeal muscles (PM*)
- 2 pharyngeal marginal cells (PMC)
- 2 pharyngeal gland cells (PGC)

- 1 pharyngeal basement membrane (PBM)
- 1 muscle class (MUS) that includes body wall muscles, vulval muscles and anal muscles
- 1 intestine class (INT)
- 1 hypoderm class (HYP)

The main network data is from the Chklovskii group (Chen..Chklovskii 2006). A modified version of their data files is available at http://wormweb.org/detail.html. A list of neurons, non-neuronal interacting cells, and the associated groups came from the Japanese CCEP group. These computer-readable data came from the following primary research:

- (White..Brenner 1986)
    - 5 animals were reconstructed in this paper: 3 adult hermaphrodites (N2T, N2U, JSE), 1 L4 larva (JSH), and 1 adult male (N2Y). The connectivity data used by the Chklovskii group (and hence used in this visualization) was primarily derived from adults N2U and JSE. Area anterior to the nerve ring was covered with adult N2T, and the gap between N2U and JSE was covered by the adult male N2Y. L4 JSH was only used to verify nerve ring connectivity. So, in actuality, the visualized network is a hermaphrodite-male hybrid and a 5-worm hybrid (Figure 10.3).

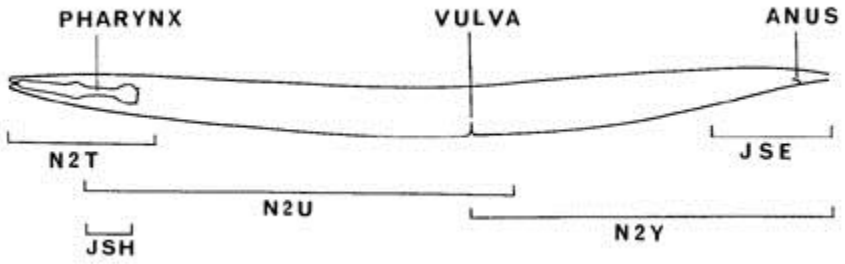

Figure 10.3: Names of worms analyzed to collect connectomic data

Reproduced from (White..Brenner 1986).

- (Durbin 1987)
- (Hall & Russell 1991)
- (Achacoso & Yamamoto 1992)

The pharynx data comes from (Albertson & Thomson 1976). At least 2 animals were compared for all observations from this paper. The raw data came from the Japanese CCEP group. This dataset has some issues:

- Some synapses are recorded as being between a single cell and a cell class. In these cases, the Neural Network assumes that connections belong to all cells of that group.
- Sometimes the type of synapse is missing. In these cases, the Neural Network either defaults to a pre-synapse or relies on comment made in the text but missing from the figure.
- A synapse is sometimes annotated as both a gap junction and a chemical synapse. In these cases, the Neural Network assumes that both are present. This causes double-counting of some synapses, so the synapse count for the pharynx isn't as accurate as for the main nervous system.
- Often the target muscle name is missing. In these cases, the Neural Network directs the synapse to the muscle that I inferred from the figure.
- Sometimes the annotations from CCEP were wrong, so I fixed them.
- I renamed several of the muscles and other non-neuronal cells to names that don't collide with and are more consistent with the main network neurons.
- I counted each line of the data file as a single synapse.
- Many synapses in the pharynx are highly variable from animal to animal, as noted in the data file. These are included in the Neural Network visualization.

The visualization was built from of an existing Javascript library called the Javascript Infovis Toolkit (http://thejit.org). The drawing of the neurons on the upper left side of the screen come from WormAtlas (http://wormatlas.org). The size of a grey arrow is proportional to the number of chemical synapses between 2 cells, and the size of the orange bar is proportional to the number of gap junctions between 2 cells.

Most importantly, just because 2 neurons are anatomically connected does not mean that they are functionally connected. Conversely, just because 2 neurons are not anatomically connected does not mean that they are not functionally connected. Functional analysis, which includes manipulations such as activation and inactivation during a behavior, as well as physiological analysis, such as calcium imaging and electrophysiology, are still the gold standards for showing that two neurons function in a neural circuit.

After curating 397 papers for the Neural Network, I have been able to calculate some interesting statistics regarding our state of knowledge of the worm's nervous system. Note that more than 2000 papers have been published about the *C. elegans* nervous system, so these statistics are lower bounds.

- There are 238 unique neuron-gene pairs where a gene is known to be both expressed in a neuron and either have a gain-of-function or loss-of-function phenotype associated with expression in that neuron. This is of 2,253 total neuron-gene pairs in the database, where the gene is expressed in the neuron, indicating that we know the function for roughly 10% of neuron-gene pairs.
- There are 552 unique genes mentioned in the database.

My hope is that by making the connectome interactive and curating relevant functional data for each neuron, we will be able to more efficiently advance our understanding of the *C.*

elegans nervous system. Hopefully such knowledge will advance our understanding of nervous systems in general across animals.

Chapter 11:

C. elegans Cell Lineage: Webapp for Cell Lineage Navigation

C. elegans is not only the only organism whose connectome is known, it is also the only organism whose cell lineage is known (Sulston & Horvitz 1977, Sulston..Thomson 1983) . Like the connectome, this knowledge has been available as a series of diagrams, but an interactive, searchable version of it was not available. A digital version of the lineage data was also not available, so I generated a file that contained the birth, death and division times for all cells based on the published diagrams, using a ruler to determine these times. Next, I used a customized version of the Javascript Infovis Toolkit (http://www.thejit.org) to make an interactive tree of the lineage, which is available at http://wormweb.org. A screenshot is shown in Figure 11.1.

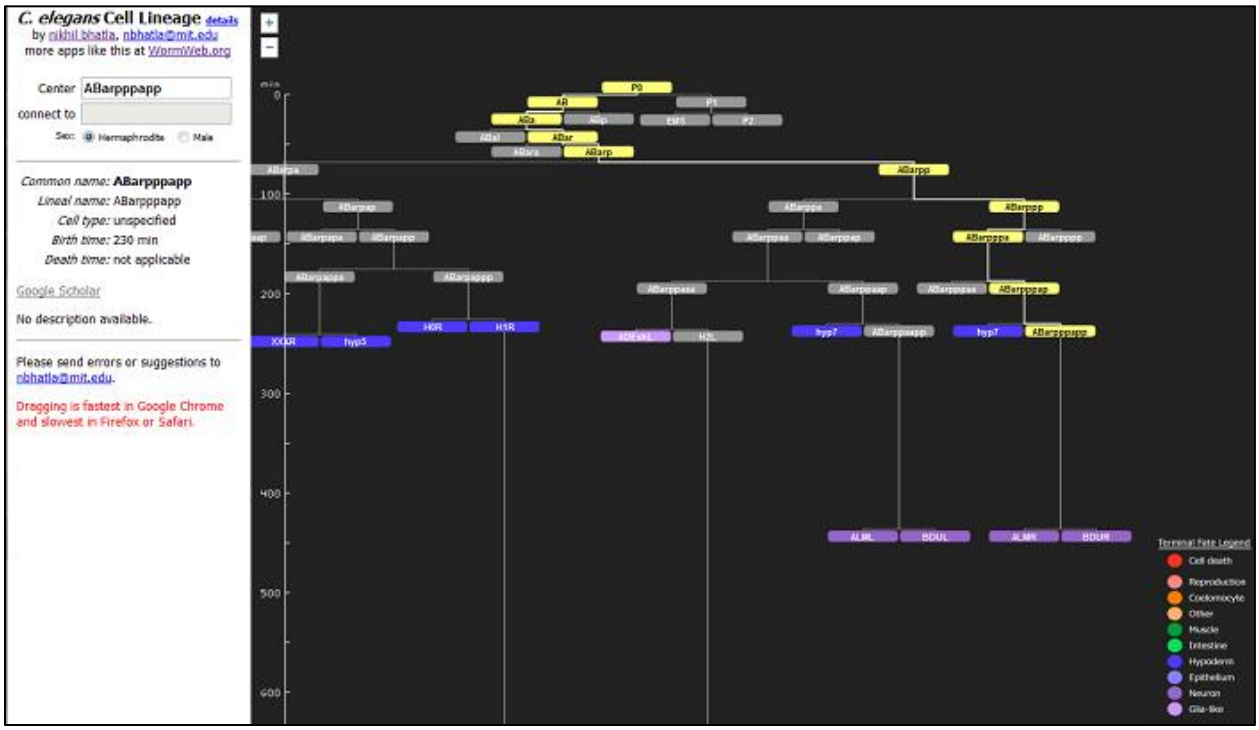

Figure 11.1: Web interface of the *C. elegans* Cell Lineage

The webapp includes features to search for cells by either lineage name or common name. Cells are color-coded base on their cell-type, with red for cells that will die, pink for cells

involved in reproduction, orange for coelomocytes, dark green for muscle, light green for intestine, dark blue for hypoderm, light blue for epithelial cells, dark purple for neurons, light purple for glia-like cells, and light orange for any other type of cell.

The panel on the left enables searching the lineage, as well as viewing the common name, lineal name, cell type, birth time, death time and a brief description of the target cell.

As with the neural network, my hope is that by digitizing the *C. elegans* cell lineage and making it more easily accessible, our knowledge of the worm will grow at a more rapid rate.

Chapter 12:

The Exon-Intron Graphic Maker

The genome is a sequence of nucleotides, and genes are functional domains that reside in this sequence. In the field of genetics, one often focuses their efforts on understanding the function of a specific gene, or set of genes. The geneticist relies on mutation, generally loss-of-function, to identify functions for genes. Genes consist of exons, portions that get translated from RNA to protein, and introns, portions that get removed before translation. Biologists find it useful to provide diagrams of their gene that indicate the exons, intron, and sites of mutation, as well as domains within the gene that code for domains within the protein. These kinds of graphics are visual representations of the structure and function of the underlying nucleotide sequence, and an example can be seen at the bottom of Figure 12.1.

When I joined the Horvitz lab, there was no efficient tool to produce these gene diagrams. Scientists would manually generate them in a graphics program such as Adobe Illustrator, which was quite tedious. So I designed a simple webapp, called the Exon-Intron Graphic Maker, to make generating gene diagrams fast and easy. The program is available at http://wormweb.org.

The interface, along with an example gene diagram, is shown in Figure 12.1. The user simply enters their gene name; 5' untranslated sequence; coding sequence with exons indicated as uppercase and introns as lowercase, or exons and introns separated by commas; the 3' untranslated sequence; locations for mutations, which can be point mutations or deletions, as well as a color to be used with the marker; protein domain locations in amino acid coordinates, as well as a name and color; and scale bar length. The Exon-Intron Graphic Maker takes what was previously a ten minute to hour long task and makes a publication-quality PDF of the gene diagram in just a few minutes.

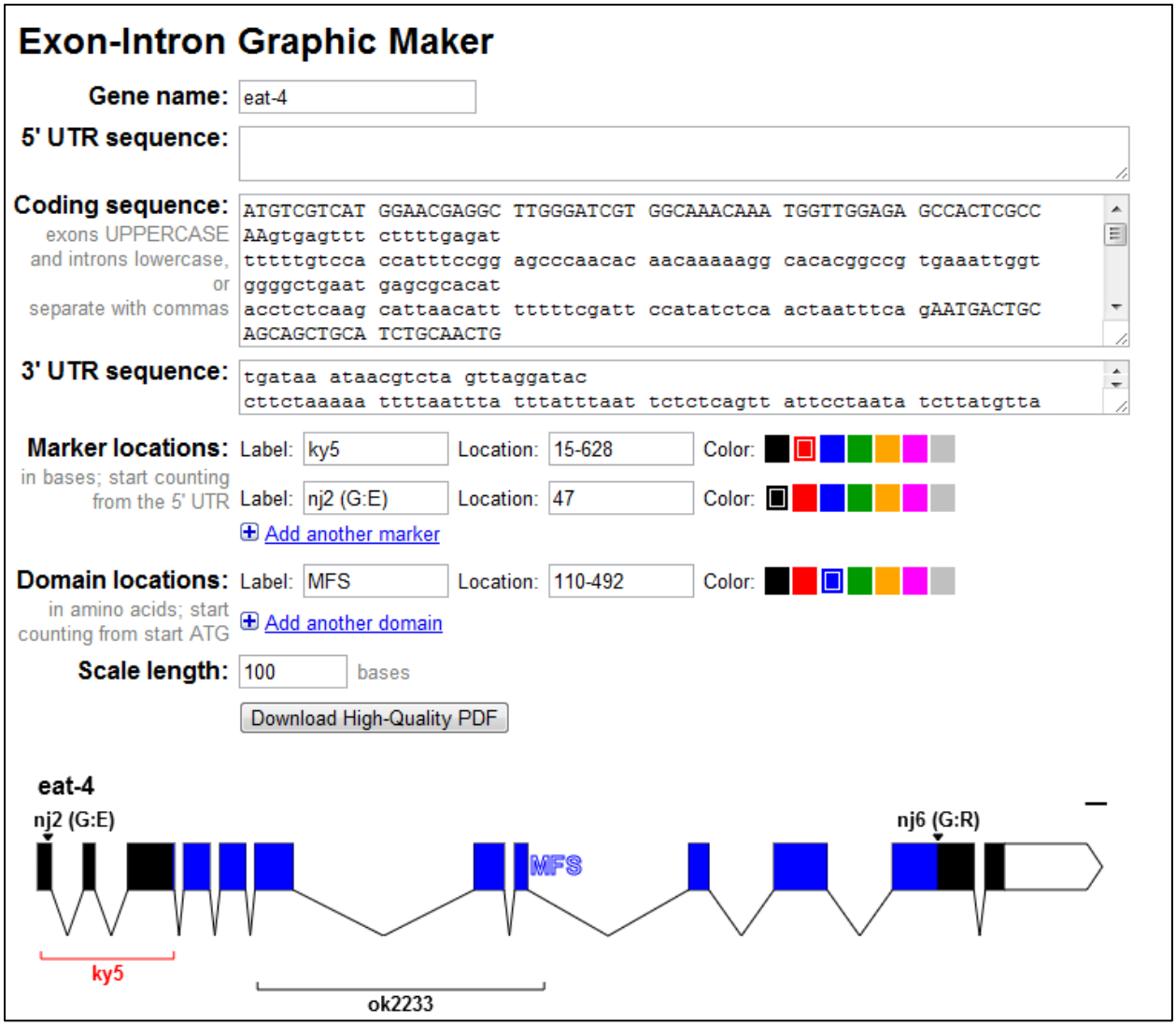

Figure 12.1: Web interface of the Exon-Intron Graphic Maker

Chapter 13:

Bacterial Chemotaxis Simulator

A. Introduction

In my efforts to understand the neural basis of behavior, I began by studying the simplest organism, the bacterium. Bacteria are capable of a behavior called chemotaxis, where they swim to the peak of an attractive gradient, such as sugar. I was impressed that a single-celled organism could exhibit such a behavior and sought to understand the mechanism that controlled this behavior. A bacterium is able to move because it has flagella, which can spin like a propeller to push a bacterium in different directions. When flagella spin in one direction (e.g. clockwise), the bacterium moves ahead, but when flagella spin in the other direction (e.g. counter-clockwise), the flagella get tangled and make the bacterium spin around. Bacteria can move smoothly along curved lines, but occasionally they slow down, twitch, and then start moving in a new direction.

While much is known about the mechanisms of chemotaxis at the protein level (Wadhams & Armitage 2004, Rao..Arkin 2004), I was interested in understanding chemotaxis at a higher computational level. Researchers have found that bacteria move in a way called a "biased random walk" (Alt 1980). When there is no attractant present, bacteria just wander, covering the space with no preference for any specific location. They move along their curved paths (called "runs"), and every so often they spin around (called "tumbles") and start in a new random direction. This is the "random walk" part of the "biased random walk".

The "bias" occurs when the attractant is present in a gradient. Bacteria rely on attractant receptors in their cell membrane that bind and sense the attractant (e.g. sugar). The presence of sugar changes the probability of whether a bacterium is going to tumble or not. When sugar concentration is increasing, the bacteria tumble less, but when sugar is decreasing, they tumble more. This concentration-dependent tumble probability introduces a "bias" into a bacterium's

normal "random walk", such that it now spends more time at higher sugar concentrations, exhibiting a place preference that it did not show in the absence of sugar.

B. The Bacterial Chemotaxis Simulator

To study the dynamics of this biased random walk process, I built a Bacterial Chemotaxis Simulator, available at http://wormweb.org. A screenshot is presented in Figure 13.1.

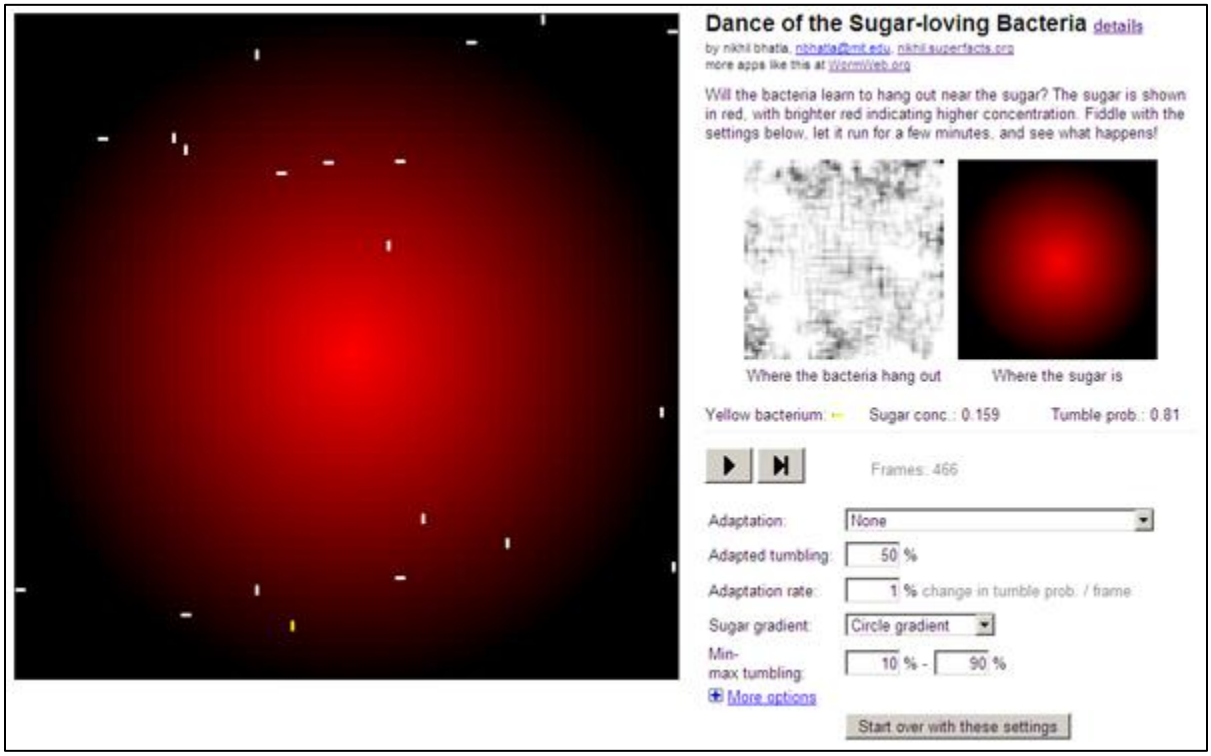

Figure 13.1: Web interface of the Bacterial Chemotaxis Simulator

The simulator is interactive in that the bacteria on the left side quickly swim around the virtual sugar gradient and their behavior is controlled by various settings, such as the adaptation rate or sugar gradient shape. Red spots indicate presence of a chemoattractant, with brightness proportional to concentration. One of the bacteria is colored yellow, and that is the bacterium

who's current tumble probability and sugar concentration are shown on the right as it moves through the environment.

I built this simulator because I wanted to get a better understanding of how bacterial chemotaxis might work. The software simulates a population of bacteria swimming through a virtual world of varying sugar concentrations, and I wanted to see what it would take to get the bacteria to properly chemotax, to swim to the highest sugar concentration and spend the most time there.

In this simulation, each bacterium gets a turn to move. On each turn, it randomly chooses whether to move forward one square, or to randomly choose a new direction to move in (i.e. tumble) and then moves one square in that direction. At the end of its turn the bacterium updates its tumble probability depending on the sugar concentration at the new location. There are many algorithms for updating tumble probability, the simplest of which is to set the tumble probability to 1 minus the current sugar concentration, which is normalized to 1. This is the default update formula in the simulator, and is specified when the **Adaptation** field is set to "none".

The simulator includes the following features in the right panel, in order from top to bottom:

- **Where the bacteria hang out:** This is the location "heat map" of where the bacteria spend time, with black shading indicating that bacteria spend more time there than spots with whiter shades. This heat map can be viewed as the result of a simulation and illustrates whether the bacteria are successfully chemotaxing. If the heat map is nearly uniformly grey, the bacteria are present everywhere equally fail to chemotax. If the shape of the heat map matches the shapes of the sugar gradient, then the bacteria are successfully chemotaxing.

- **Where the sugar is:** This is a visual representation of where the sugar is in the bacteria's environment. Brighter red indicates higher sugar concentrations.
- A row describing the current sugar concentration and tumble probability of the yellow bacterium
- **Pause/Play button**: Pauses the simulation when it's running, and plays the simulation if it is paused
- **Next frame button**: Runs only one frame (turn) of the simulation, pausing immediately after that turn is finished. You can use this to step through the simulation to watch individual bacteria.
- **Frames**: How many frames (turns) the simulation has run so far.

The following settings affect whether the bacteria successfully chemotax:

- **Adaptation**: This sets whether the bacteria adapt to the sugar they experience, and if so, how quickly they adapt.
    - **None:** The default setting, this specifies that the bacteria don't adapt at all, and the tumble probability is just updated to 1 minus the current sugar concentration on each turn.
    - **Tumble returns to steady state (linear):** When set to this option, a bacterium's tumble probability will update to approach the value of the **adapted tumbling** field, minus the difference in current vs. previous sugar concentrations. How much it will approach is specified by the **adaptation rate** field.
    - **No tumble up, tumble otherwise (2 state):** This is an update algorithm inspired from (Mittal..van Oudenaarden 2003). A bacterium's tumble probability is set to 0 if the current sugar concentration is higher than the average sugar concentration

from the last 3 turns. If it is lower than the average from the last 3 turns, the tumble probability is set to the **adapted tumbling** probability. In other words, if sugar levels are increasing, never tumble, but if they are decreasing or staying the same, tumble.

- **Adapted tumbling:** The tumble probability that is used in the adaptation algorithms described above.
- **Adaptation rate:** The rate at which a bacterium's tumble probability relaxes to the adapted tumble probability. This only affects the simulation if **Adaptation** is set to "Tumble returns to steady-state (linear)".
- **Sugar gradient:** This is the shape of the sugar gradient. There are a few options (Figure 13.2).
- **Min-max tumbling:** The first value specifies the minimum tumble probability for a bacterium, and the second value sets the maximum.

In addition to the options above, there are some extra options if you click on the "More options" link:

- **Room size:** This sets the size of the bacteria's environment, which must be square.
- **Bacteria number:** This sets the number of bacteria to simulate.
- **Bacteria speed:** This sets the update rate for the simulation.
- **Hang-out updating:** This sets how many turns have to pass before the bacterial heat map is updated.
- **Auto-stop after:** This tells the simulator when to automatically stop running the simulation.

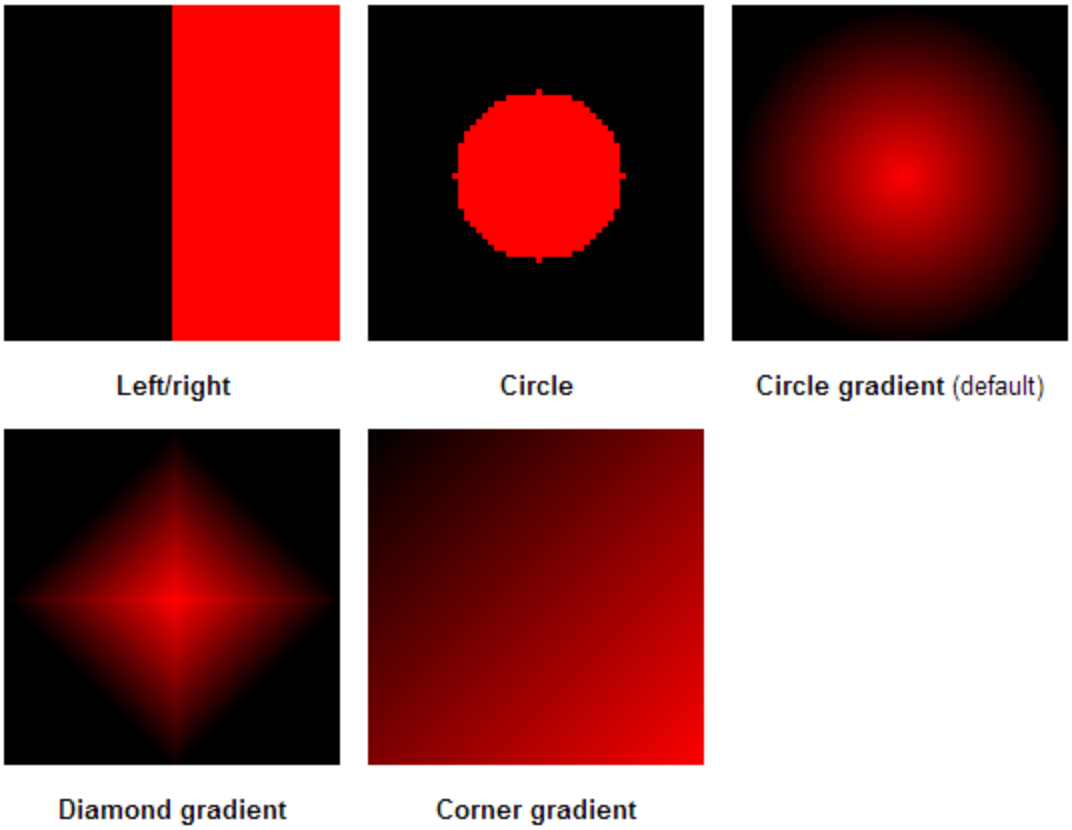

Figure 13.2: Sugar gradients available in the Bacterial Chemotaxis Simulator

C. Results

My initial impression was that a bacterium would move to the highest sugar concentration simply by tumbling less if the current sugar levels are high, and tumbling more if the current sugar levels are low. Surprisingly, this simple strategy is insufficient for chemotaxis in this simulator. What I've found instead is that it is critical for the bacterium to keep a memory of the recent sugar concentrations it has sensed. To chemotax successfully, the bacterium must change its tumble probability not only if sugar levels are changing but also if sugar levels are staying the same. If the sugar levels are relatively constant, it needs to return to a basal tumbling probability. If it doesn't, it will swim away from areas of high concentration.

After experimenting with this simulator, I learned that adaptation is critical for bacterial chemotaxis. Adaptation can be thought of as using a memory of a previous time to alter current behavior, by comparing then with now. This is also called a "temporal comparator". Figure 13.3 shows a set of heat map results for simulations where the bacterium inhabit 2 different sugar gradients using 3 adaptation algorithms. When there is no adaptation, the bacteria wander all over the environment. Watching the bacteria in the animated simulator, one will see that at low concentrations the bacteria tumble and find it difficult to leave the poor environment because they are always tumbling. Furthermore, at high concentrations the bacteria pass straight through, eventually ending up back in low concentration territory, where they get stuck tumbling.

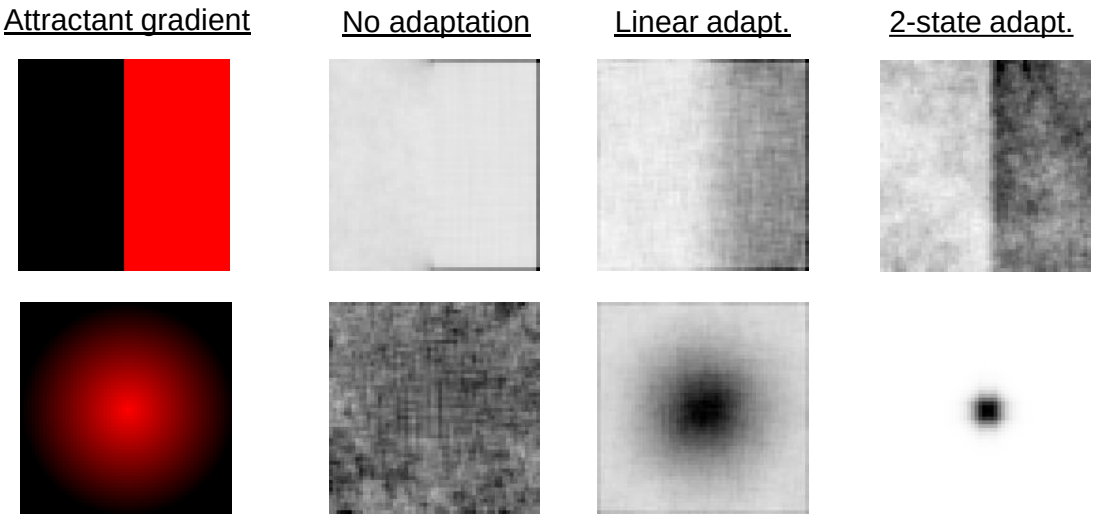

Figure 13.3: Adaptation is necessary for bacterial chemotaxis in the simulator

Each heat map is the result of a single simulation which includes: 20,000 frames of simulation, 20 bacteria, 56x56 world size, 10-90% min-max tumbling, 50% adapted tumbling, and 1% adaptation rate.

With linear adaptation, one can see the shape of the sugar gradient in the heat maps of bacteria location. This means that the bacteria are chemotaxing to some degree. Finally, with 2-state adaptation, the bacteria spend the most time at the peak of the sugar gradient, indicating that they are efficiently chemotaxing.

D. Conclusion

In conclusion, the Bacterial Chemotaxis Simulator is an educational tool for testing different behavioral models for bacteria. Using it, I learned that adaptation is critical for successful chemotaxis. At least in the simulation, bacteria cannot simply rely on the current sugar concentration to determine their next action. Even in the simplest organism of bacteria, memory is critical for success.

Chapter 14:

Conclusion

This thesis documents the work I have completed during my tenure in graduate school.

In Chapter 1, I provided an argument for three high priority research areas in biology and neuroscience: medically-relevant phenomena, artificial intelligence and consciousness.

In Chapter 2, I offered my definition of consciousness and related terms. Additionally, I explained several philosophical positions that one can take on the problem of how physical matter can generate consciousness. For the scientific study of consciousness, one must accept that consciousness exists as axiomatic. Instead of focusing on the intractable question of how consciousness exists at all, the primary goal is to identify the features of neural activity that generate subjective experience. A secondary goal of the scientific study of consciousness is to determine the features of neural activity that correspond to kinds of subjective experience, such as the difference in neural activity that causes visual perception compared with the neural activity that causes smell perception, a completely different kind of subjective experience.

In Chapter 3, I introduced my method for studying consciousness in *C. elegans*. Trace conditioning is a type of learning that correlates with awareness of stimuli contingencies in humans, and I speculated that animals that trace condition are capable of conscious awareness and so have the capacity for subjective experience. I reviewed the existing protocols for learning in *C. elegans* and determined that I needed to make a new protocol because the existing protocols were more similar to contextual conditioning than temporal conditioning like trace conditioning. I built a wormtracker called WormWatcher to assay the locomotion response of hundreds of worms to conditioning stimuli. After characterizing the locomotion response to isoamyl alcohol, octanol, light, oxygen and carbon dioxide, I tested 4 pairs of these stimuli as conditioning stimuli: isoamyl alcohol + light, isoamyl alcohol + carbon dioxide, octanol + carbon dioxide and oxygen + carbon dioxide. Worms did not learn to respond differently to the first

item in each pair after training trials where both were presented in sequence, so I was unable to find evidence for consciousness in *C. elegans*.

In the process of testing worms for learning, I measured the responses to many stimuli and discovered several novel behavioral phenotypes. In particular, I was drawn to the observation that light inhibits *C. elegans* feeding. I speculated that if I understood the neural activity the controlled this behavioral response then I might gain insight into whether worms have primitive vision, a basic form of visual perception. In Chapter 4, I described the existing knowledge of how *C. elegans* responds to light, and in Chapter 5, I described my own research on the light response of *C. elegans*. In studying the worm's response to light I uncovered several new genes (*gur-3* and *prdx-2*) that are required for the light response of a pharyngeal neuron, I2. This neuron acts as a pharyngeal light sensor. Moreover, light appears to be acting through the generation of hydrogen peroxide or another redox product, as hydrogen peroxide is sensed by the I2 neuron using the same genes that sense light.

In Chapter 6, I reported that in addition to uncovering a novel mechanism by which light is sensed, I also discovered 3 independent neural circuits that control separate phases of the feeding response to light. First, the I2 neuron secretes glutamate, likely directly onto the AVR-15 glutamate-gated chloride channel which acts in pharyngeal muscle to block contraction. Second, a neural circuit consisting of the RIP extrapharyngeal neuron and the I1 and MC pharyngeal neurons controls the amplitude of the acute inhibition of feeding cause by light. Third, a neural circuit, including the M1 pharyngeal neuron, controls a later phase of the response to light, that of rebound pumping. Taken together, these 3 neural circuits implement a motif that I termed "parallel temporal tiling", where separate neural circuits control separate phases of a behavioral response.

In Chapter 7, I argued that software is becoming a more critical part of science and that more biologists and neuroscientists would benefit from having software skills, as my research has benefitted from them. In Chapter 8, I described WormWatcher, a multi-worm tracker that I built to more accurately analyze worm locomotion behavior. Chapter 9 was about WormLips, software I developed to accurately score pumping rates in real-time. Chapters 10 and 11 discussed the 2 webapps I've developed for making accessible 2 of the crown jewels of *C. elegans* research, the neural connectome and the cell lineage. Chapter 12 presented the Exon-Intron Graphic Maker and Chapter 13 provided information on the Bacterial Chemotaxis Simulator. All of this software is or will be available at my website for scientific software, WormWeb.org.

In conclusion, although I failed to uncover evidence for consciousness in *C. elegans*, I was able to identify the molecular mechanisms and neural circuits that underly a novel behavior, that of light- and hydrogen peroxide-dependent feeding inhibition. My goal has shifted from trace conditioning to studying the neural activity that is triggered by light in the worm. If this neural activity has properties that are theorized to accompany consciousness, such as synchrony, recurrent activity, or sustained activity, perhaps I will be able to study the basic mechanisms of consciousness in the worm after all.

References

Achacoso T, Yamamoto W. (1992) *AY's Neuroanatomy of C. elegans for Computation*.

Albertson D, Thomson J. (1976) The pharynx of *Caenorhabditis elegans*. *Philosophical Transactions of the Royal Society B.*

Alt W. (1980) Biased random walk models for chemotaxis and related diffusion approximations. *Journal of Mathematical Biology*.

Amano H, Maruyama I. (2011) Aversive olfactory learniing and associative long-term memory in *Caenorhabditis elegans*. *Learning and Memory*.

Atkinson-Leadbeater K, Nuttley W, van der Kooy D. (2004) A genetic dissociation of learning and recall in *Caenorhabditis elegans*. *Behavioral Neuroscience*.

Avery L, Horvitz H. (1987) A cell that dies during wild-type *C. elegans* development can function as a neuron in a *ced-3* mutant. *Cell*.

Avery L, Horvitz H. (1989) Pharyngeal pumping continues after laser killing of the pharyngeal nervous system of *C. elegans*. *Neuron*.

Avery L. (1993) Motor neuron M3 controls pharyngeal muscle relaxation timing in *Caenorhabditis elegans*. *Journal of Experimental Biology*.

Baek J, Cosman P, Feng Z, Silver J, Schafer W. (2002) Using machine vision to analyze and classify *Caenorhabditis elegans* behavioral phenotypes quantitatively. *Journal of Neuroscience Methods*.

Bar M, Tootell R, Schacter D, Greve D, Fischl B, Mendola J, Rosen B, Dale A. (2001) Cortical mechanisms specific to explicit visual object recognition. *Neuron*.

Bargmann C. (1998) Neurobiology of the *Caenorhabditis elegans* genome. *Science*.

Bargmann C, Horvitz H. (1991) Chemosensory neurons with overlapping functions direct chemotaxis to multiple chemicals in *C. elegans*. *Neuron*.

Bargmann C, Hartwieg E, Horvitz H. (1993) Odorant-selective genes and neurons mediate olfaction in *C. elegans*. *Cell*.

Bargmann C, Marder E. (2013) From the connectome to brain function. *Nature Methods*.

Baylis H, Furuichi T, Yoshikawa F, Mikoshiba K, Sattelle D. (1999) Inositol 1,4,5-trisphosphate receptors are strongly expressed in the nervous system, pharynx, intestine, gonad and excretory cell of *Caenorhabditis elegans* and are encoded by a single gene (*itr-1*). *Journal of Molecular Biology*.

Bedford T. (1927) The nature of the action of ultra-violet light on micro-organisms. *British Journal of Experimental Pathology*.

Beets I, Janssen T, Meelkop E, Temmerman L, Suetens N, Rademakers S, Jansen G, Schoofs L. (2012) Vasopressin/oxytocin-related signaling regulates gustatory associative learning in *C. elegans*. *Science*.

Bermudez-Rattoni F, Forthman D, Sanchez M, Perez J, Garcia J. (1988) Odor and taste aversions conditioned in anesthetized rats. *Behavioral Neuroscience*.

Bernhard N, van der Kooy D. (2000) A behavioral and genetic dissection of two forms of olfactory plasticity in *Caenorhabditis elegans*: adaptation and habituation. *Learning and Memory*.

Bernstein I, Webster M. (1980) Learned taste aversions in humans. *Physiology & Behavior*.

Bienert G, Schjoerring J, Jahn T. (2006) Membrane transport of hydrogen peroxide. *Biochimica et Biophysica Acta*.

Bigelow H, Doitsidou M, Sarin S, Hobert O. (2009) MAQGene: software to facilitate *C. elegans* mutant genome sequence analysis. *Nature Methods*.
Blum H. (1932) Photodynamic action. *Physiological Review*.
Bolm M, Jansen W, Schnabel R, Chhatwal G. (2004) Hydrogen peroxide-mediated killing of *Caenorhabditis elegans*: a common feature of different *Streptococcal* species. *Infection and Immunity*.
Brockie P, Madsen D, Zheng Y, Mellem J, Maricq A. (2001) Differential expression of glutamate receptor subunits in the nervous system of *Caenorhabditis elegans* and their regulation by the homeodomain protein UNC-42. *The Journal of Neuroscience*.
Burr A. (1985) The photomovement of *Caenorhabditis elegans*, a nematode which lacks ocelli. Proof that the response is to light not radiant heating. *Photochemistry and Photobiology*.
Cardona A, Saalfeld S, Schindelin J, Arganda-Carreras I, Preibisch S, Longair M, Tomancak P, Hartenstein V, Douglas R. (2012) TrakEM2 software for neural circuit reconstruction. *PLoS One*.
Cevik M. (2014) Habituation, sensitization, and pavlovian conditioning. *Fronteirs in Integrative Neuroscience*.
Chalasani S, Chronis N, Tsunozaki M, Gray J, Ramot D, Goodman M, Bargmann C. (2007) Dissecting a circuit for olfactory behavior in *Caenorhabditis elegans*. *Nature*.
Chalfie M, Sulston J, White J, Southgate E, Thomson J, Brenner S. (1985) The neural circuit for touch sensitivity in *Caenorhabditis elegans*. *The Journal of Neuroscience*.
Chalmers D. (1995) Facing up to the problem of consciousness. *Journal of Consciousness Studies*.
Chang H, Paek J, Kim D. (2011) Natural polymorphisms in *C. elegans* HECW-1 E3 ligase affect pathogen avoidance behaviour. *Nature*.
Chao M, Komatsu H, Fukuto H, Dionne H, Hart A. (2004) Feeding status and serotonin rapidly and reversibly modulate a *Caenorhabditis elegans* chemosensory circuit. *Proceedings of the National Academy of Sciences*.
Chaves I, Pokorny R, Byrdin M, Hoang N, Ritz T, Brettel K, Essen L, van der Horst G, Batschauer A, Ahmad M. (2011) The cyrptochromes: Blue light photoreceptors in plants and animals. *Annual Review of Plant Biology*.
Chen B, Hall D, Chklovskii D. (2006) Wiring optimization can relate neuronal structure and function. *Proceedings of the National Academy of Sciences*.
Cheng D, Disterhoft J, Power J, Ellis D, Desmond J. (2008) Neural substrates underlying human delay and trace eyeblink conditioning. *Proceedings of the National Academy of Sciences*.
Chi C, Clark D, Lee S, Biron D, Luo L, Gabel C, Brown J, Sengupta P, Samuel A. (2007) Temperature and food mediate long-term thermotactic behavioral plasticity by association-independent mechanisms in *C. elegans*. *The Journal of Experimental Biology*.
Christie J, Arvai A, Baxter K, Heilmann M, Pratt A, O'Hara A, Kelly S, Hothorn M, Smith B, Hitomi K, Jenkins G, Getzoff E. (2012) Plant UVR8 photoreceptor senses UV-B by tryptophan-mediated disruption of cross-dimer salt bridges. *Science*.
Chyb S, Dahanukar A, Wickens A, Carlson J. (2003) *Drosophila Gr5a* encodes a taste receptor tuned to trehalose. *Proceedings of the National Academy of Sciences*.
Clark R, Squire L. (1998) Classical conditioning and brain systems: the role of awareness. *Science*.
Clark R, Squire L. (1999) Humam eyeblink classical conditioning: Effects of manipulating awareness of stimulus contingencies. *Psychological Science*.

Clark R, Manns J, Squire L. (2001) Trace and delay eyeblink conditioning: Contrasting phenomena of declarative and nondeclarative memory. *Psychological Science*.
Clark R, Manns J, Squire L. (2002) Classical conditioning, awareness, and brain systems. *TRENDS in Cognitive Sciences*.
Colbert H, Bargmann C. (1995) Odorant-specific adaptation pathways generate olfactory plasticity in *C. elegans*. *Neuron*.
Colbert H, Bargmann C. (1997) Environmental signals modulate olfactory acuity, discrimination, and memory in *Caenorhabditis elegans*. *Learning and Memory*.
Cowey A. (2010) The blindsight saga. *Experimental Brain Research*.
Cowey A, Stoerig P. (1995) Blindsight in monkeys. *Nature*.
Crick F, Koch C. (2003) A framework for consciousness. *Nature Neuroscience*.
Cronin C, Mendel J, Mukhtar S, Kim Y, Stirbl R, Bruck J, Sternberg P. (2005) An automated system for measuring parameters of nematode sinusoidal movement. *BMC Genetics*.
Cully D, Vassilatis D, Liu K, Paress P, Van der Ploeg L, Schaeffer J, Arena J. (1994) Cloning of an avermectin-sensitive glutamate-gated chloride channel from *Caenorhabditis elegans*. *Nature*.
Dahanukar A, Lei Y, Kwon J, Carlson J. (2007) Two *Gr* genes underlie sugar reception in *Drosophila*. *Neuron*.
de Gelder B, Tamietto M, van Boxtel B, Goebel R, Sahraie A, van den Stock J, Stienen B, Weiskrantz L, Pegna A. (2008) Intact navigation skills after bilateral loss of striate cortex. *Current Biology*.
Denning D, Hatch V, Horvitz H. (2013) Both the caspase CSP-1 and a caspase-independent pathway promote programmed cell death in parallel to the canonical pathway for apotosis in *Caenorhabditis elegans*. *PLoS Genetics*.
Dent J, Davis M, Avery L. (1997) *avr-15* encodes a chloride channel subunit that mediates inhibitory glutamatergic neurotransmission and ivermectin sensitivity in *Caenorhabditis elegans*. *The EMBO Journal*.
Dent J, Smith M, Vassilatis D, Avery L. (2000) The genetics of ivermectin resistance in *Caenorhabditis elegans*. *Proceedings of the National Academy of Sciences*.
DeYulia G, Carcamo J, Borquez-Ojeda O, Shelton C, Golde D. (2005) Hydrogen peroxide generated extracellularly by receptor-ligand interaction facilitates cell signaling. *Proceedings of the National Academy of Sciences*.
Dillon J, Hopper N, Holden-Dye L, O'Connor V. (2006) Molecular characterization of the metabotropic glutamate receptor family in *Caenorhabditis elegans*. *Biochemical Society Transactions*.
Durbin R. (1987) Studies on the development and organisation of the nervous system of *Caenorhabditis elegans*. *PhD thesis*.
Dusenbery D. (1974) Analysis of chemotaxis in the nematode *Caenorhabditis elegans* by countercurrent separation. *Journal of Experimental Zoology*.
Edwards S, Charlie N, Milfort M, Brown B, Gravlin C, Knecht J, Miller K. (2008) A novel molecular solution for ultraviolet light detection in *Caenorhabditis elegans*. *PLoS Biology*.
Edwards D, Heitler W, Krasne F. (1999) Fifty years of a command neuron: the neurobiology of escape behavior in the crayfish. *Trends in Neurosciences*.

Fang-Yen C, Avery L, Samuel A. (2009) Two size-selective mechanisms specifically trap bacteria-sized food particles in *Caenorhabditis elegans*. *Proceedings of the National Academy of Sciences*.
Fee M, Kozhevnikov A, Hahnloser R. (2004) Neural mechanisms of vocal sequence generation in the songbird. *Annals New York Academy of Sciences*.
Feng Z, Cronin C, Wittig Jr. J, Sternberg P, Schafer W. (2004) An imaging system for standardized quantitative analysis of *C. elegans* behavior. *BMC Bioinformatics*.
Fogle K, Parson K, Dahm N, Holmes T. (2011) CRYPTOCHROME is a blue-light sensor that regulates neuronal firing rate. *Science*.
Fries P, Roelfsema P, Engel A, Konig P, Singer W. (1997) Synchronization of oscillatory responses in visual cortex correlates with perception in interocular rivalry. *Proceedings of the National Academy of Sciences*.
Garcia J, Kimeldorf D, Koelling R. (1955) Conditioned aversion to saccharin resulting from exposure to gamma radiation. *Science*.
Geng W, Cosman P, Berry C, Feng Z, Schafer W. (2004) Automatic tracking, feature extraction and classification of *C. elegans* phenotypes. *IEEE Transactions on Biomedical Engineering*.
Giles A, Rankin C. (2009) Behavioral and genetic characterization of habituation using *Caenorhabditis elegans*. *Neurobiology of Learning and Memory*.
Giorgio M, Trinei M, Migliaccio E, Pelicci P. (2007) Hydrogen peroxide: a metabolic by-product or a common mediator of ageing signals. *Nature Reviews Molecular Cell Biology*.
Gomez M, De Castro E, Guarin E, Sasakura H, Kuhara A, Mori I, Bartfai T, Bargmann C, Nef P. (2001) Calcium signaling via the Neuronal Calcium Sensor-2 regulates associative learning and memory in *C. elegans*. *Neuron*.
Gray J, Karow D, Lu H, Chang A, Chang J, Ellis R, Marietta M, Bargmann C. (2004) Oxygen sensation and social feeding mediated by a *C. elegans* guanylate cyclase homologue. *Nature*.
Grill-Spector K, Kushnir T, Hendler T, Malach R. (2000) The dynamics of object-selective activation correlate with recognition performance in humans. *Nature Neuroscience*.
Hall D, Russell R. (1991) The posterior nervous system of the nematode *Caenorhabditis elegans*: Serial reconstruction of identified neurons and complete pattern of synaptic interactions. *The Journal of Neuroscience*.
Hallem E, Sternberg P. (2008) Acute carbon dioxide avoidance in *Caenorhabditis elegans*. *Proceedings of the National Academy of Sciences*.
Hallem E, Spencer W, McWhirter R, Zeller G, Henz S, Ratsch G, Miller III D, Horvitz H, Sternberg P, Ringstad N. (2011) Receptor-type guanylate cyclase is required for carbon dioxide sensation by *Caenorhabditis elegans*. *Proceedings of the National Academy of Sciences*.
Han C, O'Tuathaigh C, van Trigt L, Quinn J, Fanselow M, Mongeau R, Koch C, Anderson D. (2003) Trace but not delay fear conditioning requires attention and the anterior cingulate cortex. *Proceedings of the National Academy of Sciences*.
Hart A, Kass J, Shapiro J, Kaplan J. (1999) Distinct signaling pathways mediate touch and osmosensory responses in a polymodal sensory neuron. *The Journal of Neuroscience*.
Hartman P, Herman R. (1982) Radiation-sensitive mutants of *Caenorhabditis elegans*. *Genetics*.

Hedgecock E, Russell R. (1975) Normal and mutant thermotaxis in the nematode *Caenorhabditis elegans*. *Proceedings of the National Academy of Sciences*.
Hinton G, Osindero S, Teh Y. (2006) A fast learning algorithm for deep belief nets. *Neural Computation*.
Hockberger P, Skimina T, Centonze V, Lavin C, Chu S, Dadras S, Reddy J, White J. (1999) Activation of flavin-containing oxidases underlies light-induced production of H_2O_2 in mammalian cells. *Proceedings of the National Academy of Sciences*.
Hofmann B, Hecht H, Flohe L. (2002) Peroxiredoxins. *Biological Chemistry*.
Holldobler B, Wilson E. (2008) *The Superorganism: The Beauty, Elegance, and Strangeness of Insect Societies*.
Hoshi K, Shingai R. (2006) Computer-driven automatic identification of locomotion states in *Caenorhabditis elegans*. *Journal of Neuroscience Methods*.
Huang S, Saheki Y, VanHoven M, Torayama I, Ishihara T, Katsura I, van der Linden A, Sengupta P, Bargmann C. (2007) Left-right olfactory asymmetry results from antagonistic functions of voltage-activated calcium channels and the Raw repeat protein OLRN-2 in *C. elegans*. *Neural Development*.
Huang K, Cosman P, Schafer W. (2006) Machine vision based detection of omega bends and reversals in *C. elegans*. *Journal of Neuroscience Methods*.
Hukema R, Rademakers S, Dekkers M, Burghoorn J, Jansen G. (2006) Antagonistic sensory cues generate gustatory plasticity in *Caenorhabditis elegans*. *The EMBO Journal*.
Ikeda D, Duan Y, Matsuki M, Kunitomo H, Hutter H, Hedgecock E, Iino Y. (2008) CASY-1, an ortholog of calsyntenins/alcadeins, is essential for learning in *Caenorhabditis elegans*. *Proceedings of the National Academy of Sciences*.
Imlay J. (2008) Cellular defenses against superoxide and hydrogen peroxide. *Annual Review of Biochemistry*.
Isermann K, Liebau E, Roeder T, Bruchhaus I. (2004) A peroxiredoxin specifically expressed in two types of pharyngeal neurons is required for normal growth and egg production in *Caenorhabditis elegans*. *Journal of Molecular Biology*.
Ishihara T, Iino Y, Mohri A, Mori I, Gengyo-Ando K, Mitani S, Katsura I. (2002) HEN-1, a secretory protein with an LDL receptor motif, regulates sensory integration and learning in *Caenorhabditis elegans*. *Cell*.
Jansen W, Bolm M, Balling R, Chhatwal G, Schnabel R. (2002) Hydrogen peroxide-mediated killing of *Caenorhabditis elegans* by *Streptococcus pyogens*. *Infection and Immunity*.
Jones W, Cayirlioglu P, Kadow I, Vosshall L. (2007) Two chemosensory receptors together mediate carbon dioxide detection in *Drosophila*. *Nature*.
Jospin M, Jacquemond V, Mariol M, Segalat L, Allard B. (2002) The L-type voltage-dependent calcium channel EGL-19 controls body wall muscle function in *Caenorhabditis elegans*. *The Journal of Cell Biology*.
Jospin M, Watanabe S, Joshi D, Young S, Hamming K, Thacker C, Snutch T, Jorgensen E, Schuske K. (2007) UNC-80 and the NCA ion channels contribute to endocytosis defects in synaptojanin muntants. *Current Biology*.
Kano T, Brockie P, Sassa T, Fujimoto H, Kawahara Y, Iino Y, Mellem J, Madsen D, Hosono R, Maricq A. (2008) Memory in *Caenorhabditis elegans* is mediated by NMDA-type ionotropic glutamate receptors. *Current Biology*.

Keller C, Calkins J, Hartman P, Rupert C. (1987) UV photobiology of the nematode *Caenorhabditis elegans*: Action spectra, absence of photoreactivation and effects of caffeine. *Photochemistry and Photobiology*.
Kim K, Li C. (2004) Expression and regulation of an FMRFamide-related neuropeptide gene family in *Caenorhabditis elegans*. *The Journal of Comparative Neurology*.
Kim E, Sun L, Gabel C, Fang-Yen C. (2013) Long-term imaging of *Caenorhabditis elegans* using nanoparticle-mediated immobilization. *PLoS One*.
Kimura K, Miyawaki A, Matsumoto K, Mori I. (2004) The *C. elegans* thermosensory neuron AFD responds to warming. *Current Biology*.
Knebel A, Rahmsdorf H, Ullrich A, Herrlich P. (1996) Dephosphorylation of receptor tyrosine kinases as target of regulation by radiation, oxidants or alkylating agents. *The EMBO Journal*.
Knight D, Nguyen H, Bandettini P. (2003) Expression of conditional fear with and without awareness. *Proceedings of the National Academy of Sciences*.
Knight D, Nguyen H, Bandettini P. (2006) The role of awareness in delay and trace fear conditioning in humans. *Cognitive, Affective, & Behavioral Neuroscience*.
Knuttinen M, Power J, Preston A, Disterhoft J. (2001) Awareness in classical differential eyeblink conditioning in young and aging humans. *Behavioral Neuroscience*.
Kocabas A, Shen C, Guo Z, Ramanathan S. (2012) Controlling interneuron activity in *Caenorhabditis elegans* to evoke chemotactic behavior. *Nature*.
Kryukov V. (2012) Towards a unified model of pavlovian conditioning: short review of trace conditioning models. *Cognitive Neurodynamics*.
Kuhara A, Inada H, Katsura I, Mori I. (2002) Negative regulation and gain control of sensory neurons by the *C. elegans* calcineurin TAX-6. *Neuron*.
Kuhl P. (2004) Early language acquisition: cracking the speech code. *Nature Reviews Neuroscience*.
Kunitomo H, Sato H, Iwata R, Satoh Y, Ohno H, Yamada K, Iino Y. (2013) Concentration memory-dependent synaptic plasticity of a taste circuit regulates salt concentration chemotaxis in *Caenorhabditis elegans*. *Nature Communications*.
Kwon J, Dahanukar A, Weiss L, Carlson J. (2007) The molecular basis of CO_2 reception in *Drosophila*. *Proceedings of the National Academy of Sciences*.
Lamme V. (2006) Towards a true neural stance on consciousness. *TRENDS in Cognitive Science*.
Land M, Fernald R. (1992) The evolution of eyes. *Annual Review of Neuroscience*.
Law E, Nuttley W, van der Kooy D. (2004) Contextual taste cues modulate olfactory leaning in *C. elegans* by an occasion-setting mechanism. *Current Biology*.
Lee R, Sawin E, Chalfie M, Horvitz H, Avery L. (1999) EAT-4, a homolog of a mammalian sodium-dependent inorganic phosphate cotransporter, is necessary for glutamatergic neurotransmission in *Caenorhabditis elegans*. *The Journal of Neuroscience*.
Lipsitt L. (2006) Learning processes in the human newborn: sensitization, habituation, and classical conditioning. *Annals of the New York Academy of Sciences*.
Liu J, Ward A, Gao J, Dong Y, Nishio N, Inada H, Kang L, Yu Y, Ma D, Xu T, Mori I, Xie Z, Xu X. (2010) *C. elegans* phototransduction requires a G protein-dependent cGMP pathway and a taste receptor homolog. *Nature Neuroscience*.
Long M, Jin D, Fee M. (2010) Support for a synaptic chain model of neuronal sequence generation. *Nature*.

Lovibond P, Shanks D. (2002) The role of awareness in Pavlovian conditioning: Empirical evidence and theoretical implications. *Journal of Experimental Psychology*.
Lundberg A. (1979) Multisensory control of spinal reflex pathways. *Progress in Brain Research*.
Luo L, Gabel C, Ha H, Zhang Y, Samuel A. (2008) Olfactory behavior of swimming *C. elegans* analyzed by measuring motile response to temporal variations of odorants. *Journal of Neurophysiology*.
Ma D, Vozdek R, Bhatla N, Horvitz H. (2012) CYSL-1 interacts with the O_2-sensing hydroxylase EGL-9 to promote H_2S-modulated hypoxia-induced behavioral plasticity in *C. elegans*. *Neuron*.
Manns J, Clark R, Squire L. (2000) Awareness predicts the magnitude of single-cue trace eyeblink conditioning. *Hippocampus*.
Manns J, Clark R, Squire L. (2000) Parallel acquisition of awareness and trace eyeblink classical conditioning. *Learning and Memory*.
Manns J, Clark R, Squire L. (2001) Single-cue delay eyeblink conditioning is unrelated to awareness. *Cognitive, Affective, & Behavioral Neuroscience*.
Manns J, Clark R, Squire L. (2002) Standard delay eyeblink classical comnditioning is independent of awareness. *Journal of Experimental Psychology*.
Maren S, Phan K, Liberzon I. (2013) The contextual brain: implications for fear conditioning, extinction and psychopathology. *Nature Reviews Neuroscience*.
Marinkovic K, Schell A, Dawson M. (1989) Awareness of the CS-UCS contingencey and classical conditioning of skin conductance responses with olfactory CSs. *Biological Psychology*.
Maryon E, Coronado R, Anderson P. (1996) *unc-68* encodes a ryanodine receptor involved in regulating *C. elegans* body-wall muscle contraction. *The Journal of Cell Biology*.
Mathews E, Garcia E, Santi C, Mullen G, Thacker C, Moerman D, Snutch T. (2003) Critical residues of the *Caenorhabditis elegans* unc-2 voltage-gated calcium channel that affect behavioral and physiological properties. *The Journal of Neuroscience*.
McCormick J, Fischer J, Pachlatko J, Eisenstark A. (1976) Characterization of a cell-lethal product from photooxidation of tryptophan: hydrogen peroxide. *Science*.
McKay J, Raizen D, Gottschalk A, Schafer W, Avery L. (2004) *eat-2* and *eat-18* are required for nicotinic neurotransmission in the *Caenorhabditis elegans* pharynx. *Genetics*.
Meador K, Ray P, Echauz J, Loring D, Vachtsevanos G. (2002) Gamma coherence and conscious perception. *Neurology*.
Melloni L, Molina C, Pena M, Torres D, Singer W, Rodriguez E. (2007) Synchronization of neural activity across cortical areas correlates with conscious perception. *The Journal of Neuroscience*.
Mittal N, Budrene E, Brenner M, van Oudenaarden A. (2003) Motility of *Escherichia coli* cells in clusters formed by chemotactic aggregation. *Proceedings of the National Academy of Sciences*.
Moglich A, Yang X, Ayers R, Moffat K. (2010) Structure and function of plant photoreceptors. *Annual Review of Plant Biology*.
Mohri A, Kodama E, Kimura K, Koike M, Mizuno T, Mori I. (2005) Genetic control of temperature preference in the nematode *Caenorhabditis elegans*. *Genetics*.
Mongeluzi D, Rosellini R, Caldarone B, Stock H, Abrahamsen G. (1996) Pavlovian aversive context conditioning using carbon dioxide as the unconditional stimulus. *Journal of Experimental Psychology: Animal Behavior Processes*.

Moon S, Kottgen M, Jiao Y, Xu H, Montell C. (2006) A taste receptor required for the caffeine response in vivo. *Current Biology*.
Mori I, Ohshima Y. (1995) Neural regulation of thermotaxis in *Caenorhabditis elegans*. *Nature*.
Morrison G, Wen J, Runciman S, van der Kooy D. (1999) Olfactory associative learning in *Caenorhabditis elegans* is impaired in *lrn-1* and *lrn-2* mutants. *Behavioral Neuroscience*.
Moy T, Mylonakis E, Calderwood S, Ausubel F. (2004) Cytotoxicity of hydrogen peroxide produced by *Enterococcus faecium*. *Infection and Immunity*.
Nakatani C, Ito J, Nikolaev A, Gong P, van Leeuwen C. (2005) Phase synchronization analysis of EEG during attentional blink. *Journal of Cognitive Neuroscience*.
Nestler E, Barrot M, DiLeone R, Eisch A, Gold S, Monteggia L. (2002) Neurobiology of depression. *Neuron*.
Neumann C, Cao J, Manevich Y. (2009) Peroxiredoxin 1 and its role in cell signaling. *Cell Cycle*.
Nuttley W, Harbinder S, van der Kooy D. (2001) Regulation of distinct attractive and aversive mechanisms mediating benzaldehyde chemotaxis in *Caenorhabditis elegans*. *Learning and Memory*.
Nuttley W, Atkinson-Leadbeater K, van der Kooy D. (2002) Serotonin mediates food-odor associative learning in the nematode *Caenorhabditis elegans*. *Proceedings of the National Academy of Sciences*.
Oda S, Tomioka M, Iino Y. (2011) Neuronal plasticity regulated by the insulin-like signaling pathway underlies salt chemotaxis learning in *Caenorhabditis elegans*. *Journal of Neurophysiology*.
Ohnishi N, Kuhara A, Nakamura F, Okochi Y, Mori I. (2011) Bidirectional regulation of thermotaxis by glutamate transmissions in *Caenorhabditis elegans*. *The EMBO Journal*.
Okkema P, Harrison S, Plunger V, Aryana A, Fire A. (1993) Sequence requirements for myosin gene expression and regulation in *Caenorhabditis elegans*. *Genetics*.
Olsen S, Wilson R. (2008) Cracking neural circuits in a tiny brain: new approaches for understanding the neural circuitry of *Drosophila*. *Trends in Neurosciences*.
Omura D, Clark D, Samuel A, Horvitz H. (2012) Dopamine signaling is essential for precise rates of locomotion by *C. elegans*. *PLoS One*.
Otsu N. (1979) A threshold selection method from gray-level histograms. *IEEE Transactions on Systems, Man, and Cybernetics*.
Palva S, Linkenkaer-Hansen K, Naatanen R, Palva J. (2005) Early neural correlates of conscious somatosensory perception. *The Journal of Neuroscience*.
Papka M, Ivry R, Woodruff-Pak D. (1997) Eyeblink classical conditioning and awareness revisited. *Psychological Science*.
Pascual-Leone A, Walsh V. (2001) Fast backprojections from the motion to the primary visual area necessary for visual awareness. *Science*.
Pavlov I. (1906) The scientific investigation of the psychical faculties or processes in the higher animals. *Science*.
Pereira S, van der Kooy D. (2012) Two forms of learning following training to a single odorant in *Caenorhabditis elegans* AWC neurons. *The Journal of Neuroscience*.
Pierce-Shimomura J, Morse T, Lockery S. (1999) The fundamental role of pirouettes in *Caenorhabditis elegans* chemotaxis. *The Journal of Neuroscience*.
Piggott B, Liu J, Feng Z, Wescott S, Xu X. (2011) The neural circuits and synaptic mechanisms underlying motor initiation in *C. elegans*. *Cell*.

Pradel E, Zhang Y, Pujol N, Matsuyama T, Bargmann C, Ewbank J. (2007) Detection and avoidance of a natural product from the pathogenic bacterium *Serratia marcescens* by *Caenorhabditis elegans*. *Proceedings of the National Academy of Sciences*.
Pujol N, Link E, Liu L, Kurz C, Alloing G, Tan M, Ray K, Solari R, Johnson C, Ewbank J. (2001) A reverse genetic analysis of components of the Toll signaling pathway iin *Caenorhabditis elegans*. *Current Biology*.
Ramot D, Johnson B, Berry Jr. T, Carnell L, Goodman M. (2008) The parallel worm tracker: A platform for measuring average speed and drug-induced paralysis in nematodes. *PLoS One*.
Rankin C, Beck C, Chiba C. (1990) *Caenorhabditis elegans*: a new model system for the study of learning and memory. *Behavioral Brain Research*.
Rankin C, Broster B. (1992) Factors affecting habituation and recovery from habituation in the nematode *Caenorhabditis elegans*. *Behavioral Neuroscience*.
Rankin C, Wicks S. (2000) Mutations of the *Caenorhabditis elegans* brain-specific inorganic phosphate transporter *eat-4* affect habituation of the tap-withdrawal response without affecting the response itself. *The Journal of Neuroscience*.
Rao C, Kirby J, Arkin A. (2004) Design and diversity in bacterial chemotaxis: A comparative study in *Escherichia coli* and *Bacillus subtilus*. *PLoS Biology*.
Reddy K, Andersen E, Kruglyak L, Kim D. (2009) A polymorphism in *npr-1* is a behavioral determinant of pathogen susceptibility in *C. elegans*. *Science*.
Reddy K, Hunter R, Bhatla N, Newman D, Kim D. (2011) *Caenorhabditis elegans* NPR-1-mediated behaviors are suppressed in the presence of mucoid bacteria. *Proceedings of the National Academy of Sciences*.
Rhee S, Woo H, Kil I, Bae S. (2012) Peroxiredoxin functions as a peroxidase and a regulator and sensor of local peroxides. *The Journal of Biological Chemistry*.
Richardson A. (1893) The action of light in preventing putrefactive decomposition; and in inducing the formation of hydrogen peroxide in organic liquids. *Journal of the Chemical Society, Transactions*.
Richmond J, Davis W, Jorgensen E. (1999) UNC-13 is required for synaptic vesicle fusion in *C. elegans*. *Nature Neuroscience*.
Ruta V, Datta S, Vasconcelos M, Freeland J, Looger L, Axel R. (2010) A dimorphic pheromone circuit in *Drosophila* from sensory input to descending output. *Nature*.
Saeki S, Yamamoto M, Iino Y. (2001) Plasticity of chemotaxis revealed by paired presentation of a chemoattractant and starvation in the nematode *Caenorhabditis elegans*. *The Journal of Experimental Biology*.
Samuel A, Silva R, Murthy V. (2003) Synaptic activity of the AFD neuron in *Caenorhabditis elegans* correlates with thermotactic memory. *The Journal of Neuroscience*.
Saper C, Scammell T, Lu J. (2005) Hypothalamic regulation of sleep and circadian rhythms. *Nature*.
Schuske K, Beg A, Jorgensen E. (2004) The GABA nervous system of *C. elegans*. *Trends in Neurosciences*.
Seager W. (2012) *Natural Fabrications: Science, Emergence and Consciousness*.
Searle J. (2000) Consciousness. *Annual Review of Neuroscience*.
Sellings L, Pereira S, Qian C, Dixon-McDougall T, Nowak C, Zhao B, Tyndale R, van der Kooy D. (2013) Nicotine-motivated behavior in *Caenorhabditis elegans* requires the nicotinic acetylcholine receptor subunits *acr-5* and *acr-15*. *European Journal of Neuroscience*.

Speese S, Petrie M, Schuske K, Ailion M, Ann K, Iwasaki K, Jorgensen E, Martin T. (2007) UNC-31 (CAPS) is required for dense-core vesicle but not synaptic vesicle exocytosis in *Caenorhabditis elegans*. *The Journal of Neuroscience*.

Sporns O, Tononi G, Kotter R. (2005) The human connectome: a structural description of the human brain. *PLoS Computational Biology*.

Srinivasan R, Russel D, Edelman G, Tononi G. (1999) Increased synchronization of neuromagnetic responses during conscious perception. *The Journal of Neuroscience*.

Steger K, Shtonda B, Thacker C, Snutch T, Avery L. (2005) The *C. elegans* T-type calcium channel CCA-1 boosts neuromuscular transmission. *The Journal of Experimental Biology*.

Stern Y, Mayeux R, Rosen J, Ilson J. (1983) Perceptual motor dysfunction in Parkinson's disease: a deficit in sequential and predictive voluntary movement. *Journal of Neurology, Neurosurgery, and Psychiatry*.

Sternson S, Betley J, Cao Z. (2013) Neural circuits and motivational processes for hunger. *Current Opinion in Neurobiology*.

Sulston J, Horvitz H. (1977) Post-embryonic cell lineages of the nematode *Caenorhabditis elegans*. *Developmental Biology*.

Sulston J, Schierenberg E, White J, Thomson J. (1983) The embryonic cell lineage of the nematode *Caenorhabditis elegans*. *Developmental Biology*.

Swierczek N, Giles A, Rankin C, Kerr R. (2011) High-throughput behavioral analysis in *C. elegans*. *Nature Methods*.

Terakita A. (2005) The opsins. *Genome Biology*.

Tian L, Hires S, Mao T, Huber D, Chiappe M, Chalasani S, Petreanu L, Akerboom J, McKinney S, Schreiter E, Bargmann C, Jayaraman V, Svoboda K, Looger L. (2009) Imaging neural activity in worms, flies and mice with improved GCaMP calcium indicators. *Nature Methods*.

Tomioka M, Adachi T, Suzuki H, Kunitomo H, Schafer W, Iino Y. (2006) The insulin/PI 3-kinase pathway regulates salt chemotaxis learning in *Caenorhabditis elegans*. *Neuron*.

Tononi G. (2004) An information integration theory of consciousness. *BMC Neuroscience*.

Torayama I, Ishihara T, Katsura I. (2007) *Caenorhabditis elegans* integrates the signals of butanone and food to enhance chemotaxis to butanone. *The Journal of Neuroscience*.

Tovee M. (1994) How fast is the speed of thought?. *Current Biology*.

Troemel E, Chou J, Dwyer N, Cobert H, Bargmann C. (1995) Divergent seven transmembrane receptors are candidate chemosensory receptors in *C. elegans*. *Cell*.

Tully T, Quinn W. (1985) Classical conditioning and retention in normal and mutant *Drosophila* melanogaster. *Journal of Comparative Physiology A*.

Veal E, Day A, Morgan B. (2007) Hydrogen peroxide sensing and signaling. *Molecular Cell*.

Wadhams G, Armitage J. (2004) Making sense of it all: Bacterial chemotaxis. *Nature Reviews Molecular Cell Biology*.

Wang R, Nixon B. (1978) Identification of hydrogen peroxide as a photoproduct toxic to human cells in tissue-culture medium irradiated with "daylight" fluorescent light. *In Vitro*.

Ward A, Liu J, Feng Z, Xu X. (2008) Light-sensitive neurons and channels mediate phototaxis in *C. elegans*. *Nature Neuroscience*.

Ward S. (1973) Chemotaxis by the nematode *Caenorhabditis elegans*: Identification of attractants and analysis of the response by use of mutants. *Proceedings of the National Academy of Sciences*.

Weike A, Schupp H, Hamm A. (2007) Fear acquisition requires awareness in trace but not delay conditioning. *Psychophysiology*.
Weiskrantz L, Barbur J, Sahraie A. (1995) Parameters affecting conscious versus unconscious visual discrimination with damage to the visual cortex (V1). *Proceedings of the National Academy of Sciences*.
Weiskrantz L, Warrington E, Sanders M, Marshall J. (1974) Visual capacity in the hemianopic field following a restricted occipital ablation. *Brain*.
Wen J, Kumar N, Morrison G, Rambaldini G, Runciman S, Rousseau J, van der Kooy D. (1997) Mutations that prevent associative learning in *C. elegans*. *Behavioral Neuroscience*.
Wentworth P, Jones L, Wentworth A, Zhu X, Larsen N, Wilson I, Xu X, Goodard W, Janda K, Eschenmoser A, Lerner R. (2001) Antibody catalysis of the oxidation of water. *Science*.
Whippo C. (2006) Phototropism: Bending towards enlightenment. *The Plant Cell*.
White J, Southgate E, Thomson J, Brenner S. (1986) The structure of the nervous system of the nematode *Caenorhabditis elegans*. *Philosophical Transactions of the Royal Society of London B*.
Wood Z, Schroder E, Harris J, Poole L. (2003) Structure, mechanism and regulation of peroxiredoxins. *TRENDS in Biochemical Sciences*.
Wood Z, Poole L, Karplus P. (2003) Peroxiredoxin evolution and the regulation of hydrogen peroxide signaling. *Science*.
Woodruff-Pak D. (1999) New directions for a classical paradigm: Human eyeblink conditioning. *Psychological Science*.
Wu D, Hu Q, Yan Z, Chen W, Yan C, Huang X, Zhang J, Yang P, Deng H, Wang J, Deng X, Shi Y. (2012) Structural basis of ultraviolet-B perception by UVR8. *Nature*.
Xiang Y, Yuan Q, Vogt N, Looger L, Jan L, Jan Y. (2010) Light-avoidance-mediating photoreceptors tile the *Drosophila* larval body wall. *Nature*.
Yamamoto T, Shimura T, Sako N, Yasoshima Y, Sakai N. (1994) Neural substrates for conditioned taste aversion in the rat. *Behavioural Brain Research*.
Yeh E, Ng S, Zhang M, Bouhours M, Wang Y, Wang M, Hung W, Aoyagi K, Melnik-Martinez K, Li M, Liu F, Schafer W, Zhen M. (2008) A putative cation channel, NCA-1, and a novel protein, UNC-80, transmit neuronal activity in *C. elegans*. *PLoS Biology*.
Zeki S, Bartels A. (1999) Toward a theory of visual consciousness. *Consciousness and Cognition*.
Zhang Y, Lu H, Bargmann C. (2005) Pathogenic bacteria induce aversive olfactory learning in *Caenorhabditis elegans*. *Nature*.
Zimmer M, Gray J, Pokala N, Chang A, Karow D, Marietta M, Hudson M, Morton D, Chronis N, Bargmann C. (2009) Neurons detect increases and decreases in oxygen levels using distinct guanylate cyclases. *Neuron*.